A new marine vertebrate assemblage from the Late Neogene Purisima Formation in Central California, part II: Pinnipeds and Cetaceans

Robert W. BOESSENECKER
Department of Geology, University of Otago,
360 Leith Walk, P.O. Box 56, Dunedin, 9054 (New Zealand)
and Department of Earth Sciences, Montana State University
200 Traphagen Hall, Bozeman, MT, 59715 (USA)
and University of California Museum of Paleontology
1101 Valley Life Sciences Building, Berkeley, CA, 94720 (USA)
robert.boessenecker@otago.ac.nz

Boessenecker R. W. 2013. — A new marine vertebrate assemblage from the Late Neogene Purisima Formation in Central California, part II: Pinnipeds and Cetaceans. *Geodiversitas* 35 (4): 815-940. http://dx.doi.org/g2013n4a5

ABSTRACT
The newly discovered Upper Miocene to Upper Pliocene San Gregorio assemblage of the Purisima Formation in Central California has yielded a diverse collection of 34 marine vertebrate taxa, including eight sharks, two bony fish, three marine birds (described in a previous study), and 21 marine mammals. Pinnipeds include the walrus *Dusignathus* sp., cf. *D. seftoni*, the fur seal *Callorhinus* sp., cf. *C. gilmorei*, and indeterminate otariid bones. Baleen whales include dwarf mysticetes (*Herpetocetus bramblei* Whitmore & Barnes, 2008, *Herpetocetus* sp.), two right whales (cf. *Eubalaena* sp. 1, cf. *Eubalaena* sp. 2), at least three balaenopterids ("*Balaenoptera*" *cortesi* "var." *portisi* Sacco, 1890, cf. *Balaenoptera,* Balaenopteridae gen. et sp. indet.) and a new species of rorqual (*Balaenoptera bertae* n. sp.) that exhibits a number of derived features that place it within the genus *Balaenoptera*. This new species of *Balaenoptera* is relatively small (estimated 61 cm bizygomatic width) and exhibits a comparatively narrow vertex, an obliquely (but precipitously) sloping frontal adjacent to vertex, anteriorly directed and short zygomatic processes, and squamosal creases. Fossil odontocetes include the lipotid "river dolphin" *Parapontoporia sternbergi* (Gregory & Kellogg, 1927), four true porpoises including a bizarre new genus also known from other strata (Phocoenidae indet., Phocoenidae unnamed genera 1 and 2, and cf. *Phocoena*), an indeterminate delphinid (Delphinidae indet.) a pilot whale-like delphinid (cf. Globicephalinae indet.), an undetermined sperm whale (cf. Physeteroidea indet.), and an indeterminate odontocete. The new record of *Parapontoporia sternbergi* is noteworthy as it represents the first association of any earbones (petrosal, tympanic bulla, malleus, and incus) for the extinct genus. Discovery and description of a complete marine mammal assemblage permits faunal comparisons with other published Pliocene marine mammal assemblages from around the globe. The aggregate Pliocene marine mammal assemblage from

eastern North Pacific (ENP) shares little in common with the modern fauna, and is mostly composed of extinct genera; notably, phocoenids and odobenids were more diverse than in the ENP today. This indicates that the modern fauna of the ENP did not emerge until after the end of the Pliocene, and probably sometime during the Early Pleistocene. The Pliocene ENP assemblage is similar to that of Japan, and the North Pacific in general shares little with south Pacific, Mediterranean, or North Atlantic marine mammal assemblages, indicating the North Pacific hosted a provincial marine mammal fauna that evolved in isolation from the modern marine mammal fauna, which had already appeared in the North Atlantic by the Early Pliocene.

KEY WORDS
Marine mammals,
Pinnipedia,
Mysticeti,
Odontoceti,
Pliocene,
Pleistocene,
Purisima Formation,
new species.

RÉSUMÉ
Un nouvel assemblage de vertébrés marins de la Formation Purisima, Californie centrale, partie II : les Pinnipèdes et les Cétacés.
La nouvelle faune découverte à San Gregorio (Miocène supérieur à Pliocène supérieur) dans la Formation Purisima en Californie Centrale a permis de constituer une collection de 34 taxons de vertébrés, dont huit espèces de requins, deux de poissons osseux, trois d'oiseaux marins (décrits dans une étude antérieure) et 21 de mammifères. Les pinnipèdes comprennent un morse *Dusignathus* sp., cf. *D. seftoni*, un otarie à fourrure *Callorhinus* sp., cf. *C. gilmorei* et des os indéterminés d'otaries. Les baleines comprennent des mysticètes nains (*Herpetocetus bramblei* Whitmore & Barnes, 2008, *Herpetocetus* sp.), deux baleines franches (cf. *Eubalaena* sp. 1, cf. *Eubalaena* sp. 2), au moins trois balénoptères ("*Balaenoptera*" *cortesi* "var." *portisi* Sacco, 1890, cf. *Balaenoptera,* Balaenopteridae gen. et sp. indet.) et une nouvelle espèce de rorqual (*Balaenoptera bertae* n. sp.) qui présente des caractères dérivés permettant de la placer au sein du genre *Balaenoptera*. Cette nouvelle espèce de *Balaenoptera* est relativement petite (largeur bizygomatique estimée à 61 cm) et montre un vertex relativement étroit, un frontal avec une pente forte, une apophyse zygomatique courte et dirigée antérieurement, et un squamosal plissé. Les odontocètes fossiles comprennent un Lipotidae (dauphin de rivière) *Parapontoporia sternbergi* (Gregory & Kellogg, 1927), quatre vrais marsoins incluant un étrange nouveau genre connu dans d'autres niveaux (Phocoenidae indet., Phocoenidae genres non nommés 1 et 2, et cf. *Phocoena*), un dauphin indéterminé (Delphinidae indet.), un globicéphale (cf. Globicephalinae indet.), un cachalot indéterminé (cf. Physeteroidea indet.) et un odontocète indéterminé. La nouvelle signalisation de *Parapontoporia sternbergi* est remarquable car elle représente la première association d'os de l'oreille (petrosal, bulle tympanique et incus) pour ce genre fossile. La découverte et la description d'un assemblage complet de mammifères marins autorise une comparaison avec d'autres assemblages de mammifères marins pliocènes dans le monde. L'assemblage de mammifères marins du Pliocène de l'Est du Nord Pacifique (ENP), présente peu de similitudes avec la faune moderne et est principalement composé de genres éteints, particulièrement des phocoenidés et des odobenidés qui étaient plus diversifiés que dans l'ENP actuel. Ceci indique que la faune moderne de l'ENP n'émerge pas après la fin du Pliocène mais probablement à un moment du Pléistocène ancien. L'assemblage ENP pliocène est semblable à celui du Japon et du Nord du Pacifique en général présente peu de point communs avec ceux du Sud du Pacifique, de Méditerranée ou du Nord de l'Atlantique. Ceci indique que la faune marine de mammifère pliocène du Nord du Pacifique était marquée d'un provincialisme et a évolué de manière isolée de la faune moderne, qui était déjà apparue dans le Nord de l'Atlantique au Pliocène inférieur.

MOTS CLÉS
Mammifères marins,
Pinnipedia,
Mysticeti,
Odontoceti,
Pliocène,
Pléistocène,
Formation Purisima,
espèce nouvelle.

INTRODUCTION

The fossil record of the west coast of the United States and Mexico has long been known to yield rich assemblages of marine vertebrates of Cenozoic age (Jordan & Hannibal 1923; Kellogg 1927, 1931; Barnes 1977; Repenning & Tedford 1977; Domning 1978; Warheit 1992; Miyazaki *et al.* 1995; Barnes 1998; Deméré *et al.* 2003). Many of the earliest discovered fossil vertebrates from this region are marine mammals from Miocene and Pliocene strata, and include enigmatic odontocetes such as *Lonchodelphis occiduus* Leidy, 1858 and *Hesperocetus californicus* True, 1912, early records of fossil pinnipeds (*Pontolis magnus* True, 1903, *Desmatophoca oregonensis* Condon, 1906 and *Allodesmus kernensis* Kellogg, 1922), and the desmostylian *Desmostylus hesperus* Marsh, 1888. Subsequent discoveries in this region during the middle and late twentieth centuries have resulted in a series of major advances in the study of marine mammal evolution and paleontology, including the discovery of the oldest pinnipeds (Oligo-Miocene; Mitchell & Tedford 1973; Barnes 1979; Berta *et al.* 1989), the earliest informative discoveries of toothed mysticetes (Late Oligocene; Emlong 1966; Barnes *et al.* 1995), archaic desmostylian fossils which alleviated a host of issues concerning their phylogenetic origins (Late Oligocene; Domning *et al.* 1986), and some of the world's most complete and exquisitely preserved fossil skeletons of sirenians (Middle-Late Miocene and Pliocene; Domning 1978) and desmostylians (Early-Middle Miocene; Clark 1991; Domning & Barnes 2007). Various phylogenetic analyses have used many extinct marine mammals from the eastern North Pacific as "benchmark" taxa, including several odontocetes (Geisler & Sanders 2003; Lambert 2008a; Geisler *et al.* 2011), mysticetes (Bouetel & Muizon 2006; Marx 2011; Geisler *et al.* 2011), pinnipeds (Berta & Deméré 1986; Berta & Wyss 1994; Deméré 1994a; Deméré & Berta 2002; Barnes *et al.* 2006; Kohno 2006), sirenians (Domning 1994) and desmostylians (Beatty 2009).

Despite this long history of research on marine mammal fossils along this coast, the majority of previous studies have "cherry picked" these rich assemblages to focus upon elements within, such as a particular new marine mammal taxon. There are few assemblages for which the majority of marine vertebrate taxa have been documented. In contrast to the well-published fossil record of Neogene pinnipeds, desmostylians, and sirenians, there are comparatively few publications which are concerned with accompanying sharks, bony fish, birds, and cetaceans (Late Miocene cetaceans in particular; Barnes 1977), despite being numerically abundant in museum collections. The 2004 discovery of a new marine vertebrate assemblage in the Upper Miocene-Upper Pliocene Purisima Formation (Boessenecker 2006, 2011a) yielded enough fossils to permit study and description of an entire marine vertebrate assemblage. Previously, the fossil sharks, birds, and bony fish were described in detail by Boessenecker (2011a) and Boessenecker & Smith (2011). The purpose of this study is to describe the remainder of the assemblage, comprising 21 pinniped, odontocete, and mysticete taxa. Description of this assemblage permits comparison with the similarly aged San Diego Formation of southern California, consideration of the aggregate Pliocene marine mammal assemblage from the eastern North Pacific in general, and comparison with other published marine mammal assemblages from across the globe.

Institutional abbreviations

CAS	California Academy of Sciences, San Francisco;
FP	uncataloged specimens of Frank A. Perry collection, housed at University of California Museum of Paleontology, Berkeley;
SCMNH	Santa Cruz Museum of Natural History, Santa Cruz;
SDNHM	San Diego Natural History Museum, San Diego;
UCMP	University of California Museum of Paleontology, Berkeley;
VMS	Sierra College Natural History Museum-marine mammal collection, Rocklin.

MATERIALS AND METHODS

Fieldwork

Most of the fossil material examined during this study was excavated by the author under a California State Parks Paleontological Collections permit

during 2005-2006 and 2010-2011. Some earlier collected specimens reside in collections at Sierra College (Rocklin, California, USA) and the University of California Museum of Paleontology (Berkeley, California, USA). A stratigraphic column was recorded in order to establish a stratigraphic context for the assemblage, previously presented in Boessenecker (2011a) and Boessenecker & Smith (2011), and shown in Figure 1. Fossil specimens were subsequently curated at the University of California Museum of Paleontology in Berkeley, California. Detailed locality information is available on request to researchers from UCMP or the author.

Physical and digital preparation

Marine mammal fossils collected from these localities were mechanically and chemically prepared at the Department of Earth Sciences and Museum of the Rockies at Montana State University in Bozeman, Montana, and the University of California Museum of Paleontology. Vertebrate fossils were prepared using hand tools pneumatic airscribes, and sandblasters. Specimens with calcareous cemented matrix were placed in acid baths using dilute (5-10%) acetic acid. 3D models were prepared by from HRXCT scans by M. Colbert at the UT Austin High Resolution X-ray CT facility.

Terminology and orientation

Anatomical terminology for pinnipeds follows that of Deméré & Berta (2005, and sources therein), while anatomical terminology for cetacean crania follows that of Mead & Fordyce (2009), with some of the suggested modifications of Ekdale *et al.* (2011). With regards to orientation, cetacean petrosals and tympanic bullae are described as if in isolation using traditional orientation based on named anatomical landmarks (e.g., lateral tuberosity on petrosal, medial and lateral lobes of tympanic bullae), following Mead & Fordyce (2009: 4).

Comparisons

To properly identify marine mammal fossils during this study, comparisons were made with a wide variety of modern osteological specimens, fossil specimens in museum collections, and the paleontological literature. Osteological specimens of modern marine mammals were examined at the California Academy of Sciences (San Francisco, California), Museum of the Rockies (Bozeman, Montana) Museum of Vertebrate Zoology at the University of California (Berkeley, California), the San Diego Natural History Museum (San Diego, California), and the University of Otago Geology Museum (Dunedin, New Zealand).

Phylogenetic analysis

A cladistic analysis was employed to place *Balaenoptera bertae* n. sp. within a phylogenetic context. *Balaenoptera bertae* n. sp. was coded in the data matrix of Marx (2011), and analyzed in TNT version 1.1 (Goloboff *et al.* 2008) with the "traditional search option". Characters were analyzed under equal weights, with 10 000 random stepwise-addition replicates and tree bisection reconnection branch swapping, saving 10 trees per replicate. The most parsimonious trees are reported herein as strict consensus trees with collapsed zero-length branches, Bremer support values, and branch support based on symmetric resampling using 2000 replicates.

Geochronologic framework

The Pliocene-Pleistocene boundary was recently changed from 1.806 Ma to 2.588 Ma due to the inclusion of the Gelasian Stage within the Pleistocene and modification of the Quaternary (Gibbard *et al.* 2009). Although this change is based on chronostratigraphy, it does not reflect the biostratigraphic integrity of the traditionally defined Pleistocene epoch (Aubry *et al.* 2009). Thus, for the purposes of this paper, the traditional definition of the Plio-Pleistocene boundary at the 1.806 Ma Gelasian-Calabrian stage boundary (Gradstein *et al.* 2004) is retained following the recommendations of Hilgen *et al.* (2012), including a twofold division of the Pliocene, with the Early Pliocene being constituted by the Zanclean and Piacenzian stages, and the Late Pliocene being constituted by the Gelasian stage. This study follows Boessenecker (2011a, c) and Boessenecker & Smith (2011) in utilizing the traditional Plio-Pleistocene boundary, but differs from these previous studies in using a twofold (rather than threefold) division.

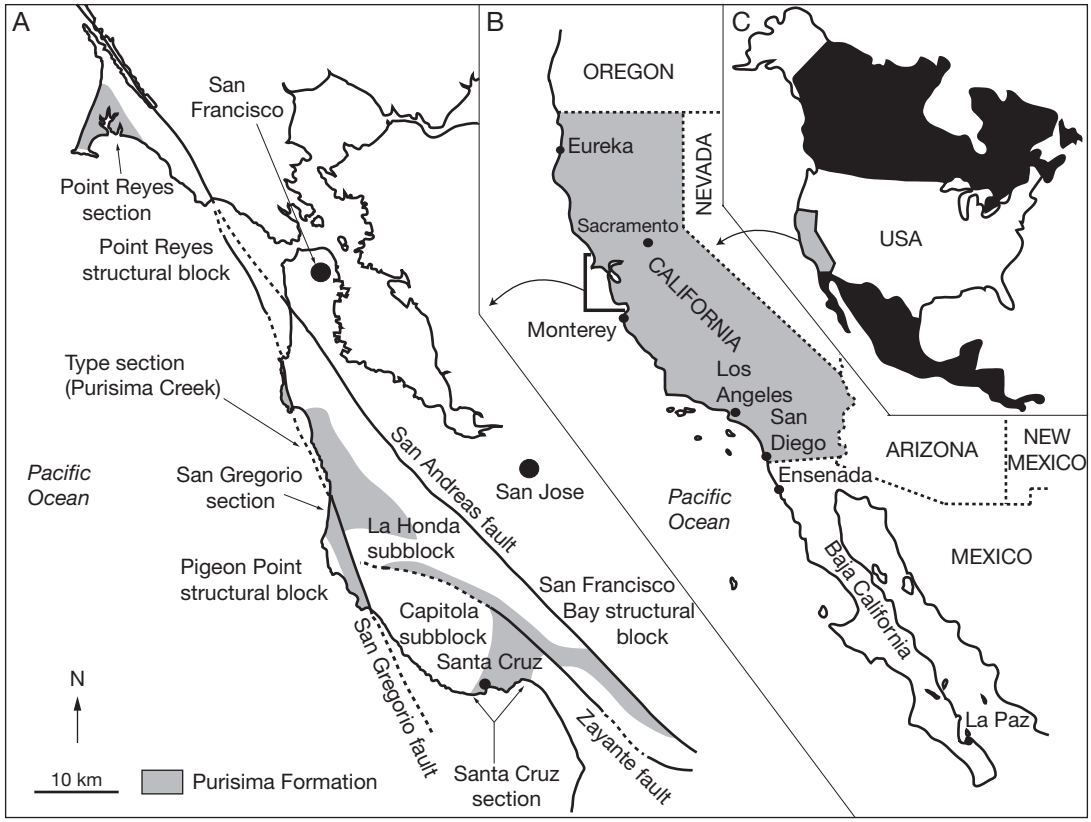

FIG. 1. — Geologic map of the Purisima Formation: **A**, generalized geologic map of the Purisima Formation in the greater San Francisco Bay area, showing outcrops (in gray) and major faults and structural blocks; **B**, map of California and Baja California; **C**, inset map of North America. Modified from Boessenecker (2011a).

GEOLOGIC AND PALEONTOLOGIC BACKGROUND

GEOLOGY

The marine mammal fossils reported here were collected from the Purisima Formation near Halfmoon Bay, California. The Purisima Formation is exposed in various tectonic subblocks in Northern California (Fig. 1) in the vicinity of Point Reyes (Point Reyes structural block), Pillar Point (Pigeon Point structural block), Halfmoon Bay (Pigeon Point structural block and the La Honda subblock of the Santa Cruz Structural block), Año Nuevo Point (Pigeon Point structural block), and Santa Cruz (Capitola subblock of the Santa Cruz structural block; Powell *et al.* 2007). The Purisima Formation is typically latest Miocene and Pliocene in age wherever it is exposed (Cummings *et al.* 1962; Galloway 1977; Clark *et al.* 1984; Powell 1998; Powell *et al.* 2007). Owing to the disparate locations of these various exposures and the multiple strike-slip faults that separate them, correlation between exposures has been difficult (Powell *et al.* 2007). Furthermore, these exposures also vary in terms of stratigraphic completeness (many exposures do not include the top or base of the unit), thickness, outcrop quality, fossil content, and fossil preservation (Powell 1998; Boessenecker 2011a), also hampering intraformational correlations. The Purisima Formation is similar in lithology and age to the Upper Etchegoin Formation and San Joaquin Formation of the southwestern San Joaquin Valley,

and appears to have had a sediment source and been close to this region prior to separation along the San Andreas and San Gregorio faults (Powell *et al.* 2007). The Santa Cruz, San Gregorio, Pillar Point, and Point Reyes sections of the Purisima Formation have been separated from their site of deposition via strike-slip faulting by approximately 180, 250, 270, and 350 km (respectively; Powell *et al.* 2007).

The Purisima Formation near Santa Cruz (Fig. 1A) is the best understood in terms of its stratigraphic and biostratigraphic framework, depositional environment, and invertebrate and vertebrate fossil assemblages (Clark 1981; Norris 1986; Powell *et al.* 2007), and was designated as an alternate reference section for the Purisima Formation by Powell *et al.* (2007). Better understanding of the exposures near Santa Cruz is also related to the relatively poor exposures of the type section of the Purisima Formation in the cliffs near Purisima Creek (San Mateo County), which is currently no longer accessible by foot and has been neglected by researchers in comparison to the Santa Cruz section (Powell *et al.* 2007). The Santa Cruz section of the Purisima Formation is 6.9 to 2.5 Ma based upon biostratigraphy, magnetostratigraphy, and radiometric dating (Clark 1981; Madrid *et al.* 1986; Powell 1998; Powell *et al.* 2007). The Purisima Formation in this area includes sandstones, mudrocks, diatomites, minor phosphatic and glauconitic bonebeds; this is reflective of shelf deposition from the outer to inner shelf, and a brief initial transgression followed by a regression reflected by a thin transgressive systems tract and a thick highstand systems tract (Norris 1986; Powell *et al.* 2007; Boessenecker, unpublished data). Hereafter in this study it will be referred to as the "Santa Cruz section of the Purisima Formation" or the "Purisima Formation near Santa Cruz".

A second section of the Purisima Formation at Point Reyes (Fig. 1A) has been the subject of stratigraphic disagreements. Originally named the Drake's Bay Formation, it was later reidentified as including the Santa Margarita Sandstone, Santa Cruz Mudstone, and Purisima Formation, similar to the sequence in Santa Cruz County (Clark *et al.* 1984). A 7.9 ± 0.3 Ma K-Ar date on glauconite from the Santa Margarita Sandstone at Point Rey was reported by Clark (1997).

The Purisima Formation in the La Honda subblock (Fig. 1A) was divided into five members (Cummings *et al.* 1962), which are from oldest to youngest, the Tahana Sandstone, Pomponio Mudstone, San Gregorio Sandstone, Lobitos Mudstone, and Tunitas Sandstone. Exposures in the type area are depauperate with respect to vertebrate fossils. Further south, the North-South trending San Gregorio fault separates the La Honda subblock (on the east side) from the Pigeon Point structural block (on the west), and the Purisima Formation is exposed on both sides of the fault. Purisima Formation strata to the west of the San Gregorio fault were originally mapped as the Tahana Sandstone Member by Cummings *et al.* (1962); the Tahana Sandstone Member is strictly Late Miocene, based on microfossils (Powell *et al.* 2007). This section (Fig. 2; herein referred to as the San Gregorio section of the Purisima Formation following Powell *et al.* 2007) was also considered to be of Late Miocene age by Gavigan (1984), who reported Late Miocene mollusks from the locality. Durham & Morgan (1978) summarized mollusks from the upper part of the San Gregorio section, concluding that it was Early Pliocene (or Late Miocene of European usage at the time) based on the occurrence of pectinids in the genus *Lituyapecten* MacNeil, 1961; they correlated the San Gregorio section with the Ohlson Ranch, "Merced" (= Wilson Grove Formation), and Falor Formations. The Ohlson Ranch and Falor Formations are Pliocene and Pleistocene in age (respectively; Peck 1960; Nilsen & Clark 1995); Powell (1998) notes that the Purisima specimens probably belong to *Lituyapecten purisimaensis* Arnold, 1906, which is only known from the Purisima Formation and therefore of little use in correlation. Furthermore, Powell *et al.* (2004a) noted *Lituyapecten* occurs in Late Miocene strata of the Wilson Grove Formation, and therefore not useful for indicating a Pliocene age. Gigantic traces from this section were named as the new ichnospecies *Teichichnus pescaderoensis* Stanton & Dodd, 1984; the only other stratigraphic unit yielding such traces in the eastern North Pacific was the Plio-Pleistocene Wildcat Group at Centerville Beach in the Eel River Basin (Stanton & Dodd 1984), tentatively suggesting a Pliocene (rather than Miocene) age for this section. The Late Miocene

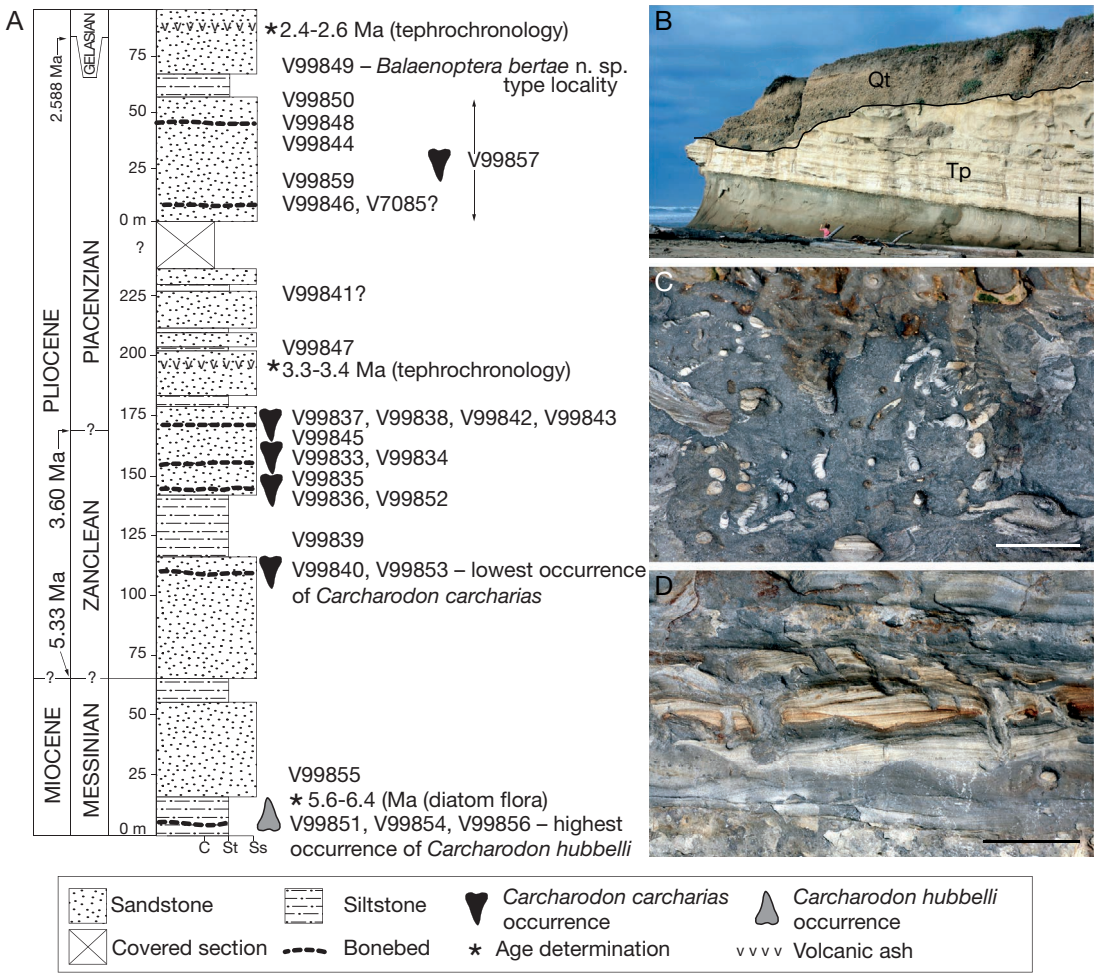

FIG. 2. — Stratigraphy of the Purisima Formation: **A**, Stratigraphic column of the San Gregorio section of the Purisima Formation (in meters), showing stratigraphic position of UCMP vertebrate localities, dated ash beds, diatom floras, and species of *Carcharodon*; thickness measurements start over above missing section in uppermost part due lack of overlapping strata; epoch and stage boundaries marked as "?" are estimated; modified from Boessenecker (2011a); Pliocene-Pleistocene boundary after Hilgen *et al*. (2012); **B**, photograph of 3-4 m thick ash within Purisima Formation at mouth of San Gregorio Creek correlated with 2.5 Ma Ishi Tuff (Powell et al. 2007); **C**, trace fossils in pervasively bioturbated sandstone, Purisima Formation, mouth of San Gregorio Creek; **D**, swaley cross-stratified sandstone, mouth of San Gregorio Creek. Abbreviations: **Qt**, Pleistocene terrace deposits; **Tp**, Purisima Formation; **C**, claystone; **St**, siltstone; **Ss**, sandstone. Scale bars: A, 2 m; B, C, 10 cm.

age reported by Gavigan (1984) was challenged by Sarna-Wojcicki *et al.* (1991), who reported a Late Pliocene ash correlation of 2.5 Ma for a thick unit of tephra at the mouth of San Gregorio Creek (Fig. 2A, B). An additional ash bed slightly lower in the section (Fig. 2A) subsequently yielded an ash correlation of 3.35 Ma (Powell *et al.* 2007). Because of these ashes and the presence of the Pliocene mollusk *Patinopecten healeyi* Arnold, 1906, Powell *et al.* (2007) concluded that the San Gregorio section of the Purisima Formation does not represent the Tahana Member. Additionally, Powell *et al.* (2007) reported a latest Miocene diatom flora (6.4-5.6 Ma) from the base of the San Gregorio section.

Because of these apparently mutually exclusive age determinations, Boessenecker (2011a) utilized

TABLE 1. — The aggregate vertebrate assemblage from the San Gregorio section of the Purisima Formation in San Mateo County, California. Modified from Boessenecker (2011a) and Boessenecker & Smith (2011). Bold indicates taxa described in this study; *, denotes taxa represented only in latest Miocene portion of San Gregorio section; †, denotes taxa represented only in Pliocene portion of San Gregorio section.

Chondrichthyes
Carcharodon hubbelli *
Carcharodon carcharias †
Cetorhinus maximus
Isurus oxyrhincus †
Hexanchidae indet. *
Pristiophorus sp. †
Raja sp., cf. *R. binoculata* †
cf. *Sphyrna* †
Osteichthyes
Paralichthys sp. †
Thunnus sp. †
Aves
Mancalla lucasi †
Morus sp. †
Pelagornis sp. †
Mammalia
Pinnipedia
Dusignathus* sp., cf. *D. seftoni †
Callorhinus* sp., cf. *C. gilmorei †
Otariidae indet. †
Odontoceti
Odontoceti indet. †
Delphinidae indet. †
cf. Globicephalinae indet. †
Parapontoporia sternbergi †
Phocoenidae indet. †
Phocoenidae unnamed genus 1 *
Phocoenidae unnamed genus 2†
cf. *Phocoena* †
Physeteroidea indet. †
Mysticeti
cf. *Eubalaena* sp. 1 *
cf. *Eubalaena* sp. 2 †
***Balaenoptera bertae* n. sp.** †
"*Balaenoptera*" *cortesi* "var." *portisi* †
cf. *Balaenoptera* *
Balaenopteridae indet. morphotype 1 †
Balaenopteridae indet. morphotype 2
Herpetocetus bramblei *
***Herpetocetus* sp.** †

non-mammalian marine vertebrates from the San Gregorio section as an independent test of prior biostratigraphic and tephrochronologic age determinations. Marine vertebrates from the middle and upper parts of the section corroborated the Early to Late Pliocene (Piacenzian-Gelasian) ash correlations (Boessenecker 2011a), while marine vertebrates from the lower part of the San Gregorio section were indeed most similar to marine vertebrate assemblages of latest Miocene age. This framework rectifies most previous age determinations for this section, with the exception of Gavigan (1984). The age implications of the marine mammal taxa found at this locality are discussed below, expanding the account by Boessenecker (2011a).

The San Gregorio section (Fig. 2) is approximately 80 m thick, and is composed of massive, pervasively bioturbated (Fig. 2C) very fine- to fine-grained sandstones and siltstones with rare ash beds (Fig. 2B), bonebeds (Fig. 3C), shell pavements, and shell stringers (Cummings *et al.* 1962; Durham & Morgan 1978; Stanton & Dodd 1984; Norris 1986; Boessenecker 2011a); rare hummocky and swaley cross-stratification is present at certain horizons within the upper and middle parts of the section (e.g., Fig. 2D). This section reflects middle to outer shelf (or transition zone and offshore) deposition (Stanton & Dodd 1984; Norris 1986; Boessenecker 2011a), and records an overall regression, as reflected by up-section increases in grain size, the frequency of shell and bone beds and pavements, and decreasing prevalence of bioturbation.

VERTEBRATE PALEONTOLOGY

Two studies have previously discussed the marine vertebrate fossil assemblage from the San Gregorio section of the Purisima Formation. Fossil sharks, rays, bony fish, and birds were described by Boessenecker (2011a). Vertebrate fossils occasionally occur isolated within the sediment (Fig. 3A), but typically occur within laterally extensive bonebeds which manifest as *c.* 10-20 cm thick pavements with a mixture of terrigenous pebbles, unabraded phosphatic nodules, and mollusk shells with approximately 2-5 clasts or bioclasts per horizontal meter of outcrop. Two bonebeds also exhibit phosphatized, reworked bone: UCMP locality V99836 includes a 20 cm thick mollusk-rich bed with abundant well-rounded and polished phosphatic nodules and phosphatized bone fragments (Fig. 3C); a second bonebed extending

over 2 km represented by UCMP localities V99837, V99838, V9942, and V99843 lack calcareous material, but is comprised by a *c.* 10-30 cm zone of matrix-supported conglomerate (occasionally clast-supported where formed in dense "clumps') primarily consisting of well-rounded and polished phosphatic nodules and vertebrate skeletal elements. Marine mammal remains are occasionally (but very rarely) articulated or associated (Fig. 3B).

Fossil vertebrates reported from the San Gregorio assemblage (Table 1) by Boessenecker (2011a: table 1) are cowsharks (cf. *Hexanchus*), sawsharks (*Pristiophorus* sp.), angel sharks (*Squatina* sp.), basking sharks (*Cetorhinus maximus* Gunnerus, 1765), great white sharks (*Carcharodon* sp., *Carcharodon carcharias* Linnaeus, 1758), shortfin makos (*Isurus oxyrinchus* Rafinesque, 1810), hammerhead sharks (cf. *Sphyrna*), skates (*Raja* sp., cf. *R. binoculata* Girard, 1855), tuna (*Thunnus* sp.), flounder (*Paralichthys* sp.), a gannet (*Morus* sp.), and an extinct penguin-like auk (*Mancalla lucasi* Smith, 2011; Boessenecker 2011a). While that study was in review, the author discovered a fossil of the gigantic bony toothed bird *Pelagornis* sp. (Table 1), later described by Boessenecker & Smith (2011). Subsequently, Ehret *et al.* (2012) described the new species *Carcharodon hubbelli* Ehret, MacFadden, Jones, DeVries, Foster & Salas-Gismondi, 2012 from the Late Miocene of Peru, and *Carcharodon* sp. of Boessenecker (2011a) is herein reidentified as *C. hubbelli*. Overall, there are 14 non-mammalian taxa reported and described by Boessenecker (2011a) and Boessenecker & Smith (2011). These two studies also included a brief list of 13 marine mammal taxa; the current study has expanded this list to 21 marine mammals (Table 1), as described herein.

The comparatively larger fossil vertebrate assemblages from the Santa Cruz section of the Purisima Formation have been the focus of more studies. A few studies have reported sharks (Perry 1977; Domning 1978; Stewart & Perry 2002), although none of these included descriptions, and the diverse shark assemblage requires further study. No published descriptions of fossil birds exist, but bird fossils have been mentioned by Perry (1977) and Warheit (1992); the bird assemblage is now large and diverse, including a wide variety of alcids, sulids, and other marine taxa. Fossil pinnipeds have been described in a number of published studies, including the walrus *Dusignathus santacruzensis* Kellogg, 1927 and the fur seal *Thalassoleon macnallyae* Repenning & Tedford, 1977. Various walrus and fur seal postcrania were described by Mitchell

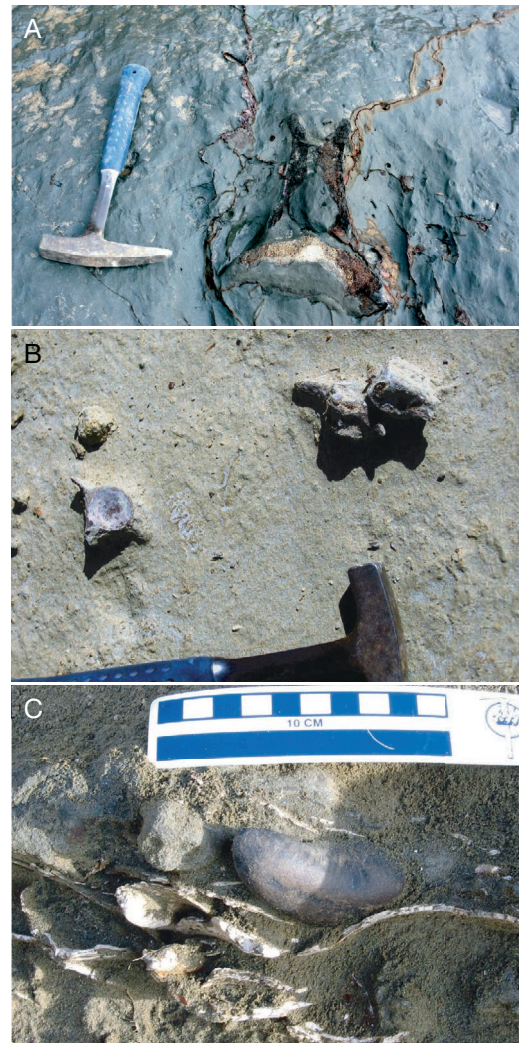

FIG. 3. — Vertebrate fossils in the Purisima Formation: **A**, isolated mysticete vertebra, middle part of San Gregorio section; **B**, associated odontocete vertebrae, upper part of San Gregorio section, UCMP locality V-99846; **C**, *Herpetocetus* sp. tympanic bulla (UCMP 219117) in shell-rich, calcium carbonate cemented phosphatic bonebed, middle part of San Gregorio section, UCMP locality V-99836.

(1962). Boessenecker & Perry (2011) described indeterminate otariid forelimb bones with circular puncture marks in them, which were identified as probable marine mammal bite marks. Additionally, a new genus of toothless odobenine walrus (Barnes & Perry 1989) awaits formal publication. Several members of the diverse cetacean assemblage (Barnes 1977) have been reported, including the bizarre small-bodied mysticete *Herpetocetus bramblei* (Boessenecker & Geisler 2008; Whitmore & Barnes 2008) and the long-snouted lipotid dolphin *Parapontoporia wilsoni* Barnes, 1985, in addition to two globicephaline whales (Boessenecker *et al.* 2013). Lastly, fossil sirenian bone fragments were reported by Domning (1978).

Other localities in the Purisima Formation have yielded diverse marine vertebrate assemblages, principally exposures at Point Reyes (latest Miocene-Early Pliocene, Messinian-Zanclean equivalent; Marin County) and near Pillar Point (Pliocene; San Mateo County). Marine vertebrates from Pillar Point include indeterminate mysticete bones, an undescribed phocoenid porpoise, earbones of an unidentified delphinoid dolphin, and forelimb bones of the walrus *D. santacruzensis* (Glen 1959; Repenning & Tedford 1977). Exposures at Point Reyes have yielded the giant salmon *Oncorhynchus rastrosus* Cavender & Miller 1972, the fur seal *T. macnallyae*, a balaenid right whale (*Balaenula* sp.), an apparently modern rorqual (*Balaenoptera* sp.), a sperm whale ("*Scaldicetus*" sp.), the beluga-like monodontid *Denebola* sp., and an unidentified odontocete (Barnes 1977; Repenning & Tedford 1977; Domning 1978). Repenning & Tedford (1977) also reported a partial forelimb of the walrus *D. santacruzensis* from the Drake's Bay Formation, which they considered to be coeval with the Purisima Formation; however, this specimen was collected from the glauconitic base of the Santa Margarita Sandstone and is thus *c.* 7.9 Ma in age (Clark *et al.* 1984; Clark 1997), and older than the Early Pliocene strata of the Purisima Formation along Drake's Bay. Furthermore, this specimen appears to represent an odobenid closer to *Imagotaria* Mitchell, 1968 (Boessenecker pers. obs.). Recent field research by the author has resulted in some additions to the assemblage, including teeth of great white sharks (*C. carcharias*) and cow sharks (*Hexanchus* sp.), new mandibles, teeth, and partial skeletons of the fur seal *Thalassoleon* Repenning & Tedford, 1977, a nearly complete skull and an isolated partial femur of a large dusignathine walrus, earbones of the balaenopterid mysticete "*Megaptera*" *miocaena* Kellogg, 1922, partial skulls and mandibles of the small mysticete *Herpetocetus* Van Beneden, 1872, partial crania and earbones of an unidentified possible phocoenid, and a petrosal and mandible fragment of a hydrodamaline sea cow.

SYSTEMATIC PALEONTOLOGY

Order CARNIVORA Bowditch, 1821
Suborder PINNIPEDIA Illiger, 1811
Family ODOBENIDAE Allen, 1880
Genus *Dusignathus* Kellogg, 1927

Dusignathus sp., cf. ***D. seftoni***

REFERRED MATERIAL. — VMS 2, a complete right radius; UCMP 219005, a partial right radius, UCMP 219006, a partial atlas, and UCMP 219001, a partial cervical vertebra, collected by R.W. Boessenecker and C. Dailey from UCMP localities V99834 and V99848.

STRATIGRAPHIC OCCURRENCE. — Middle and upper parts of the San Gregorio section of the Purisima Formation, Early to Late Pliocene (*c.* 5-2.5 Ma, Zanclean-Gelasian equivalent; Fig. 2).

DESCRIPTION

These specimens are all relatively large in comparison to the otariid specimens described below. The radii (Fig. 4) are at least twice the size of *Callorhinus* sp., cf. *C. gilmorei*. The description is primarily based on VMS 2; however, the distal end of VMS 2 is poorly preserved, and the description of the distal end is based instead upon UCMP 219005. The radii are relatively straight and transversely flattened. Although damaged, the radial head bears an expanded and concave proximal articular surface. The shaft is proximally cylindrical, and distally becomes anteroposteriorly expanded near the pronator teres process. The pronator teres process is positioned just slightly proximal to the midpoint of the radius, and occurs

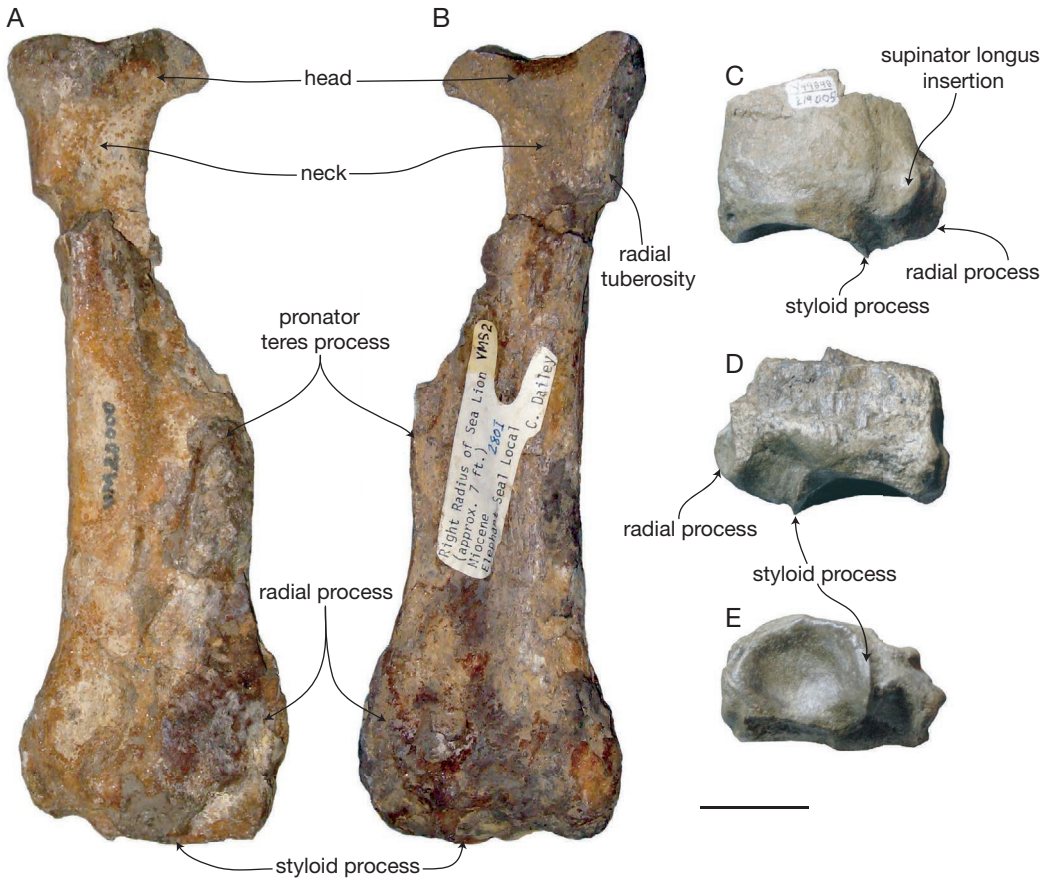

FIG. 4. — Radii of *Dusignathus* sp., cf. *D. seftoni*: **A**, VMS 2, right radius in lateral view; **B**, VMS 2, medial view; **C**, UCMP 219005, fragment of right radius, in lateral view; **D**, UCMP 219005 in medial view; **E**, UCMP 219005 in distal view. Scale bar: 3 cm.

as an angle on the anterior margin of the radius (Fig. 4A); the lateral surface of the pronator teres process is slightly rugose. The distal end is massive, transversely thicker, and anteroposteriorly deeper than the proximal shaft. Although the radial process is damaged in VMS 2, in UCMP 219005 it is transversely robust, distally directed, and extends nearly to the level of the distal scapholunar articulation surface (Fig. 4C, D). The supinator longus insertion is present as a small knob. The scapholunar articulation of UCMP 219005 is deeply concave and oval in distal aspect, with a prominent styloid process. The medial surface of the shaft is shallowly concave, while the lateral surface is slightly convex.

Nearly the complete left side of the atlas (UCMP 219006) is preserved (Fig. 5A-C). Anteriorly, there is a large, concave, and crescentic articular surface for the left occipital condyle. The neural canal would have been large and circular. The neural arch is anteroposteriorly broad and dorsally bears a small, transversely oriented foramen. The posterior articular surface is flat, small, oval, and positioned laterally to the neural canal. The transverse process is large, positioned at the middle of the centrum, and in dorsal aspect, is triangular and dorsally flat and shelf-like. A large, circular, transverse foramen perforates the transverse process. The ventral root of the transverse process is cylindrical, and the ventral arch of the centrum is curved and bar-like.

UCMP 219001 is a partial cervical vertebra with a rectangular articular surface of body (Fig. 5D, E). In lateral aspect, the anterior and posterior articular surfaces are vertically oriented and parallel, but the body of the centrum is oriented anterodorsally so that the anterior face is dorsally higher than the posterior face. The ventral surface of the neural canal is nearly flat, and rectangular in dorsal aspect. The transverse process is broken, but ventrolaterally projecting, tabular, and massive; a circular transverse foramen perforates the transverse process.

Comparisons

These specimens exhibit one odobenid synapomorphy, an expanded distal end of the radius with an enlarged and distally projected radial process (Deméré 1994a); this feature is damaged in VMS 2, but clearly preserved in UCMP 219005. These new specimens are similar to radii referred to *Dusignathus santacruzensis* by Repenning & Tedford (1977), although radii of *D. santacruzensis* (see Mitchell 1962: fig. 3; and Repenning & Tedford 1977: pl. 16.5) are typically more robust and transversely wider than the San Gregorio specimens and *Dusignathus seftoni* Deméré, 1994. These Purisima Formation specimens share a transversely compressed cross-section with *D. seftoni*. Both radii can be separated from the larger dusignathine *Gomphotaria* in their much smaller size and more prominent pronator teres process (on VMS 2). UCMP 219005 and VMS 2 differ from radii of the "toothless" odobenine *Valenictus chulavistensis* Deméré, 1994 in being transversely flattened and lacking a pachyosteosclerotic bone histology in broken cross-section (Deméré 1994b). They further differ from *Valenictus* and other odobenine walruses such as *Aivukus* Repenning & Tedford, 1977, *Odobenus* Brisson, 1762, and *Pliopedia* Kellogg, 1921 in exhibiting a more prominent pronator teres process (Repenning & Tedford 1977), and having an anteroposteriorly deeper shaft. Furthermore, the similarity of the radii to *D. seftoni* rather than to *D. santacruzensis* or any other dusignathine suggests tentative referral to *D. seftoni*.

The cervical vertebra can be referred to *Dusignathus* due to the similarity with those of SDNHM 905000, a partial skeleton of *D. seftoni* from the San Diego Formation. The atlas (UCMP 219006) exhibits pointed and triangular transverse processes that are laterally (not dorsolaterally) oriented, unlike the atlas of *V. chulavistensis*, the only other odobenid from the San Diego Formation (Deméré 1994b). Neither vertebra is pachyosteosclerotic as in *Valenictus*. Although these vertebrae cannot be compared to the latest Miocene to Early Pliocene odobenine *Pliopedia pacifica* Kellogg, 1921 (only known from a weathered braincase and appendicular elements), *Pliopedia* has not been found in Piacenzian or Gelasian equivalent strata (Repenning & Tedford 1977), and the similarity to *D. seftoni* and clear separation from *Valenictus* suggests tentative referral of these vertebrae to *Dusignathus.*

Remarks

The only postcranial element originally referred to *D. seftoni* was an isolated humerus (Demere 1994b). New cranial and postcranial fossils of this taxon have emerged and are present in SDNHM collections. The radii described here compare best with SDNHM 92134, an isolated undescribed radius of *D. seftoni* from the San Diego Formation. These specimens tentatively extend the geographic range of *D. seftoni* into Northern California, although more diagnostic remains of Pliocene walruses from this region are necessary for further evaluation. Although fossils of odobenine walruses are absent from the San Gregorio section of the Purisima Formation, odobenine specimens are known from the Pliocene part of the Santa Cruz section including partial tusks (Odobeninae indet., UCMP 190024), a partial femur (cf. *Valenictus* sp., SCMNH 21366), and a complete skull (cf. *Valenictus* sp., UCMP 219091) Although fragmentary, these specimens (in concert with those of *Callorhinus* sp., cf. *C. gilmorei*) document a change from the Late Miocene pinniped assemblage from slightly older horizons of the Purisima Formation (e.g., UCMP localities V99875, V99876, V99877, V90042, V6875, lowermost 75 m of the Santa Cruz section of the Purisima Formation, Messinian equivalent) to a Pliocene assemblage similar to that of the San Diego Formation.

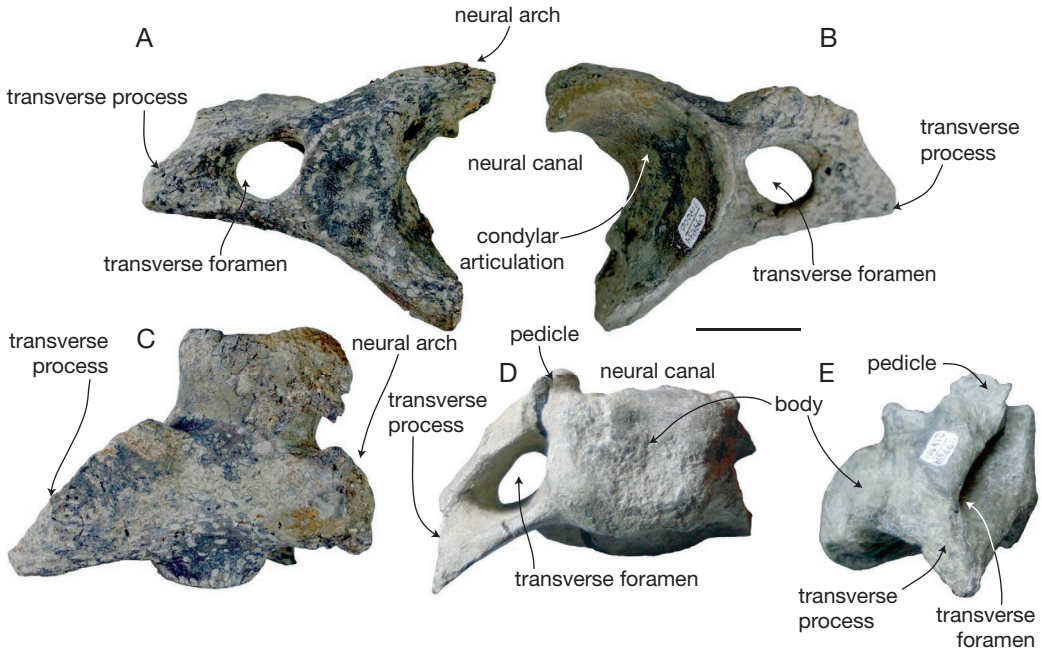

Fig. 5. — Vertebrae of *Dusignathus* sp., cf. *D. seftoni*: **A**, UCMP 219006, fragment of left side of atlas in posterior view; **B**, UCMP 219006 in anterior view; **C**, UCMP 219006 in dorsal view; **D**, UCMP 219001, partial cervical vertebra in anterior view; **E**, UCMP 219001 in lateral view. Scale bar: 3 cm.

Family Otariidae Gill, 1866
Genus indet.

Species indet.

Referred material. — UCMP 86298, right 5th metacarpal; UCMP 13799, partial phalanx, collected by L. Olivera from UCMP locality V7085.

Stratigraphic occurrence. — Middle and upper parts of the San Gregorio section of the Purisima Formation, Early to Late Pliocene (*c.* 5-2.5 Ma, Zanclean-Gelasian equivalent; Fig. 2).

Description

The isolated right fifth metacarpal (UCMP 86298) is well-preserved, small, and short with a robust proximal end (Fig. 6A-D); it measures 39.38 mm in length. The shaft is straight, rectangular, and dorsoventrally flattened. The proximal end is dorsoventrally expanded (17.95 mm dorsoventral depth) and transversely compressed (13.91 mm transverse width) with a proximal ventral tubercle, and a dorsoventrally oriented, arcuate, and transversely convex articular facet. A small concavity is present on the medial and lateral surfaces of the proximal end. The distal surface is nearly flat, and transversely wider than the proximal end (15.33 mm transverse width). The isolated manual or pedal phalanx (UCMP 13799) is damaged and missing the proximal end (Fig. 6E, F). The shaft is dorsoventrally flattened and elongate (42.89 mm in length). The distal end is flattened and rectangular in dorsal view, measures 10.52 mm in transverse width, has a saddle-shaped trochlea, and slight convex tubercles are developed on the medial and lateral sides.

Comparisons and remarks

The metacarpal is referred to Otariidae indet. based on its shortness, gracile proportions, and similarity with extant otariids, and lack of similarity with more robust odobenid metacarpals. The partial phalanx is referred to Otariidae indet. based on its small size and gracile morphology, compared to typical phalanges of odobenids (e.g., Repenning & Tedford 1977: pl. 11). The fifth metacarpal (UCMP 86298) compares well

TABLE 2. — Measurements (in mm) of *Callorhinus* sp., cf. *C. gilmorei* humerus (UCMP 86247). Measurements given to nearest hundredth of a millimeter.

Total length, distal end to greater trochanter	108.52
Total length, distal end to head	106.31
Transverse width across epicondyles	37.38
Narrowest transverse width of shaft	14.37
Anteroposterior width, midshaft	19.23
Greatest anteroposterior diameter, medial lip of trochlea	15.20
Transverse width, distal articular surface	22.03
Greatest anteroposterior diameter, radial capitulum	15.83

TABLE 3. — Measurements (in mm) of *Callorhinus* sp., cf. *C. gilmorei* radii. Measurements given to nearest hundredth of a millimeter.

	UCMP 219138	UCMP 219139
Total width	133.75	111.31
Depth at pronator teres insertion	–	24.98
Greatest width, proximal	30.41	23.84
Least width, proximal	18.49	16.02
Greatest width, distal	44.11	32.42

with specimens of extant *Callorhinus ursinus* Linnaeus, 1758, and shares the extremely short length of the shaft, relatively small size, and small ventral tubercle on the shaft (Fig. 6A-D). UCMP 86298 is smaller and less robust than fifth metacarpals of *Zalophus* Gill, 1866 and *Eumetopias* Gill, 1866; it differs from *Zalophus* in lacking an extremely globose proximal end, and it differs from *Eumetopias* in having a proportionally shorter shaft. These specimens may represent *Callorhinus* sp., cf. *C. gilmorei*, but since these specimens only exhibit features typical of the family Otariidae, there is insufficient evidence for a referral.

Genus *Callorhinus* Gray, 1859

Callorhinus sp., cf. ***C. gilmorei*** Berta & Deméré, 1986

Thalassoleon sp. – Boessenecker 2006: 43A.

REFERRED MATERIAL. — UCMP 219003, anterior fragment of lower canine; UCMP 219147, upper third incisor; UCMP 86297, partial left humerus; UCMP 219139 and 219138, two right radii; UCMP 219122, right calcaneum; and UCMP 219149, right astragalus. Collected by R.W. Boessenecker and L. Olivera from UCMP localities V7085, V99833, V99838, V99839, and V99859.

STRATIGRAPHIC OCCURRENCE. — Middle and upper parts of the San Gregorio section of the Purisima Formation, Early to Late Pliocene (*c.* 5-2.5 Ma, Zanclean-Gelasian equivalent; Fig. 2).

DESCRIPTION

The right upper third incisor (UCMP 219147) is small (14.55 mm crown length), caniniform, strongly recurved, and bears well-developed posterior and anterior cristae (Fig. 7A-D). The crown measures 6.05 mm in transverse width, and 8.66 mm anteroposterior width. A posteriorly curving longitudinal crista occurs on the lingual side of the tooth, and is posterobasally convergent with a slight posterolingual cingulum. Faint longitudinal wrinkles occur in the enamel. The crown and root of UCMP 219147 both have an oval cross section. The root is slightly damaged, and a thin layer of the outer surface of the root is missing; this is interpreted to be taphonomic, and this preservation is also seen in shark, pinniped, and cetacean teeth from other localities in the Purisima Formation.

A fragment (UCMP 219003) of the anterior portion of a canine represents a lower canine because of its curvature (Fig. 7E, F); upper canines of early diverging otariids (*Callorhinus*, *Thalassoleon*) are relatively straight, while lower canines are more posteriorly curved. The crown is conical, posteriorly curved, and exhibits longitudinally wrinkled enamel and an open pulp cavity is exposed on the broken surface.

The partial left humerus (UCMP 86297) is relatively small (108.52 mm total length; Table 2), slender, has a hemispherical humeral head, and is missing most of the deltopectoral crest and the lesser and greater trochanters (Fig. 7G-J). The preserved portion of the deltopectoral crest (partially reconstructed) is transversely thin. A triangular, knob-like medial entepicondyle is positioned along the distomedial margin. The lateral entepicondyle is anteroposteriorly thin and bladelike with an arcuate margin in anterior aspect. The trochlea is saddle-shaped and concave posteriorly and distally. The radial capitulum is convex, and exhibits the same

anteroposterior diameter as the medial lip of the trochlea. A shallow olecranon fossa is present on the posterior side, proximal to the trochlea.

The two right radii (UCMP 219139 and 219138) are relatively small (111.31 and 133.75 mm total length, respectively; Table 3) and slender and missing the distal epiphyses (Fig. 8), indicating young ontogenetic age. UCMP 219138 is slightly larger than UCMP 219139 and is damaged anteriorly. The proximal surface of the radial head is oval in proximal aspect, slightly concave, and the articular surface has a "stepped" morphology so that the lateral surface is less proximally elevated. The radial tuberosity is positioned distal to the head on the medial surface, forming a raised, rugose, and circular plateau. The shaft of both specimens is transversely thin and flattened. The shaft widens anteroposteriorly toward the pronator teres process, which is preserved in UCMP 219139. When accounting for the missing distal epiphysis, the pronator teres process is positioned about ⅓ of the element's length from the proximal end. The medial surface is gently concave, and the lateral surfaces are slightly convex and smooth. The shaft is widest distally.

The right astragalus (UCMP 219149) is small (34.62 mm total length; Table 4) and slightly damaged on the plantar side (Fig. 9D, E). The dorsal tibial articulation is divided into two gently convex ridges on the trochlear surface, separated by a shallow median furrow. The head of the astragalus has an anteriorly convex articular facet for the navicular (Fig. 9D); the neck is slightly constricted relative to the head. The sustentacular facet is small, smooth, and slightly convex, and located on the plantar side of the neck. The sustentacular facet is bordered anteriorly and laterally by a shallow groove. The astragalar sulcus is transversely oriented and separates the sustentacular facet from the calcaneo-astragalar facet. The calcaneo-astragalar facet is oval-shaped and concave. The posterior margin of the astragalus is convex, and slight indentations occur at the posterior ends of the lateral and medial processes. The lateral process is a small, laterally projecting knob, and the medial process is a small rectangular knob on the posteromedial surface.

The well-preserved right calcaneum (UCMP 219122) is small (59.34 mm total length; Table 4) and roughly rectangular, with a robust calcaneal process (Fig. 9A-C). The proximal surface of the calcaneal process is smooth and gently convex, with

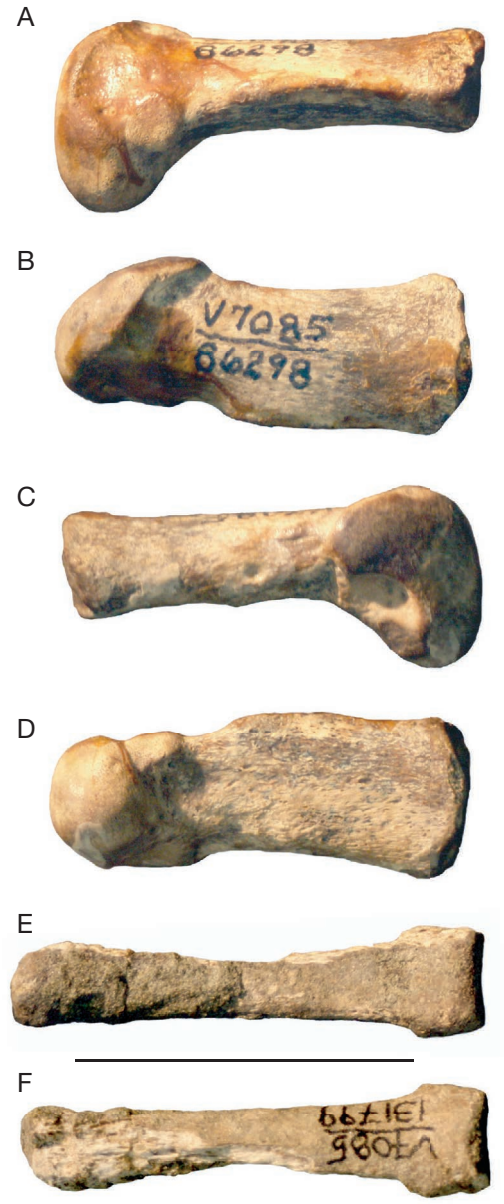

Fig. 6. — Metacarpal and phalanx of Otariidae gen. et sp. indet.: **A**, UCMP 86298, fifth right metacarpal in lateral view; **B**, UCMP 86298 in dorsal view; **C**, UCMP 86298 in medial view; **D**, UCMP 86298 in plantar view; **E**, UCMP 131799, manual or pedal phalanx in dorsal view; **F**, UCMP 131799 in plantar view. Scale bar: 3 cm.

TABLE 4. — Measurements (in mm) of *Callorhinus* sp., cf. *C. gilmorei* tarsal elements; *, denotes incomplete measurement due to breakage. Measurements given to nearest hundredth of a millimeter.

	Astragalus UCMP 219149	Calcaneum UCMP 219122
Total length	34.62	59.34
Transverse width, calcaneal tuber	–	26.89
Transverse width, proximal	–	31.00*
Dorsoventral depth, calcaneal tuber	–	19.94
Dorsoventral depth at cuboid facet	–	20.80
Transverse width at navicular facet	21.20	–
Dorsoventral depth at navicular facet	11.29	–
Transverse width of trochlea	15.94	–
Angle between neck and trochlea	33°	–

a shallow vertical groove for the gastrocnemius and soleus tendons. The medial calcaneal tubercle is small and situated on the medial surface of the calcaneal process. The calcaneal process is cylindrical and proximally rugose. The calcaneoastragalar facet is oriented posteromedially and is lunate in shape, dorsally convex, and slopes anteromedially. The lateral calcaneal tubercle is a slight ridge. The medial margin of the calcaneal process is concave, while the sustentacular facet is dorsally concave and projects medially as a triangular process. The peroneal tubercle is abraded away. The secondary shelf of the sustentaculum is developed as a narrow groove along the anteromedial margin of the sustentacular facet, and widens anteriorly. A slight groove occurs between the calcaneo-astragalar facet and the sustentacular facet, and a slight fossa lies lateral to the sustentacular facet. The cuboid facet occupies the slightly concave and oval shaped anterior surface of the calcaneum.

COMPARISONS

Specimens referred to *Callorhinus* sp., cf. *C. gilmorei* all exhibit otariid characteristics and small size, and constitute all otariid specimens from the San Gregorio section of the Purisima Formation, and are considered to represent a single otariid taxon. Some of these elements (incisor, radius, astragalus, calcaneum) exhibit features diagnostic of *Callorhinus gilmorei* Berta & Deméré, 1986 from the San Diego Formation (including new material within SDNHM collections), but several elements (canine, humerus) only possess features characteristic of the family. Although potentially belonging to a separate otariid taxon, they are tentatively included in the same taxon based on their small size and similarity with *C. gilmorei* material from the San Diego Formation. Furthermore, *C. gilmorei* is the only otariid present in the California Pliocene (Miyazaki *et al.* 1995; Boessenecker 2011c), with the exception of *Thalassoleon macnallyae* from the latest Miocene and earliest Pliocene of the Purisima Formation (Point Reyes and Santa Cruz sections), and cf. *Thalassoleon* from the earliest Pliocene Salada and San Mateo Formations (Barnes 1998; Deméré *et al.* 2003), to which these specimens cannot be referred. *T. macnallyae* is the only other otariid known from the Purisima Formation, and along with other specimens of *Thalassoleon*, consistently exhibit more plesiomorphic characteristics than these new specimens, in addition to larger overall size (approximately 150-200% larger). Additional diagnostic material is necessary to refine this preliminary identification.

The upper third incisor is relatively small and close in its morphology to *C. gilmorei* and *Callorhinus ursinus*. It differs from *Arctocephalus pusillus* Schreber, 1775, *Eumetopias jubatus* Schreber, 1775, *Hydrarctos lomasiensis* Muizon, 1978, *Neophoca* Gill, 1866, *Otaria* Peron, 1816, *Phocarctos* Peters, 1866, *Proterozetes ulysses* Barnes, Ray & Koretsly, 2006, *Thalassoleon mexicanus* Repenning & Tedford, 1977, and *Zalophus*, in having a small, gracile crown with an oval cross-section (Fig. 7D; Repenning *et al.* 1971). An isolated upper third incisor (UCMP 219433) referable to *T. macnallyae* from locality V-6875 in the Purisima Formation is similar in size and cross-section, but differs from this specimen in possessing a lingual bulge at the base of the crown.

The humerus (UCMP 86297) exhibits typical otariid characteristics including a relatively straight shaft in lateral/medial aspect (as opposed to sinuous

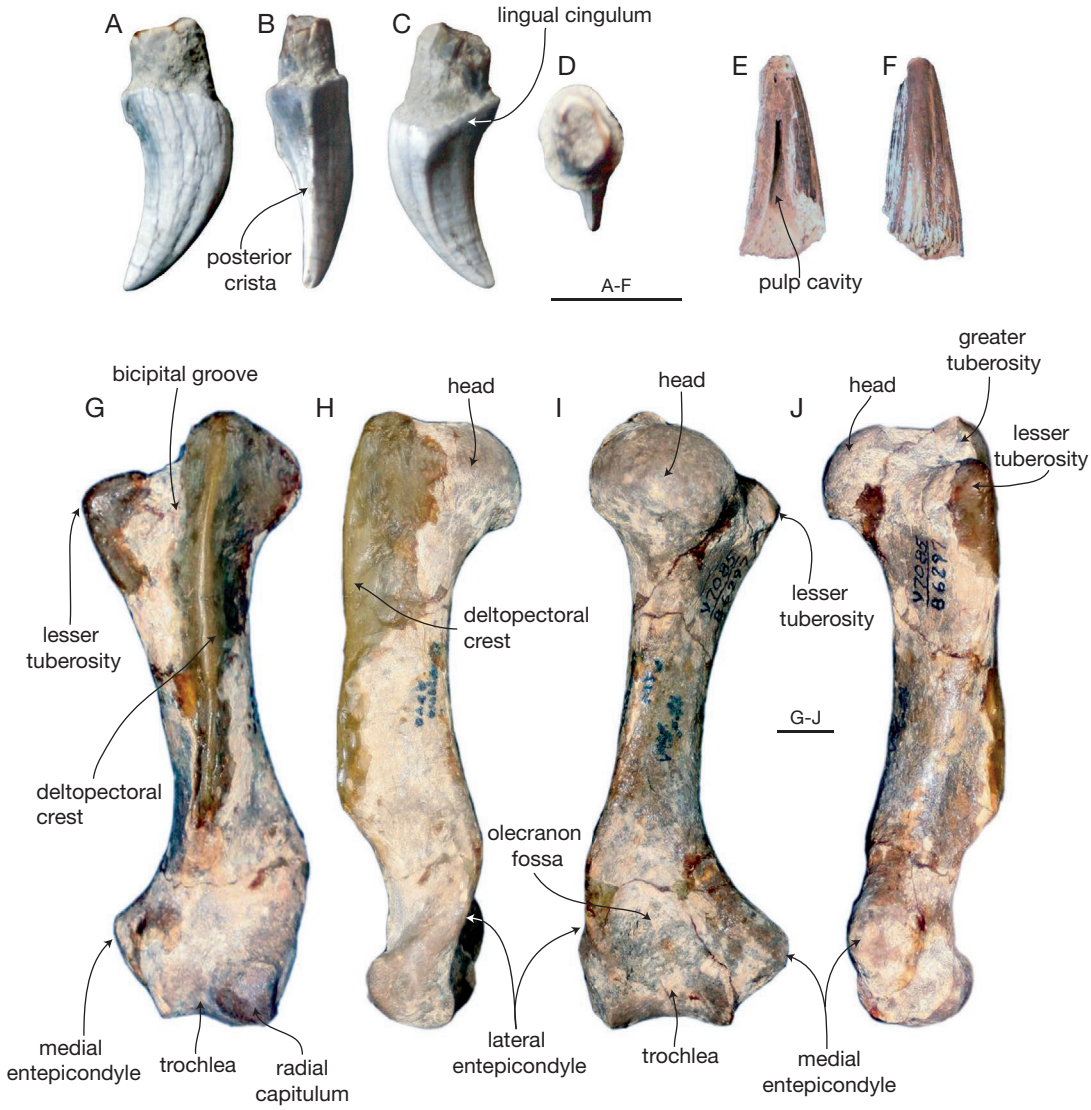

FIG. 7. — Skeletal elements of *Callorhinus* sp., cf. *C. gilmorei*: **A**, UCMP 219147, right upper third incisor, in lateral view; **B**, UCMP 219147 in lingual view; **C**, UCMP 219147 in mesial view; **D**, UCMP 219147 in basal view; **E**, UCMP 219003, fragment of lower canine in lingual view; **F**, UCMP 219003 in labial view; **G**, UCMP 86297, partial left humerus in anterior view (deltopectoral crest partially reconstructed); **H**, UCMP 86297 in lateral view; **I**, UCMP 86297 in posterior view; **J**, UCMP 86297 in medial view. Scale bars: 1 cm.

as in phocids), the medial lip of the distal trochlea having the same diameter as the radial capitulum (the medial lip is of a greater diameter in odobenids; Deméré 1994a), and a small, triangular medial entepicondyle (which is knob-like in most Late Neogene odobenids). Despite its small size, it has fully fused proximal and distal epiphyses, indicating it is an adult; it is here interpreted as an adult female. UCMP 86297 compares well with modern *Callorhinus* and *Arctophoca* Gill, 1866 humeri, as well as *C. gilmorei* humeri from the San Diego Formation (SDNHM 25398 and 38296). This specimen

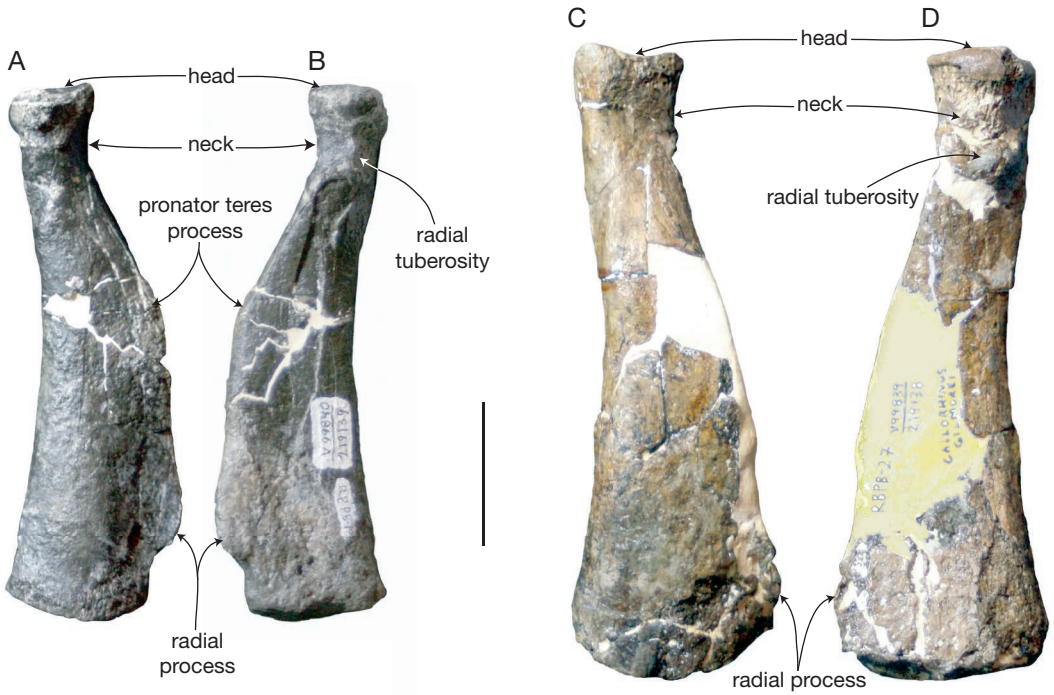

FIG. 8. — Radii of *Callorhinus* sp., cf. *C. gilmorei*: **A**, UCMP 219139, right radius in lateral view; **B**, UCMP 219139 in medial view; **C**, UCMP 219138, partial right radius in lateral view; D, UCMP 219138 in medial view. Scale bar: 3 cm.

exhibits fully fused epiphyses, while similarly sized humeri of *T. mexicanus* and *T. macnallyae* remain unfused, and adult humeri of *Thalassoleon* spp. are substantially larger than those of adult *C. ursinus* and *C. gilmorei* (SDNHM 38296). The small adult size of this humerus indicates referral to *C. gilmorei*.

The radii (UCMP 219138 and 219139) exhibit several otariid features, including a relatively straight and transversely compressed shaft, exhibiting a radial process that does not extend further distally than the distal scapholunar articulation facet, and having a pronator teres process that is positioned relatively far proximally (Fig. 8). These specimens are too small to represent an odobenid, and also lack the well developed bony ridges and processes on the distal end associated with extensor tendons, which typify odobenid radii. Ridges on the lateral side of the radius are also typical for many extant otariids as well as *T. mexicanus* (Repenning & Tedford 1977; Deméré & Berta 2005). UCMP 219138 and 219139 differ from *T. mexicanus*, *T. macnallyae*, and *Eumetopias* in having a more proximally placed pronator teres process, and their much smaller size. Extant *Callorhinus* and *Arctophoca* exhibit pronator teres processes that are more proximally positioned than in UCMP 219138; the pronator teres process is positioned similarly in *Zalophus*. These specimens compare best with fossil radii of *C. gilmorei* (i.e. SDNHM 25549, 35268) in their size and the proximal position of the pronator teres process.

The astragalus is relatively small (Fig. 9D, E), and too small to represent an odobenid or a sea lion (Otariinae), but approximately the same size and nearly identical to extant *Callorhinus*. This specimen differs from the otariine *Eumetopias* in its smaller size, having a relatively larger calcaneo-astragalar facet, a more circular sustentacular facet, a transversely narrower head, a smaller medial process, and tibial trochleae that are more medially rotated. This specimen differs from *Zalophus* in its slightly smaller size, a smaller and more convex navicular facet, lacking a medial spur off the head, more

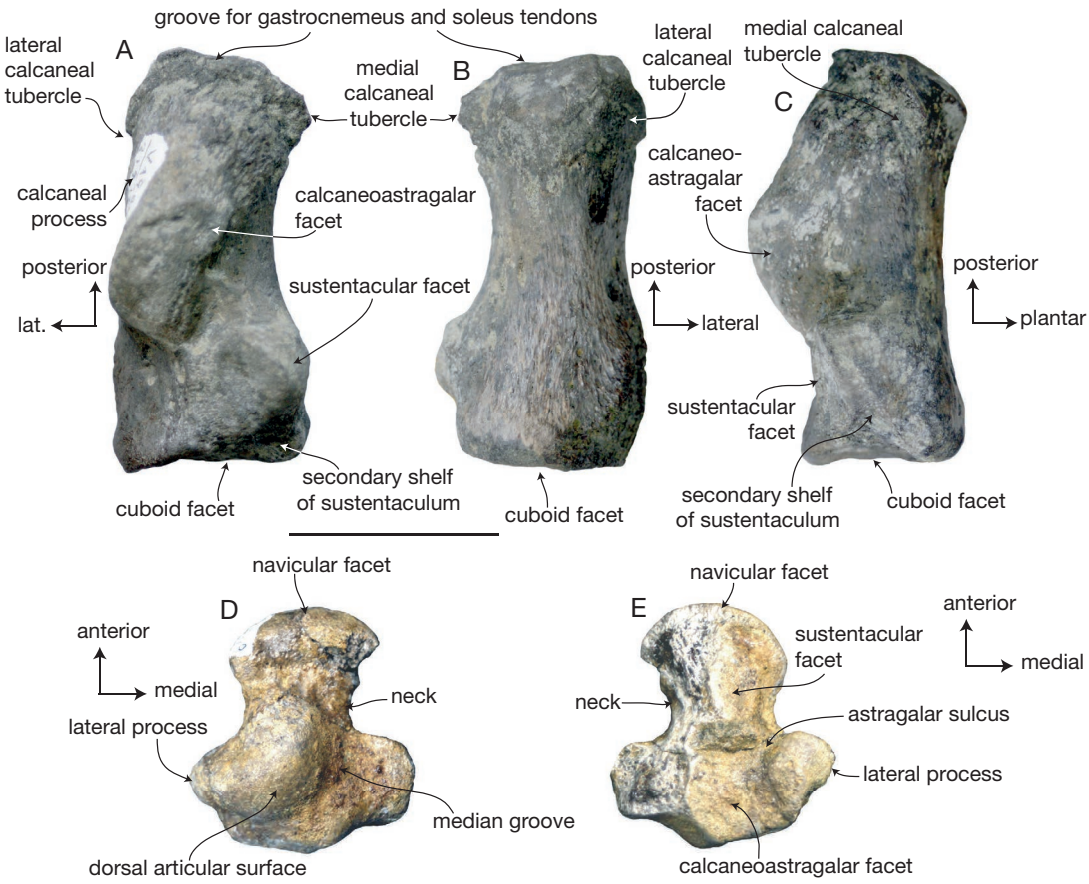

FIG. 9. — Tarsal elements of *Callorhinus* sp., cf. *C. gilmorei*: **A**, UCMP 219122, right calcaneum in dorsal view; **B**, UCMP 219122 in plantar view; **C**, UCMP 219122 in medial view; **D**, UCMP 219149, left astragalus in dorsal view; **E**, UCMP 219149 in plantar view. Scale bar: 3 cm.

equally sized medial and lateral processes, and a larger calcaneo-astragalar facet. UCMP 219149 differs from *T. mexicanus* in having a narrower neck, smaller head, and in lacking a distinct anterior extension of the dorsal articular surface onto the neck of the astragalus. It compares relatively well with UCMP 219482, a recently collected disarticulated hindlimb of *T. macnallyae* from the Purisima Formation near Santa Cruz, but differs in having a wider neck, narrower astragalar sulcus, larger lateral and medial processes; it also differs from UCMP 219482 in lacking an anterior extension of the dorsal articular surface. The lack of an anterior extension of the dorsal articular surface precludes UCMP 21949 from referral to *Thalassoleon*; an isolated astragalus of *C. gilmorei* (SDNHM 25570) from the San Diego Formation is similarly small, lacks an anterior extension of the dorsal articular surface, and does not appreciably differ from the Purisima specimen. The preclusion of referral to *Thalassoleon* or any extant otariid, small size, and similarity with *C. gilmorei* and *C. ursinus* suggest referral to the former.

The calcaneum differs from odobenids in its tiny size and lack of a medial tuber of the calcaneal process, while it differs from phocid calcanea in being transversely broader and having large cuboid and calcaneo-astragalar facets (Fig. 9A, B). UCMP

219122 differs from *T. mexicanus* in having a slight sustentacular shelf (Fig. 9A; completely lacking in *Thalassoleon* spp., and present in all extant otariids; Robinette & Stains 1970; Deméré & Berta 2005), and a shorter calcaneo-astragalar facet. *Eumetopias* is much larger, exhibits a wider secondary sustentacular shelf, a narrower neck, and a smaller cuboid facet than UCMP 219122 (Robinette & Stains 1970). *Zalophus* has a slightly wider secondary sustentacular shelf, a longer calcaneo-astragalar facet, and a more robust calcaneal process than the fossil (Robinette & Stains 1970). *Otaria* differs from UCMP 219122 in having a bilobate calcaneo-astragalar facet, a narrower secondary sustentacular facet, and a broader neck (Robinette & Stains 1970). *Arctophoca* and *Arctocephalus* have similar proportions to UCMP 219122, but have a smaller cuboid facet, and like all other extant otariids, have a wider secondary sustentacular facet (Robinette & Stains 1970). This specimen differs from *C. ursinus* in having a more robust calcaneal process, a smaller secondary sustentacular shelf, and a shorter calcaneo-astragalar facet that does not extend as far proximally. UCMP 219122 shares with an isolated calcaneum of *C. gilmorei* from the San Diego Formation (SDNHM 65334) a secondary sustentacular shelf that is narrow, posteriorly tapering, and groove-like, to the exclusion of other fossil otariids.

Remarks

These isolated bones and teeth consistently exhibit features that are more derived than the fossil otariids *T. mexicanus* and *T. macnallyae*, but are slightly plesiomorphic relative to extant otariids. Several features preclude referral to *Thalassoleon*, including the morphology of the radius, astragalus, and calcaneum. Additionally, all specimens are nearly identical in size and morphology to corresponding elements of *C. gilmorei* (from the San Diego Formation) and nearly identical in morphology to the extant *C. ursinus* (which is somewhat larger than the Purisima Formation fossils), suggesting identification as the former. In summary, these specimens possess features – among fossil otariids from the eastern North Pacific – which are known only in *C. gilmorei*. However, some specimens preserve features characteristic of the family only, and this collection of isolated elements is only tentatively identified as this taxon. *Callorhinus gilmorei* was originally described from the Pliocene San Diego Formation of southern California and Baja California (Berta & Deméré 1986), and has also been reported from the Upper Pliocene Rio Dell Formation of Northern California (Boessenecker 2011c), and the Upper Pliocene of Japan (Kohno & Yanagisawa 1997). These tentatively identified specimens of *C. gilmorei* now record this fur seal from the Pliocene of central California as hypothesized by Boessenecker (2011c), suggesting that it inhabited most of the California coastline during the Pliocene in addition to Southern California and Baja California (Berta & Deméré 1986) and Northern California (Boessenecker 2011c), and document the presence of at least two pinnipeds in the San Gregorio assemblage.

Order CETACEA Brisson, 1762
Suborder MYSTICETI Flower, 1864
Family Balaenidae Gray, 1821

cf. *Eubalaena* sp. 1

Referred material. — UCMP 219100, a small partial right tympanic bulla; and UCMP 219481, a small partial right tympanic bulla. Collected by R.W. Boessenecker from UCMP locality V99851.

Stratigraphic occurrence. — Lowermost part of the San Gregorio section of the Purisima Formation, latest Miocene (6.4-5.6 Ma, Messinian equivalent; Fig. 2).

Description

Except where noted, this description is based primarily on UCMP 219100. This tympanic bulla has a large involucrum with a greatly expanded medial surface which is anteriorly truncated (Fig. 10A-C). Several elongate, deep, and anterolaterally directed transverse creases occur on the involucrum. Posteriorly, the involucrum is much deeper dorsoventrally. A deep sulcus runs adjacent to the involucral ridge; the involucral ridge is slightly retracted from the ventral margin, and diverges posteriorly from the main ridge. The ventral surface is relatively smooth and convex and lacks a keel-like main ridge. Laterally adjacent to the main ridge there is an indistinct

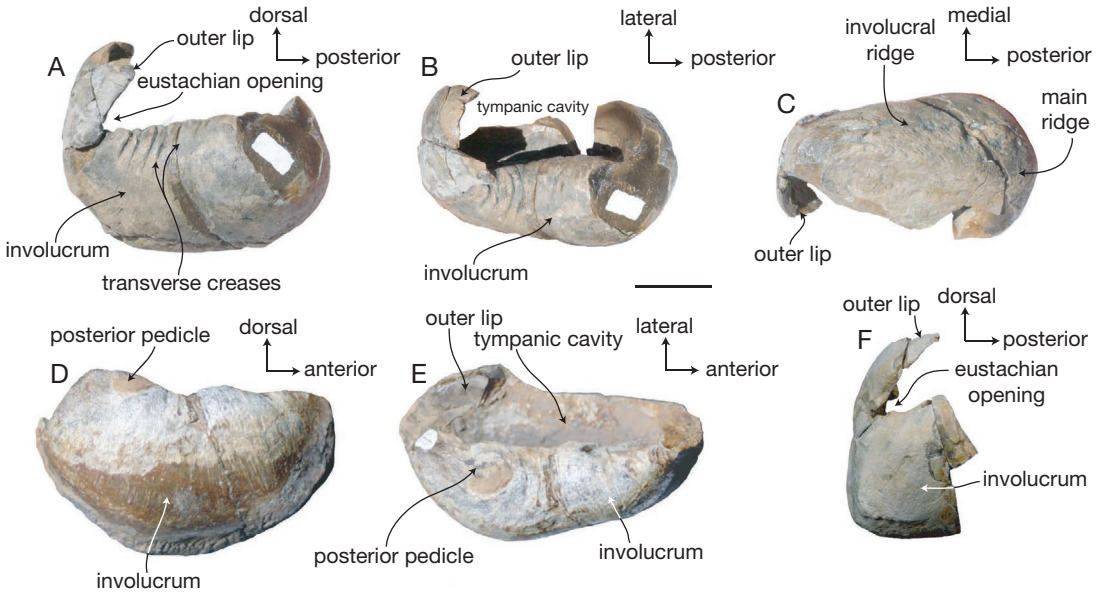

Fig. 10. — Tympanic bullae of balaenid mysticetes: **A**, UCMP 219100, partial right tympanic bulla of cf. *Eubalaena* sp. 1 in medial view; **B**, UCMP 219100 in dorsal view; **C**, UCMP 219100 in ventral view; **D**, UCMP 219099, partial left tympanic bulla of cf. *Eubalaena* sp. 2 in medial view; **E**, UCMP 219099 in dorsal view; **F**, UCMP 219481, fragment of right tympanic bulla of cf. *Eubalaena* sp. 1 in medial view. Scale bar: 3 cm.

longitudinal furrow. The posteromedial portion of the bulla is rather robust and inflated in medial aspect. A fragment of the anterior portion of the outer lip is present, and it is broadly convex in anterior view. This results in a eustachian opening that is narrow; anteriorly this margin is slit-like and has an angle of *c.* 45° (between the involucrum and outer lip). UCMP 219481 also exhibits a narrow eustachian opening, although it has an anteroventral corner of the eustachian opening that is more acutely defined and not broadly curved as in UCMP 219100 (Fig. 10F).

Remarks and comparisons

These tympanic bullae share many features with extant *Eubalaena* Gray, 1864, including an elevated anterior lobe and a narrow eustachian opening (Ekdale *et al.* 2011). Nevertheless, the involucral and main ridges are posteriorly divergent, whereas in extant *Eubalaena* they are parallel. They differ from balaenopterids in having a convex dorsal margin of the involucrum in medial and lateral aspect; balaenopterid bullae generally differ from those of extant balaenids in having a relatively straight medial margin of the involucrum that is not broadly arched in dorsal view (Oishi & Hasegawa 1995b; Ekdale *et al.* 2011). These bullae differ from *Balaena* Linnaeus, 1758 in being relatively transversely broader; bullae of extant *Balaena* are transversely flattened relative to those of *Eubalaena* (Ekdale *et al.* 2011). The tympanic bulla of *Caperea* Gray, 1864 is similar in size, but transversely narrower than UCMP 219100; it exhibits a posteroventrally expanded involucrum and a rectangular eustachian opening, unlike UCMP 219100 and 219481 (Ekdale *et al.* 2011). UCMP 219100 differs from *Balaenella* Bisconti, 2005 in having a rounded anteroventral margin that is not shaped into a corner (Bisconti 2005), although this is seen in UCMP 219481 and *Eubalaena*. UCMP 219100 and 219481 differ from the tympanic bulla of *B. balaenopsis* Van Beneden, 1872 in exhibiting a narrow, triangular eustachian opening; UCMP 219100 further differs in exhibiting a more transversely inflated bulla, and UCMP 219481 differs in exhibiting a corner-like anteroventral margin. The tympanic bulla of *Bal-*

TABLE 5. — Measurements (in cm) of mysticete tympanic bullae. Abbreviations: **e**, denotes estimated measurement, in this case due to adhering matrix. Measurements given to nearest hundredth of a millimeter.

Specimens	Taxon	Length of bulla	Width of involucrum	Greatest depth of bulla
UCMP 219100	cf. *Eubalaena* sp. 1	94.97	54.94	54.37
UCMP 219099	cf. *Eubalaena* sp. 2	109.49	60 (e)	63.45
UCMP 219478	Balaenopteridae indet. morphotype 1	97.7	46.1	51.7
UCMP 219097	Balaenopteridae indet. morphotype 1	88.64	33.30	41.46
UCMP 219098	Balaenopteridae indet. morphotype 2	81.49	39.88	40.99
UCMP 219107	Balaenopteridae indet. morphotype 2	80.29	35.37	40.70
UCMP 219117	*Herpetocetus* sp.	58.64	27.51	34.57

aenula astensis Trevisan, 1942 is more transversely compressed than UCMP 219100, and exhibits a eustachian opening that is less acutely triangular and slit-like than UCMP 219100 and 219481, although it is somewhat narrower than the broadly rounded eustachian opening in *B. balaenopsis*. A balaenid tympanic bulla (UCMP 29852; identified as *Balaenula* sp. by Barnes 1977) from the Purisima Formation at Point Reyes (Early Pliocene) is similar in size, but appears to be transversely thinner and exhibits a flatter medial surface of the involucrum relative to UCMP 219100 and 219481. Although they are relatively small (Table 5), these specimens share enough features with *Eubalaena* to be tentatively identified to this genus.

cf. *Eubalaena* sp. 2

REFERRED MATERIAL. — UCMP 219099, a partial left tympanic bulla collected by R.W. Boessenecker from UCMP locality V99846.

STRATIGRAPHIC OCCURRENCE. — Uppermost part of the San Gregorio section of the Purisima Formation, Early to Late Pliocene (3.35-2.5 Ma, Piacenzian-Gelasian equivalent; Fig. 2).

DESCRIPTION

This larger tympanic bulla is missing most of its outer lip, and is similar in most regards to the above described specimens of cf. *Eubalaena* sp. 1. It differs from UCMP 219100 in its larger size and several other features; the description of this specimen follows that for cf. *Eubalaena* sp. 1 except for the differences outlined below. This specimen further differs from UCMP 219100 by having a much more medially convex involucrum in ventral aspect (Fig. 10D, E). Furthermore, it has a well-defined concave longitudinal furrow laterally adjacent to the main ridge. The main ridge also forms a well-developed ventral keel, and unlike UCMP 219100, the main and involucral ridges are parallel.

REMARKS AND COMPARISONS

The great dorsoventral depth and massive medial face of the involucrum identify this specimen as a balaenid (Oishi & Hasegawa 1995b; Ekdale *et al.* 2011). It differs from *Balaena* in being transversely thicker, and shares similar large size and transverse thickness with extant *Eubalaena*, although it is incomplete (Table 5; Ekdale *et al.* 2011). The much larger size and younger (Early-Late Pliocene) age of the specimen suggest it is not conspecific with UCMP 219100. Several tympanic bullae of this same size and morphology are known from the Santa Cruz section of the Purisima Formation (UCMP 29852, 167800, SCMNH 9990.07, 21654, 21658; latest Miocene-Early Pliocene, Messinian-Zanclean equivalent, 6.9-4.5 Ma).

Family BALAENOPTERIDAE Gray, 1864
Genus *Balaenoptera* Lacépède, 1804

Balaenoptera bertae n. sp.
(Figs 11-15)

HOLOTYPE. — UCMP 219078, a partial skull lacking the premaxillae, maxillae, nasals, jugals, tympanic bullae, and bodies of the petrosal, excavated by R. W. Boessenecker,

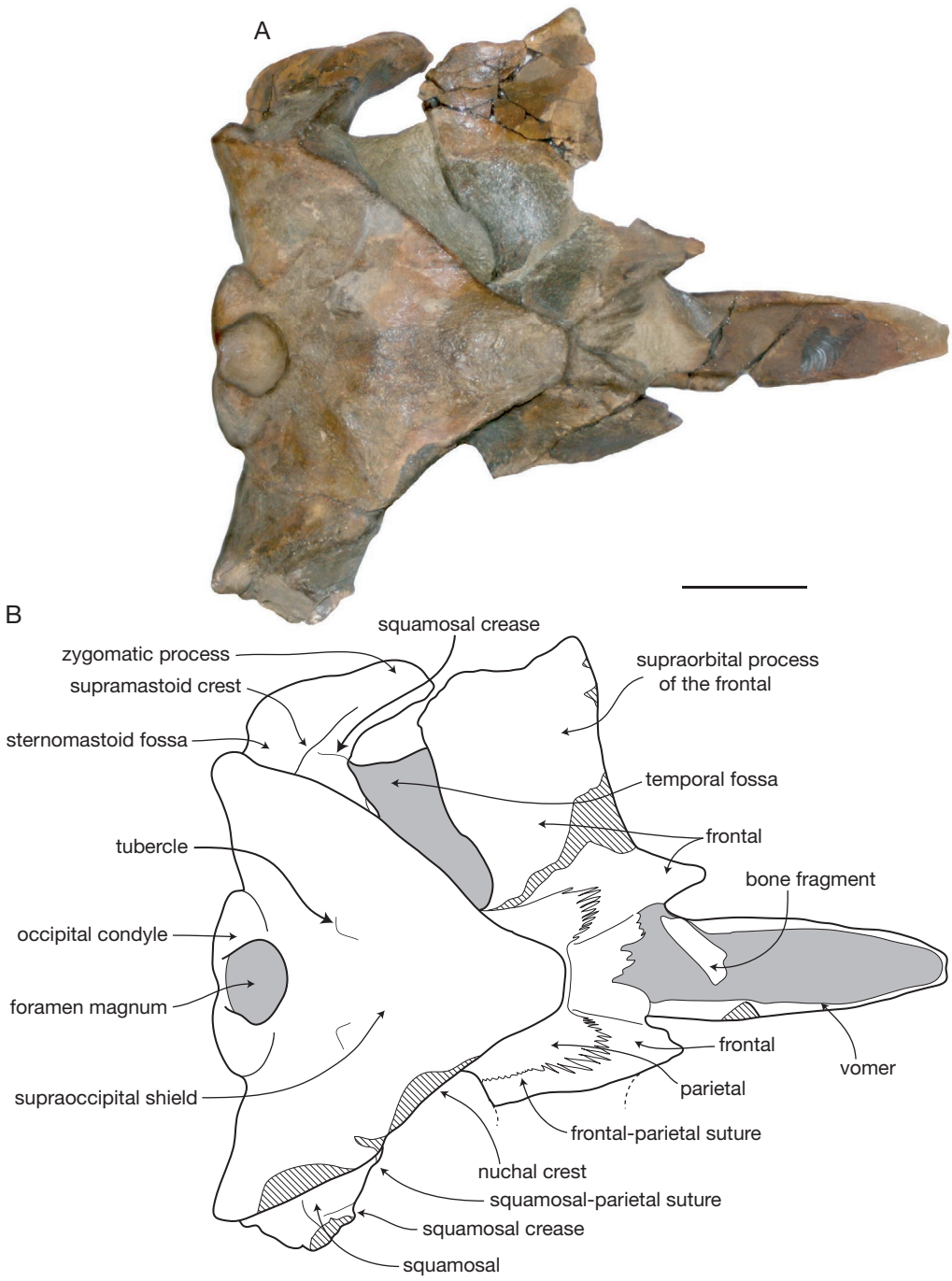

FIG. 11. — Holotype cranium of *Balaenoptera bertae* n. sp., UCMP 21907, in dorsal view: **A**, photograph; **B**, interpretive line drawing. Cross hatching denotes broken or missing bone, and gray denotes adhering matrix. Scale bar: 10 cm.

E. Johnson, T. Palladino, and M. Berrini from UCMP locality V99849 from August 12-15, 2005.

TENTATIVELY REFERRED SPECIMENS. — UCMP 131815, a partial juvenile cranium including the vertex, supraorbital processes of the frontals, palatines, and tips of the zygomatic processes collected in 1985 by a UCMP party from UCMP locality V85027; UCMP uncataloged, an isolated squamosal from UCMP locality V99868.

ETYMOLOGY. — Honouring Dr Annalisa Berta (San Diego State University), for her many contributions to the study of fossil cetaceans and pinnipeds.

DIAGNOSIS. — *Balaenoptera bertae* n. sp. is a small balaenopterid (estimated bizygomatic width of 61.4 cm), smaller in size than extant *Balaenoptera acutorostrata* Lacépède, 1804, characterized by: broadly triangular occipital shield that laterally overhangs the temporal fossa and exhibits a flattened apex, large occipital condyles, little to no parietal exposed dorsally at the transversely narrow vertex, squamosal with short, anteriorly directed zygomatic process, posteriorly elongate postglenoid process, prominent squamosal crease, frontal with rectangular supraorbital process with transversely oriented anterior margin, frontal that is abruptly depressed below the vertex and obliquely oriented so that this surface and anterior wing of parietal are visible in dorsal aspect, large petrosal fossa (*sensu* Mead & Fordyce 2009), and a posterior process of the petrotympanic that is relatively short and inflated.

STRATIGRAPHIC OCCURRENCE. — Uppermost part of the San Gregorio section of the Purisima Formation (*sensu* Powell *et al.* 2007) that is bracketed below by an ash bed correlated with the 3.3-3.4 Ma Putah Tuff (Powell *et al.* 2007) and above by another ash bed correlated with the 2.5 ± 0.2 Ma Ishi Tuff. This indicates an age of 3.35-2.5 Ma, or Early to Late Pliocene (Piacenzian-Gelasian equivalent).

TYPE LOCALITY. — UCMP locality V99849, Pliocene Purisima Formation. Detailed locality information available on request from UCMP or the author.

DIFFERENTIAL DIAGNOSIS

Balaenoptera bertae n. sp. is a member of the extant genus *Balaenoptera* and shares with all extant species of *Balaenoptera* a squamosal crease, relatively short and anteriorly oriented zygomatic processes, a bulge at the squamosal-parietal suture in the posterior temporal fossa, and a truncated apex of the occipital shield.

Balaenoptera bertae n. sp. differs from:

– *Archaebalaenoptera castriarquati* Bisconti, 2007, in having a broader occipital shield with a laterally sinuous margin that overhangs the temporal fossa and an anteriorly truncated apex, a transversely thinner vertex measuring only 10% of bizygomatic width (compared to 24% bizygomatic width in *A. castriarquati*), short and blunt anteriorly directed zygomatic process that lack supramastoid crest that extends to the zygomatic apex, and having an anteroposteriorly shorter supraorbital process of the frontal;

– "*Balaenoptera*" *cortesi* "var." *portisi*, in having a squamosal crease, shorter and more anteriorly oriented zygomatic process that lacks a supramastoid crest that extends to the anteroventrally oriented zygomatic apex, transversely wide postglenoid process, an anteroposteriorly short supraorbital process with a transversely oriented anterior margin and laterally prominent antorbital process, a shallow sternomastoid fossa, and a large petrosal fossa;

– "*Balaenoptera*" *ryani* Hanna & McLellan, 1924, in having a posteriorly broad occipital shield, little to no parietal exposed at the vertex, and an anteriorly truncated occipital shield;

– *Balaenoptera acutorostrata*, in its smaller size, apex of the occipital shield narrow and only 10% of bizygomatic width (25% bizygomatic width in *B. acutorostrata*), lacking a lateral triangular extension of the parietal between the squamosal and nuchal crest, exhibiting a ventrolaterally sloping (rather than vertical) surface of the parietal and frontal lateral to the supraorbital process of the frontal, transversely oriented anterior margin of the supraorbital process of the frontal in dorsal aspect (as opposed to being posterolaterally oriented), and a blunt distal apex of the inflated compound posterior process of the petrotympanic;

– *Balaenoptera bonaerensis* Burmeister, 1867, in its smaller size, apex of the occipital shield narrow and only 10% of bizygomatic width (22% bizygomatic width in *B. bonaerensis*), exhibiting a ventrolaterally sloping (rather than vertical) surface of the parietal and frontal lateral to the supraorbital process of the frontal, and transversely oriented anterior margin of the supraorbital process of the frontal in dorsal aspect (as opposed to being posterolaterally oriented), and a blunt distal apex of the inflated compound posterior process of the petrotympanic;

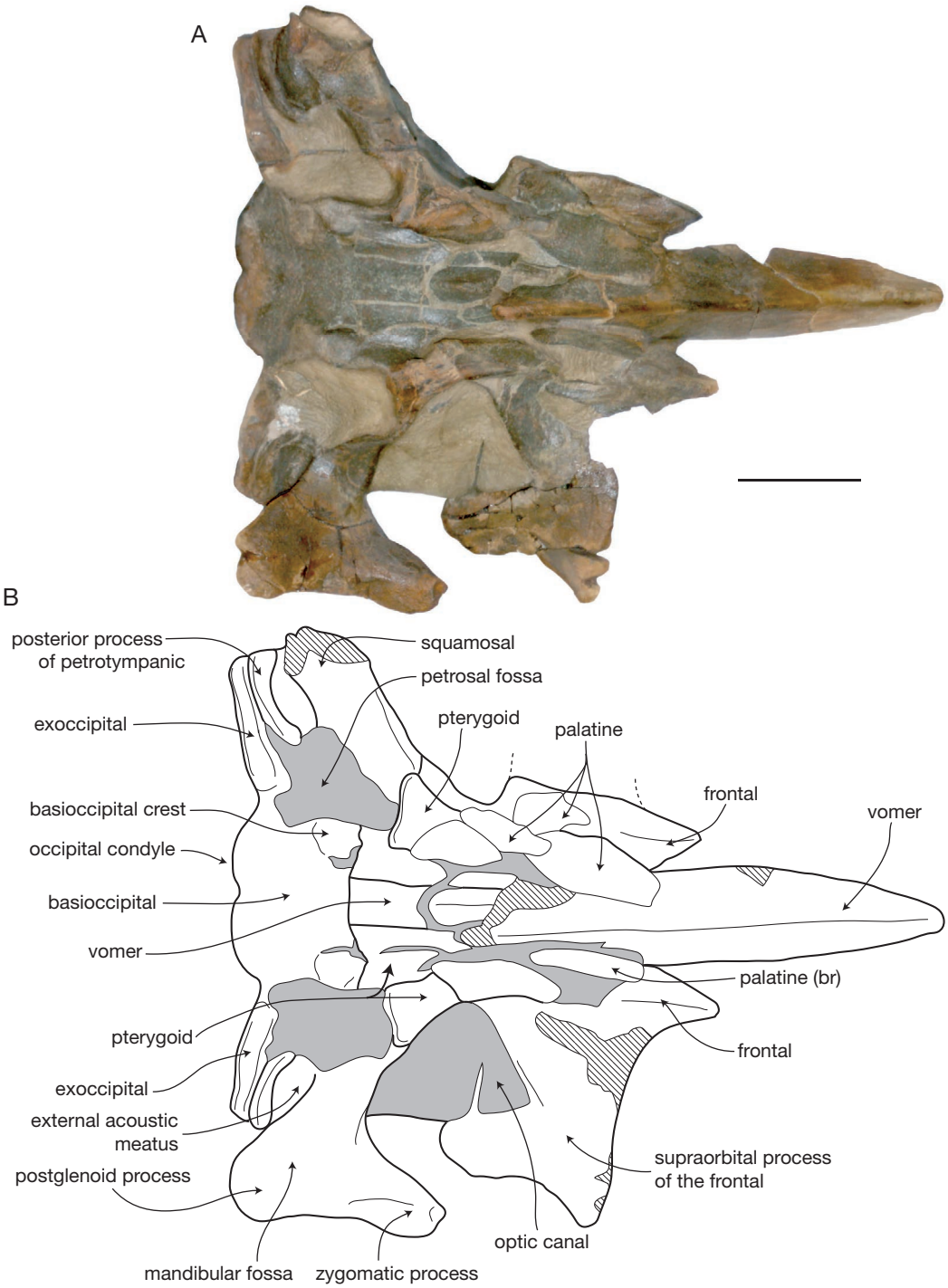

FIG. 12. — Holotype cranium of *Balaenoptera bertae* n. sp., UCMP 21907, in ventral view: **A**, photograph; **B**, interpretive line drawing. Cross hatching denotes broken or missing bone, and gray denotes adhering matrix. Scale bar: 10 cm.

– *Balaenoptera borealis* Lesson, 1824, in its much smaller size, apex of the occipital shield narrow and only 10% of bizygomatic width (26% bizygomatic width in *B. borealis*), exhibiting a ventrolaterally sloping (rather than vertical) surface of the parietal and frontal lateral to the supraorbital process of the frontal, shorter and blunt zygomatic process of the squamosal, shallower squamosal crease, a more posteriorly projecting postglenoid process, a supraorbital process of the frontal that lacks a dorsal ridge, with a more concave lateral margin and transversely oriented anterior margin, larger occipital condyles, a much larger petrosal fossa, and a blunt distal apex of the inflated compound posterior process of the petrotympanic;
– *Balaenoptera edeni* Anderson, 1879, in its much smaller size, apex of the occipital shield narrow and only 10% of bizygomatic width (18% bizygomatic width in *B. edeni*), larger occipital condyles, shorter zygomatic process of the squamosals, a more laterally prominent preorbital process, exhibiting a ventrolaterally sloping (rather than vertical) surface of the parietal and frontal lateral to the supraorbital process of the frontal, supraorbital process of the frontal that lacks a dorsal ridge, and a blunt distal apex of the inflated compound posterior process of the petrotympanic;
– *Balaenoptera musculus* Linneaus, 1758, in its much smaller size, in having a supraoccipital that is more broadly triangular with horizontal (rather than dorsolaterally) nuchal crests that dorsally overhang the temporal fossa, apex of the occipital shield narrow and only 10% of bizygomatic width (22% bizygomatic width in *B. musculus*), exhibiting a ventrolaterally sloping (rather than vertical) surface of the parietal and frontal lateral to the supraorbital process of the frontal, shorter zygomatic process of the squamosal that is anteriorly directed (rather than anterolaterally directed), larger petrosal fossa and occipital condyles, posteriorly directed postglenoid process (not posterolaterally directed as in *B. musculus*), a supraorbital process of the frontal with transversely oriented anterior margin and posterolaterally oriented posterior margin (as opposed to posterolaterally and posteromedially, as in *B. musculus*) and a blunt distal apex of the inflated compound posterior process of the petrotympanic;
– *Balaenoptera omurai* Wada, Oishi & Yamada, 2003, in its smaller size, in having a shorter and blunt zygomatic process of the squamosal, apex of the occipital shield narrow and only 10% of bizygomatic width (24% bizygomatic width in *B. omurai*), a more transversely oriented anterior margin of the supraorbital process of the frontal (as opposed to posterolaterally as in *B. omurai*), exhibiting a ventrolaterally sloping (rather than vertical) surface of the parietal and frontal lateral to the supraorbital process of the frontal, in lacking a sheet of the parietal that medially overlaps the supraorbital process of the frontal, and possessing a blunt distal apex of the inflated compound posterior process of the petrotympanic;
– *Balaenoptera physalus* Linneaus, 1758, in its much smaller size, apex of the occipital shield narrow and only 10% of bizygomatic width (25% bizygomatic width in *Balaenoptera physalus*), exhibiting a ventrolaterally sloping (rather than vertical) surface of the parietal and frontal lateral to the supraorbital process of the frontal, zygomatic process of the squamosal that is shorter and blunt, transversely narrower postglenoid process, a transversely oriented anterior margin of the supraorbital process of the frontal (as opposed to posterolaterally as in *B. physalus*), larger petrosal fossa, and a blunt distal apex of the inflated compound posterior process of the petrotympanic ;
– *Balaenoptera siberi* Pilleri & Pilleri, 1989, in possessing an anteriorly truncated and narrow apex of the occipital shield, only 10% of bizygomatic width (18% bizygomatic width in *B. siberi*), a squamosal crease, an anteriorly directed zygomatic process with a supramastoid crest that does not extend to the zygomatic apex, a zygomatic process that is dorsoventrally thicker, a paroccipital process that is less posterolaterally directed and not as prominent posteriorly, well defined crease between the squamosal and paroccipital process, and a transversely oriented anterior margin of the supraorbital process of the frontal;
– *Cetotheriophanes capellinii* (Brandt, 1873), in having a broader apex of the occipital shield that measures 10% of bizygomatic width (4% in *C. capellinii*) that is anteriorly truncated, a shorter intertemporal region, a more anteriorly thrusted occipital shield, a shorter zygomatic process of the squamosal, and

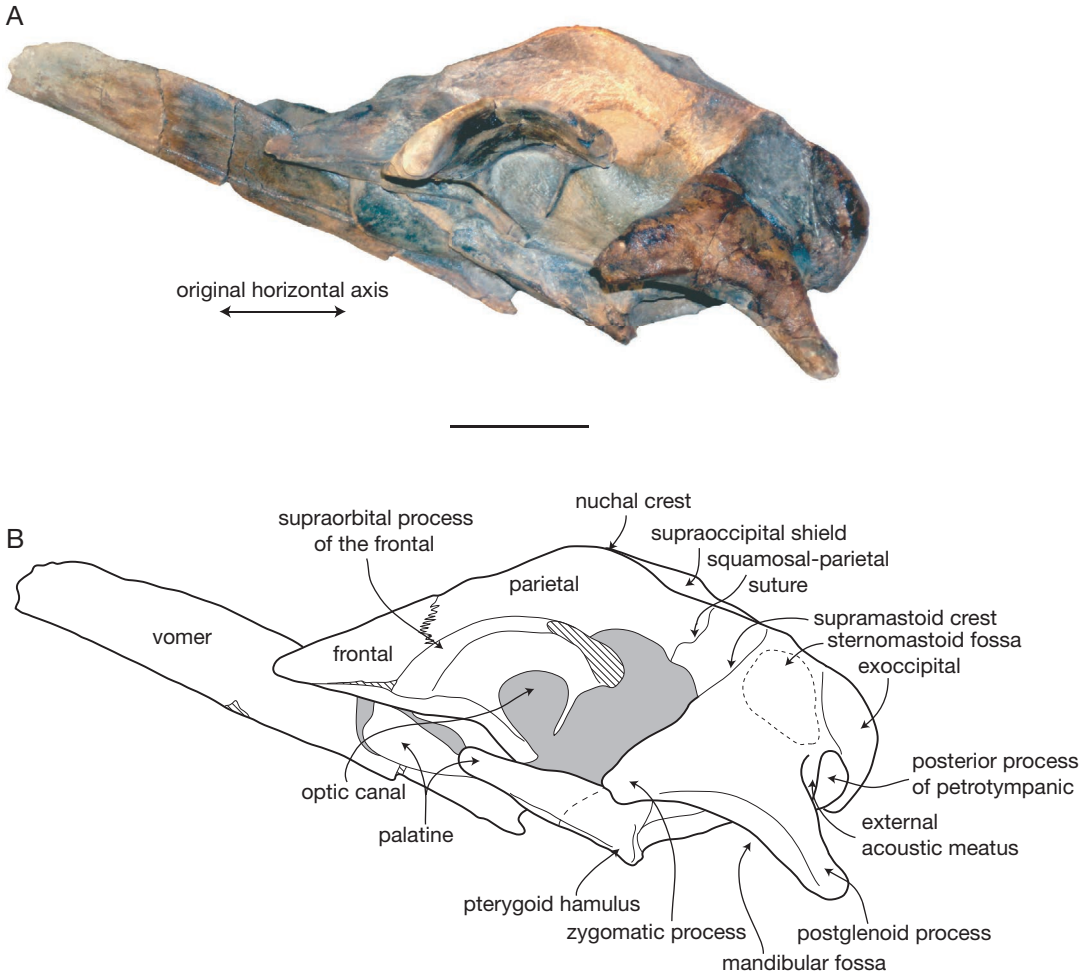

FIG. 13. — Holotype cranium of *Balaenoptera bertae* n. sp., UCMP 219078, in lateral view: **A**, photograph; **B**, interpretive line drawing. Cross hatching denotes broken or missing bone, and gray denotes adhering matrix. Scale bar: 10 cm.

longer postglenoid processes of the squamosal that are visible in dorsal aspect;
– *Diunatans luctoretmurgo* Bosselaers & Post, 2010, in having a narrow apex of the occipital shield measuring only 10% of bizygomatic width (24% bizygomatic width in *D. luctoretmurgo*), more sinuous lateral margin of the occipital shield, a slightly narrower zygomatic process that is less laterally offset from the braincase, pterygoid that is ventrally flat and not ventrally rounded in lateral aspect, and a posterior process of the petrotympanic that is anteromedially curved;
– *Megaptera novaeangliae* Brisson, 1762, in its much smaller size, in having a squamosal crease, shorter and more anteriorly oriented zygomatic process that lack a supramastoid crest that extends to the zygomatic apex, transversely narrow and posteriorly projecting postglenoid process of the squamosal, a less transversely and anteroposteriorly broad supraorbital process of the frontal, a transversely oriented anterior margin of the supraorbital process (as opposed to posterolaterally oriented), anteriorly truncated and narrow apex of the occipital shield measuring only 10% of bizygomatic width (14%

TABLE 6. — Measurements (in cm) of the skull of *Balaenoptera bertae* n. sp. (UCMP 219078). *, denotes partial measurement to midline and multiplied by two. Measurements given to nearest tenth of a centimeter.

Total length as preserved	64.5
Transverse width across condyles	16.4
Transverse width of foramen magnum	7.2
Dorsoventral depth of foramen magnum	7.3
Breadth across exoccipitals	42.1
Breadth across postglenoid processes	55.6*
Zygomatic width	61.4*
Interorbital width	55.6*
Breadth across antorbital processes	63.0*
Length of temporal fossa	8.75
Transverse width of temporal fossa	19.6
Intertemporal width	16.6
Posterior cranium to zygomatic process	20.4
Posterior cranium to antorbital process	35.4
Transverse width across basioccipital crests	13.9
Width of supraoccipital at vertex	4.5
Length of supraoccipital	29.0

bizygomatic width in *M. novaeangliae*), large petrosal fossae, and occipital condyles that are not set out on a distinct neck
– "*Megaptera*" *hubachi* Dathe, 1983, in having a squamosal crease, shorter and more anteriorly oriented zygomatic process that lacks a supramastoid crest that extends to the zygomatic apex, a more anteriorly thrust occipital shield with a slightly transversely narrower apex measuring 10% of bizygomatic width (compared to 14% in "*M.*" *hubachi*), an occipital shield that laterally overhangs the temporal fossa to a greater degree, a well defined crease between the paraoccipital process of the exoccipital and the squamosal, transversely narrow and posteriorly elongate postglenoid process of the squamosal, a laterally prominent antorbital process of the frontal, transversely oriented anterior margin of the supraorbital process, an inflated posterior process of the petrotympanic, and by lacking paired tuberosities on the supraoccipital and an anterior indentation in the apex of the occipital shield;
– "*Megaptera*" *miocaena* Kellogg, 1922, in its smaller size, in having a squamosal crease, shorter and more anteriorly oriented zygomatic process that lacks a supramastoid crest that extends to the zygomatic apex, less anteriorly thrust occipital shield that is roughly triangular and with more widely diverging lateral margins, vertex that is more anteriorly constricted and transversely narrower and measuring 10% of bizygomatic width (compared to 21% in "*M.*" *miocaena*), an anteroposteriorly broader supraorbital process of the frontal lacking a posterolaterally oriented ridge on its dorsal surface and with a laterally prominent antorbital process, a planar and transversely oriented posterior margin of the supraorbital process of the frontal, a well defined crease between the paroccipital process and squamosal, and an occipital shield that is dorsally convex in lateral aspect;
– *Parabalaenoptera baulinensis* Zeigler, Chan & Barnes, 1997, in having a squamosal crease, shorter and more anteriorly oriented zygomatic processes that lack a supramastoid crest that extends to the zygomatic apex, a clearly defined crease between the paroccipital process of the exoccipital and the squamosal, transversely broader apex of the occipital shield that measures 10% of bizygomatic width (8.7% in *P. baulinensis*) large occipital condyles, transversely oriented anterior and posterolaterally oriented posterior margin of the supraorbital process of the frontal (posterolaterally and posteromedially oriented in *Parabalaenoptera* Zeigler, Chan, & Barnes, 1997, respectively), anterolaterally oriented nuchal crests (oriented dorsolaterally in *Parabalaenoptera*), and a transversely narrow and posteriorly elongate postglenoid process of the squamosal;
– *Plesiobalaenoptera quarantellii* Bisconti, 2010, in having a less elongate and more inflated and anteromedially curved posterior process of the petrotympanic;
– *Protororqualus cuvieri* (Fischer, 1829), in having a squamosal crease, shorter and more anteriorly oriented zygomatic process that lack a supramastoid crest that extends to the zygomatic apex, a supraoccipital apex that is anteriorly squared-off at the vertex and transversely wider, measuring 10% of bizygomatic width (compared to 5% in *P. cuvieri*), little to no parietal exposure at the vertex, laterally prominent antorbital process, and a posteriorly elongate postglenoid process of the squamosal.

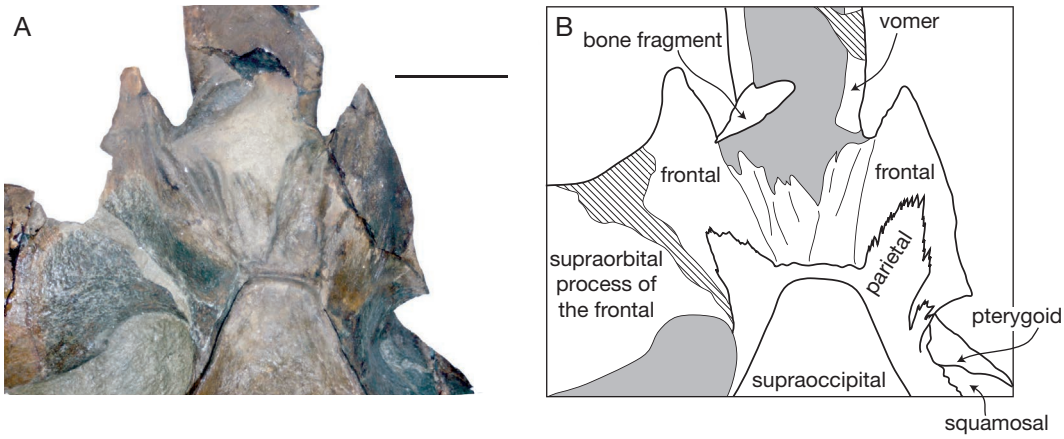

FIG. 14. — Vertex of holotype cranium of *Balaenoptera bertae* n. sp., UCMP 219078: **A**, dorsal view of vertex; **B**, interpretive line drawing. Gray color denotes matrix, and cross-hatching represents damaged or missing bone. Scale bar: 10 cm.

DESCRIPTION

The holotype is a partial skull including a nearly complete braincase, complete left squamosal and frontal, and vomer; the maxillae, premaxillae, and nasals are missing as well as both right and left tympanic bullae and petrosals (with the exception of the posterior processes; Figs 11-15). Measurements of the holotype are presented in Table 6. UCMP 219078 was found upside-down, and many bones of the ventral portion of the skull (as well as the left supraorbital process of the frontal) are fractured and displaced (Fig. 16). The vomer is broken posteriorly, and is rotated anterodorsally (Fig. 13). The left supraorbital process exhibits a long, anterolaterally oriented fracture, and the portion of the bone lateral to this fracture has rotated so that the supraorbital process is oriented dorsolaterally, and the postorbital process is no longer in contact with the zygomatic process. A reconstruction of the skull of *B. bertae* n. sp. is depicted in Figure 17.

Occipital shield

In dorsal view the occipital shield is broad and triangular with a transversely narrow apex that is rectilinear and transversely oriented in dorsal view (Figs 11A, 15A). The anteriormost portion of the shield is longitudinally concave, and posterior to this, it is dorsally strongly convex along the sagittal plane. A pair of faint tubercles occur in the middle of the supraoccipital, anterior to each occipital condyle. The nuchal crests are formed dorsally by the supraoccipital, are oriented anterolaterally, and overhang the temporal fossa so that the medial wall of the temporal fossa is not visible in dorsal aspect.

Exoccipital

The posterior margin of the exoccipital is posterolaterally oriented (Figs 11A, 12A). In dorsal view, the lateral margin of the occipital shield is slightly sinuous. The occipital condyles are relatively large. There are no clear dorsal condyloid fossae. Ventral to the foramen magnum, a shallow furrow extends between the occipital condyles.

Squamosal

The squamosal has a posteriorly elongate postglenoid process that is paddle-shaped (in dorsal and ventral view), dorsoventrally compressed, and posteroventrally directed (Figs 11B, 13A, 15C). The posterior margin of the postglenoid process is semi-circular in dorsal aspect. In lateral aspect, the ventral border of the mandibular fossa is strongly concave (Fig. 13), and both the zygomatic and postglenoid processes are somewhat ventrally directed, and in dorsal and ventral aspect, the zygomatic process is nearly anteriorly directed (Figs 11, 12). The zygomatic process is relatively short, blunt, and triangular in cross-section. The supramastoid crest runs along the dorsal

margin of the squamosal from the lateral margin of the occipital shield, but does not extend far onto the zygomatic process. A distinct dorsoventrally oriented and anteriorly facing squamosal crease occurs on the anterior surface of the squamosal, at the base of the zygomatic process. Along the posteromedial wall of the temporal fossa near the parietal-squamosal suture, a faint squamosal cleft occurs and runs parallel to the parietal-squamosal suture. In dorsal aspect, postglenoid process terminates well anterior to the exoccipital. A vertical crease occurs at the squamosal-exoccipital suture at the posterolateral edge of the cranium (Fig. 11A). The posterolateral surface of the squamosal is relatively planar. Ventrally, the mandibular fossa is transversely broad, and anteroposteriorly concave.

Basicranium

Portions of the basicranium are badly shattered (Figs 11B, 12B). The posterior sheet and wings of the vomer and palatines are broken. The basioccipital is broad and shallowly concave between the relatively small and knoblike basioccipital crests. The basioccipital crest is elongate and transversely convex. The petrosal fossa is large, subrectangular, anteriorly bordered by the pterygoid, medially by the medial lamina of the pterygoid, laterally by the squamosal, and posteriorly by the exoccipital (Figs 11B, 12B, 15C). Ventrally, the exoccipital forms a transversely oriented ridge that is posterolaterally directed. Posterolaterally, the exoccipital contacts the posterior surface of the posterior process of the petrotympanic. The posterior process of the petrotympanic curves anteromedially, is distally swollen, and bears a sharp ventral crest (Fig. 15B, C). The posterior meatal crest anteriorly overlaps the posterior process of the petrotympanic, and anterior to this thin plate, the squamosal exhibits a posterolaterally directed, trough-like external acoustic meatus positioned posterodorsally to the postglenoid process. The anterior meatal crest continues medially on the squamosal from the postglenoid process and forms the anterior margin of the external acoustic meatus.

The vomer is nearly complete, and anteriorly protrudes beyond the anterior margin of the frontals (Figs 11-13). Dorsally, the transversely concave mesorostral canal is filled with matrix. Anteriorly, the vomer becomes transversely narrower. The vomer is V-shaped in cross-section and bears a sharp ventral crest. Posteriorly, the ventral ridge of the vomer becomes lower to merge with the flat wings of the vomer. The latter becomes relatively wider posteriorly, ventrally flooring the basicranium, contacting the medial lamina of the pterygoid, and underlapping the anterior portion of the basioccipital. Posteriorly, the vomer is broad and flat. The basisphenoid is not exposed. The now-fractured palatine appears to have been slightly convex transversely, medially contacting the vomer, and posteriorly contacting the pterygoid. The palatal surface of the pterygoid is triangular in shape and positioned along the anterior margin of the petrosal fossa, with a blunt, tongue-shaped hamulus. The pterygoid hamulus does not appear to be broken or to possess finger-like posteromedial projection as in species of extant *Balaenoptera*, and this may tentatively considered to be natural. Medially, the blunt pterygoid hamulus overhangs the medial lamina of the pterygoid. The medial lamina is anteroposteriorly elongate, ventrally flat, and laterally forms the ventrally directed pharyngeal crest that is confluent with the basioccipital crest and forms the medial margin of the petrosal fossa.

Vertex

The vertex of UCMP 219078 is transversely narrow, reflecting the narrow apex of the supraoccipital (Figs 11A; 12A; 14). A thin band of the parietal is exposed between the sutures for the rostral elements and the supraoccipital (Fig. 14). As the rostral elements are missing, it is not possible to ascertain the length of the nasals and morphology of the ascending processes of the maxillae and premaxillae. The articular surface on the frontals for the rostral elements is corrugated and exhibits a series of anteroposteriorly oriented grooves and ridges; seven ridges are present on the left side; the right side is not as well-preserved. The region of the vertex as preserved on the frontal appears asymmetrical with the left side having extending further anterolaterally and with a larger angle to the midline; this is due to the slight counterclockwise rotation of the left supraorbital process of the frontal.

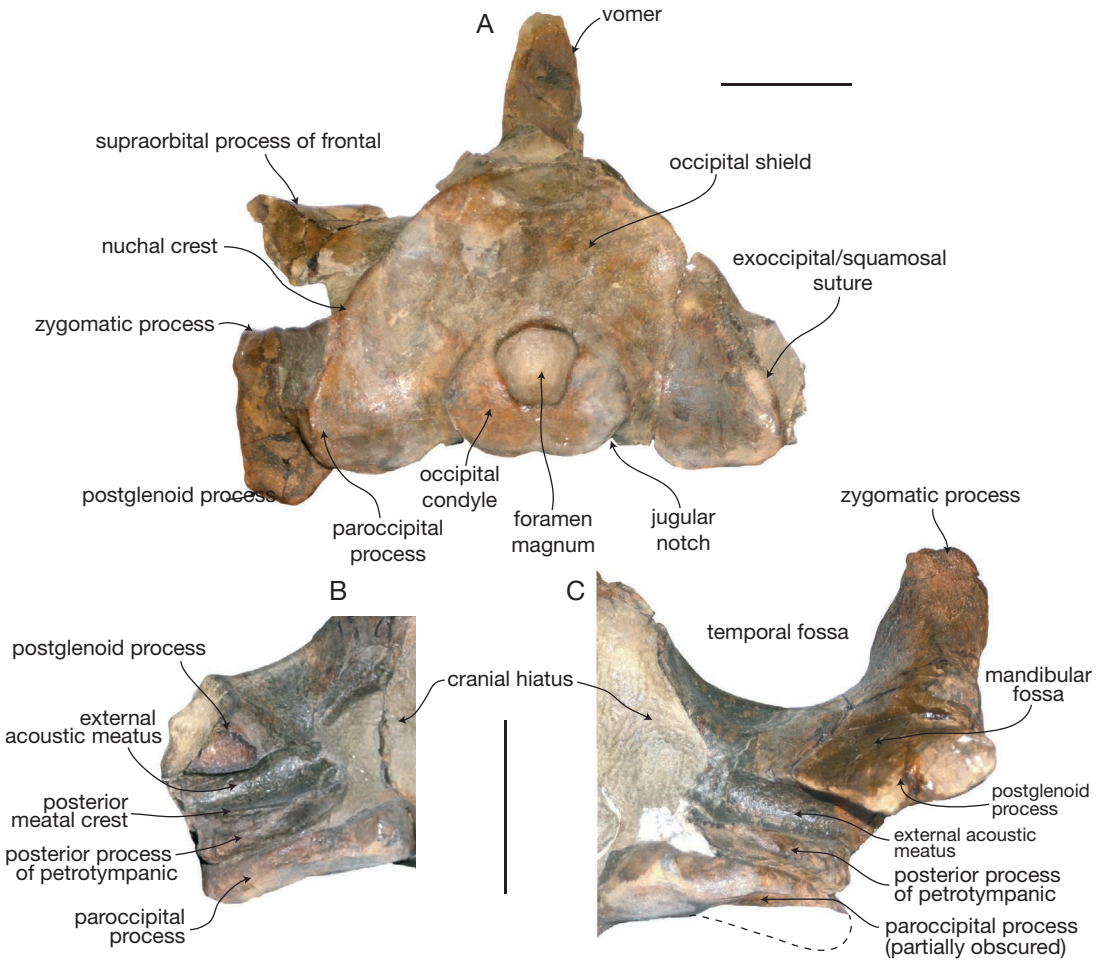

FIG. 15. — Holotype skull of *Balaenoptera bertae* n. sp., UCMP 219078: **A**, skull in posterodorsal view; **B**, right auditory region in ventral view; **C**, left auditory region in ventral view. Left paroccipital process is complete, but obscured by plaster display cradle. Scale bars: 10 cm.

Frontal

The well-preserved left frontal (Figs 11-13) has a sharp, triangular prong anteriorly. Lateral to this prong, the anterior margin of the supraorbital process is straight and transversely oriented in dorsal view (Fig. 17). The base of the supraorbital process is broken and displaced dorsally along the medial crack; the postorbital process is broken off, and when the original orientation of the supraorbital process is taken into account, it would have probably dorsally overlapped or contacted the zygomatic process (Fig. 17). The orbital margin of the supraorbital process is concave in dorsal view, and the dorsal surface of the supraorbital process is slightly anteroposteriorly arched. The posterior margin of the supraorbital process of the frontal is oriented transversely. Medially, the frontal drops sub-vertically from the vertex to the near-horizontal supraorbital process, which is horizontally oriented. The frontal drops near vertically from the vertex, so that it faces dorsolaterally, and the overlapping sheet of the parietal can be seen in dorsal aspect. The optic canal opens anterolaterally and is positioned posteriorly on the ventral surface of the supraorbital

process of the frontal (Fig. 12), defined by two ridges – the posteriorly placed infratemporal crest, and an anterolaterally directed ridge anterior to the canal. This anterior ridge is laterally confluent with the preorbital process, which projects slightly laterally.

Parietal

The parietal forms most of the medial wall of the temporal fossa, is exposed along the anterior portion of the vertex, and forms the ventral contribution to the nuchal crests on either side of the occipital shield (Fig. 13B). The lateral surface of the parietal in the temporal fossa is concave. Slightly anteromedial to the junction of the nuchal crest and the supramastoid crest of the squamosal, the parietal-squamosal suture descends ventrally along a bulge in the wall of the temporal fossa; it is oriented ventromedially, and does not turn posteriorly to form a long lateral finger of the parietal as in *B. acutorostrata*.

Ontogeny

Several features of the skull suggest that the holotype cranium of *B. bertae* n. sp. represents an immature individual. These include relatively large occipital condyles, large petrosal fossae, and a relatively short compound posterior process of the petrotympanic. Additionally, several cranial sutures remain unfused, including the squamosal-parietal suture and the frontal-parietal suture; young ontogenetic age may explain the ease at which basicranial elements were lost or fractured (see Taphonomy). These features suggest that UCMP 219078 was not finished growing, and highlights the possibility that the morphology may not be representative of the adult form. In concert with the size of UCMP 219078 and development of these features in comparison with juveniles of extant *Balaenoptera*, the holotype of *B. bertae* n. sp. is interpreted as an old juvenile or subadult. The primary features used for diagnosing *B. bertae* n. sp. include the narrow transverse width of the vertex and the dorsolaterally facing surface lateral to the vertex, permitting the anterior wing of the parietal (and proximal portion of frontal) to be visible in dorsal aspect. Examination of juvenile and neonatal specimens of *B. acutorostrata* and *B. physalus* (CAS, USNM collections) indicates these features do not change during postnatal development. For example, small juveniles of *B. acutorostrata* (e.g., CAS 22180) exhibit a relatively wide apex of the occipital shield, and a vertical slope adjacent to the vertex. These diagnostic features can thus reasonably be interpreted as present in fully grown adults of *B. bertae* n. sp. Although the compound posterior process of the petrotympanic is relatively short, it is inflated with a blunt distal apex; in extant adult *Balaenoptera* spp., the distal apex is tapered. Examination of juvenile *Balaenoptera* indicates the distal apex is also tapered, unlike the condition in *Balaenoptera bertae* n. sp., suggesting an additional derived feature that does not appear to be affected by ontogenetic patterns observed in extant relatives. Furthermore, the posterior process extends laterally to the level of the lateral extremity of the paroccipital process, unlike immature specimens of extant *Balaenoptera*; during ontogeny, the posterior process increases in length and lags behind the exoccipital during early development (Bisconti 2001). Examination of the petrosal fossae of juvenile *B. acutorostrata* indicates that even in neonates, the fossae are smaller relative to skull size than in UCMP 219078, suggesting that the large size is autapomorphic for *B. bertae* n. sp., and possibly a paedomorphic trait. In summary, although several features suggest immaturity, other features suggest that growth was nearly completed; additionally, most of the diagnostic features for *B. bertae* n. sp. do not appear to be affected by ontogenetic changes in extant *Balaenoptera*.

Taphonomy

The skull of *B. bertae* n. sp. exhibits several noteworthy preservational features (Fig. 16). UCMP 219078 was preserved in a monotonous succession of massively bedded, pervasively bioturbated fine-grained sandstone. This facies, typically lacking any primary sedimentary structures due to thorough homogenization of the sediment by bioturbators, was interpreted by Norris (1986) as reflecting a middle shelf (or transition zone) depositional setting. Other evidence for a lag deposit such as abundant, large terrigenous or phosphatic clasts or abundant mollusks is absent from this stratum. The rostral bones (premaxillae, maxillae, and nasals), tympanic bullae, middle ear ossicles, and bodies of the pet-

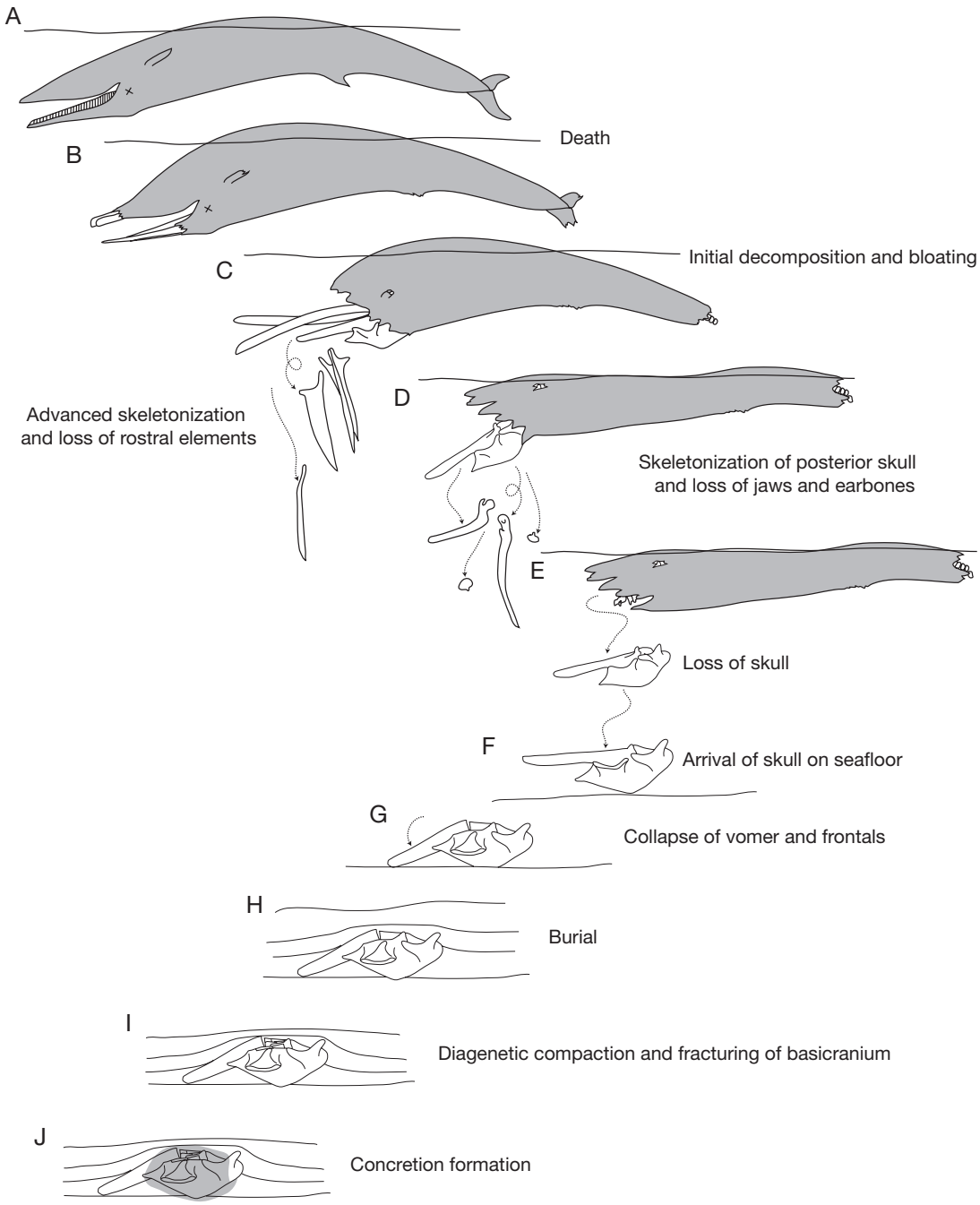

FIG. 16. — Possible taphonomic pathway of the holotype specimen of *Balaenoptera bertae* n. sp.: **A**, death; **B**, initial decay, bloat, and floating; **C**, advanced skeletonization of the facial region and loss of rostral elements; **D**, continued skeletonization of the facial region and the loss of petrotympanics and mandibles; **E**, loss of the cranium from the carcass; **F**, arrival of the skull on the seafloor in the ventral-up position; **G**, collapse and rotation of the vomer and frontals and contact with the seafloor; **H**, burial; **I**, diagenetic compaction and fracturing of basicranial elements; **J**, formation of a concretion during later diagenesis.

rosals are missing, and no postcrania were found during excavation. The vomer and other basicranial elements are shattered, and the left supraorbital process of the frontal and vomer are broken and rotated dorsally. UCMP 219078 was found ventral-up in massively bedded, bioturbated sandstone with dispersed mollusks and pebbles. The cranium was likely too large to be overturned by currents and probably represents the original orientation of the skull upon arrival at the sea floor. The lack of postcrania suggests that the skull arrived on the sea floor as an isolated element. The lack of evidence for a lag deposit or erosional surface at this horizon suggests that postcrania were not dissociated by transport and submarine erosion.

Many cetacean carcasses float ventral up (Schäfer 1972) and it is possible that the orientation of the skull reflects this; it also may reflect the hydrodynamically stable orientation of the skull as it sank. The rostral elements could have been lost during the bloat and float stage (Fig. 16A-C). Due to exaggerated movement of craniovertebral joint in modern floating cetacean carcasses, the skull is lost not long after the mandibles (e.g., Fig. 16E; Schäfer 1972), which is reflected in some cetacean assemblages (Bianucci *et al.* 2010). How the basicranial elements shattered is less clear, but some features of the fossil help to constrain the timing of deformation. Parts of the skull inside the concretion are shattered, indicating that this happened prior to formation of the concretion. Rotation and displacement of the vomer and supraorbital process of the frontal would not have been possible once entombed in sediment, and must have occurred prior to burial. The sequence of events for the holotype individual of *B. bertae* n. sp. is inferred as follows: bloating and floating of the whale after death (whether immediate or after refloating; Fig. 16A); initial decomposition and loss of the jaws and rostral elements (Fig. 16B, C); advanced decay and skeletonization of the head results in the loss of the earbones (Fig. 16D), and eventual loss of the skull (Fig. 16E). At that time, the skull sinks to the sea floor ventral-up (Fig. 16F), and at some point between its arrival on the seafloor and burial, the vomer and supraorbital process rotate and come into contact with the seafloor (Fig. 16G). Eventually the skull is buried (Fig. 16H). Long after burial, diagenetic compaction fractures the basicranial elements (Fig. 16I), and a concretion forms around the braincase (Fig. 16J).

Phylogenetic analysis

Balaenoptera bertae n. sp. was coded for the 150 characters of Marx (2011) as follows:

```
??????????????1??????????00012?210?1?
??11???01????????10120111302102100 11?0
101?111?????????21?????????????????????
????????????????????????????????????????
```

Incorporation of *B. bertae* n. sp. into the matrix of Marx (2011) and cladistic analysis supported inclusion (with low branch support) of this new taxon within *Balaenoptera* (Fig. 18). In the strict consensus tree, *B. bertae* n. sp. appears within a basal polytomy with *Balaenoptera physalus*, *B. edeni*, *B. acutorostrata*, and *B. bonaerensis*. Within *Balaenoptera*, the Peruvian fossil *B. siberi* is sister to a *B. omurai* + *B. musculus* clade, forming the only resolved clade within *Balaenoptera*; however, this relationship is weakly supported (Fig. 18). Topology among other mysticete taxa did not change relative to the phylogenetic results of Marx (2011: fig. 3), although branch and bremer support values slightly decreased across Balaenopteroidea, and support for Eschrichtiidae slightly increased (Fig. 18). Most notably, the moderately supported *B. borealis*-*B. bonaerensis*-*B. acutorostrata* clade (Marx 2011: fig. 3) collapsed in this analysis, perhaps owing to the inclusion of the somewhat incomplete *B. bertae* n. sp. Increased resolution of balaenopterid phylogeny would be possible with the inclusion of additional balaenopterid taxa into this matrix (such as *D. luctoretmurgo*, *C. capellinii*, *P. quarantellii*, and "*B.*" *cortesi* "var." *portisi*) and additional balaenopterid-specific characters, including petrotympanic characters recently discussed by Ekdale *et al.* (2011), and other skull features such as a squamosal crease, which in the current study was only identified in modern and fossil species of *Balaenoptera*.

Balaenoptera bertae n. sp. as a balaenopterid

Balaenoptera bertae n. sp. exhibits several balaenopterid characteristics, including an abruptly depressed

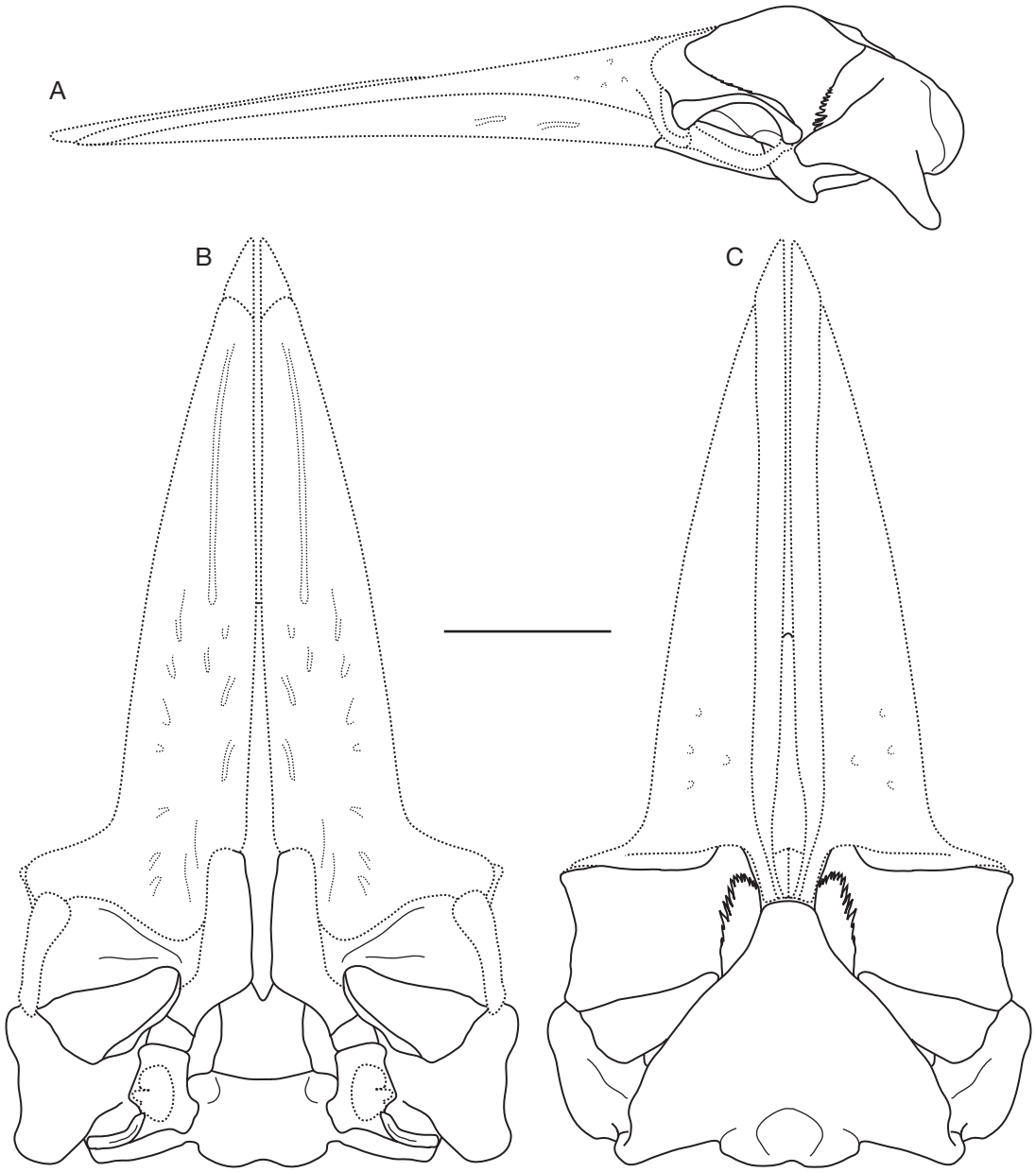

FIG. 17. — Reconstruction of the skull of *Balaenoptera bertae* n. sp.; **A**, lateral view; **B**, ventral view; **C**, dorsal view. Scale bar: 20 cm.

supraorbital process of the frontal, an anteriorly thrusted occipital shield that laterally overhangs the temporal fossa, and telescoping of the rostral elements and supraoccipital such that the parietal is only exposed as a narrow transverse band at the vertex (Figs 11-15, 17; Zeigler *et al.* 1997; Deméré *et al.* 2005; Bisconti 2007a, b, 2010a; Bosselaers & Post 2010). *Balaenoptera bertae* n. sp. shares with

all extant *Balaenoptera* spp. and *M. novaeangliae* a broadly triangular occipital shield that laterally overhangs much of the temporal fossa so that it obscures most of the parietal and medial wall of the temporal fossa in dorsal view (Figs 11, 17; Deméré *et al.* 2005). In many fossil balaenopterids, the crania are less extremely telescoped and the supraoccipital is not thrust as far anteriorly and overhangs less of the temporal fossa (e.g., *Archaebalaenoptera* Bisconti, 2007, "*B.*" *cortesi* "var." *portisi*, *C. capellinii*, *Protororqualus* Bisconti, 2007) or only overhangs the anterior portion of the temporal fossa so that the posterior half of the medial wall is visible in dorsal aspect (*P. baulinensis*, "*M.*" *hubachi*, "*M.*" *miocaena*). Most species of *Balaenoptera*, including *B. bertae* n. sp., exhibit a slight convex bulge along the medial wall of the temporal fossa at the position of the squamosal-parietal suture; *Megaptera* Gray, 1846 lacks this bulge, and is thus the only balaenopterid where the inner wall of the temporal fossa is completely obscured in dorsal view. In *B. musculus*, the occipital shield is transversely narrow, and the medial wall is so bulged that nearly the entire medial wall is visible in dorsal aspect (interpreted here to be a reversal).

The morphology of the squamosal varies widely within balaenopterids. Most fossil balaenopterids (e.g., *A. castriarquati*, "*B.*" *cortesi* "var." *portisi*, *P. baulinensis*, and *P. cuvieri*) appear to exhibit an elongate, laterally divergent zygomatic process with well-defined supramastoid crest that run along most of the length of the zygomatic process, while lacking a squamosal crease (Zeigler *et al.* 1997; Deméré *et al.* 2005; Bisconti 2007a, b). An elongate and laterally flaring zygomatic process is regarded as the primitive condition amongst balaenopteroids (Deméré *et al.* 2005), and among fossil and extant balaenopterids, characterize all taxa (including *Megaptera*) except for *D. luctoretmurgo* and *Balaenoptera* spp., which have relatively short and anteriorly directed zygomatic process. *B. musculus* is exceptional amongst extant *Balaenoptera* in its elongate and laterally flaring zygomatic process. The most extreme condition within balaenopterids characterizes *B. acutorostrata*, *B. bertae* n. sp., and *D. luctoretmurgo*, all of which have short and nearly anteriorly oriented zygomatic process. Postglenoid process morphology also varies within the Balaenopteridae, and it is short and indistinct in basal balaenopterids (e.g., *Archaebalaenoptera*, *Parabalaenoptera*, *Protororqualus*) and posteriorly elongate in *Balaenoptera*, *Diunatans* Bosselaers & Post, 2010, and *Megaptera*. These latter taxa (including *B. bertae* n. sp.) also exhibit a posterolaterally directed postglenoid process. The early diverging balaenopterid "*B.*" *cortesi* "var." *portisi* also exhibits posteriorly elongate postglenoid process, but it is posteriorly and not posterolaterally oriented. A squamosal crease is present in taxa with anteriorly oriented zygomatic processes. While a squamosal crease is absent in *D. luctoretmurgo* (Bosselaers & Post 2010) and *B. siberi*, it is present in all extant species of *Balaenoptera* and *B. bertae* n. sp., and absent in *M. novaeangliae* (Kellogg 1922; Deméré *et al.* 2005). This feature may be a possible synapomorphy of *Balaenoptera*.

Balaenoptera bertae n. sp. may be distinguished from all extant balaenopterids by the lack of a fingerlike posterior projection of the pterygoid hamulus (Fig. 11B). The condition of this character is unknown in many fossil taxa, either because the ventral side of the skull has not been prepared (e.g., *Archaebalaenoptera*, *B. siberi*), is completely missing (*Cetotheriophanes* Brandt, 1873, *Plesiobalaenoptera* Bisconti, 2010), or is too damaged to tell (e.g., "*B.*" *cortesi* "var." *portisi*, "*M.*" *miocaena*, *Parabalaenoptera*). "*Megaptera*" *hubachi* also appears to lack a posteriorly directed finger of the pterygoid hamulus. Fingerlike pterygoid hamuli are widely distributed among modern and fossil mysticetes such as cetotheriids *sensu stricto*, cetotheres *sensu lato* (*sensu* Bouetel & Muizon 2006), and extant *Eschrichtius robustus* (Lilljeborg, 1861).

Balaenoptera bertae n. sp. as a member of *Balaenoptera*

In general, *B. bertae* n. sp. exhibits characteristics that are relatively derived in comparison to most fossil balaenopterids. In comparison to extant species of *Balaenoptera*, *B. bertae* n. sp. is characterized by a mosaic of primarily derived and a few plesiomorphic characters. Aside from the derived features outlined above (also see Differential diagnosis), plesiomorphic characteristics of *B. bertae* n. sp. include a transversely narrow vertex and supraoccipital apex, and a supraor-

FIG. 18. — Strict consensus tree of the phylogenetic analysis executed, including *Balaenoptera bertae* n. sp. within the data matrix of Marx (2011). Basal parts of the tree outside the *Caperea* + Balaenopteroidea clade are not shown; support values are Bremer support and GC frequency values. †, denotes extinct taxa.

bital process of the frontal which is separated from the vertex by a dorsolaterally oriented and steeply sloping surface (of the frontal and parietal), instead of a vertically oriented (and laterally facing) surface (Fig. 11). While a narrower vertex is plesiomorphic (Deméré *et al.* 2005; Bisconti 2007b), most basal balaenopterids exhibit a vertically oriented anterior lateral wall of the braincase and an abruptly depressed supraorbital process of the frontal, and the condition of the supraorbital process in *B. bertae* n. sp. may not necessarily be archaic. Likewise, *B. bertae* n. sp. does exhibit an abruptly depressed supraorbital process of the frontal, although offset by an oblique, dorsolaterally oriented surface rather than a vertical surface as in all other balaenopterids (Fig. 14A) and may be autapomorphic. An additional feature of *B. bertae* n. sp. is the apparent anteroposterior shortness of the vertex (judging by the anterior tips of the frontals, which approximate the posterior margin of the bony nares). In most extant balaenopterids, the anteriormost point of the supraoccipital is relatively far posteriorly, near the posterior margin of the supraorbital process of the frontal (or posterior to a transverse line dividing the supraorbital process into anterior and posterior halves). This condition characterizes most fossil balaenopterids as well, including *Archaebalaenoptera*, *B. siberi*, "*B.*" *cortesi* "var." *portisi*, *C. capellinii*, "*M.*" *hubachi*, *Parabalaenoptera*, and *Protororqualus.* In *B. bertae* n. sp., *B. bonaerensis*, "*M.*" *miocaena*, and *M. novaeangliae*, the anterior margin of the occipital shield is positioned within the anterior ¼ of the medial part of the supraorbital process of the frontal. This feature indicates that *B. bertae* n. sp. exhibits the most telescoped occipital shield of any species of *Balaeno-*

ptera. Only one fossil balaenopterid appears to have a more anteriorly thrusted occipital shield, the Early Late Miocene "*M.*" *miocaena*; in this fossil taxon, the supraoccipital is thrust anteriorly to the level of the preorbital process of the frontal. The apex of the occipital shield is roughly at the postorbital process in basal balaenopterids like *Archaebalaenoptera* and *Protororqualus*, indicating that the condition in *B. bertae* n. sp. is relatively derived even when compared with extant balaenopterids. However, this may be an illusion caused by the apparent anteroposterior shortness of the supraorbital process of the frontal (Fig. 17C) of *B. bertae* n. sp. relative to other balaenopterids, which appears to be an autapomorphic feature.

As demonstrated in the phylogenetic analysis, *Balaenoptera bertae* n. sp. represents a fossil species of the extant taxon *Balaenoptera*. Fossil species attributed to *Balaenoptera* by Deméré *et al.* (2005) include *Balaenoptera davidsonii* Cope, 1872 (Pliocene San Diego Formation of California), *B. siberi* (uppermost Miocene of Peru), *Balaenoptera borealina* Van Beneden, 1880 (Pliocene of Belgium), *Balaenoptera minutis* Van Beneden, 1880 (formerly *Burtinopsis* Van Beneden, 1872; Pliocene of Belgium), *Balaenoptera rostratella* Van Beneden, 1880 (Pliocene of Belgium), and *Balaenoptera sibbaldina* Van Beneden, 1880 (Pliocene of Belgium). Because P. J. Van Beneden did not designate any holotypes and because all the syntype material of the Belgian Pliocene taxa appear to represent multiple individuals or chimaeras, or are not considered to be diagnostic enough to be designated as lectotypes, Bosselaers & Post (2010) proposed that all Belgian Pliocene balaenopterid taxa (as well as *Megapteropsis robusta* Van Beneden, 1872 and *Plesiocetus garopii* Van Beneden, 1859) should be considered *nomina dubia*. Deméré *et al.* (2005) referred a skull (San Diego Formation, Pliocene, California) to *B. davidsonii*, which was previously only known by mandibles (Deméré 1986), although this specimen now appears to represent a different taxon (T. A. Deméré pers. comm. 2011). While *B. siberi* was placed within *Balaenoptera* in the phylogenetic analysis of Deméré *et al.* (2005) and Marx (2011), Bosselaers & Post (2010) did not consider *B. siberi* to be a member of the genus as it exhibited "basal features". Features that distinguish it from extant *Balaenoptera* and *B. bertae* n. sp. include relatively slender and widely flaring zygomatic process, a supramastoid crest that continues nearly to the zygomatic apex, a broadly rounded supraoccipital apex, lack of a squamosal crease, and lack of a well-defined separation of the paroccipital process and squamosal in dorsal aspect. On one hand, several other basal balaenopterids exhibit a derived and wide vertex like *Balaenoptera* (e.g., *Archaebalaenoptera*, *Parabalaenoptera*), while exhibiting plesiomorphic squamosal morphology (slender and widely flaring zygomatic processes and no squamosal crease); perhaps the morphology of *B. siberi* is exactly what could be expected of an archaic species within *Balaenoptera*. However, a recent phylogenetic analysis by Bisconti (2010b) suggests that *B. siberi* may lie outside *Balaenoptera*, as a sister taxon of *Diunatans*. The generic placement of *B. davidsonii* and *B. siberi* requires additional fossil material and phylogenetic studies. This study documents a convincing example of an extinct species of *Balaenoptera* from the Pliocene, and additional records of extinct (or extant) members of this genus from the Pliocene may await discovery.

Remarks

Previous molecular analyses have utilized fossil calibrations in an attempt to constrain the timing of molecular divergence of various mysticete clades. Recent studies have yielded dates for the balaenopterid-eschrichtiid clade in the Middle to Late Miocene (13.8 Ma; McGowen *et al.* 2009; 13-12 Ma, Dornburg *et al.* 2012). However, molecular divergence dating is problematic for this clade due to the phenomenon of *Balaenoptera* paraphyly (by inclusion of *Megaptera* and occasionally *Eschrichtius* Gray, 1864 within *Balaenoptera*), which is frequently recovered in molecular analyses (Rychel *et al.* 2004; McGowen *et al.* 2009; Dornburg *et al.* 2012; but see Nikaido *et al.* 2006, and Steeman *et al.* 2009), although *Megaptera* and *Eschrichtius* fall outside the genus *Balaenoptera* in nearly all morphology-based cladistic analyses (Steeman 2007; Marx 2011). Further complications arise when considering the choice of fossil calibrations. Dornburg *et al.* (2012) used "*M.*" *hubachi* as a calibration for the *B. physalus-M. novaeangliae* clade; however, some morphology-based analyses have failed to demonstrate a close relationship between "*M.*" *hubachi* and extant *M. novaeangliae*, and it

TABLE 7. — Measurements (in cm) of mysticete petrosals. Measurements given to nearest tenth of a millimeter. Total length refers to length of the petrosal body, and does not include the posterior process (preserved only in UCMP 219114 among these specimens).

	UCMP 219135 "*Balaenoptera*" *cortesi* "var." *portisi*	**UCMP 219136** cf. *Balaenoptera*	**UCMP 219114** *Herpetocetus* sp.	**UCMP 219115** *Herpetocetus* sp.
Total length as preserved	78.85	86.40	53.34	54.43
Length of pars cochlearis	80.18	59.89	33.11	29.02
Anteroposterior length of promontorium	39.06	37.91	14.46	14.86
Length of anterior process	62.48	65.35	35.35	33.87
Transverse width of anterior process	21.01	23.01	9.80	6.83

is considered not to belong to *Megaptera* (Deméré *et al.* 2005; Bisconti 2010b). Problems of *Balaenoptera* monophyly notwithstanding, perhaps more appropriate fossil calibrations could be found in fossil species of *Balaenoptera*, as previously reported fossil records of *Megaptera* have turned out to be archaic balaenopterids with superficial similarities to *Megaptera* ("*M.*" *hubachi*; "*M.*" *miocaena*) or fragmentary remains from the Pliocene (Whitmore & Kaltenbach 2008). Both *B. bertae* n. sp. and *B. siberi* have been found to fall within *Balaenoptera* (Marx 2011; this study; but see Bisconti 2010b) although further testing is necessary for both taxa. Regardless of molecular divergence dating, fossils such as *B. bertae* n. sp. and *B. siberi* demonstrate that "true" *Balaenoptera* had evolved by the Early Pliocene, and possibly by the latest Miocene.

"***Balaenoptera***" ***cortesi*** "var." ***portisi*** Sacco, 1890

REFERRED MATERIAL. — UCMP 219135, a right petrosal collected by R.W. Boessenecker from UCMP locality V99840.

STRATIGRAPHIC OCCURRENCE. — Middle part of the San Gregorio section of the Purisima Formation, Early Pliocene (*c.* 5-3.35 Ma; Zanclean-Piacenzian equivalent; Fig. 2).

DESCRIPTION

The pars cochlearis of this large petrosal (Table 7) is dorsally elongate (Fig. 19A), with an elongate, posteroventrally directed posterior cochlear crest; adjacent to this crest is the small, circular fenestra cochleae. The groove for the tensor tympani muscle is situated anteroventral to the pars cochlearis, on the medial surface of the anterior process. The anterior process is triangular and bladelike, curves medially at its apex, and rugose along its medial margin (Fig. 19A, C). In medial aspect, the ventral margin of the anterior process is straight and directed anterodorsally. The lateral tuberosity is oriented posteroventrally and positioned at the base of the anterior process. The anterior pedicle for the tympanic bulla is positioned just dorsal to the lateral tuberosity; dorsal to the pedicle is a shallow mallear fossa. The facial sulcus is oval and dorsal to the mallear fossa; an elongate trough is not developed as in some modern *Balaenoptera*. The oval-shaped fenestra vestibuli is medially adjacent to the facial sulcus and at the base of pars cochlearis. The neck for the posterior process is robust and quadrate in cross-section, and the small posterior pedicle is present anteromedially on the neck. The anteroposteriorly elongate, rectangular, and shallow stylomastoid fossa is positioned on the posterior surface of the pars cochlearis and base of the posterior process. Further anterior along the dorsal surface of the petrosal are the perilymphatic and endolymphatic foramina, which are situated in a common groove an separated from the stylomastoid fossa by a thin crest. The internal acoustic meatus is deep and cavernous (resulting from the extreme dorsal elongation of the pars cochlearis) with a circular canal for the vestibulocochlear nerve (= spiral cribriform tract of Mead & Fordyce 2009) and an oval-shaped facial canal (Fig. 19D). The crista transversa is deeply recessed (34 mm) within the internal acoustic meatus. The vestibulocochlear nerve canal is 43 mm deep, and the facial canal is 48 mm deep. An additional unidentified foramen

is present anterodorsally to the facial canal on the dorsal edge of the pars cochlearis; it is unclear whether or not this foramen is the hiatus fallopii. The lateral surface of the petrosal is rugose and gently convex.

Remarks and comparisons

This petrosal compares best with the holotype petrosal of "*Balaenoptera*" *cortesi* "var." *portisi* from the Pliocene of Italy (Sacco 1890), as well as SDNHM 68698, a petrosal preserved with a partial skull from the Upper Pliocene San Diego Formation of southern California referred to "*B.*" *cortesi* "var." *portisi* by Deméré *et al.* (2005). Deméré (1986) and Deméré *et al.* (2005) further indicated that the holotype mandible of "*Balaenoptera*" *floridana* Kellogg, 1944, as well as the Italian Pliocene balaenopterid *Cetotheriophanes capellinii* may also be congeneric or conspecific with this taxon. "*B.*" *cortesi* "var." *portisi* does not belong in *Balaenoptera* and requires a new genus name and reevaluation (Deméré *et al.* 2005). In particular, UCMP 219135 shares many distinctive features with of "*B.*" *cortesi* "var." *portisi* such as a dorsally elongate pars cochlearis, a straight anterior margin of the anterior process, an anterior process that is pointed anterodorsally rather than anteriorly, and a flattened, bladelike anterior process. Crania of "*B.*" *cortesi* "var." *portisi* preserving this petrosal morphology differ from *Balaenoptera bertae* n. sp. in exhibiting more elongate and widely flaring zygomatic processes, lacking a squamosal crease, an anteroposteriorly more elongate supraorbital process of the frontal, and an occipital shield that is more anteriorly elongate and attenuate; it is thus unlikely that UCMP 219135 is referable to *B. bertae* n. sp.

Some features of this specimen are shared with *Megaptera novaeangliae*, including the extreme elongation of the pars cochlearis, and having the perilymphatic and endolymphatic foramina situated in a common groove. However, UCMP 219135 differs from *Megaptera* in having deep canals for the facial and vestibulocochlear nerves, in having the internal acoustic meatus positioned in the middle of the pars cochlearis (instead of the posterior aspect as in extant *Megaptera*), and in having a smaller and less acutely pointed lateral tuberosity. UCMP 219135 differs from extant *Balaenoptera* spp. in the extreme elongation of the pars cochlearis, and an anterior process that is directed anterodorsally (relative to the long axis of the pars cochlearis), rather than anteriorly in extant *Balaenoptera* and *Megaptera* (Ekdale *et al.* 2011).

Two additional specimens from the Purisima Formation undoubtedly represent this taxon. A large cranial fragment (UCMP uncataloged, field no. FP 192) from the Santa Cruz section of the Purisima Formation exhibits a well-preserved and identical petrosal; furthermore, a partial cranium (SCMNH 21292) exhibits squamosal morphology that is identical to the holotype of "*B.*" *cortesi* "var." *portisi* and referred skulls from the San Diego Formation (SDNHM 65769 and 68698).

This fossil represents an additional occurrence of "*B.*" *cortesi* "var." *portisi* from the eastern North Pacific along with that from the San Diego Formation reported by Deméré *et al.* (2005). Along with other records of this taxon from the Pliocene of Florida and Italy (Portis 1885; Kellogg 1944; Deméré *et al.* 2005), this indicates that this taxon (whether several species within a genus, or a single species) was cosmopolitan and formerly inhabited the eastern North Pacific, the western North Atlantic, and the Mediterranean Sea during the Pliocene.

cf. *Balaenoptera*

Referred material. — UCMP 219136, a right petrosal, collected by R.W. Boessenecker from UCMP locality V99851.

Stratigraphic occurrence. — Lowermost part of the San Gregorio section of the Purisima Formation, latest Miocene (6.4-5.6 Ma; Messinian equivalent; Fig. 2).

Description

This large partial petrosal exhibits a low, and ventrally flattened pars cochlearis that is roughly oval-shaped in ventral aspect and somewhat elongated dorsally (Fig. 20; Table 7). A small, thin, and bladelike posterior cochlear crest occurs posteroventrally on the pars cochlearis. The fenestra cochleae is small and circular and occurs within a small fossa. The anterior process is acutely triangular, transversely thick, and a longitudinal keel occurs on the ventral side at its apex. The anterior pedicle sits atop a rectangular plateau on the medial surface of the anterior process. A well-

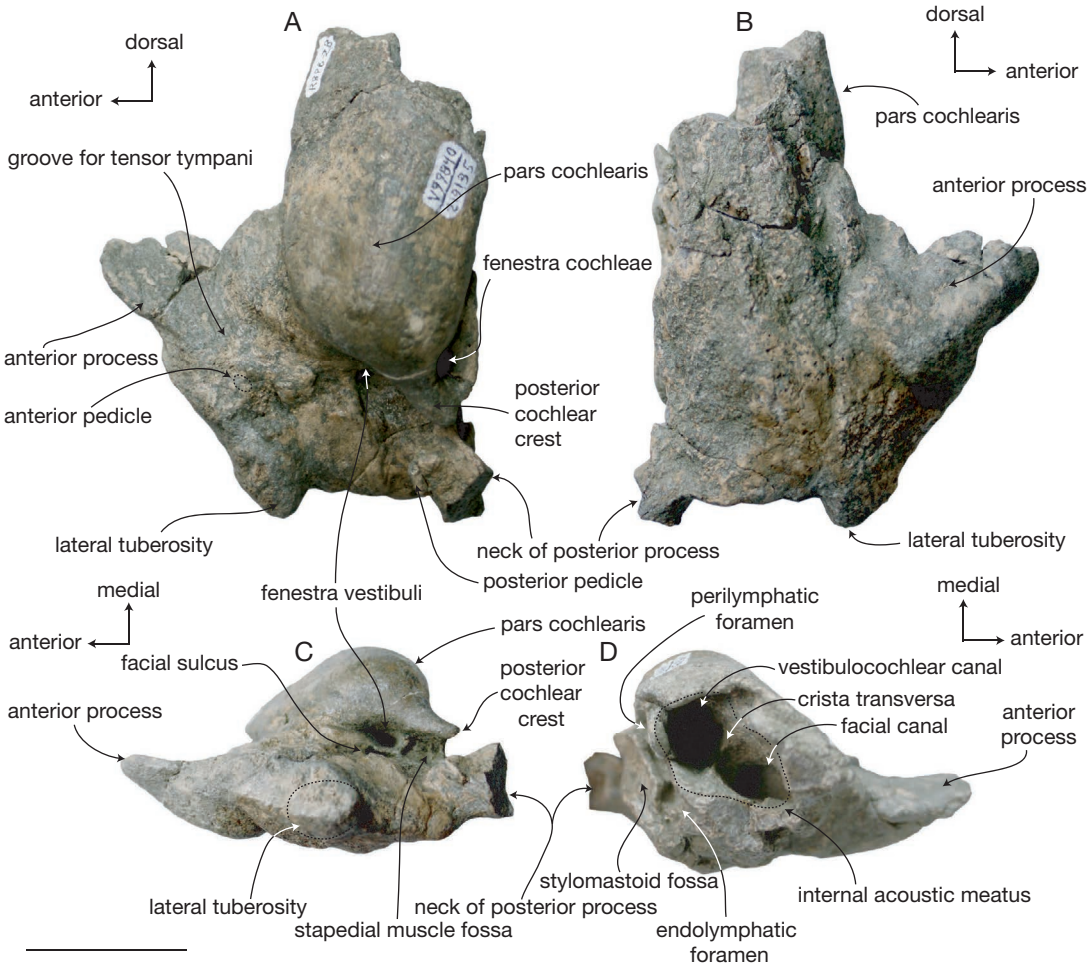

FIG. 19. — Right petrosal of "*Balaenoptera*" *cortesi* "var." *portisi* (UCMP 219135); **A**, medial view; **B**, lateral view; **C**, ventral view; **D**, dorsal view. Scale bar: 3 cm.

developed and knob-like lateral tuberosity is present on the lateral margin of the anterior process, anterior to the position of the fenestra vestibuli. The oval-shaped fenestra vestibuli is positioned at the posteroventral end of the pars cochlearis, and a posteriorly oriented facial sulcus is present dorsolaterally to the fenestra vestibuli. A small, rectangular, and concave fossa for the stapedial muscle is positioned lateral to the posterior cochlear rest and posterior to the fenestra vestibuli. A relatively small, oval shaped, and deep suprameatal fossa occurs on the anterodorsal side of the pars cochlearis. The vestibulocochlear canal and facial canal are located on the posterodorsal portion of the pars cochlearis. Both canals are circular and small, closely appressed, with a thin crista transversa. The endolymphatic and perilymphatic foramina are positioned posterior to the vestibulocochlear nerve canal, and occur in a deep fossa which is deeper at the dorsal end near the endolymphatic foramen (Fig. 20D). Both foramina are slit-like and open dorsally. The shallowly concave stylomastoid fossa is small, rectangular, and positioned dorsal to the fenestra cochleae. The dorsal side of the petrosal and anterior process is convex and rugose.

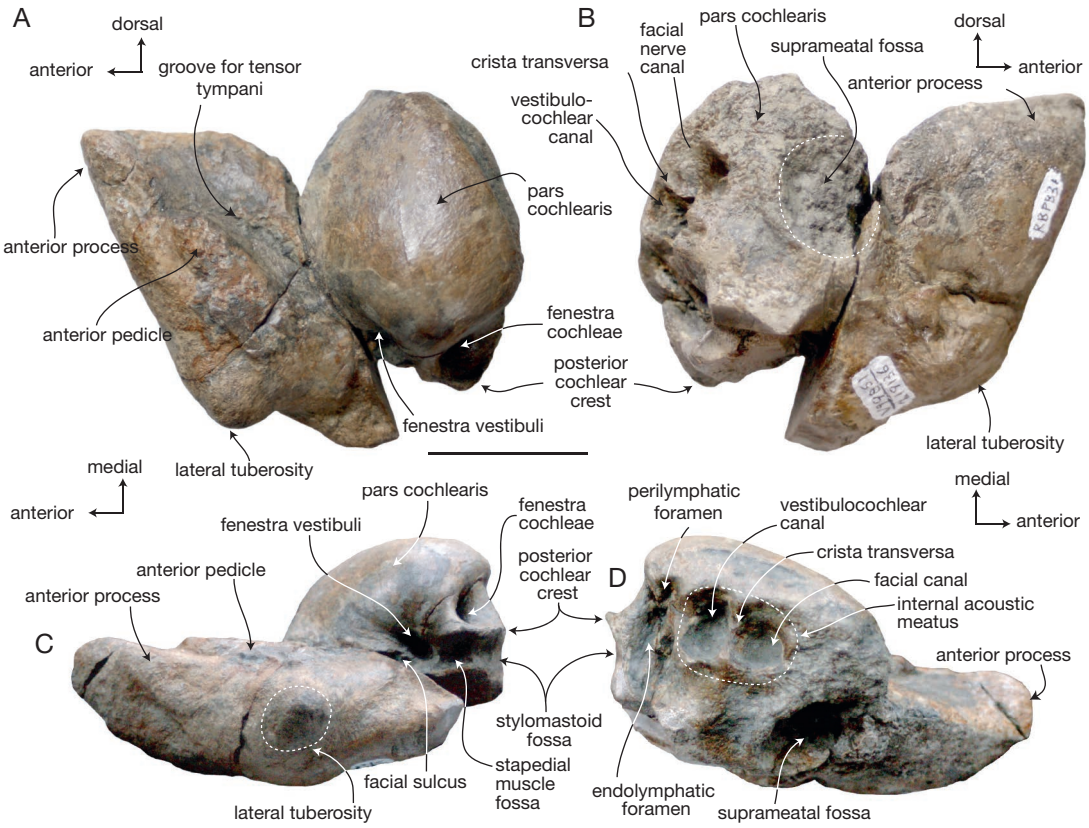

Fig. 20. — Right petrosal of cf. *Balaenoptera* (UCMP 219146); **A**, medial view; **B**, lateral view; **C**, ventral view; **D**, dorsal view. Scale bar: 3 cm.

Remarks and comparisons

This petrosal is identified as a balaenopterid because of the relatively wide and triangular anterior process and the medially elongated pars cochlearis. It differs from "*Balaenoptera*" *cortesi* "var." *portisi* (including UCMP 219135, described above) and *Megaptera novaeangliae* in lacking extreme medial elongation of the pars cochlearis, and in having a transversely thick anterior process. The cranial nerve canals of UCMP 219136 are located on the posterodorsal portion of the pars cochlearis, like extant *Balaenoptera* spp. and *M. novaeangliae* (Ekdale *et al.* 2011); this differs from many extinct balaenopterids including "*B.*" *cortesi* "var." *portisi*, *Diunatans luctoretmurgo*, and *Plesiobalaenoptera quarantellii*, in which the cranial nerve canals are centrally positioned on the dorsal face of the pars cochlearis (Bosselaers & Post 2010; Bisconti 2010a).

This specimen is tentatively referred to *Balaenoptera* owing to several features. The pars cochlearis of UCMP 219136 is more similar to extant *Balaenoptera* than to *Megaptera* or any described extinct balaenopterids; however, the anterior process differs from every modern species within *Balaenoptera* in being dorsally rather than anteriorly directed. Among extant *Balaenoptera*, the morphology of the pars cochlearis is closest to *Balaenoptera acutorostrata*; although the anterior process is of similarly short length between *B. acutorostrata* and UCMP 219136, it is anteriorly directed in extant *B. acutorostrata* and anterodorsally deflected in UCMP 219136. UCMP 219136 also differs from all extant species of *Balaenoptera* in this feature. This indicates that at least two balaenopterids are represented in the San Gregorio assemblage based

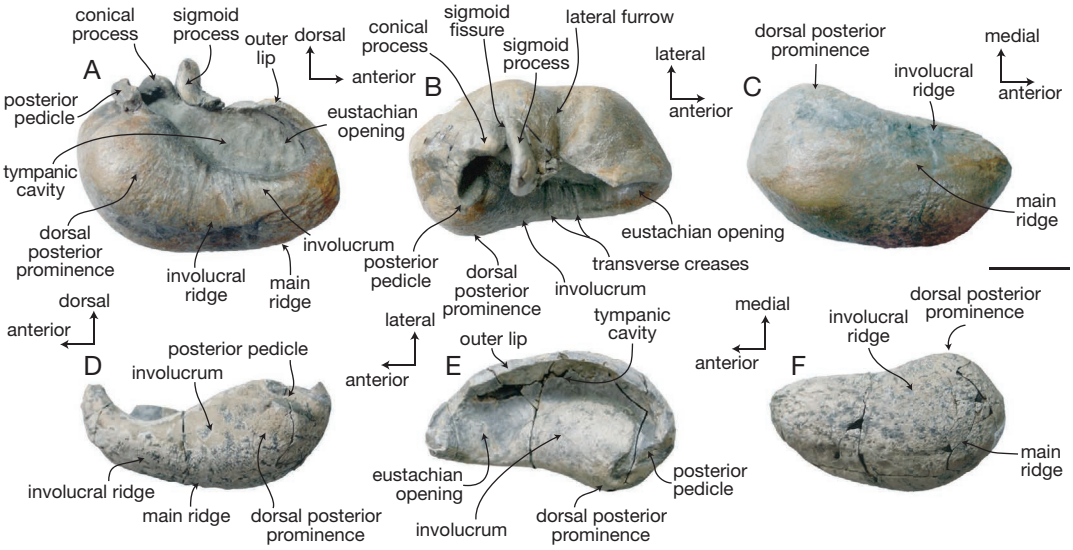

Fig. 21. — Tympanic bullae of Balaenopteridae gen. et sp. indet., morphotype 1; **A**, UCMP 219478, left tympanic in medial view; **B**, UCMP 219478 in dorsal view; **C**, UCMP 219478 in ventral view; **D**, UCMP 219097 in medial view; **E**, UCMP 219097 in dorsal view; **F**, UCMP 219097 in ventral view. Scale bar: 3 cm.

on petrosal morphology. UCMP 219136 is nearly identical in morphology to a fossil balaenopterid (SDNHM 80102) formerly identified as *Balaenoptera davidsonii* (Deméré *et al.* 2005), which now appears to represent a separate balaenopterid taxon (T. A. Deméré pers. comm. 2011). The skull of SDNHM 80102 lacks squamosal creases and has elongate zygomatic processes, unlike *Balaenoptera bertae* n. sp., and it is thus unlikely that UCMP 219136 is a petrosal of *B. bertae* n. sp.

Balaenopteridae gen. et sp. indet.

aff. *Plesiocetus* – Boessenecker 2006: 43A.

Referred material. — UCMP 219137, a right posterior process of a petrotympanic UCMP 219098, 219097, 219107, 219478, one left and three right tympanic bullae, and UCMP 219141, a fragment of the posterior end of a left mandible, collected by R.W. Boessenecker from UCMP localities V99834, V99835, V99836, V99840, and V99851.

Stratigraphic occurrence. — Lower and middle parts of the San Gregorio section of the Purisima Formation, latest Miocene to Early Pliocene (6.4-3.35 Ma; Messinian-Piacenzian equivalent; Fig. 2).

Description

Two balaenopterid morphotypes are represented by fossil tympanic bullae (Table 5). Morphotype 1 includes UCMP 219097 and 219478; except where noted, the description of this morphotype is based primarily on UCMP 219478 (Morphotype 2 described below). In medial and lateral aspect, the tympanic bulla is roughly oval (Fig. 21A), with subequally sized anterior and posterior lobes. A vertical shelf or flange along the anteromedial margin is absent. The involucrum is smooth, gently convex, and tapers anteriorly. The involucrum bears some faint transverse striations (Fig. 21A, D) and a well-developed dorsal posterior prominence (*sensu* Oishi & Hasegawa 1995b; Fig. 21C, F). In medial view, the tympanic cavity is anteriorly oval -shaped, and narrows posteriorly where it is pinched between the involucrum and sigmoid process. The conical process is blunt, low, and ventrally concave. The lateral furrow is broad and situated at the midpoint of the bulla. The sigmoid fissure (= posterior border of sigmoid process) is transversely oriented, deep, and ventrally shallows (Fig. 21B). The involucral and main ridges are posteriorly divergent and faintly developed. The

TABLE 8. — Measurements (in mm) of the posterior process of mysticete petrosals. Measurements given to nearest hundredth of a millimeter.

Specimens	Species	Length of posterior process	Greatest depth of posterior process
UCMP 219137	cf. *Balaenoptera*	167.65	59.18
UCMP 219114	*Herpetocetus* sp.	35.96	33.17
UCMP 219116	*Herpetocetus* sp.	38.73	36.39

TABLE 9. — Measurements (in cm) of mandibles of *Herpetocetus* Van Beneden, 1872. Curvilinear measured along lateral surface of mandible. Abbreviation: **(inc)**, incomplete measurement due to breakage. Measurements given to nearest tenth of a millimeter.

	UCMP 219077 *Herpetocetus* sp.	**UCMP 219079** *Herpetocetus bramblei*
Total length as preserved	48.78 (inc)	119.70
Depth at coronoid process	6.18	7.55
Length of coronoid crest	9.91	12.41
Depth at inward elevation	4.14	5.87
Depth at mandibular condyle	4.25	7.72
Greatest anteroposterior length of condyle	5.27	6.21
Transverse width of condyle	3.55	4.34
Depth at angular process	1.99	2.68
Width of angular process	–	6.41
Total length (curvilinear)	–	128.80

involucral ridge is separated from the main ridge along the ventral margin (Fig. 21A, D).

The tympanic bullae (UCMP 219098 and 219107) of Morphotype 2 are generally similar to those of Morphotype 1, but differ in a few characteristics, including their smaller size (Fig. 22; Table 5). No dorsal posterior prominence is developed. Slight transverse striations occur on the involucrum of UCMP 219098 (Fig. 22A), while more deeply incised transverse creases occur in UCMP 219107 (Fig. 22B). The involucral ridge is straight and retracted from the ventral margin (in dorsal aspect), and is roughly parallel with the main ridge. A vertical shelf or flange along the anteromedial margin is absent. The lateral surface of the outer lip is greatly inflated (Fig. 22C), and tympanic bullae of Morphotype 2 are relatively transversely wider than in Morphotype 1. The conical process is acutely triangular in medial aspect (Fig. 22A).

The isolated posterior process of the petrotympanic (UCMP 219137) is large (Table 9), anteroposteriorly flattened, and slightly curved posterolaterally (Fig. 23). It tapers laterally to become bladelike, and exhibits a sharp ventral crest. Along the anterior side of this crest, a shallow facial sulcus is present. Medially, the posterior process turns anteromedially toward the neck.

The mandible fragment (UCMP 219141) preserves part of the condyle, the angular process, and the ventral margin of the mandibular foramen, but lacks everything anterior to the mandibular foramen (Fig. 24). The mandibular condyle is large, hemispherical, and prominent laterally. The angular process is much smaller, and in medial and lateral views is shaped as a tabular process running ventral to the condyle along the ventral margin of the mandible. A transversely oriented groove separates the mandibular condyle from the angular process; the angular process is broadly visible in lateral view (Fig. 24B). The mandibular foramen is posterodorsally oriented, large, and transversely broad. The posteriormost section of the mandible is straight and parasagittally oriented, while anteriorly, the mandible bends strongly laterally, indicating a large degree of bowing of the horizontal ramus (Fig. 24A) as in *Balaenoptera* spp. and *Megaptera novaeangliae*.

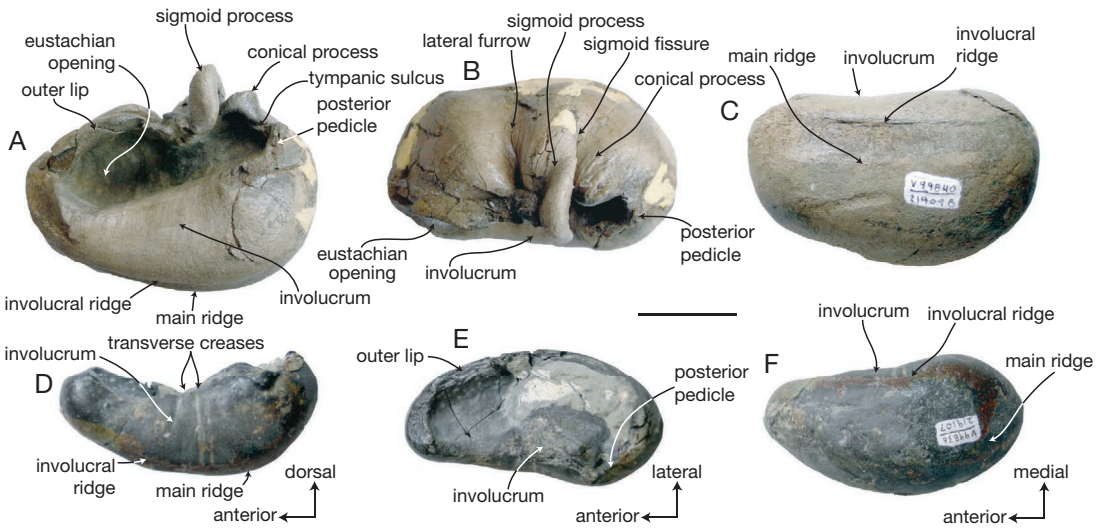

Fig. 22. — Tympanic bullae of Balaenopteridae gen. et sp. indet., morphotype 2; **A**, UCMP 219098, right tympanic bulla in medial view; **B**, UCMP 219098 in dorsal view; **C**, UCMP 219098 in ventral view; **D**, UCMP 219107, partial right tympanic bulla in medial view; **E**, UCMP 219107 in dorsal view; **F**, UCMP 219107 in ventral view. Scale bar: 3 cm.

Remarks and comparisons

These tympanic bullae (morphotypes 1 and 2) are referred to the Balaenopteridae based on their oval outline in medial aspect, simple sub-cylindrical involucra, lack of a dorsoventrally expanded and medially flattened involucrum as in Balaenidae, and being dorsoventrally shallower and transversely wider than extant *Eschrichtius robustus*; furthermore, their much larger size and lack of a median furrow precludes their assignment to Cetotheriidae (Oishi & Hasegawa 1995b; Ekdale *et al.* 2011). Morphotype 1 tympanic bullae share in common with extant *Megaptera* a large and robust dorsal posterior prominence, a feature which is lacking in most extant species of *Balaenoptera* as well as *Plesiobalaenoptera*, although some species of *Balaenoptera* exhibit a weakly developed dorsal posterior prominence. A slight dorsal posterior prominence occurs in *Diunatans luctoretmurgo*, although its bulla is substantially larger than UCMP 219478 and 219097 and differs in having a much more robust involucrum than the Purisima Formation specimens. These specimens differ in several regards from most extant *Balaenoptera* spp., including their smaller size (except *Balaenoptera acutorostrata* and *Balaenoptera bonaerensis*, which have smaller tympanic bullae). Most extant species of *Balaenoptera* exhibit an involucral ridge that is separated from the posterior margin (except *Balaenoptera musculus*), similar to *Megaptera novaeangliae* and these Purisima specimens. In dorsal view, the anterior portion of the involucra of these specimens and *M. novaeangliae* are much more constricted and have a large rounded eustachian opening; the latter feature is relatively smaller in *Balaenoptera*. These specimens are somewhat smaller than tympanic bullae of extant *M. novaeangliae*, and are transversely narrower with a less convex lateral surface. Due to the variability of bullar morphology in fossil and modern balaenopterids, Morphotype 1 bullae are only identified to the family level, despite similarities with *Megaptera*. It is unclear whether these specimens are referable to *Balaenoptera bertae* n. sp.

Morphotype 2 tympanic bullae differ from those of Morphotype 1 (see above) and extant *Megaptera* in lacking a robust dorsal posterior prominence (Fig. 24). The present specimens differ from *Balaenoptera*, *Diunatans*, and *Plesiobalaenoptera* in lacking a transversely flattened anteromedial shelf, in having a substantially more inflated lateral surface

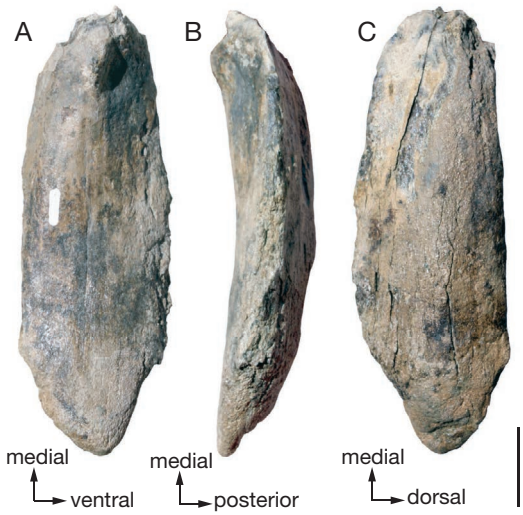

FIG. 23. — UCMP 219137, posterior process of right petrotympanic of Balaenopteridae gen. et sp. indet.: **A**, posterior process in anterolateral view; **B**, posterior process in ventral view; **C**, posterior process in posteromedial view. Scale bar: 3 cm.

of the outer lip, a sigmoid process that is positioned further posteriorly, and their much smaller size. UCMP 219098 further differs from *Plesiobalaenoptera* in lacking a distinctly convex anterior lobe in dorsal view and having a relatively larger eustachian opening; it further differs from *Balaenoptera* and *Plesiobalaenoptera* in having a smooth main ridge not developed into a slight ventral keel (Bisconti 2010a). These specimens lack the derived features of most previously described balaenopterids, and are relatively archaic in comparison to these taxa. However, they differ from all known balaenopterid and stem-balaenopteroid (= cetotheres *sensu lato*) taxa in exhibiting an extremely inflated lateral surface and a posteriorly positioned sigmoid process. Additional tympanic bullae from California similar to Morphotype 2 bullae include UCMP uncataloged (Field number FP 302, UCMP locality V90042) from an Upper Miocene (*c.* 5.33 Ma) locality in the Purisima Formation near Santa Cruz, and UCMP 88665 from the Upper Miocene San Luis Rey River Local Fauna of the San Mateo Formation (6-8 Ma) near Oceanside, California. Tympanic bullae agreeing in morphology to Morphotype 2 have occasionally been identified as "*Plesiocetus*" Van Beneden, 1859 (Barnes 1977; Oishi & Hasegawa 1995a). However, as detailed by Deméré *et al.* (2005), the generic taxon "*Plesiocetus*" has been applied incorrectly to a large number of different taxa, to the point where the application of this taxon has been inconsistent and confusing. Because of confusion surrounding the taxon "*Plesiocetus*" (Deméré *et al.* 2005; Bosselaers & Post 2010), future identifications should be avoided and Morphotype 2 bullae are only identified to the family level herein. It is unclear whether these specimens are referable to *B. bertae* n. sp.

The posterior process of a petrotympanic (UCMP 219137) shares with Balaenopteridae an elongate and strap-like posterior process with parallel dorsal and ventral margins (Fig. 23). It differs from herpetocetine mysticetes in being more elongate and larger in size and lacking a plug-like morphology with a flattened distal apex (Whitmore & Barnes 2008). It differs from *Eschrichtius* in being longer and lacking a ventrally expanded crest, and is precluded from assignment to the Balaenidae in being anteroposteriorly flattened, distally tapering in ventral view, and lacking a broad and well defined sulcus for the facial nerve. UCMP 219137 differs from *B. bertae* n. sp. its much larger size, and in lacking a slightly inflated distal apex that is not tapered and bladelike.

The mandible fragment (UCMP 219141) is also not identifiable beyond the family level because of its incompleteness. It exhibits two balaenopterid features. The first feature, a concave lateral margin of the posterior part of the mandible, results from the sigmoid curvature of the mandible; and the posterior ⅓ of the mandible in balaenopterids is medially bowed (while the anterior ⅔ is laterally bowed). The second feature is a robust angular process that is visible laterally, but does not extend posteriorly to the mandibular condyle; the angular process is not developed in balaenids, and in *Eschrichtius*, it is indistinct and not separated from the condyle by a crease as in UCMP 219141 and all balaenopterids. Based on its size, it can be eliminated from *B. bertae* n. sp., which is perhaps one-half the size of UCMP 219141. It is possible that it may belong to cf. *Balaenoptera*, "*B.*" *cortesi* "var." *portisi*, but is too incomplete to be identified beyond the family level.

Family CETOTHERIIDAE Brandt, 1872
Subfamily HERPETOCETINAE Steeman, 2007, *sensu* Whitmore & Barnes (2008)
Genus *Herpetocetus* Van Beneden, 1872

Herpetocetus bramblei
Whitmore & Barnes, 2008

REFERRED MATERIAL. — UCMP 219079, a complete left mandible collected by R.W. Boessenecker from UCMP V99854.

STRATIGRAPHIC OCCURRENCE. — Lowermost part of the San Gregorio section of the Purisima Formation, latest Miocene (6.4-5.6 Ma; Messinian equivalent; Fig. 2).

DESCRIPTION

This complete large (Table 9) mandible is relatively straight in lateral view and strongly laterally bowed in dorsal view ; it exhibits nearly continuous curvature along its length (Fig. 25). The horizontal ramus is twisted along its longitudinal axis so that posteriorly, the medial surface is vertical and faces medially, and anteriorly the medial surface of the ramus is obliquely oriented and faces dorsomedially (Fig. 25C, F). The anterior end is slightly dorsoventrally expanded, and a well-developed symphyseal groove occurs near the ventral border along the anteriormost part of the ramus (Fig. 25A, D). Below the symphyseal groove, the anteroventral extremity is extremely transversely compressed; a sharp ventral keel occurs on the anterior ⅓ of the mandible, whereas posteriorly, the ventral margin is rounded and lacks a crest. The mandible is planoconvex in cross section with a flat medial surface along its anterior 60 cm; the lateral surface becomes flattened towards the anterior end of the mandible (Fig. 26). Laterally adjacent to the blunt dorsal crest of the ramus is a series of eight mental foramina oriented tangentially to the arc of the mandible; each foramen opens anteriorly into a groove that extends for several centimeters. Where they overlap, the groove of the posterior foramen extends slightly lateral to the more anterior foramen. These grooves are shorter posteriorly, and the anteriormost foramen is open along the dorsal surface rather than adjacent to the dorsal crest (Fig. 25E, F). Gingival foramina are not evident on the medial surface.

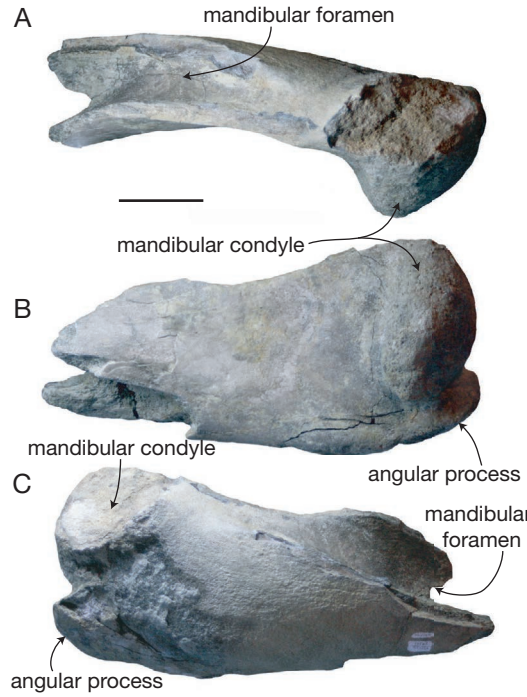

FIG. 24. — UCMP 219141, posterior fragment of left mandible of Balaenopteridae gen. et sp. indet.: **A**, mandible in dorsal view; **B**, mandible in lateral view; **C**, mandible in medial view. Scale bar: 10 cm.

The dorsal crest increases in height posteriorly towards the coronoid process. At the position of the coronoid process the medial surface is flat and vertically oriented. The coronoid process is elongate and elevated, and highest anteriorly where it is developed into a slight knob and is laterally hooked in cross-section (Figs 25, 26). A large and deep fossa for the temporalis insertion occurs on the lateral side of the coronoid process. In dorsal aspect, the apex of the coronoid process is anterolaterally directed. The coronoid crest decreases in height posteriorly and merges with a well defined ridge, which forms the medially directed inward elevation. A thin crest continues posterolaterally from the inward elevation, forming a thin plate that dorsally overhangs the mandibular foramen and merges with the mandibular condyle. The mandibular condyle is laterally offset from the mandible, and faces posterodorsally. The articular surface of

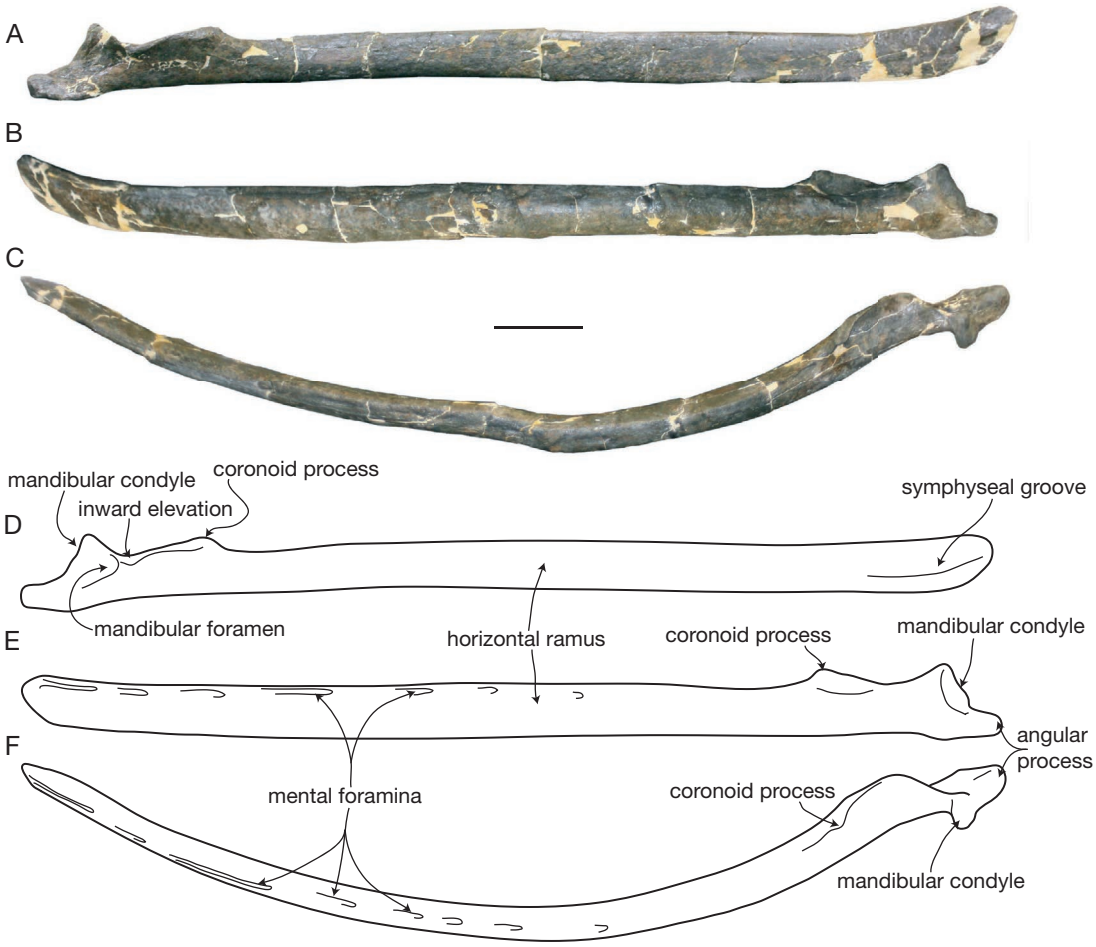

Fig. 25. — UCMP 219079, left mandible of *Herpetocetus bramblei* Whitmore & Barnes, 2008; **A**, medial view; **B**, lateral view; **C**, dorsal view; **D-F**, interpretive line drawing corrected for distortion in medial, lateral, and dorsal view (respectively). Scale bar: 10 cm.

the condyle is nearly flat, and in articular aspect, has a strongly convex lateral margin and a nearly flat medial margin, giving the condyle a "D"-shape. Along the posterolateral rim of the condyle is a sharp crest. The dorsal margin of the mandibular condyle is elevated above the apex of the coronoid process (Fig. 25A, B). The large mandibular foramen opens below the inward elevation with a V-shaped anterior margin of the opening. Ventrally, a thin crest forms the ventromedial margin of the foramen. The angular process is transversely broad and shelf-like; it extends posterior to the mandibular condyle. A knob for the digastric insertion occurs at the posterior end of the process, and there is a medial expansion of the angular process in dorsal aspect (Fig. 25A, C).

Comparisons

This specimen shares an anteroposteriorly elongate and laterally hooked coronoid process, laterally offset, posterodorsally facing and flattened mandibular condyle, and a posteriorly elongate and dorsoventrally flattened angular process with *Piscobalaena nana* Pilleri & Siber, 1989, *Herpetocetus*, and Herpetocetinae indet. (Boessenecker 2011b) to the exclusion of all other mysticetes, indicat-

ing that it represents a cetotheriid. However, the lack of an tongue-shaped anterior extension of the mandibular foramen margin precludes it from *Piscobalaena* Pilleri & Siber, 1989 and Herpetocetinae indet. (Boessenecker 2011b), and the more extreme elongation of the angular process identify this specimen as *Herpetocetus*.

Identification of the mandible UCMP 219079 as *Herpetocetus bramblei* is based on shared morphological features with UCMP 82465, similar geochronologic age, and the large size (for a herpetocetine) of both specimens. The holotype specimen of *Herpetocetus bramblei* (UCMP 82465) was collected from the uppermost Miocene part of the Santa Cruz section of the Purisima Formation (UCMP locality V-6875), and includes a partial braincase, a petrosal, a fragment of the supraorbital process of the frontal, a fragment of the maxilla, and a partial mandible. (Whitmore & Barnes 2008) The holotype mandible of *H. bramblei* lacks the anterior and posterior ends, and was estimated to be 90 cm long (Whitmore & Barnes 2008) and exhibits a dorsoventral depth similar to UCMP 219079. Given the similar dimensions of these specimens, it is likely that Whitmore & Barnes (2008) underestimated the mandibular length of *H. bramblei*, and the holotype mandible may have been 120 cm long, like UCMP 219079. Despite the lack of the supposedly distinctive posterior end of the mandible (see Boessenecker 2011b), the *H. bramblei* holotype exhibits other features consistent with the lectotype specimen of *Herpetocetus scaldiensis* Van Beneden, 1872 (e.g., longitudinal twisting of the ramus, planoconvex cross section, dorsoventral expansion of the anterior end of the mandible; Whitmore & Barnes 2008); however, these features also occur in *P. nana* (Bouetel & Muizon 2006) and indeterminate herpetocetine mandibles from the basal Upper Miocene Santa Margarita Sandstone (Boessenecker 2011b). However, Whitmore & Barnes (2008) mentioned the remarkably flat medial surface of the holotype mandible of *H. bramblei*, a feature shared with UCMP 219079. In addition to this feature, UCMP 219079 can be referred to *H. bramblei* based on its relatively large size. The middle of the horizontal ramus of the *H. bramblei* holotype mandible is roughly 60-70 mm in height, larger and more robust than all previously published herpetocetine specimens; similarly,

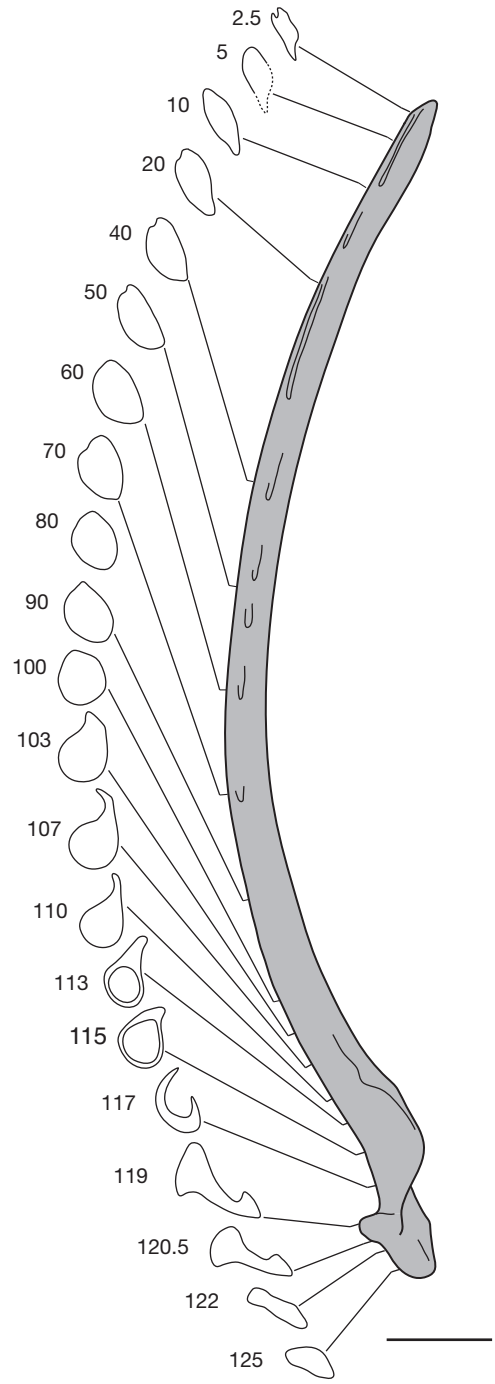

FIG. 26. — Cross sections of UCMP 219079, left mandible of *Herpetocetus bramblei* Whitmore & Barnes, 2008. Numbers adjacent to cross sections indicate distance from anterior tip (measured along the arc in centimeters). Scale bar: 10 cm.

UCMP 219079 is 60-65 mm high at the middle of the ramus. The mandible of the referred specimen (NSMP-PV 19540) of *Herpetocetus* "*sendaicus*" (Hatai, Hayasaka & Masuda, 1963) (Bouetel & Muizon 2006: fig. 31a; NSMP-PV 19540 may represent a separate taxon, as the holotype bulla of *Mizuhoptera sendaicus* is not diagnostic at the species level; Boessenecker 2011b) differs from UCMP 219079 in having a dorsally high coronoid process that is higher at its posterior end, a more laterally flaring angular process, and in its substantially smaller size. *H.* "*sendaicus*" shares with *H. bramblei* a mandibular condyle that is elevated higher than the coronoid process. The lectotype mandible (IRSNB M.379; formerly IRSNB 14) of *H. scaldiensis* differs from *H. bramblei* in having a shorter, laterally narrower angular process, a mandibular condyle not elevated above the coronoid process, a less steeply inclined articular surface of the condyle; it is also slightly smaller in overall size.

Remarks

Boessenecker (2011b) urged caution regarding the referral of isolated cetotheriid mandibles because of the presence of unusually geologically early *Herpetocetus*-like mandibles in the basal Upper Miocene Santa Margarita Sandstone (12-9 Ma; Repenning & Tedford 1977). Given the unknown mandible morphology of the slightly older herpetocetine *Nannocetus eremus* Kellogg, 1929 as well as the similarity of the potential herpetocetine *P. nana* (Bouetel & Muizon 2006: fig. 17), it is possible that the supposedly distinctive morphology of the *H. scaldiensis* lectotype may not be unique to *Herpetocetus* and may instead be characteristic of a more inclusive group of herpetocetines (Boessenecker 2011b). If the lectotype mandible of *H. scaldiensis* is not diagnostic, then the utility of the genus is uncertain and may necessitate taxonomic reevaluation (Boessenecker 2011b). Despite these issues, cranial specimens indicate that *Herpetocetus* is the only cetotheriid in the North Pacific during the Pliocene (*c.* 5.33-2 Ma; Oishi & Hasegawa 1995a, b; Whitmore & Barnes 2008; Boessenecker 2011b). In the context of latest Miocene and Pliocene specimens, it is reasonable to identify this specimen as *Herpetocetus* (Boessenecker 2011b).

Regarding the age of *H. bramblei*, Whitmore & Barnes (2008) indicated the type locality is "probably somewhat" younger than the basal glauconite of the Purisima Formation; the basal glauconite has been radiometrically dated at 6.79 Ma (recalibrated by Powell *et al.* 2007; reported as 6.7 Ma by Whitmore & Barnes 2008). The recent work of Powell *et al.* (2007) allows a more refined age determination for the type locality. The type locality of *H. bramblei* is the Crab Marker horizon of Madrid *et al.* (1986), and identified as the 5.33 Ma Miocene-Pliocene boundary by Powell *et al.* (2007); this stratigraphic level is bracketed below by the basal glauconite date (6.79 Ma). UCMP 219079 was collected from the base of the San Gregorio section of the Purisima Formation, and this locality has yielded a diatom flora correlative with the latest Miocene *Nitzchia reinholdii* Zone (Powell *et al.* 2007), indicating an age of 6.4-5.6 Ma. Thus, the ages of UCMP 219079 and the *H. bramblei* holotype are in accord, relative to the geochronologically younger *Herpetocetus* sp. material described below. Other new material (some topotypic) referable to *H. bramblei* (all from the Purisima Formation in Santa Cruz County) including multiple crania, earbones, and mandibles was summarized by Boessenecker & Geisler (2008).

Herpetocetus sp.

Referred material. — UCMP 219479, a partial juvenile right squamosal, UCMP 219114, a right petrosal with attached compound posterior process, UCMP 219115, a left petrosal lacking posterior process, UCMP 219116, isolated posterior process of a left petrotympanic, UCMP 219117, a partial right tympanic bulla, and UCMP 219077, a partial right mandible, collected by R.W. Boessenecker from UCMP localities V99836, V99840, and V99859.

Stratigraphic occurrence. — Middle and upper parts of the San Gregorio section of the Purisima Formation, Early to Late Pliocene (*c.* 5-2.5 Ma; Zanclean-Gelasian equivalent; Fig. 2).

Description

The squamosal (UCMP 219479) represents a juvenile or neonate based on its small size and lack of fused sutures with adjoining bones (e.g., alisphenoid, parietal, exoccipital). Dorsally, the squamosal is broadly

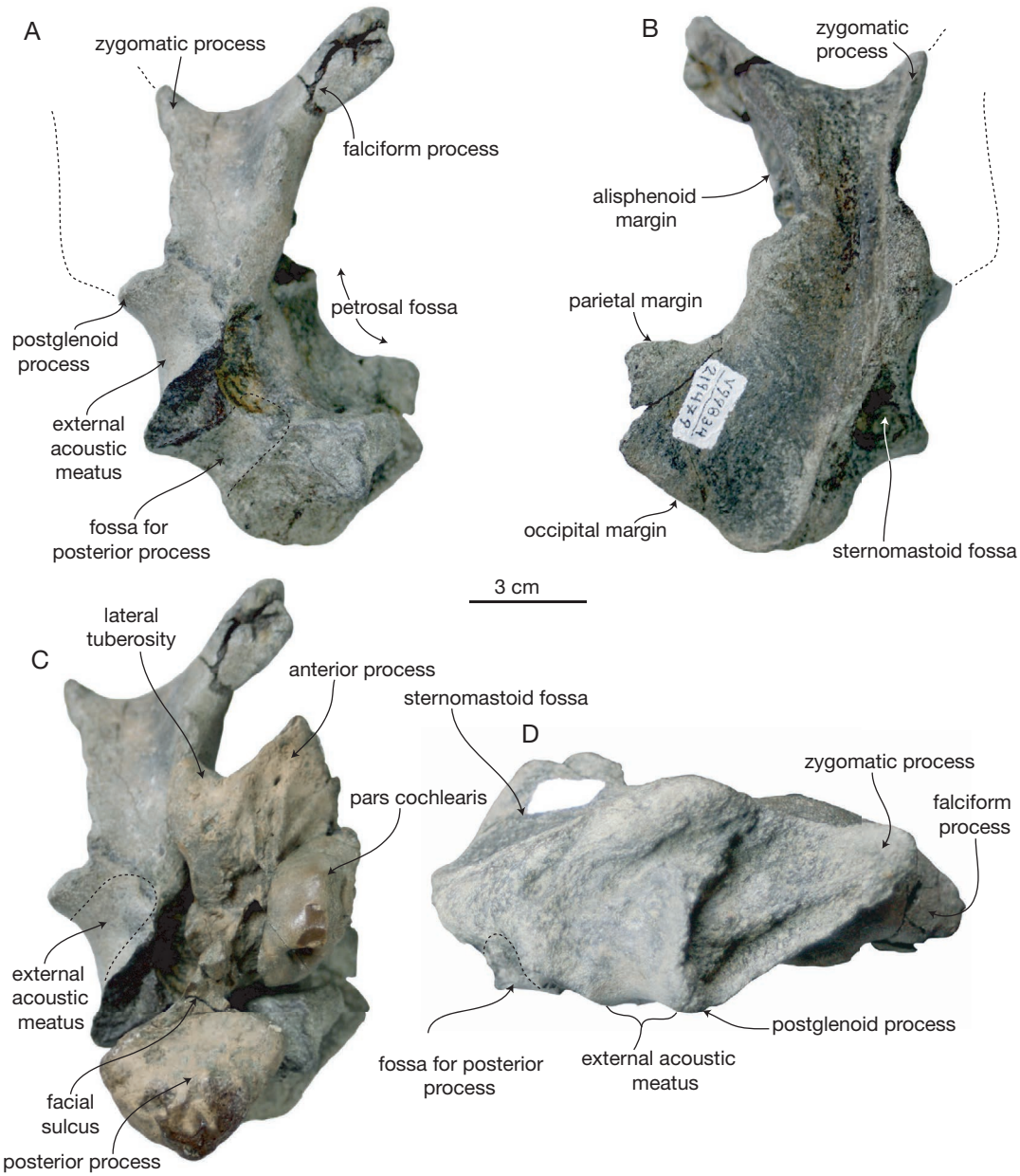

FIG. 27. — UCMP partial right squamosal (UCMP 219479) of *Herpetocetus* sp.; **A**, ventral view; **B**, dorsal view; **C**, ventral view with right petrosal and posterior process (UCMP 219114) in articulation; **D**, lateral view (without petrosal). Scale bar: 3 cm.

convex where it forms the dorsolateral roof of the braincase and exhibits a longitudinal and elongate fossa along the lateral margin (Fig. 27). Lateral to the fossa, the supramastoid crest is elongate, sharp, linear, and anteriorly oriented. Two ascending plates of the squamosal extend medial to the supramastoid crest; the squamosal plate extends dorsomedially from the posterior portion of the squamosal, while the

falciform process runs anteromedially to form the anterior margin of the braincase (Fig. 27B). There is a large division between the squamosal plate and falciform process; in more complete crania of *Herpetocetus*, this wedge-shaped division accommodates the postparietal foramen (Whitmore & Barnes 2008), the parietal (dorsally) and hypertrophied alisphenoid (anterodorsally). The zygomatic and postglenoid processes of UCMP 219479 are lost. Only a fragment of the medial edge of the zygomatic is present, but it shows that the process was anteriorly oriented. A knob-like process occurs along the supramastoid crest above the external acoustic meatus. The sternomastoid fossa is small, concave, triangular, and positioned posterior to the external acoustic meatus and immediately below the supramastoid crest (Fig. 27D). The lateral surface of the squamosal is otherwise flat. Ventrally, the external acoustic meatus is formed as a transversely oriented concavity posterior to the postglenoid process. Posteriorly, another semi-cylindrical concave fossa is present, oriented posterolaterally, and would have received the posterior process of the petrotympanic. The medial margin of the squamosal is concave where it forms the lateral wall of the petrosal fossa (Fig. 27A). A corrugated articular surface for the alisphenoid is present dorsomedially.

The isolated petrosals (UCMP 219114, 219115) are small (pars cochlearis length 29-33 mm; Table 7) and roughly lenticular in ventral view (Fig. 28). The pars cochlearis is small and medially elevated (Fig. 28A, E); the tensor tympani muscle origin is marked by deep groove on the medial surface of the anterior process (Fig. 28C, F). The anterior process is transversely compressed and bladelike, and appears rectangular in medial aspect. Dorsally adjacent to the groove for the tensor tympani muscle, a longitudinal ridge is present on the medial surface of the anterior process (Fig. 28C, G). The posterior cochlear crest has a strongly convex posterior margin in medial aspect; in ventral aspect it is well developed, and strongly overhangs both the stapedial muscle fossa and the stylomastoid fossa (Fig. 28C, G, H). The dorsal side of UCMP 219115 is convex and lacks a suprameatal fossa, while in UCMP 219114, it is nearly planar with a shallow suprameatal fossa. The canal for the vestibulocochlear nerve is large and circular, and is separated from the facial canal by a thick crista transversa (Fig. 28B, F). In dorsal aspect, the slit-like hiatus fallopii is confluent with the anterior margin of the facial canal, giving the facial canal a teardrop shape. Relative to the endolymphatic foramen, the perilymphatic foramen is much smaller (Fig. 28B); both are oriented slightly anterodorsally. At the position of the anterior part of the pars cochlearis, the lateral tuberosity is present along the ventral margin of the anterior process; it is ventrolaterally projecting as a flattened triangular flange in UCMP 219114 (Fig. 28A) and a large knob in UCMP 219115 (Fig. 28E). In UCMP 219115, a short groove (that widens and deepens anteriorly) is present along the anterior half of the lateral tuberosity, separating the lateral tuberosity and anterior process. Medial to the lateral tuberosity the broken anterior pedicle occurs as a small, anteroposteriorly short and bladelike crest. Between the anterior pedicle and the pars cochlearis is a relatively large, shallow mallear fossa. The fenestra vestibuli is oval and positioned posteromedial to the mallear fossa; the facial canal opens lateral to the fenestra vestibuli, and opens into the facial sulcus. The facial sulcus and fenestra vestibuli are separated by a thin crest (Fig. 28A). Posterior to the lateral tuberosity, a small convex ridge-like squamosal flange (*sensu* Geisler & Luo 1996) is ventrally prominent. The lateral surface of the petrosal is broadly convex in both specimens (Fig. 28A, B, E, F). Medially adjacent to the squamosal flange, the posterior pedicle is preserved in both specimens as a transversely thin crest.

The posterior process (UCMP 219115, 219116) is short (Table 8) and plug-shaped (Figs 28A-D; 29D-F); in UCMP 219115, there is a thin, constricted neck. The lateral surface of the posterior process is flat, triangular, and slightly rugose. The dorsolateral apex is anteroposteriorly tapered (Figs 28D; 29F). The short, deep facial sulcus occurs on the ventral side, and is bounded anterolaterally by a large, high, bladelike ridge (Figs 28D; 29F). Posteromedial to the facial sulcus is an anteroposteriorly thick, transversely oriented ridge, which is anteromedially convex and spherical. Medially adjacent to the neck of the posterior process is a small but well defined circular pit.

The partial right tympanic bulla (UCMP 219117) is abraded and missing most of the outer

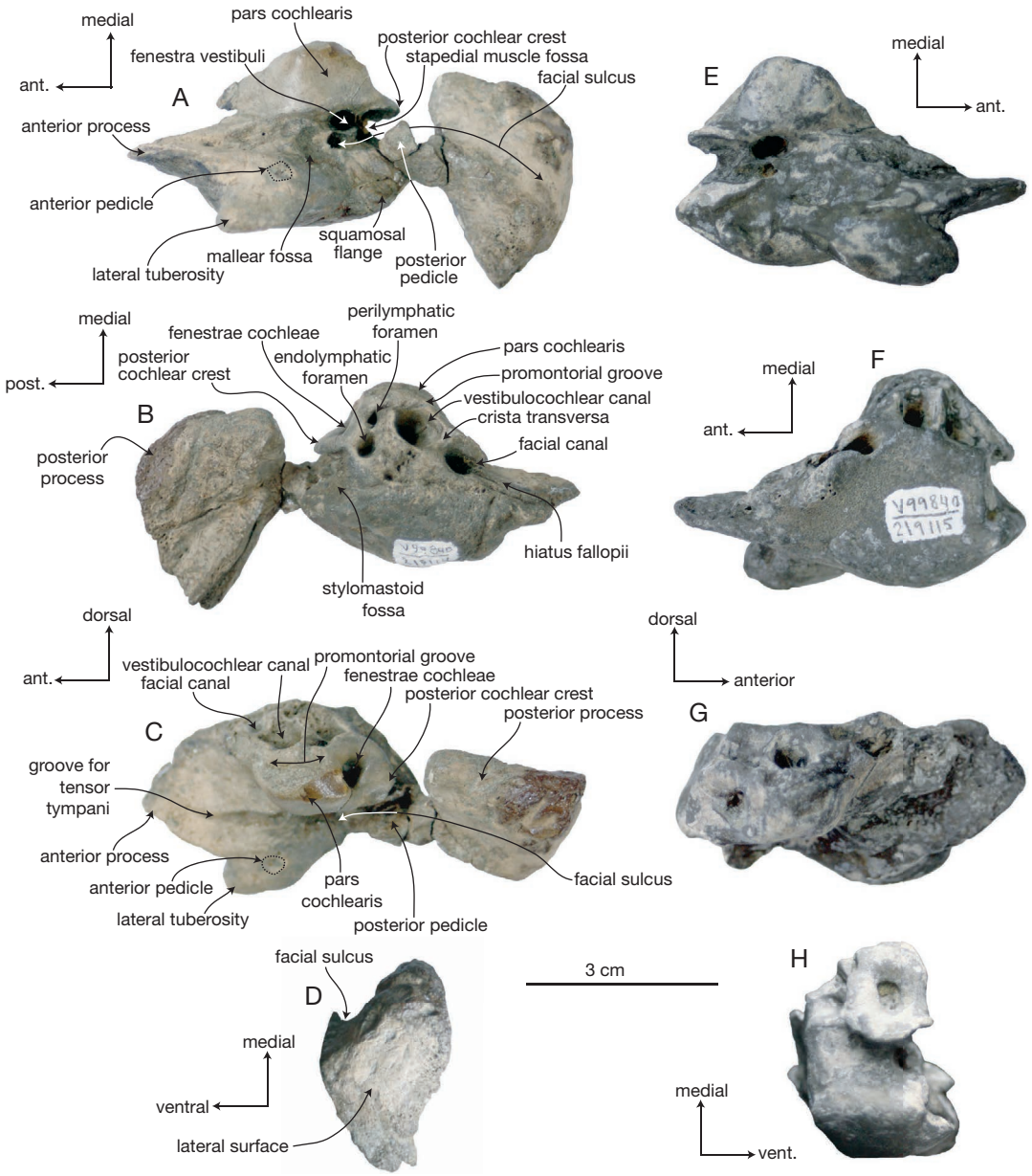

FIG. 28. — Petrosals of *Herpetocetus* sp.; right petrosal with attached compound posterior process, UCMP 219114 in **A**, ventral view; **B**, dorsal view, and **C**, medial view; **D**, compound posterior process of UCMP 219114 in posterolateral view; left petrosal UCMP 219115 in **E**, ventral view, **F**, dorsal view, **G**, medial view, and **H**, posterior view. Scale bar: 3 cm.

lip (Fig. 29A-C; Table 5). The involucrum is relatively thick with a well developed dorsal posterior prominence (Fig. 29B, C). In ventral aspect, the bulla is posteriorly bilobate: a fossa-like median furrow separates the medial and lateral lobes. The involucral and main ridges are posteriorly divergent

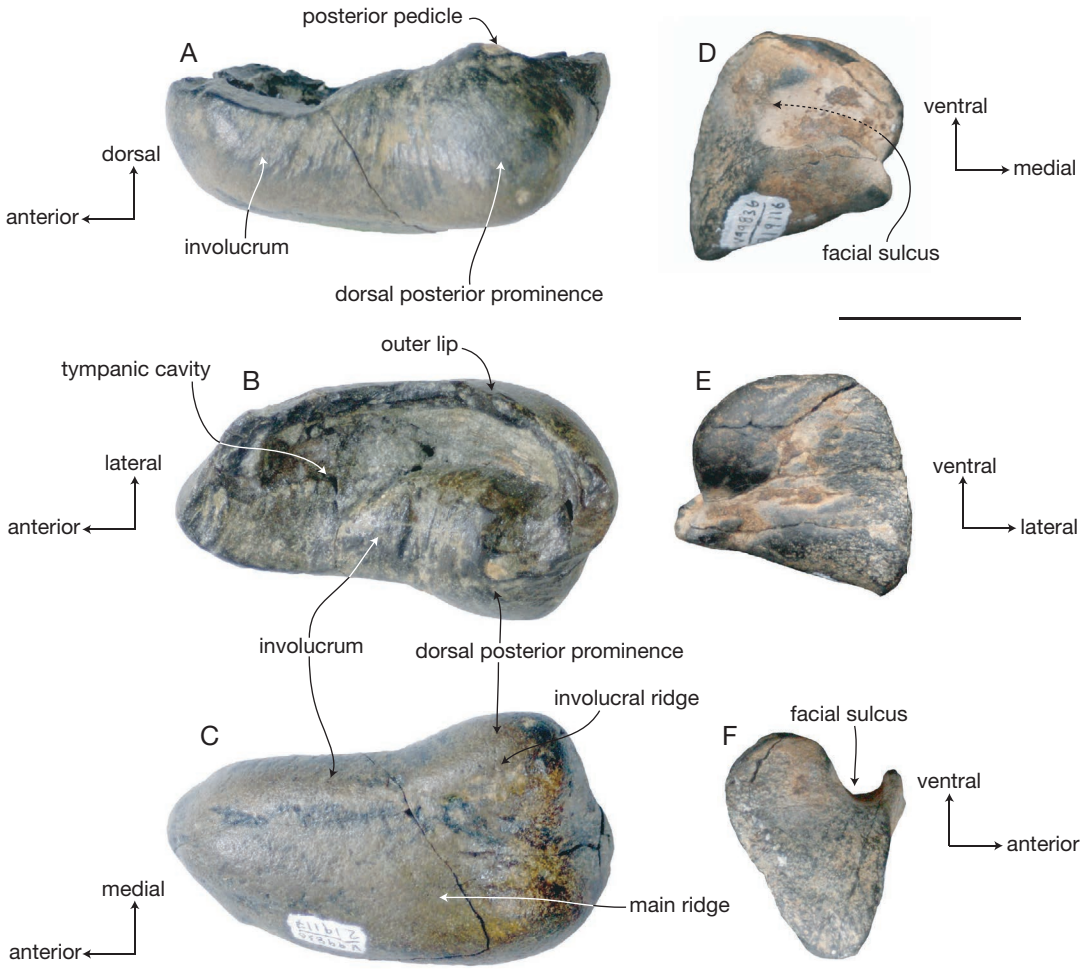

Fig. 29. — Petrotympanic elements of *Herpetocetus* sp.; **A**, UCMP 219117, partial right tympanic bulla in medial view; **B**, UCMP 219117 in dorsal view; **C**, UCMP 219117 in ventral view; **D**, UCMP 219116, compound posterior process of left petrotympanic in anterior view; **E**, UCMP 219116, posterior process of left petrosal in posterior view; **F**, UCMP 219116, posterior process of left petrosal in posterolateral view. Scale bar: 3 cm.

and widely separated (Fig. 29C). In medial aspect, the anterior portion of the involucrum is constricted, and the medial surface of the involucrum bears fine transverse striations.

The anterior half of the mandible (UCMP 219077) is missing, but the posterior portion is well-preserved (Fig. 30; Table 6) and similar to UCMP 219079 with a few exceptions (Table 6). Laterally adjacent to the dorsal crest, three mental foramina are preserved and open into anteriorly extending sulci (Fig. 30A). Two small gingival foramina occur on the medial surface, medially adjacent to the dorsal crest anterior to the coronoid process, also anteriorly opening but with shorter sulci than the gingival foramina. A large, deep, and anteroposteriorly elongate fossa on the lateral surface of the coronoid process extends anteriorly as a narrow concavity for the temporalis insertion below the anterior crest of the coronoid process. The mandibular condyle is laterally bilobate, with a slight fossa occurring on the lateral side dividing the condyle into dorsal and ventral lobes. A deep fossa occurs on the ventral

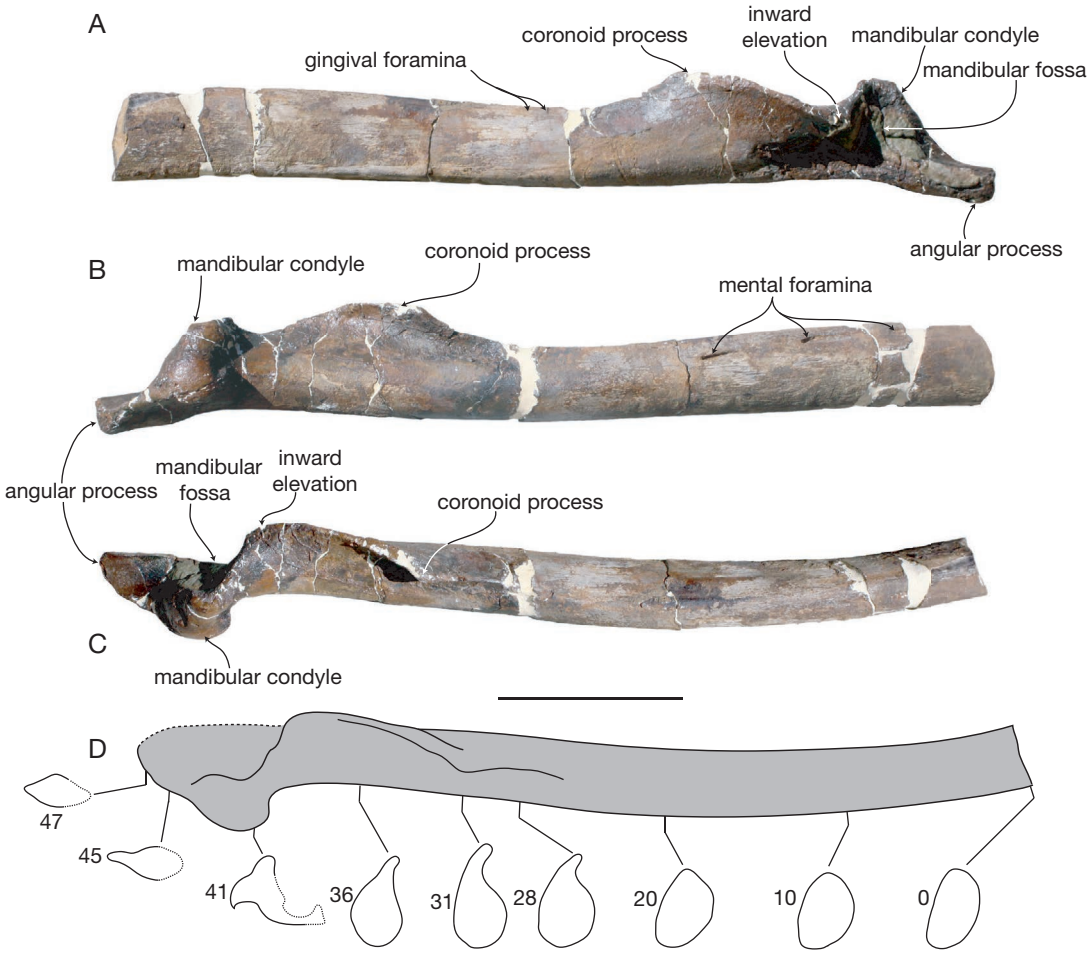

Fig. 30. — Partial right mandible of *Herpetocetus* sp. (UCMP 219077); **A**, medial view; **B**, lateral view; **C**, dorsal view; **D**, interpretive line drawing in dorsal view with cross section outlines (lateral direction in cross-sections is to left side). Numbers adjacent to cross sections indicate distance from broken anterior surface (measured in centimeters). Scale bar: 10 cm.

side of the condyle, forming a sharp ventromedially curving crest (Fig. 30D). The angular process extends far posterior to the condyle and dorsally exhibits a longitudinal groove.

Comparisons

These specimens can be referred to *Herpetocetus* owing to several characteristics. The squamosal (UCMP 219479) matches those of *Herpetocetus* as described by Whitmore & Barnes (2008) in possessing a large fossa for the posterior process of the petrotympanic, an elongate anteroposteriorly oriented trough-like fossa on the squamosal medial to the supramastoid crest, and a large wedge-shaped dorsomedial margin to accommodate the alisphenoid and postparietal foramen. The squamosal differs from *Herpetocetus bramblei* in exhibiting a small sternomastoid fossa that does not extend anterior to the level of the external acoustic meatus. The petrosals bear a laterally compressed, bladelike anterior process (which characterizes *Herpetocetus* and *Nannocetus* Kellogg, 1929; Geisler & Luo 1996; Whitmore & Barnes 2008), a large lateral projection (*sensu* Geisler & Luo 1996; = lateral tuberosity, Mead & Fordyce 2009)

of the anterior process (unique to *Herpetocetus*; Geisler & Luo 1996; Whitmore & Barnes 2008), and a short plug-shaped posterior process (a potential synapomorphy of herpetocetines; Bouetel & Muizon 2006; Steeman 2007; Whitmore & Barnes 2008). The squamosal (UCMP 219479) was placed in articulation with UCMP 219114 (Fig. 27C), a petrosal with attached posterior process from a separate individual (see description above); the tight articulation of these two elements strongly supports the identification of these as the same taxon.

The tympanic bulla (UCMP 219117) is referred to *Herpetocetus* sp. because of its small size, distinct dorsal posterior prominence, median groove, distinct transverse creases on the involucrum, and close phenetic similarity to previously published tympanic bullae of *Herpetocetus* (Whitmore & Barnes 2008). A newly referred (and nearly complete) skull of *H. bramblei* (UCMP 219111) introduced by Boessenecker & Geisler (2008) includes both petrosals and a tympanic bulla, the latter of which is not preserved in the holotype. The isolated tympanic bulla (UCMP 219117) differs from the well-preserved tympanic bulla of UCMP 219111 in its smaller size, less distinct transverse creases, much lower dorsal posterior prominence, a shallower furrow on the medial surface between the dorsal prominence and the posterior lobe, and lacking a sharp spur on the ventral tip of the dorsal posterior prominence. UCMP 219117 differs from *Herpetocetus transatlanticus* Whitmore & Barnes, 2008, the referred specimen of *H.* "*sendaicus*", and the holotype bulla of *H. sendaicus*, in having a transversely narrower involucrum with a smaller and more defined dorsal posterior prominence. It also differs from *Piscobalaena* and *Nannocetus* in exhibiting a more strongly developed dorsal posterior prominence and having a more constricted anterior portion of the involucrum.

The mandible (UCMP 219077) exhibits characteristic features of *Herpetocetus*, including an elongate and laterally hooked coronoid process, a posteromedial sloping mandibular condyle, and a posteriorly projecting and shelf-like angular process (see above remarks under *H. bramblei*; Boessenecker 2011b; Whitmore & Barnes 2008). This specimen is unique among herpetocetines (and possibly among mysticetes) in having a fossa on the lateral surface of the condyle, giving it a bilobate morphology. It is further distinct from *Piscobalaena, H.* "*sendaicus*", *H. bramblei*, and indeterminate herpetocetine mandibles (Boessenecker 2011b) in having a fossa for the temporalis insertion that extends anteriorly beyond the coronoid process; this feature is slightly developed in *H. scaldiensis*. UCMP 219117 is roughly the same size as the mandible of *H.* "*sendaicus*", and is much smaller than UCMP 219076 described above. As mentioned above, the mandibular morphology of herpetocetines may not be diagnostic at the genus level (Boessenecker 2011b), but some subtle mandibular features may be taxonomically useful among species of *Herpetocetus*.

Remarks

These specimens appear to represent an undescribed species of *Herpetocetus* morphologically distinct from and geochronologically younger than *H. bramblei*; additional material of this taxon is recorded from the Santa Cruz section of the Purisima Formation (see below). The squamosal, petrosals, and mandible exhibit several differences with *H. bramblei* (see above). These specimens are from higher up in the San Gregorio section than the mandible of *H. bramblei* (UCMP 219079), and occur in younger strata with occasional *Patinopecten healelyi* shells, the latter indicating a Pliocene age (Powell *et al.* 2007). The mandible (UCMP 219077) was collected from between two tephra layers dated at 2.5 and 3.35 Ma, indicating an Early to Late Pliocene age (Piacenzian-Gelasian equivalent) for this specimen. All other specimens were collected below the 3.35 Ma tephra, and above the aforementioned 6.4-5.6 Ma (Late Miocene) diatom flora; they are likely Early-Late Pliocene (Zanclean-Piacenzian equivalent) in age due to their association with Pliocene mollusks and *Carcharodon carcharias* teeth (Boessenecker 2011a). These specimens are all younger than the 6.79-5.33 Ma age for the type locality of *H. bramblei*. Likewise, these specimens differ from *H. bramblei*. The squamosal (UCMP 219479) exhibits a small sternomastoid fossa that does not extend anteriorly past the external acoustic meatus (Fig. 27D); in *H. bramblei*, the sternomastoid fossa is much larger. A similarly small sternomastoid fossa occurs in a

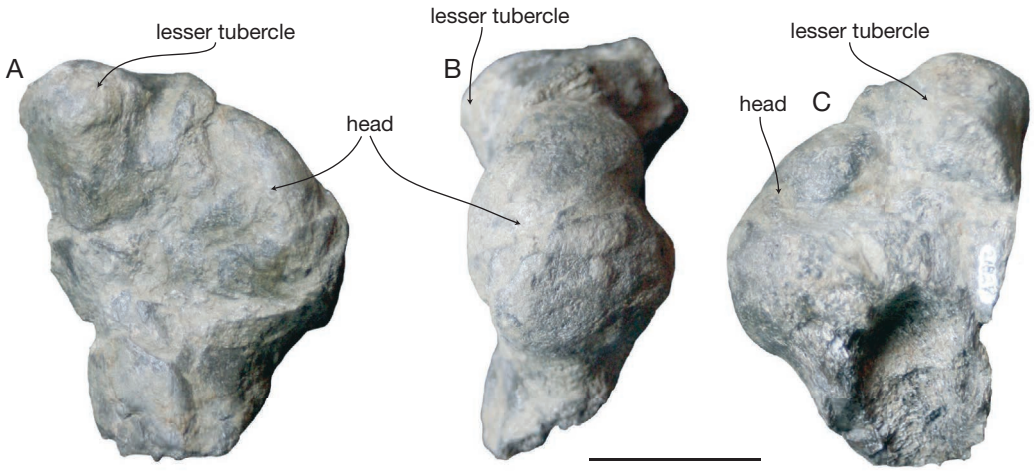

FIG. 31. — Partial humerus of Odontoceti gen. et sp. indet.: **A**, UCMP 219175, anterior or posterior view; **B**, UCMP 219175 in medial view; **C**, UCMP 219175 in anterior or posterior view. Scale bar: 3 cm.

Herpetocetus sp. braincase (UCMP 219121) from the Lower Pliocene Purisima Formation near Santa Cruz (5.33-4.5 Ma; Zanclean equivalent). The petrosals (UCMP 219114 and 219115) are relatively similar to the holotype of *H. bramblei*, but both differ from it in having a posteriorly elongate and transversely thin posterior cochlear crest, and a thick crista transversa; the crista transversa in the *H. bramblei* holotype is thin, and the posterior cochlear crest is short. The *H. bramblei* holotype petrosal further differs in having elongate prongs of bone on the dorsal surface, and having a circular facial canal which lacks an anterior fissure (as opposed to the teardrop shaped facial canal described above in UCMP 219114 and 219115). UCMP 219115 also differs from *H. bramblei* (and all other herpetocetines) in exhibiting a bulbous lateral projection of the anterior process (Fig. 28E).

These specimens are distinct from *H. bramblei*, and indicate the presence of a second, younger undescribed species within the Purisima Formation. Additional material from the lower Pliocene section of the Purisima Formation (Zanclean-Piacenzian equivalent) near Santa Cruz includes a skull with earbones (UCMP 219121) and several isolated petrosals (UCMP 219118, 219119) that share this same morphology. As this more diagnostic material is from a locality separate from material described herein, it is beyond the scope of this study to describe this new taxon, and will be considered in a separate study.

Suborder ODONTOCETI Flower, 1867

Odontoceti gen. et sp. indet.

REFERRED MATERIAL. — UCMP 219175, one partial left humerus collected by R.W. Boessenecker from UCMP locality V99854.

STRATIGRAPHIC OCCURRENCE. — Lowermost part of the San Gregorio section of the Purisima Formation, latest Miocene (6.4-5.6 Ma; Messinian equivalent; Fig. 2).

DESCRIPTION

The partial humerus (UCMP 219175) is missing the distal end, and is slightly transversely crushed (Fig. 31). UCMP 219175 is tentatively identified as a left humerus, and is relatively large for an odontocete. The humeral head is large and oval in articular aspect, and was possibly circular prior to diagenetic compaction. The lesser tubercle is anteroposteriorly broad and oval-shaped in proximal aspect. An anteromedially oriented crest occurs on the proximal end, connecting the humeral head and the lesser tubercle. The humeral head is narrower than the lesser tuber-

cle, and is oriented dorsomedially (Fig. 31). UCMP 219175 appears to lack a greater tubercle.

Remarks and comparisons

This specimen (UCMP 219175) differs from all fossil and modern phocoenids and many non-globicephaline delphinids (except *Tursiops* Gervais, 1855) in its larger size; although a humerus is not yet known for *Parapontoporia* Barnes, 1984, this specimen is almost certainly too large to belong to it. UCMP 219175 is similar in size and morphology to *Albireo whistleri* Barnes, 1984. This specimen differs from kogiid humeri in lacking a prominent deltopectoral crest, and by having a lesser tubercle that is wider than the humeral head (Kazár & Bohaska 2008). UCMP 219175 differs from pontoporiids in its much larger size and exhibiting a transversely wider lesser tubercle (Kazár & Bohaska 2008). This specimen differs from larger physeteroids in lacking a proximally small lesser tubercle and having a relatively thinner shaft (Kazár & Bohaska 2008); it is not a ziphiid because of its possession of a larger and more prominent lesser tubercle. This specimen further differs from non-globicephaline delphinids in having a more elongate shaft (Kazár & Bohaska 2008). Because this specimen is similar to both the monodontid *Delphinapterus* Lacépède, 1804, *Albireo* Barnes, 1984, and globicephaline delphinids, it is not identified to a more exclusive clade.

Infraorder DELPHINIDA Muizon, 1988
Superfamily Lipotoidea Muizon, 1988
Family Lipotidae Zhou, Qian & Li, 1978
sensu Geisler *et al.* (2011)
Genus *Parapontoporia* Barnes, 1984

Parapontoporia sternbergi
(Gregory & Kellogg, 1927)

Referred material. — UCMP 219700, a nearly complete skull missing the tip of the rostrum and the pterygoid, with associated right and left petrotympanics and fragment of right mandible, collected by R.W. Boessenecker and C. Pirrone from UCMP locality V99884.

Stratigraphic occurrence. — Middle part of the San Gregorio section of the Purisima Formation, Early Pliocene (*c.* 3.35 Ma; Piacenzian equivalent; Fig. 2).

Description

Measurements of this specimen are presented in Tables 10-12. The skull of UCMP 219700 is nearly complete; the petrotympanics were found near the vertex. CT imaging of the left petrotympanic complex revealed the malleus and incus in articulation, but failed to identify the stapes; rather than being absent, it is likely poorly visible in CT data due to the highly concretionary matrix surrounding the petrotympanics. UCMP 219700 exhibits a relatively small braincase and an elongate and attenuate rostrum (Figs 32-34) that is nearly triangular in cross section, dorsoventrally deep, with a flat, narrow palate. The rostrum tapers anteriorly, and is transversely broad and dorsoventrally deep at its base. Posteriorly, a deep rostral basin on the dorsal surface of the rostrum is formed by the maxilla and premaxilla; this basin extends from the anterior facial region to about 5 cm anterior to the antorbital notch (Fig. 32). The facial region is pentagonal in dorsal aspect and slightly wider than long (Fig. 32), and the right ascending process of the maxilla is distinctly wider than the left.

The premaxillae of UCMP 219700 form most of the dorsal surface of the rostrum; they are transversely convex and nearly touch medially, exposing a narrow (<1 mm wide) and open mesorostral gutter with parallel margins. On the dorsolateral surface of the rostrum, there is a deep lateral groove at the premaxilla-maxilla contact (Fig. 33A, C), which extends along the length of the rostrum anterior to the rostral basin, giving the rostrum a trilobate cross section. On the middle of the rostrum, the premaxilla faces dorsolaterally and together the premaxillae form a dorsal median ridge. About 7-8 cm anterior to the antorbital notch, the premaxilla is dorsally flattened; the premaxilla gradually widens posteriorly. About 5 cm anterior to the antorbital notch the premaxilla is twisted and faces dorsomedially. Posterior to the antorbital notch, the nasal portion of the premaxilla is transversely wide; the right nasal process of the premaxilla is obscured by the mandible and adherent matrix (Fig. 32). The left nasal process is dorsally flat and plate-like, and widest anteriorly; the premaxillary foramen perforates the premaxilla anterolateral to the bony nares and is confluent with a deep, elongate poste-

TABLE 10. — Measurements (in cm) of odontocete crania. *, denotes partial measurement to midline and multiplied by two; **(inc)**, denotes incomplete measurement due to breakage. Measurements given to nearest tenth of a centimeter.

	UCMP 219700 *Parapontoporia sternbergi*	**UCMP 219123** cf. *Phocoena*	**UCMP 219503** Phocoenidae unnamed genus 2
Total length as preserved	40.4 (inc)	18.4 (inc)	34.8
Length of rostrum	28.9 (inc)	–	17.9
Depth at base of rostrum	4.3	2.83	2.9
Breadth of base of rostrum	5.2*	7.8*	8.1
Width across antorbital processes	10.5	–	13.2
Width across postorbital processes	12.9	–	15.2
Zygomatic width	12.8	–	15.8*
Width across condyles	5.4	–	7.8
Breadth across premaxillary eminences	–	4.6*	4.9
Height of premaxillary eminences	–	1.4	1.5
Posterior width of braincase	10.9	–	13.6
Width of bony naris	2.6*	–	2.9
Length of bony naris	2.6	–	3.2
Width of foramen magnum	2.5	–	4.0
Height of foramen magnum	2.4	–	2.5
Height of temporal fossa	4.3	–	3.2
Length of temporal fossa	5.8	–	7.1
Height of skull at vertex	11.3	–	14.3

TABLE 11. — Measurements (in mm) of odontocete petrosals. Measurements given to nearest tenth of a millimeter.

	UCMP 219700 (left) *Parapontoporia sternbergi*	**UCMP 219700** (right) *P. sternbergi*	**UCMP 219480** Phocoenidae unnamed genus 1
Total length as preserved	32.6	32.3	28.5
Length of pars cochlearis	14.1	14.2	17.2
Transverse width of inner acoustic meatus	3.6	3.6	4.2
Length of inner acoustic meatus	5.5	5.5	9.2
Length of anterior process	20.8	20.8	14.9

TABLE 12. — Measurements (in mm) of odontocete tympanic bullae. Measurements given to nearest tenth of a millimeter.

Specimens	**Taxon**	**Greatest length as preserved**	**Dorsoventral depth of involucrum**	**Greatest transverse width of tympanic bulla**
UCMP 219174	Delphinidae indet.	28.3	8.9	17.1
UCMP 219175	Phocoenidae indet.	28.4	7.8	14.1
UCMP 219034	cf. Globicephalinae indet.	41.0	10.5	21.8
UCMP 219700	*Parapontoporia sternbergi* (left)	32.2	23.0	19.9
UCMP 219700	*Parapontoporia sternbergi* (right)	34.1	23.8	20.4

rolateral sulcus which continues to the position of the posterior margin of the bony nares. The nasal process tapers posteriorly and curves posterolaterally around the bony naris; the ascending process bears a round termination that does not contact the nasal, but extends posterior to the anterior margin of the nasal.

The maxilla forms the ventral, lateral, and dorsolateral portions of the rostrum of UCMP 219700. 44 and 50 alveoli are preserved on the left and right

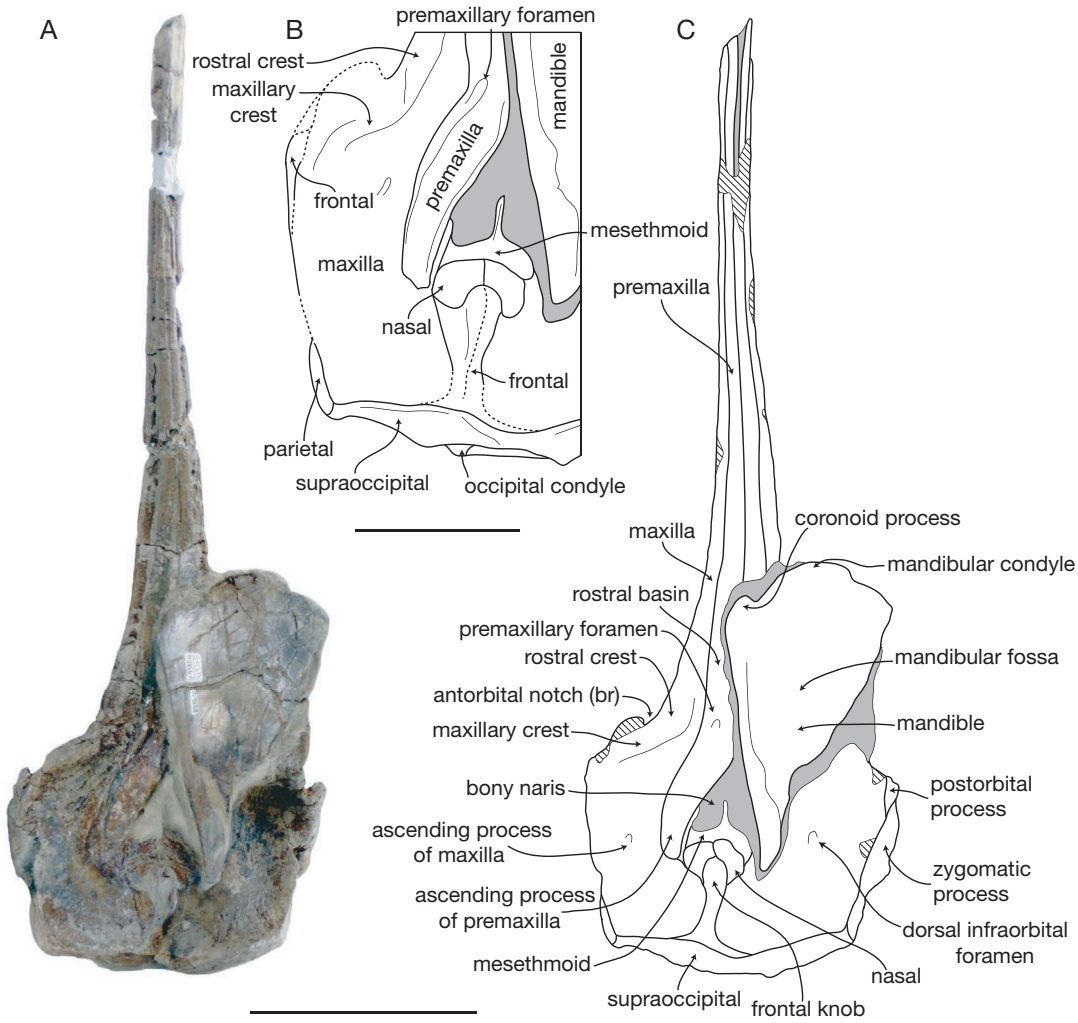

FIG. 32. — UCMP 219700, skull and partial mandible of *Parapontoporia sternbergi* (Gregory & Kellogg, 1927); **A**, dorsal view; **B**, interpretive line drawing in of left facial region of skull in dorsal view; **C**, interpretive line drawing in dorsal view; gray indicates adhering matrix, and cross-hatching indicates damaged bone. Scale bars: A, C, 10 cm; B, 5 cm.

maxillae (respectively); 32 and 25 of these are well-preserved and indicated in the illustration (Fig. 33). The rostral portion of the maxilla is laterally convex in cross section. Anterior to the antorbital notch, the maxilla forms a large, dorsolaterally directed boss-like rostral crest (*sensu* Mead & Fordyce 2009; = maxillary eminence of Barnes 1985b); this ridge extends dorsally above the level of the premaxillae to form the lateral margin of the rostral basin (Figs 32, 33). A slight fossa occurs on the ventrolateral surface of the maxilla below this ridge. On the ventral surface of the anterior portion of the rostrum, there is a deep median groove between the ventrolaterally facing tooth rows. Posteriorly, the palatal surface of the maxilla widens and the ventral surface becomes flattened; further anteriorly, the palatal surface of the maxilla is transversely convex. The alveolar row ends at the level of the anterior part of the rostral basin, approximately 5 cm anterior to the antorbital notch. The palate is ventrally convex in cross section

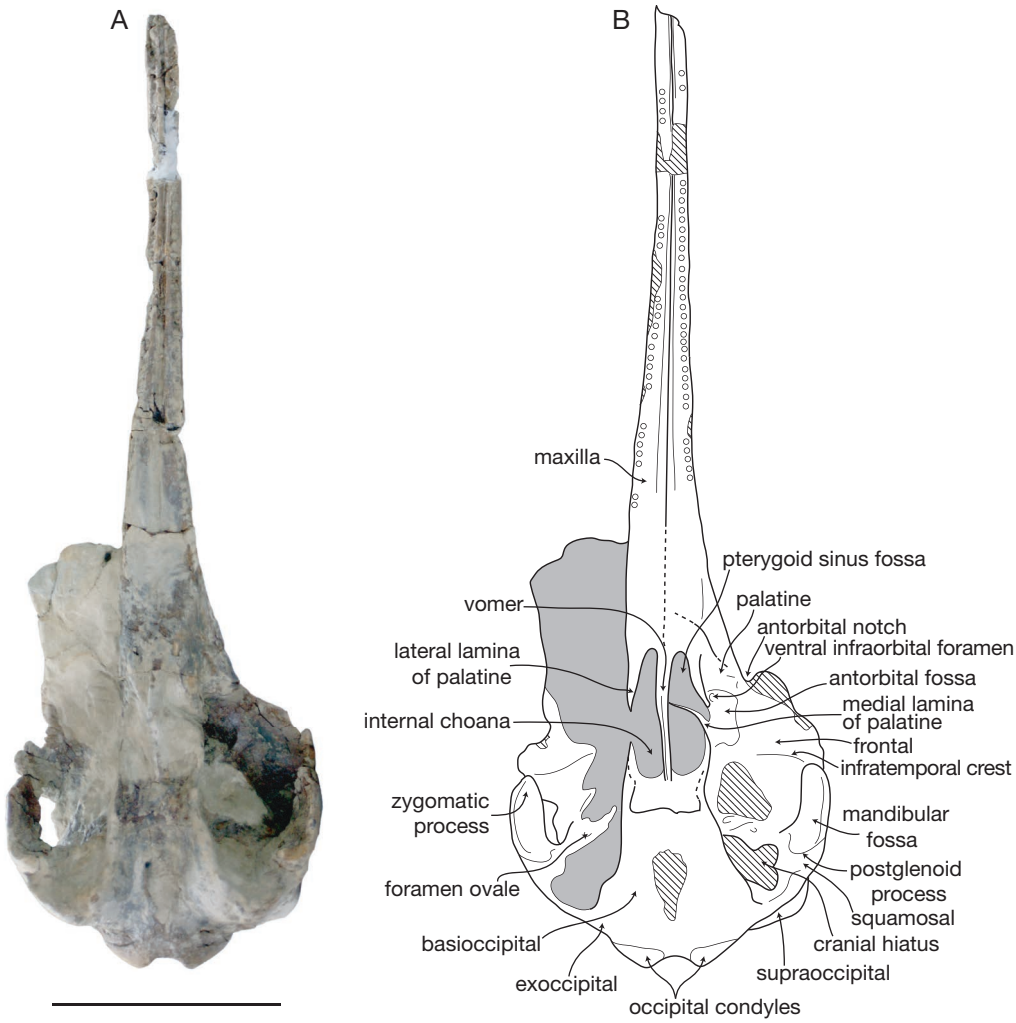

FIG. 33. — UCMP 219700, skull and partial mandible of *Parapontoporia sternbergi* (Gregory & Kellogg, 1927); **A**, ventral view; **B**, interpretive line drawing in ventral view; gray indicates adhering matrix, and cross-hatching indicates damaged bone. Scale bar: 10 cm.

at the base of the rostrum. The maxillo-palatine suture appears to be anteromedially oriented and its lateral portion emanating medial to the antorbital notch. The rostral crest (*sensu* Mead & Fordyce 2009) ends posteriorly in a subtle boss anteromedial to the antorbital notch; it is posteriorly continuous with an anteromedially oriented maxillary crest (*sensu* Mead & Fordyce 2009) positioned posterior to the antorbital process. The left antorbital process is missing, but would have been positioned on the elevated maxillary crest, which demarcates the anterior margin of a shallow anteromedially directed trough on the maxilla (Figs 32, 33). This trough is laterally adjacent to the premaxillary sac fossae. The ascending process of the maxilla is posteriorly broad and plate-like. Medial to the antorbital process, a large dorsal infraorbital foramen opens posteriorly into a deep sulcus. Posteriorly, the ascending process curves around and posterior to the bony nares and toward the frontal knob.

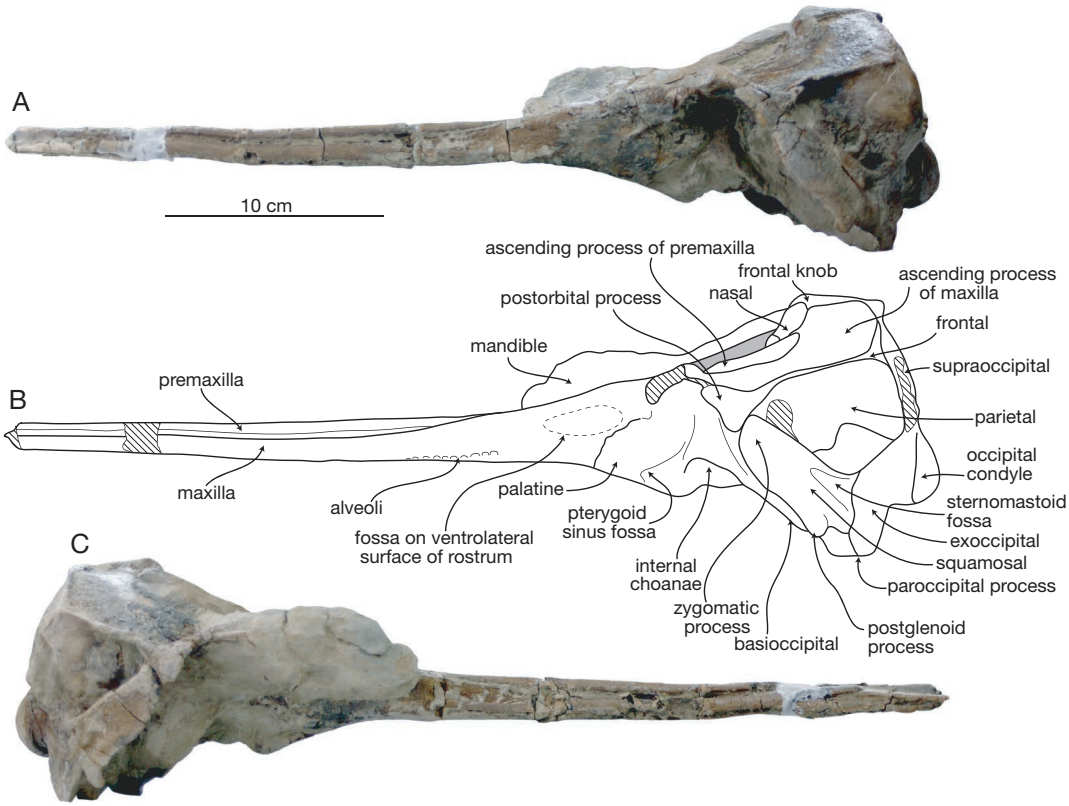

Fig. 34. — UCMP 219700, skull and partial mandible of *Parapontoporia sternbergi* (Gregory & Kellogg, 1927); **A**, left lateral view; **B**, interpretive line drawing in left lateral view; gray indicates adhering matrix, and cross-hatching indicates damaged bone; **C**, right lateral view. Scale bar: 10 cm.

Together the bony nares are heart-shaped, as they are anteriorly narrow between the premaxillary sac fossae and posteriorly divided by the nasal septum (Fig. 32A). The mesethmoid ridge is vertically oriented and bladelike plate that separates the bony nares; posteriorly it widens to the flat, transversely oriented lateral wings of the mesethmoid. The mesethmoid dorsally overlaps the frontal and the anteroventral margin of the nasals.

The vertex of UCMP 219700 is formed by a prominent frontal knob, which the nasal overlaps anteriorly (Figs 32, 33). The nasals are asymmetrical, subrectangular in shape, transversely convex, and steeply slope away from the frontal knob. The vertex is offset to the left, and a low nuchal crest is formed by the frontal-supraoccipital contact, which runs dorsomedially to meet the vertex. The right nasal and maxilla are wider than their counterparts on the left, and the longitudinal dorsal crest of the frontal knob is twisted clockwise (in dorsal aspect). A short and low crest corresponding to the median suture of the frontals runs posteriorly from the frontal knob to the occipital shield and the nuchal crest; it deviates slightly to the left and is offset from the sagittal plane by approximately 10 mm. A small pit is located on the supraoccipital posterior to the vertex and below the nuchal crest. An interparietal is not visible at the vertex, and the supraoccipital appears to directly abut the frontal.

The frontal of UCMP 219700 is exposed only at the vertex, the dorsal surface of the temporal

fossa and orbit, and along the lateral edge of the facial region (Figs 32-34). The postorbital process is triangular and robust in lateral view, but ventrally short, and contacting the apex of the zygomatic process of the squamosal; it is unclear if this contact is natural or due to compaction. Posteriorly, the frontal forms the concave dorsal wall of the temporal fossa, ventromedially contacting the parietal. The infratemporal crest is low, extends medially from the postorbital process, and is approximately transversely oriented. Anteromedial to the postorbital process, the antorbital fossa is large, subrectangular, posteriorly deep, and anteriorly shallow. The ventral infraorbital foramen opens anteriorly within the fossa; the medial wall of the antorbital fossa is formed by the delicate and thin lateral lamina of the palatine. The sphenopalatine foramen is hidden by matrix. The ventral exposure of the frontal/maxilla contact lies between the preorbital ridge and the antorbital fossa.

No details of the lacrimojugal are apparent, owing to damage to the antorbital region and adhering matrix; furthermore, poor preservation of the ventral part of the cranium has obscured the sutures with the frontal and maxilla. However, a small crest of the maxilla extends posteroventrally from the medial margin of the antorbital notch to articulate with the lacrimal. The anterior portion of the palatines is obscured by matrix, but the lateral laminae are exposed, and the pterygoids are lost. Anterior to the choana, the fossa for the pterygoid sinus is large (Fig. 33); the lateral lamina of the palatine is parasagittally oriented and wafer-thin. The medial lamina of the palatine forms the anterolateral wall of the nasal passage, and is laterally convex.

Only the vomerine crest of the vomer is exposed, in the vicinity of the internal choanae (Fig. 33); it is dorsally contiguous with the transversely thin nasal septum. In specimens of *Parapontoporia sternbergi* described by Barnes (1985b), the vomer is also exposed ventrally on the base of the rostrum; in UCMP 219700, this region is insufficiently preserved to tell if a similar exposure was present. The ventral tubercle extends ventrally and anterior to the internal choanae. The vomerine crest extends posteriorly towards the transversely concave basisphenoid.

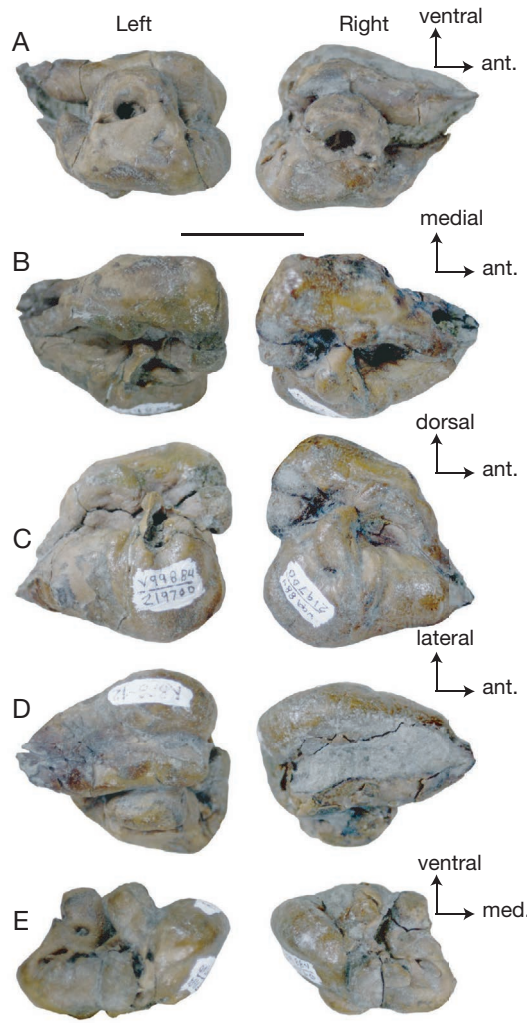

FIG. 35. — Petrotympanics of UCMP 219700, *Parapontoporia sternbergi* (Gregory & Kellogg, 1927); **A**, medial view; **B**, dorsal view; **C**, lateral view; **D**, ventral view; **E**, posterior view. Scale bar: 20 mm.

Owing to poor preservation of the basicranium, the morphology of the alisphenoid and ventral portion of the parietal cannot be ascertained. The basioccipital of UCMP 219700 is trapezoidal in ventral view, transversely concave, longitudinally flat in its medial region, and has ventrally extending crests on either side that are anteromedially oriented (Fig. 33A). Lateral to the basioccipital, a fissure marks the petrosal fossa, which is demarcated anteriorly and laterally by the falciform process of

the squamosal, medially by the basioccipital, and posteriorly by the exoccipital. The foramen ovale is laterally directed and opens medially on the alisphenoid, although the alisphenoid-squamosal suture cannot be discerned. A large portion of the left anteroventral surface of the braincase is missing, forming a large window into the braincase. The zygomatic process is robust, anterodorsally directed, with a flat lateral surface. The sternomastoid fossa is present as a shallow crease below the sharp supramastoid crest. The mandibular fossa is slightly concave and anteriorly facing. Anteriorly, the zygomatic process bears a rectangular apex in lateral view, which contacts the postorbital process.

The parietal forms the posterolateral and widest portion of the braincase and is exposed mostly in the temporal fossae, where it is laterally convex and smooth (Fig. 33A, B). Ventrally, the parietal contacts the squamosal, and posteriorly extends to the posterolateral corner of the braincase to meet the supraoccipital.

The posterolateral surface of the exoccipital of UCMP 219700 is flat and extends ventrolaterally as a broad paroccipital process (Fig. 33). A deep dorsal condyloid fossa occurs dorsolateral to each occipital condyle. Each condyle is set out on a distinct, short condyloid pedicle. The occipital shield is nearly vertical and bisected medially by a shallow sagittal trough; although large windows are broken into the supraoccipital on both sides dorsal to the condyles (it is unclear whether or not these are natural fontanelles), the left and right dorsolateral surfaces of the supraoccipital clearly form paired convex surfaces corresponding to the cerebral hemispheres.

The description of the petrotympanic complex is based primarily on the left side, unless otherwise stated. The tympanic bulla (Figs 35, 36; Table 12) is slightly larger than the petrosal, with a laterally convex outer lip. The outer posterior prominence is ventrally swollen in ventral view and broadly convex. The median furrow is well-defined and deep along ⅔ of the ventral surface, and shallows anteriorly; medially it is delimited by the involucral ridge, which is sharp and diverges posteromedially. The inner posterior prominence is narrower and does not extend as far posteriorly as the outer posterior prominence, and in dorsal view it exhibits an abrupt posteromedial corner. The involucrum is narrow anteriorly, widens posteriorly toward the inner posterior pedicle, and is sinuous along its long axis in dorsal view. The tympanic cavity is most cavernous posteriorly, and narrows anteriorly toward the small Eustachian outlet. The anterior tip of the tympanic bulla is sharp, but lacks a prominent spine. The accessory ossicle was digitally sectioned and kept in articulation with the tympanic bulla for images of the 3D reconstruction (Fig. 36F, G); it is pillow-shaped with a small, medial lobate ridge for articulating with the fovea epitubaria of the petrosal. The lateral furrow is distinct but shallow, transversely oriented, and present at the level of the accessory ossicle. The sigmoid process is small, dorsally prominent, and transversely oriented; ventrally, the sigmoid fissure (*sensu* Ekdale *et al.* 2011) is curved and turns anteriorly so that in lateral view the fissure is posteriorly convex. Likewise, the sigmoid process here turns anteroventrally; no apparent tympanic sulcus is visible. The conical process is between the posterior and sigmoid processes, low, and transversely flattened. The posterior process is set off on a distinct neck from the inner posterior pedicle, ventrally rugose, and has a smooth, convex and oval-shaped articular facet for the posterior process of the petrotympanic; the small elliptical foramen separates the inner and outer posterior pedicles.

The petrosal (Figs 35; 36A-D) is small and compact with an elongate anterior process (Table 11). The pars cochlearis is large, subspherical, anteromedially thrusted, and slightly dorsoventrally shallower than it is long. Posterolaterally it is perforated by the fenestra vestibuli, and just anterior to the fenestra vestibuli, two additional unidentified paired foramina open anteroventrally on the ventral surface of the pars cochlearis; they are much smaller than the fenestra vestibuli. The homology of these foramina is unclear; nor is it clear whether these are present on the other petrosal. No promontorial groove is present (Fig. 36D). Dorsally the large internal acoustic meatus is nearly circular and deep; the dorsal opening of the facial canal is separated from the spiral cribriform tract by a low, crista transversa.

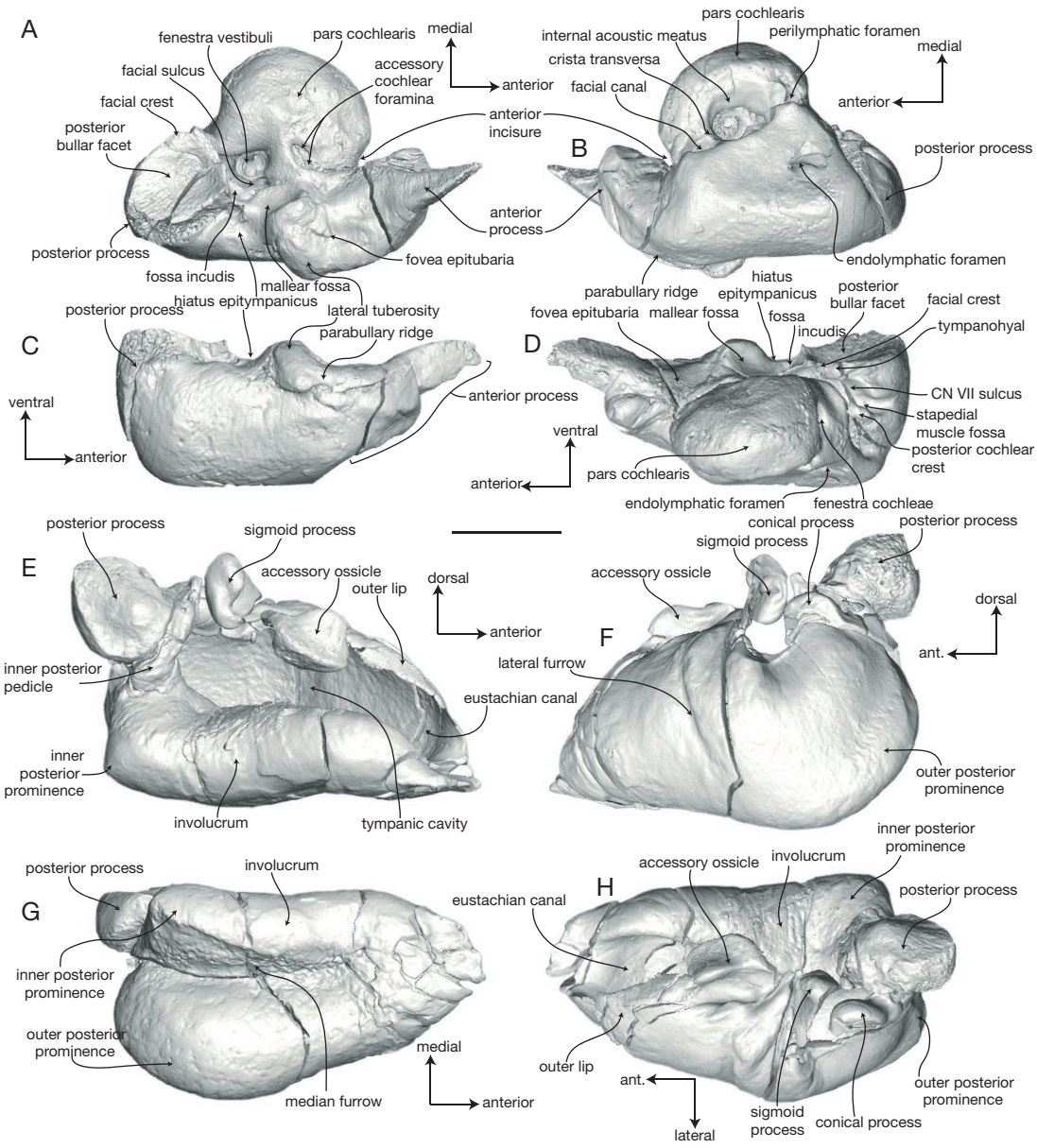

FIG. 36. — CT images of left petrosal and tympanic bulla of UCMP 219700, *Parapontoporia sternbergi* (Gregory & Kellogg, 1927); **A**, petrosal in ventral view; **B**, petrosal in dorsal view; **C**, petrosal in lateral view; **D**, petrosal in medial view; **E**, tympanic bulla in medial view; **F**, tympanic bulla in lateral view; **G**, tympanic bulla in ventral view; **H**, tympanic bulla in dorsal view. Scale bar: 5 mm.

The perilymphatic foramen is oval-shaped and positioned just posterior to the internal acoustic meatus. Lateral to the internal acoustic meatus, the dorsal surface of the petrosal exhibits an elongate triangular facet, which in its posterior part is pierced by the slit-like endolymphatic foramen. Although no dorsal crest is obvious on the dorsal face, the homologous portion of the dorsal face

of the petrosal is formed into a gentle pyramidal apex. The posterior process is short with a convex posterior margin, and a small, teardrop-shaped, smooth and concave posterior bullar facet. A medially prominent facial crest is elevated along the medial margin of the facet. In ventral view, this crest obscures the posterior cochlear crest and the posteriorly directed facial sulcus. The facial sulcus continues anteriorly to the ventral opening of the facial canal, which is laterally adjacent to the fenestra vestibuli. Medially adjacent to the posterior cochlear crest, the large and oval shaped fenestra rotunda opens on the posterior surface of the pars cochlearis. A small, concave fossa incudis is positioned anterior to the posterior bullar facet and faces anteroventrally, while a larger mallear fossa occurs between the base of the anterior process and the ventral opening of the facial canal. The hiatus epitympanicus is wide and shallow. The anterior process is large, subrectangular in ventral view, and has a prominent anterior spine on the anteroventral angle. It is separated from the pars cochlearis by an acutely excavated anterior incisure (Fig. 36A, B). The parabullary ridge is delimited dorsolaterally by a distinct sulcus, and posteroventrally it terminates in the large lateral tuberosity. The ventral face of the anterior process is concave (Fig. 36C), and in the area of the fovea epitubaria (e.g., medial to the parabullary ridge), the accessory ossicle articulates with the petrosal. The anterodorsal angle is formed into a prominent medial tubercle. The anterior spine is sharp, transversely compressed, sword-like, and extends anteriorly; its ventral margin articulates with the anterodorsal edge of the outer lip of the tympanic bulla, just anterior to the accessory ossicle (Fig. 36C). When in articulation with the bulla set flat on its ventral surface, the ventral face of the petrosal faces laterally rather than ventrally.

The malleus is small, anteroposteriorly elongate, and formed into two lobes: an anterior lobe including the tubercule, and a posterior lobe with the head of the malleus (Fig. 37E-H). The manubrium is conical and extends ventrally. The anterior process extends laterally to fuse with the sigmoid process of the tympanic bulla. The lateral foramen for the chorda tympani opens dorsally and is encircled by the tube-like anterior process; it is unclear if there is an open canal for the chorda tympani. The tubercule is oriented anteriorly, and includes a small muscular process for the insertion of the tensor tympani muscle. The articular facet for the incus is positioned posteromedially and is formed as two small, convex, pad-like surfaces that are offset at about 100°; the dorsal surface is roughly twice the area of the ventral surface (Fig. 37G). A distinct groove completely encircles the articular surfaces.

The incus is small and has a large head for articulation with the malleus (Fig. 37A-D), with two concave articular facets. The articular facets are offset by a longitudinal ridge; the dorsal surface is slightly larger than the ventral surface. The crus longum is conical and projects anteromedially; at its apex, it turns dorsally, and exhibits a small button-like lenticular process for articulation with the stapes. The crus breve is shorter, and extends posteromedially as a short, cylindrical process with a truncated, flat apex; there is a shallow saddle between the crus breve and crus longum.

A fragment of the posterior right mandible of UCMP 219700 is preserved and exposed in medial view (Fig. 32); this part of the mandible has not been previously described for *Parapontoporia*. The lateral wall of the greatly enlarged mandibular foramen is medially smooth and shallowly concave. The condyle is obscured by matrix, medially concave, and dorsoventrally elongate. A sharp, ventrally oriented ridge forms the dorsomedial margin of the mandibular foramen. The coronoid process is low, transversely flattened, posteriorly directed, with a finger-like outline. The dorsal margin of the mandible is straight and smooth.

Taphonomy

UCMP 219700 was recovered from a vertical succession of stacked 0.5-1 m thick tabular very fine sandstone beds with erosive soles, hummocky-cross stratifications at their base and massive, bioturbated sandstone at their tops. This is typical of event deposition in the lower shoreface and transition zone by hyperpycnal flows (Norris 1986; Duke *et al.* 1991). The skull of UCMP 219700 was discovered in a horizontal, ventral-up position,

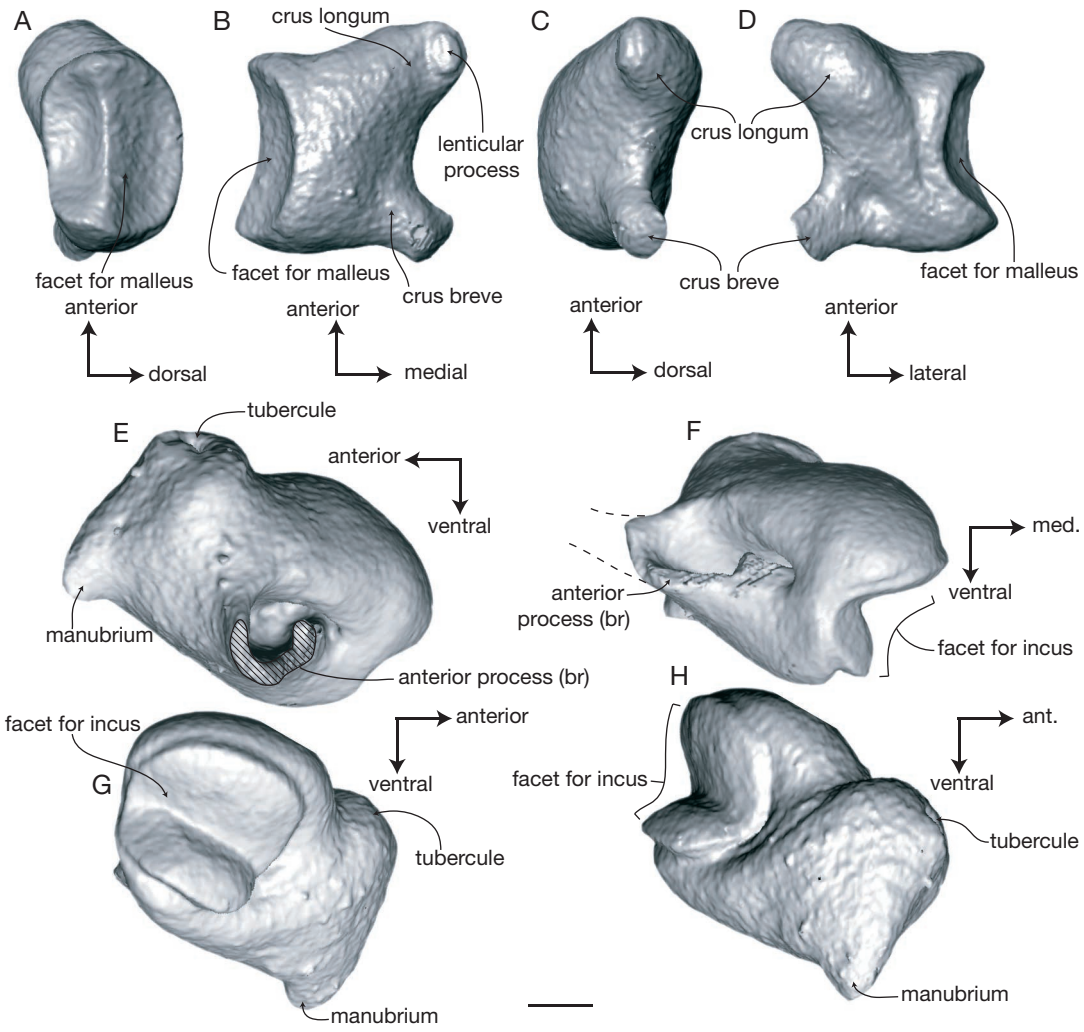

FIG. 37. — CT images of middle ear ossicles from left petrotympanic complex of UCMP 219700, *Parapontoporia sternbergi* (Gregory & Kellogg, 1927); **A**, incus in lateral or mallear view; **B**, incus in dorsal or stapedial view; **C**, incus in medial view; **D**, incus in lateral view; **E**, malleus in lateral or tympanic view; **F**, malleus in posterior view; **G**, malleus in medial view; **H**, malleus in anteroventral view. Dashed line indicates broken anterior process. Scale bar: 1 mm.

and aside from the associated mandible fragment and petrotympanics, no other associated bones (including postcrania) were found during the excavation. This suggests that these four skeletal elements arrived on the seafloor as a unit, possibly connected by soft tissue (e.g., Fig. 38); observations of floating cetacean carcasses demonstrate that the length of the skull causes soft tissue in the neck to degrade faster than other parts of the carcass, resulting in the loss of the head early on during decomposition (Schäfer 1972); this phenomenon has been the hypothesized for the preservation of isolated beaked whale crania in the Miocene of Peru (Bianucci *et al.* 2010). The anterior portion of the rostrum is missing, and the tips of the premaxillae and maxillae are modified into thin, pointed splints and are slightly splayed apart anteriorly, indicating that the tip of the rostrum has been abraded

(possibly being dragged through the sediment by a neutrally buoyant carcass, prior to re-floating). It is also possible that the rostrum protruded from the sediment water interface and was damaged by sediment abrasion, but unlikely given that the skull was oriented parallel to bedding. The mandible fragment and both petrotympanics were found in contact with the dorsal surface of the facial region of the skull (and thus stratigraphically below the skull). Modern cetaceans decay within an "integumentary sack" (Schäfer 1972), and it is possible that the dolphin floated ventral up, and the earbones and mandible fragment settled into the dorsal side, followed by subsequent loss of the head. Alternatively, the earbones and mandible fragment could have been loosely connected to the skull by remaining soft tissues, arriving on the seafloor adjacent to the dorsal-up skull, and the skull could have rolled over onto the three associated elements. Fracturing of the mandible could have been caused by perimortem injury or impact of the carcass into hard substrate (i.e. within the surf zone). A hypothetical interpretation of the taphonomic history of UCMP 219700 is shown in Figure 38.

It is worth noting that UCMP 219700 is only one of two specimens of *Parapontoporia* preserved with petrotympanics, which is particularly interesting given that numerous skulls of *P. sternbergi* and *Parapontoporia wilsoni* are now known from the San Diego and Purisima Formations (respectively) in LACM, SDNHM, and UCMP collections. The petrotympanic complex of odontocetes only exhibits loose bony connections to the rest of the skull (Mead & Fordyce 2009), and as a result they are often disarticulated and absent from fossil specimens. The other specimen of *Parapontoporia* (SDNHM 53169) includes a nearly complete skull with articulated mandibles and petrotympanic complex, and was collected from the siltstone member of the Capistrano Formation in Orange County, a unit deposited far below storm weather wave base in low energy, quiescent offshore settings (Ingle 1979). UCMP 219700 was preserved in sediments characterized by rapid (but intermittent) event sedimentation, and it is likely that it was rapidly covered by a blanket of sediment, preserving the petrotympanics and mandible fragment with the skull. Most of the crania of *P. wilsoni* from the Santa Cruz section of the Purisima Formation were collected from UCMP locality V-6875, a time-averaged bonebed, or from shallow shoreface sandstones generally characterized by frequent current disturbance. The San Diego Formation was predominantly deposited under higher energy, shoreface-transition zone settings (Deméré 1983). Although other odontocetes have been found with associated petrotympanics in the San Diego Formation, *Parapontoporia* has not. Perhaps the small body size of *Parapontoporia* contributed to relatively quick decomposition relative to larger odontocetes. It is hypothesized here that this pattern reflects taphonomic bias against preservation of associated petrotympanics in shallower, higher energy settings.

Comparisons

UCMP 219700 shares with platanistine platanistids a rostrum that is transversely compressed, but differs in retaining a triangular cross section; it differs from pomatodelphine platanistids a rostrum that is not dorsoventrally compressed (Barnes *et al.* 2010); it further differs from many platanistids and allodelphinids (e.g., *Araeodelphis* Kellogg, 1957; *Zarhachis* Cope, 1868; *Zarhinocetus* Barnes & Reynolds, 2009) in lacking an inflated boss-like antorbital process of the maxilla. Platanistids such as *Platanista* Wagler, 1830 and *Zarhachis* differ from UCMP 219700 in exhibiting enlarged plate-like maxillary crests. UCMP 219700 differs from Pontoporiidae in lacking premaxillary eminences, and differs from *Brachydelphis* Muizon, 1988 in exhibiting a longer rostrum, and from *Pontoporia blainvillei* Gervais & d'Orbigny, 1844 in exhibiting a relatively wider and asymmetrical facial region. Odontocetes of the family Iniidae (e.g., *Inia* d'Orbigny, 1834 and *Meherrinia* Geisler, Godfrey & Lambert, 2012) differ from UCMP 219700 in exhibiting crania with relatively narrow facial regions, which, in the case of *Inia*, approximates a rectangular shape. This specimen exhibits several of Muizon's (1988a) delphinidan synapomorphies, including a contribution to the lateral lamina by the palatine, frontals narrower

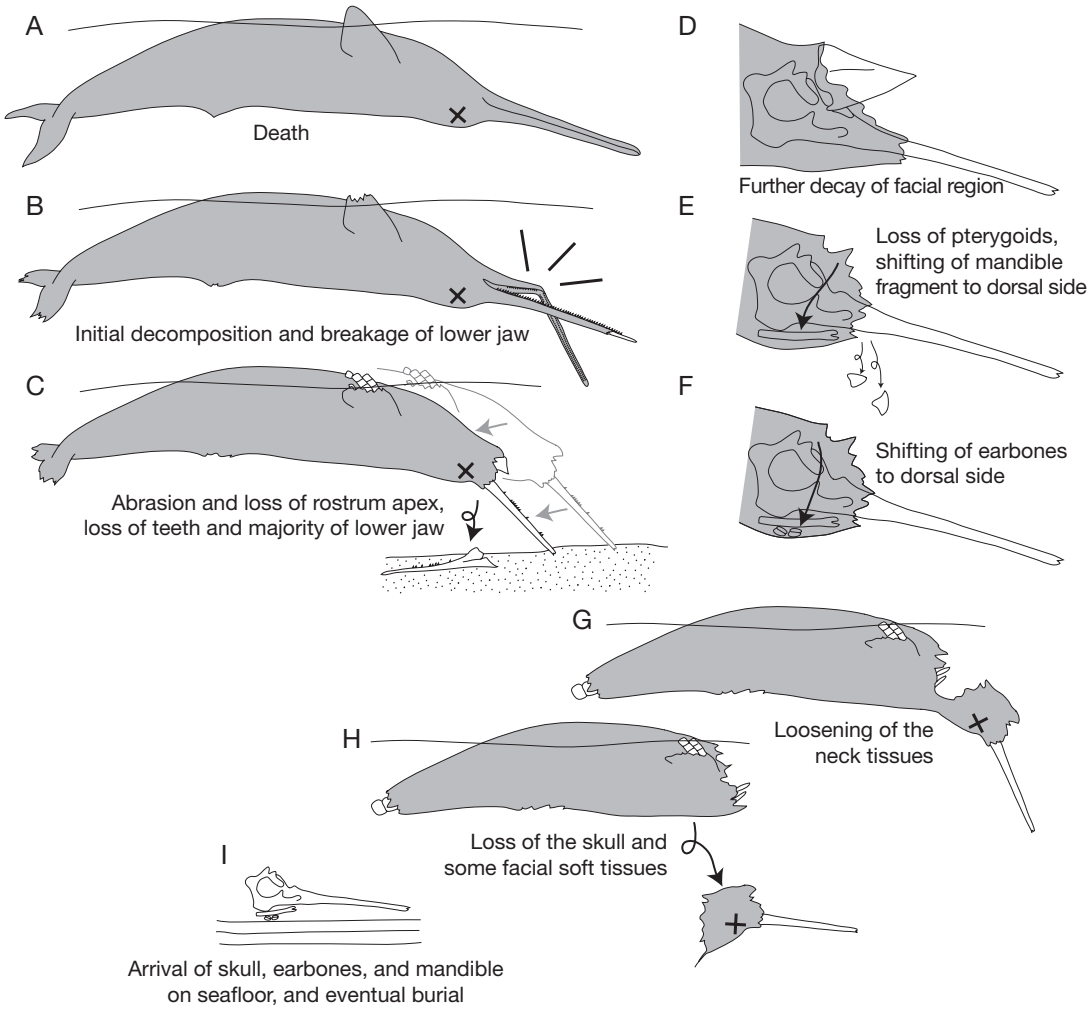

Fig. 38. — Possible taphonomic pathway of UCMP 219700, *Parapontoporia sternbergi* (Gregory & Kellogg, 1927); **A**, death; **B**, initial decomposition and breakage of lower jaw; **C**, abrasion of rostrum apex, loss of teeth, and loss of missing portions of lower jaw; **D**, continued decay and skeletonization of facial region; **E**, loss of pterygoids and shifting of mandible fragment to bottom of carcass (dorsal side of skull); **F**, shifting of petrotympanics to bottom of carcass (dorsal side of skull); **G**, loosening of soft neck tissues connecting skull to carcass; **H**, loss of skull with adhering soft tissue; **I**, arrival of skull, petrotympanics, and mandible fragment on seafloor in ventral-up position and eventual burial.

than nasals on the vertex, a well-developed lateral tuberosity of the petrosal, and a well-developed processus muscularis of the malleus.

This fossil represents an occurrence of the Pliocene lipotid dolphin *P. sternbergi*, based on several cranial features. The cranium of UCMP 219700 shares in common with other species of *Parapontoporia* an elongate, narrow, and attenuate rostrum with deep longitudinal lateral grooves along the premaxilla-maxilla contact, high tooth count, rostral basin, maxillae with robust and inflated rostral crests, cranial asymmetry, and small size (lateral grooves are also present in other Miocene longirostrine odontocetes such as *Lipotes* Miller, 1918, allodelphinids, eurhinodelphinids, iniids, platanistids, and squalodelphinids). Like other

specimens of *P. sternbergi*, UCMP 219700 differs from both *Pontoporia* Gray, 1846 and *Lipotes* in having a higher (probable) tooth count per quadrant; UCMP 219700 has an estimated 48 alveoli per quadrant as preserved, not including alveoli from the missing portion of the rostrum; in comparison to complete crania of *Parapontoporia pacifica* Barnes, 1984 and *P. sternbergi*, approximately 40% of the rostrum is missing (Barnes 1985). If the rostrum were complete, UCMP 219700 would probably preserve 80 teeth per quadrant as in *P. sternbergi* and *P. pacifica*, in comparison to 32-36 in *Lipotes* and 48-61 in *Pontoporia* (Barnes 1985b);. UCMP 219700 exhibits a vertex that is offset to the left side of the cranium, with a right ascending process of the maxilla that is wider than the left, thereby differing from *Pontoporia* in having an asymmetrical skull, like *Lipotes*. UCMP 219700 differs from *Lipotes* in lacking a swelling of the maxillae at the base of the rostrum, exhibiting a narrower rostrum with a rostral basin, a relatively larger braincase, wider occipital shield, and a pentagonal-shaped facial region that laterally obscures most of the temporal fossae and zygomatic processes. Conversely, UCMP 219700 shares several cranial features in common with *Lipotes* to the exclusion of *Pontoporia*, including an anteriorly wider and less rectangular facial region, and nasal process of the premaxillae that posteriorly curve medially around the bony naris and nearly contact the nasals. *Parapontoporia*, *Lipotes*, and UCMP 219700 additionally share a zygomatic process of the squamosal with a concave dorsal margin, pterygoid sinus fossa that extends further anterior to the orbit, and a frontal knob that extends further dorsally than the dorsal margin of the occipital shield (Geisler & Sanders 2003).

The skull of UCMP 219700 differs from that of *P. pacifica* in exhibiting a rostral basin, more anteriorly elongate rostral crests, and lacking such a well defined posterolateral sulcus on the premaxilla. UCMP 219700 differs from *P. wilsoni* in exhibiting a slightly shallower rostral basin, less inflated rostral crests, a facial region slightly wider than long, and a more anteriorly thrusted vertex. *Parapontoporia sternbergi* and UCMP 219700 share several of these features in common to the exclusion of *P. wilsoni*, including a facial region that is wider than long and a shallower rostral basin (Barnes 1985b), and a vertex that is positioned further anteriorly. *P. sternbergi* and *P. wilsoni* share a rostral basin (although it is more deeply excavated in the latter), while the dorsal surface of the rostrum in *P. pacifica* is nearly flat (Barnes 1985b). These comparisons indicate referral of UCMP 219700 to *P. sternbergi*.

The discovery of UCMP 219700 is important as it is the first reported skull of *Parapontoporia* for which an associated petrosal is known. Barnes (1985b) stated that no crania of *Parapontoporia* with associated earbones had yet been identified, and none have been reported since; as identified above, this appears to be a taphonomic issue. The petrotympanic morphology of UCMP 219700 confirms Barnes' (1985b) referral of isolated petrosals to *P. sternbergi*. Curiously, although Barnes (1985b) placed *Parapontoporia* within the Pontoporiidae, he referred isolated petrosals based on their similarity with *Lipotes vexillifer* Miller, 1918, rather than *Pontoporia blainvillei* (Barnes 1985b: 16). The referred petrosals share several features with *Lipotes*, including a long and pointed anterior process with a prominent medial tubercle, a distinct parabullary ridge, a small posterior bullar facet, a deep anterior incisure, and a relatively small and circular internal acoustic meatus (Barnes 1985b); all of these features are confirmed in UCMP 219700. Like the referred petrosals from the San Diego Formation, the petrosal of UCMP 219700 differs from *Pontoporia* in having a relatively larger anterior process with an anterior spine that articulates with the anteromedial edge of the outer lip of the tympanic bulla, exhibiting a large medial tubercle on the anterior process, a smaller lateral tuberosity, possessing a well-defined anterior incisure, and a more circular internal acoustic meatus.

UCMP 219700 additionally presents the first tympanic bulla, malleus, and incus reported for *Parapontoporia*. The tympanic bullae of UCMP 219700 and *Lipotes* are similar, to the exclusion of other extant "river dolphins" (*Inia*, *Pontoporia*, and *Platanista*); similarities include the sharp anterior tip (unlike the rounded anterior tip as in

Pontoporia or the anterior spine present in *Platanista*), the small and sinuous involucrum like in other Delphinida (and unlike the grossly inflated involucrum in *Platanista*), the broadly inflated posterolateral surface and transversely broad outer posterior prominence (unlike *Pontoporia* and *Inia*). The involucrum is posterodorsally excavated or constricted in medial aspect, a synapomorphy of Delphinida (Muizon 1988a). Another feature of UCMP 219700 which appears to be lacking in *Inia* and *Pontoporia* is a sword-like anterior spine of the petrosal which articulates with the outer lip of the tympanic bulla (Fig. 36C).

Remarks

The confirmation of this petrotympanic morphology for *Parapontoporia* is important as it has been considered a key taxon for morphology-based phylogenetic analyses of the Odontoceti, including Muizon (1988a), Geisler & Sanders (2003), Geisler *et al.* (2011). Phylogenetic analyses have placed *Parapontoporia* sister to *Lipotes* within a monophyletic Platanistoidea (Geisler & Sanders 2003), or sister to *Lipotes* as a basal member of the Delphinida (Muizon 1988a; Geisler *et al.* 2011, 2012). The now large sample size of *Parapontoporia* spp. from the Late Neogene of California and Baja California will offer multiple opportunities for new avenues of study, including statistical analyses of morphological variation, as well as detailed analyses of morphological changes of *Parapontoporia* crania and petrosals from different rock units with well-resolved stratigraphy and ages, potentially allowing detailed study of morphological changes through time and reevaluation of various hypotheses by Barnes (1985b).

Three species of *Parapontoporia* have been described from the Neogene of California and Baja California. *P. sternbergi* (originally described as *Stenodelphis sternbergi* by Gregory & Kellogg 1927) is known principally from the Pliocene San Diego Formation (Barnes 1985b), but other incomplete material has been referred to this species (e.g., petrosals, rostral and mandible fragments) from the San Joaquin Formation (Barnes 1973) and Wilson Grove Formation (Barnes 1977; formerly "Merced" Formation). Barnes (1985b) described a well-preserved and nearly complete cranium of *P. sternbergi* from the San Diego Formation in addition to several petrosals (see above), and there now exists a much larger sample size from the San Diego Formation within SDNHM collections, including several nearly complete crania and mandibles, partial crania, and dozens of isolated petrosals. Two additional species of *Parapontoporia* were described by Barnes (1984) and Barnes (1985b), including *P. pacifica* from the Almejas Formation, and *P. wilsoni* from the Purisima Formation near Santa Cruz. There now also exists a substantially larger collection of topotypic material of *P. wilsoni* from the Purisima Formation near Santa Cruz, including several nearly complete and partial crania, mandibles, and dozens of isolated petrosals and tympanic bullae.

Although UCMP 219700 and *P. wilsoni* are both from the Purisima Formation, the type locality of *P. wilsoni* is now known to be UCMP locality V6875, the "Crab Marker Bed" of Madrid *et al.* (1986), which has been locally identified as the 5.33 Ma Miocene-Pliocene boundary (Powell *et al.* 2007). Barnes (1985b) reported the type locality as Manresa State Beach, but this is further up section and beyond the top of the Purisima Formation (F.A. Perry, pers. comm.). This 5.33 Ma age assignment is based on identification of the stratum as the Mio-Pliocene boundary based upon paleomagnetic data (Powell *et al.* 2007). A more conservative age assignment is based on bracketing dates above and below UCMP V6875: a 5.3 ± 0.3 Ma ash correlation and paleomagnetically dated 4.5 Ma horizon (Madrid *et al.* 1986; Powell *et al.* 2007), establishing this locality as earliest Pliocene (5.3-4.5 Ma). The type locality of *P. wilsoni* is therefore somewhat older than the strata in the San Gregorio section that yielded UCMP 219700, here identified as the species *P. sternbergi*, which was collected 2-3 m below a 3.35 Ma ash bed (Powell *et al.* 2007), and contemporaneous with the Pliocene (Piacenzian-Gelasian equivalent; San Diego Formation (which yielded the holotype and numerous referred specimens of *P. sternbergi*). This new find indicates that two species of *Parapontoporia* are truly represented within the Purisima Formation at different stratigraphic levels.

Family Delphinidae Gray, 1821

Delphinidae gen. et sp. indet.

Referred material. — UCMP 219174, an isolated tympanic bulla collected by R. W. Boessenecker from UCMP locality V99853.

Stratigraphic occurrence. — Middle part of the San Gregorio section of the Purisima Formation, Early Pliocene (*c.* 5-3.35 Ma; Zanclean-Piacenzian equivalent; Fig. 2).

Description

This specimen is small (Table 12) and rectangular in dorsal aspect (Fig. 39B, E, I). The posterior process is small, dorsoventrally shallow, and bears several longitudinal striations on the posterior bullar facet. The inner and outer posterior prominences are similar in transverse width, but the outer posterior prominence is positioned slightly further posterior to the inner posterior prominence (Fig. 39I). The involucrum of UCMP 219174 is anteriorly inflated (Fig. 39E). In medial aspect, the inner posterior prominence of UCMP 219174 forms an acute angle at its apex.

Remarks and comparisons

This specimen exhibits one synapomorphy of the Delphinida, an anteriorly inflated involucrum (Muizon 1988a). It also exhibits one delphinid synapomorphy, a ventral crest on the medial lobe that terminates posterior to the midpoint of the bulla (Geisler & Sanders 2003). It is similar in morphology to UCMP 219034 (tentatively referred to a globicephaline below), except for its much smaller size. This specimen is generally similar to tympanic bullae of extant delphinine delphinids, and represents a single occurrence of a small-bodied delphinid in the San Gregorio assemblage.

Subfamily Globicephalinae Gray, 1866

cf. Globicephalinae gen. et sp. indet.

Referred material. — UCMP 219034, a partial right tympanic bulla, collected by R.W. Boessenecker from UCMP locality V99842; UCMP 219162, a partial tooth collected by R.W. Boessenecker from UCMP locality V99833.

Stratigraphic occurrence. — Middle part of the San Gregorio section of the Purisima Formation, Early Pliocene (*c.* 5.6-3.35 Ma; Zanclean-Piacenzian equivalent; Fig. 2).

Description

The isolated tooth (UCMP 219162) is missing part of the root, and the tip of the crown was abraded away during life (Fig. 40). While the lingual and labial directions are obvious on this specimen, anterior and posterior are not, and thus it is unclear if it is an upper or a lower tooth. The conical root is elongate, straight, oval in cross section, and basally tapering (Fig. 40C). The crown is conical, with smooth enamel, a lingually curved tip, and oval in cross section (Fig. 40A, B). The crown and root are anteroposteriorly compressed.

The tympanic bulla (UCMP 219034) is missing most of the outer lip as well as the posterior process; it is large for an odontocete (41 mm in length; Table 12). The involucrum is robust and sinuous in medial view, and anteriorly, the involucrum is inflated in medial aspect (Fig. 39C, F, J). A ventromedial keel is present on the medial lobe, but terminates at about the midpoint of the bulla. The dorsal crest of the involucrum is anteriorly high and sharp, and in dorsal aspect, it has a sinuous outline (Fig. 39C). Faint transverse creases occur on the medial and dorsal surfaces of the involucrum. The inner posterior prominence is dorsoventrally narrow and does not extend as far posteriorly as the outer posterior prominence; the outer posterior prominence is large and hemispherical (Fig. 39J).

Remarks and comparisons

The tooth (UCMP 219162) is larger than all non-globicephaline delphinids (including *Orcinus* Fitzinger, 1860 and *Hemisyntrachelus* Brandt, 1873 for the purposes of this study), including *Tursiops*; it is also larger than the teeth of some globicephalines (*Feresa* Gray, 1870, *Grampus* Gray, 1828, *Orcaella* Gray, 1866, *Peponocephala* Nishiwaki and Norris, 1966). In terms of size and morphology, UCMP 219162 compares best with teeth of the fossil globicephalines *Hemisyntrachelus* (Bianucci 1996) and *Protoglobicephala mexicana* Aguirre-Fernández, Barnes, Aranda-Manteca & Fernández-Rivera, 2009. UCMP 219162 further differs from *Grampus* in having an

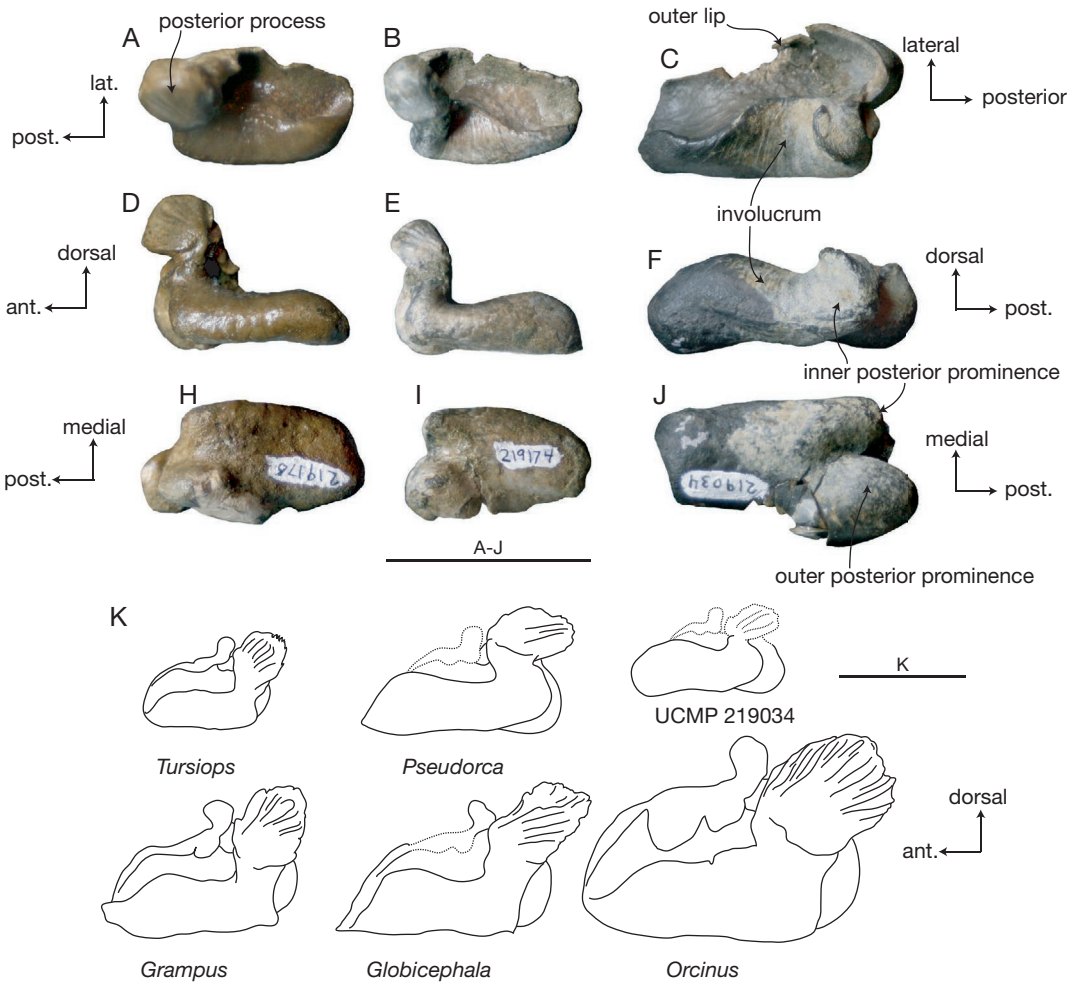

Fig. 39. — Tympanic bullae of delphinoid odontocetes; **A**, UCMP 219176, Phocoenidae gen. et sp. indet. in dorsal view; **B**, UCMP 219174, Delphinidae gen. et sp. indet. in dorsal view; **C**, UCMP 219034, cf. Globicephalinae gen. et sp. indet. in dorsal view; **D**, UCMP 219176 in medial view; **E**, UCMP 219174 in medial view; **F**, UCMP 219034 in medial view; **H**, UCMP 219176 in ventral view; **I**, UCMP 219174 in ventral view; **J**, UCMP 219034 in ventral view; **K**, comparison of interpretive line drawings of extant delphinids; specimen numbers for extant specimens are as follows: *Globicephala macrorhynchus* Gray, 1846, CAS 16466; *Grampus griseus* Cuvier, 1812, CAS 13461; *Orcinus orca* Linnaeus, 1758, CAS 23814; *Pseudorca crassidens* Owen, 1846, AMNH 18965; *Tursiops truncatus* Gray, 1866, CAS 16183). Scale bars: 3 cm.

elongate root with a closed pulp cavity; the roots of the few mandibular teeth of *Grampus* remain open during ontogeny (Boessenecker, pers. obs.). UCMP 219162 differs from *Delphinapterus* in lacking a curved root. Although teeth of the eastern North Pacific monodontid *Denebola brachycephala* Barnes, 1984 were not described or figured by Barnes (1984), the morphology of UCMP 219162 suggests that it does not belong to a monodontid. UCMP 219162 is similar in size and morphology to *Globicephala macrorhynchus* Gray, 1846, and *Globicephala melas* Traill, 1809, and substantially smaller than teeth of *Pseudorca* Reinhardt, 1862 and *Orcinus*. Although it lacks the more extremely developed anteroposterior root compression of *Pseudorca* and *Orcinus*, UCMP 219162 is similar in tooth morphology to

Globicephala Lesson, 1828 and *Protoglobicephala* Aguirre-Fernandez, Barnes, Aranda-Manteca & Fernandez-Rivera, 2009, and is tentatively identified as an indeterminate globicephaline.

Because of the large size of the tympanic bulla, UCMP 219034 cannot be identified as a small odontocete like *Parapontoporia* (see below), any fossil or extant phocoenid, or any small-bodied delphinid (e.g., *Tursiops* and all other non-globicephaline delphinids), although it is within the size range of globicephaline delphinids (e.g., pilot whales) as well as the beluga, *Delphinapterus*. This specimen differs from the enigmatic delphinoid *Albireo whistleri* in being transversely narrower with a transversely narrower involucrum with a sinuous (rather than straight) lateral margin; furthermore, *Albireo whistleri* exhibits a convex medial margin of the involucrum (straight in UCMP 219034), and an inner posterior prominence that extends as far posterior as the lateral posterior prominence. UCMP 219034 differs from *Denebola brachycephala*, *Delphinapterus*, and *Monodon* Linnaeus, 1758 in lacking a ventral surface of the bulla that is dorsally arched in medial and lateral view. UCMP 219034 further differs from *Denebola* Barnes, 1984 in being transversely narrower in ventral view, and possessing an inner posterior prominence that is transversely narrower and does not extend as far posteriorly as the outer posterior prominence. UCMP 219034 further differs from *Delphinapterus* in having a larger and more spherical outer posterior prominence, and in lacking an elongate ridge confluent with the inner posterior prominence on the medial surface. Because of these differences, UCMP 219034 is not identifiable as a monodontid.

UCMP 219034 exhibits one delphinid synapomorphy, a ventromedial keel of the tympanic bulla that terminates near the midpoint of the bulla (Geisler & Sanders 2003). UCMP 219034 differs from *Orcinus*, *Globicephala*, and *Pseudorca* in its smaller size, but is larger than *Grampus* and *Orcaella* (Fig. 39). The anterior inflation of the involucrum appears to characterize monodontids and most delphinids, except *Orcinus* and *Orcaella*. UCMP 219034 lacks the prominent anterior spine which characterizes *Globicephala* and *Grampus*. Although similar in involucral morphology, this specimen differs from the extinct delphinids *Arimidelphis sorbinii* Bianucci, 2005, *P. mexicana*, *Hemisyntrachelus oligodon* Pilleri & Siber, 1989, and *Hemisyntrachelus cortesii* Fischer, 1829 in having a more posteriorly projecting outer posterior prominence (Pilleri & Siber 1989a; Bianucci 1996; Bianucci 2005; Aguirre-Fernández *et al.* 2009).

UCMP 219034 shares a large and spherical outer posterior prominence with *Pseudorca* and *Globicephala*, which is lacking in *Delphinapterus*, *Grampus*, *Orcinus*, and non-globicephaline delphinids. Although being slightly smaller in absolute size, this specimen shares the most similarities among all globicephalines with *Pseudorca*; however, given the uncertain diagnostic utility of isolated odontocete bullae, UCMP 219034 is only tentatively identified to the subfamily Globicephalinae. UCMP 219034 and 219162 appear to represent additional (albeit fragmentary) records of globicephalines from the Pliocene of the eastern North Pacific along with *Protoglobicephala* from Baja California (Aguirre-Fernández *et al.* 2009). Additional globicephaline fossils from the Santa Cruz section of the Purisima Formation including a partial skull (UCMP 219233) and two petrosals (UCMP 219487 and 219488) were reported by Boessenecker *et al.* (2013). Nevertheless, globicephalines appear to be relatively rare in Late Neogene strata of the eastern North Pacific.

Family Phocoenidae Gray, 1825

Phocoenidae gen. et sp. indet.

Referred material. — UCMP 219176, an isolated left tympanic bulla collected by R. W. Boessenecker from UCMP locality V99847.

Stratigraphic occurrence. — Middle part of the San Gregorio section of the Purisima Formation, Early-Late Pliocene (3.35-2.5 Ma; Piacenzian-Gelasian equivalent; Fig. 2).

Description

The tympanic bulla is small (Table 12), and rectangular in dorsal aspect (Fig. 39A, D, H). UCMP 219176 has a small, equidimensional and pachyostotic posterior processes, with slightly convex and nearly smooth posterior bullar facet with faint lon-

gitudinal striations. The inner and outer posterior prominences are similar in transverse width, but the outer posterior prominence is positioned slightly further posterior to the inner posterior prominence (Fig. 39H). The involucrum of UCMP 219176 is gracile and lacks a strongly inflated anterior portion. In dorsal aspect, the inner posterior prominence of UCMP 219174 forms a more acute angle at its apex than in 219176. Although the outer lip is damaged, a slight inflection at the margin of the broken portion suggests it had a lateral furrow.

Remarks and comparisons

UCMP 219176 exhibits one synapomorphy of Delphinida, an anteriorly inflated involucrum (Muizon 1988a). Furthermore, this specimen exhibits two phocoenid synapomorphies: a short posterior process with a smooth articular surface (Muizon 1984), and a pachyostotic posterior process (Muizon 1988a). This specimen differs from *Albireo whistleri* in its smaller size, lacking a transversely massive involucrum with a convex medial margin in dorsal view, and exhibiting an outer posterior prominence that extends further posteriorly than the inner posterior prominence. UCMP 219176 differs from Delphinidae gen. et sp. indet. (UCMP 219174) described above in exhibiting a ventral crest on the medial lobe that extends further anteriorly, and in having a larger posterior process with a smooth posterior bullar facet; in UCMP 219174, the facet is more strongly striated. This specimen is identical to extant phocoenids and an undescribed fossil phocoenid (SDNHM 65276) from the San Diego Formation (Racicot *et al.* 2007; this taxon is equivalent to Phocoenidae unnamed genus 2 described below), and may be synonymous with any of the other phocoenids reported herein.

Phocoenidae unnamed genus 1

Phocoenidae species C – Barnes 1977: 321-343.

Referred material. — From the San Gregorio Section of the Purisima Formation: UCMP 219480, an isolated left petrosal collected by R.W. Boessenecker from UCMP locality V99851.

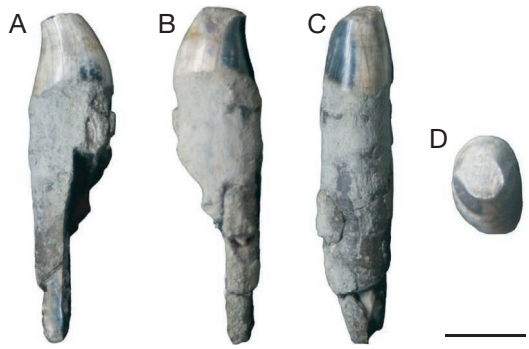

Fig. 40. — Partial tooth of cf. Globicephalinae gen. et sp. indet. in: **A**, anterior or posterior view (UCMP 219162); **B**, anterior or posterior view (UCMP 219162); **C**, lingual view (UCMP 219162); **D**, apical view (UCMP 219162). Scale bar: 1 cm.

From the Santa Cruz Section of the Purisima Formation: UCMP 128285, partial skeleton including skull, UCMP 219504, nearly complete skull; UCMP 219486, petrosal; SCMNH 21221, petrosal; 21222, petrosal; 21224, petrosal.

Stratigraphic occurrence. — Lowermost part of the San Gregorio section of the Purisima Formation, latest Miocene to earliest Pliocene (6.4 to *c.* 5 Ma; Messinian-Zanclean equivalent; Fig. 2).

Description

UCMP 219480 is a medium-sized (28.5 mm in length; Table 11) odontocete petrosal from the base of the San Gregorio section of the Purisima Formation (Fig. 41). The specimen has a large, prominent, and anteroposteriorly broad pars cochlearis. The internal acoustic meatus is teardrop shaped, transversely narrow, and anterolaterally oriented (Fig. 41B). The facial canal appears to be coalesced with the internal acoustic meatus due to the deeply recessed crista transversa. No dorsal crest or tuberosity is present; the dorsal face is smooth, rectangular, and slightly convex. A low parabullary ridge runs along the lateral margin of the petrosal from the base of the anterior process to the epitympanic hiatus; there is no anterior bullar facet (Fig. 41A, B). Toward the extremities of the anterior and posterior processes, the dorsal surface slopes ventrally (in medial aspect). The anterior process is large, blunt, and swollen; in ventral aspect, it is kidney shaped and curves anteromedially. In medial aspect it is bilobate and

appears to curve ventrally. The anterior incisure forms a well-defined crease between the pars cochlearis and the anterior process; ventrally there is a broad, smooth, and concave fovea epitubaria. The short posterior process is dorsoventrally thick and in medial aspect, its posterior margin is broadly curved and lacks a sharp posterior crest. Although the distal part of the posterior process is abraded, the proximal part of the posterior bullar facet is ventrally deflected. In ventral aspect, the long axis of the pars cochlearis forms an angle of approximately 130° with the long axis of the pars cochlearis.

Remarks and comparisons

This petrosal (UCMP 219480) exhibits one delphinoid feature (lateral side of petrosal smooth; Geisler & Sanders 2003), and two phocoenid synapomorphies: a posterior process that is ventrally deflected, and an angle between the posterior process and long axis of the pars cochlearis less than 135° (Murakami *et al.* 2012a, b). This specimen differs from petrosals of Phocoenidae unnamed genus 2 (see below) in its larger size, larger, bilobate anterior process (rather than small and conical), and proportionately smaller posterior process. It further differs from another undescribed broad-headed phocoenid from the San Diego Formation (SDNHM 38340) in lacking a medially directed anterior process and circular internal acoustic meatus. UCMP 219480 appears to represent a taxon distinct from cf. *Phocoena* (based on petrosals of modern *Phocoena* spp.) and Phocoenidae unnamed genus 2 (= "Phocoenidae new genus" of Racicot *et al.* 2007), based on referred petrosals from the San Diego Formation (Barnes 1973: fig 2g-j). Isolated petrosals from the Santa Cruz section of the Purisima Formation (UCMP 95963, 219486, UCMP uncatalogued, field no. FP-177, SCMNH 21221, 21222, 21224) share with this specimen a large, anteroposteriorly broad pars cochlearis with a small teardrop-shaped internal acoustic meatus, a small and ventromedially deflected posterior process, and an inflated anterior process that is bilobate at its apex. Other petrosals matching this morphology (listed above) consistently exhibit a sharp triangular projection at the posterolateral apex of the posterior process; this appears abraded in UCMP 219480. This feature is noteworthy as it is unique to petrosals of this morphotype within the available sample of odontocete petrosals from the Purisima Formation. These isolated petrosals (UCMP 95963, 219480, 219486, etc.) share these characteristics with a petrosal associated with a partial skeleton from the Purisima Formation near Santa Cruz (UCMP 128285) which was identified as "Phocoenidae species C" by Barnes (1977). This specimen and another cranium (UCMP 219504) exhibit a combination of delphinid and phocoenid characteristics, including an asymmetrical skull with a right premaxilla extending further posteriorly than the left and contacting the nasal (a delphinid synapomorphy), as well as premaxillary eminences, a frontal knob, and spatulate teeth (phocoenid synapomorphies). In addition to this undescribed taxon and *Haborophocoena toyoshimai* Ichishima & Kimura, 2005, several additional delphinid-like phocoenids have been described recently from the Pliocene of Japan including *Archaeophocaena teshioensis* Murakami, Shimada, Hikida & Hirano, 2012, *Haborophocoena minutis* Ichishima & Kimura, 2009, and *Miophocaena nishinoi* Murakami, Shimada, Hikida & Hirano, 2012 (Ichishima & Kimura 2009; Murakami *et al.* 2012b). Given this mixture of characteristics, it is interesting to note that an isolated petrosal of Phocoenidae unnamed genus 1 (UCMP 95963) was identified by Barnes (1977) as aff. *Tursiops*. Although similar in some regards to delphinid petrosals (e.g., *Tursiops*), UCMP 219480 and other petrosals of this unnamed taxon (listed above) differ in having a much larger anterior process and smaller posterior bullar facet that lacks striations. Delphinoid features include relatively short anterior and posterior processes and the lack of an anterior bullar facet (Fordyce 1994; delphinidan features according to Muizon 1988a). Identification of UCMP 219480 is based on skull features of crania of this unnamed taxon (UCMP 128285, 219504).

Petrosals of Phocoenidae unnamed genus 1 (including UCMP 219480) are most similar to the Early Pliocene *H. toyoshimai* and the Late Miocene *M. nishinoi*; UCMP 219480 shares two features in common with *Haborophocoena* Ichishima & Kimura, 2005 to the exclusion of other phocoenids, notably

an unusually robust and swollen anterior process (also shared with *Miophocaena* Murakami, Shimada, Hikida & Hirano, 2012), and a posterolaterally directed posterior process with a spine (present in UCMP 219486, SCMNH 21221, 21222, and 21224; also shared with *Pterophocaena nishinoi* Murakami, Shimada, Hikida & Hirano, 2012). UCMP 219480 differs from *Pterophocaena* Murakami, Shimada, Hikida & Hirano, 2012 in having a more inflated and bilobate anterior process, and differs from *Miophocaena* in having a smaller internal acoustic meatus. Interestingly, crania of this undescribed taxon from the Purisima Formation (Phocoenidae unnamed genus 1) also share several features with *Haborophocoena*, including large size, an elongate rostrum, an asymmetrical facial region, a frontal knob, relatively flat facial plane and low premaxillary eminences. Consideration of the generic identity of this taxon and relationship with *Haborophocoena* awaits description of more complete cranial material from the Santa Cruz section of the Purisima Formation. Fossils of Phocoenidae unnamed genus 1 have thus far not been found outside the Purisima Formation in California.

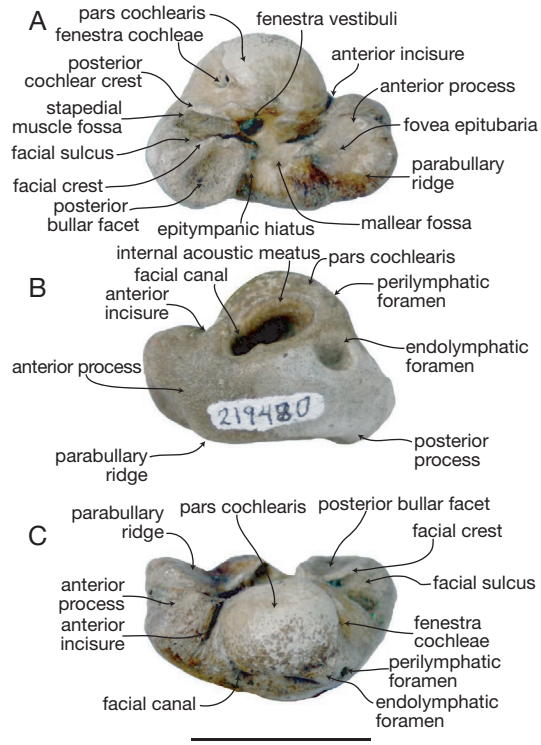

FIG. 41. — Left petrosal of Phocoenidae unnamed genus 1 (UCMP 219840); **A**, ventral view; **B**, dorsal view; **C**, medial view. Scale bar: 20 mm.

Phocoenidae unnamed genus 2

Odontoceti incertae sedis – Barnes 1973: 37-42.

?Phocoenidae – Barnes 1977: 331, table 5.

Phocoenidae new genus – Racicot *et al.* 2007: 132A.

REFERRED MATERIAL. — UCMP 219503, nearly complete skull collected by R.W. Boessenecker and C. Argento from UCMP locality V99854; and UCMP 219076, a pair of fused mandibles from UCMP locality V99859.

STRATIGRAPHIC OCCURRENCE. — Middle and upper parts of the San Gregorio section of the Purisima Formation, Early to Late Pliocene (*c.* 5-2.5 Ma; Zanclean-Gelasian equivalent; Fig. 2).

DESCRIPTION

UCMP 219503 is a small (Table 10) partial skull missing part of the apex of the rostrum, most of the basicranium including both petrotympanics and the right squamosal, and the pterygoids (Fig. 42). The dorsal surface is damaged and the left supraorbital and ascending processes of the maxilla are broken away, and the left premaxillary eminence is damaged. The rostrum is relatively long, triangular, dorsoventrally compressed, and the dorsal surface is slightly transversely convex . The rostral portion of the premaxilla is long and dorsally flat with nearly parallel medial and lateral margins. Posteriorly, the premaxilla is wider than the exposed rostral portion of the maxilla (Fig. 42A). The anteromedial sulcus is elongate and extends anteriorly to the midpoint of the rostrum, defining the acute prenarial triangle. Both premaxillary foramina are obscured by matrix, but are positioned anterior to the premaxillary eminence. The premaxillary eminence is convex and dorsally elevated; in dorsal aspect, the lateral margins of the eminences are slightly convex (Fig. 42A-C). The eminence is dorsally flat and overhangs laterally; the right eminence is transversely wider and slightly anteroposteriorly longer than the left. The

ascending process of the premaxilla is reduced to a small conical process that slightly overlaps the maxilla posterior to the premaxillary eminence. The premaxilla-maxilla suture runs along the base of the eminences.

The rostral portion of the maxilla has a narrow dorsal exposure, and it tapers anteriorly (Fig. 42A). Posteriorly, the rostral portion of the maxilla is raised and faces dorsomedially. A distinct anterolaterally oriented rostral crest (*sensu* Mead & Fordyce 2009) is present medial to the antorbital notch on the dorsal surface of the maxilla, and anteriorly forms a small tubercle. Posteriorly adjacent to this crest is the anteriormost dorsal infraorbital foramen. Laterally adjacent to the rostral crest is a posteromedially oriented furrow that is confluent with the antorbital notch; medial to the rostral crest, an elongate shallow longitudinal trough is positioned along the medial margin of the maxilla. The antorbital process is large and knoblike, and composed of the maxilla, frontal, and the lacrimal (Fig. 42A, B). Posteromedially, the maxilla forms part of the margin of the bony naris; a slight sulcus runs parallel to this margin, which demarcates a narrow cylindrical ridge running posteriorly from the tip of the premaxilla and along the lateral side of the bony naris. Adjacent to the bony nares, the maxilla is dorsally concave where it forms a transversely narrow fossa for the inferior vestibule, whereas it is convex further posteriorly. Posteriorly, the dorsal surface of the maxilla is bordered by the frontal and posteromedially by the mesethmoid and nasals. Where the left ascending maxilla is broken away, a reniform, anterolaterally oriented matrix cast of the dorsal lobe of the pterygoid sinus occurs on the dorsal side of the frontal bone and lateral to the bony nares, and medial to the postorbital process of the frontal. In life, this sinus would have been situated between the frontal and ascending process of the maxilla. The palate is smooth and flat anteriorly, and transversely convex posteriorly (Fig. 42D). Adjacent to the palatine, the maxilla is transversely concave. Poorly preserved alveolar grooves are present; well-preserved alveoli are only present on the right maxilla, along the middle of the preserved portion of the rostrum.

The right nasal is damaged, and the left nasal is large, inflated, and sub-spherical; both nasals are positioned on the anterior surface of the frontal knob (Fig. 42A, C). Much of the left frontal is visible where the left supraorbital and ascending processes of the maxilla have broken away. The lateral margin of the frontal (and facial region of the skull) forms a slight corner in dorsal view at the position of the postorbital process. The ventrally projecting postorbital process, better preserved on the left side, is narrow and triangular in lateral aspect. Posteriorly, the suture between the frontal and the supraoccipital along the nuchal crest is difficult to detect and appears fused. The left nuchal crest is eroded away; the right nuchal crest is tall, anteroposteriorly thin, highest adjacent to the frontal knob, and decreases in height laterally (Fig. 42A, B). Posterior to the vertex, the nuchal crest forms a posteriorly directed and sharp crest. There is a deep fossa in the right side of the frontal knob, where it meets the nuchal crest; this feature is damaged on the left side. The frontal knob is tall and dorsally prominent; the nasal-frontal sutures are clear, but it is unclear whether the interparietal is exposed or not. The frontoparietal suture in the region of the temporal fossa is indistinct. The parietal is gently convex and exposed within the temporal fossa. The temporal fossa is proportionally long but dorsoventrally low in height, triangular, and is delineated dorsally by the frontal, anteriorly by the postorbital process, ventrally by the zygomatic process, and posteriorly by the temporal crest.

There are large (and presumably natural) fenestrae in the supraoccipital dorsolateral to the occipital condyles; these appear to have been enlarged due to breakage. A median furrow rises from the foramen magnum to the vertex. A small, posteriorly overhanging crest is present on the posterior side of the frontal knob. The occipital condyles are convex, D-shaped, and not defined by a prominent edge or neck. The foramen magnum is oval shaped, and narrower ventrally. The jugular notch is a slight incision between the paroccipital process of the exoccipital and the basioccipital crest. Only the posteriormost portion of the flat basioccipital and left basioccipital crest are preserved; the basisphenoid is lost.

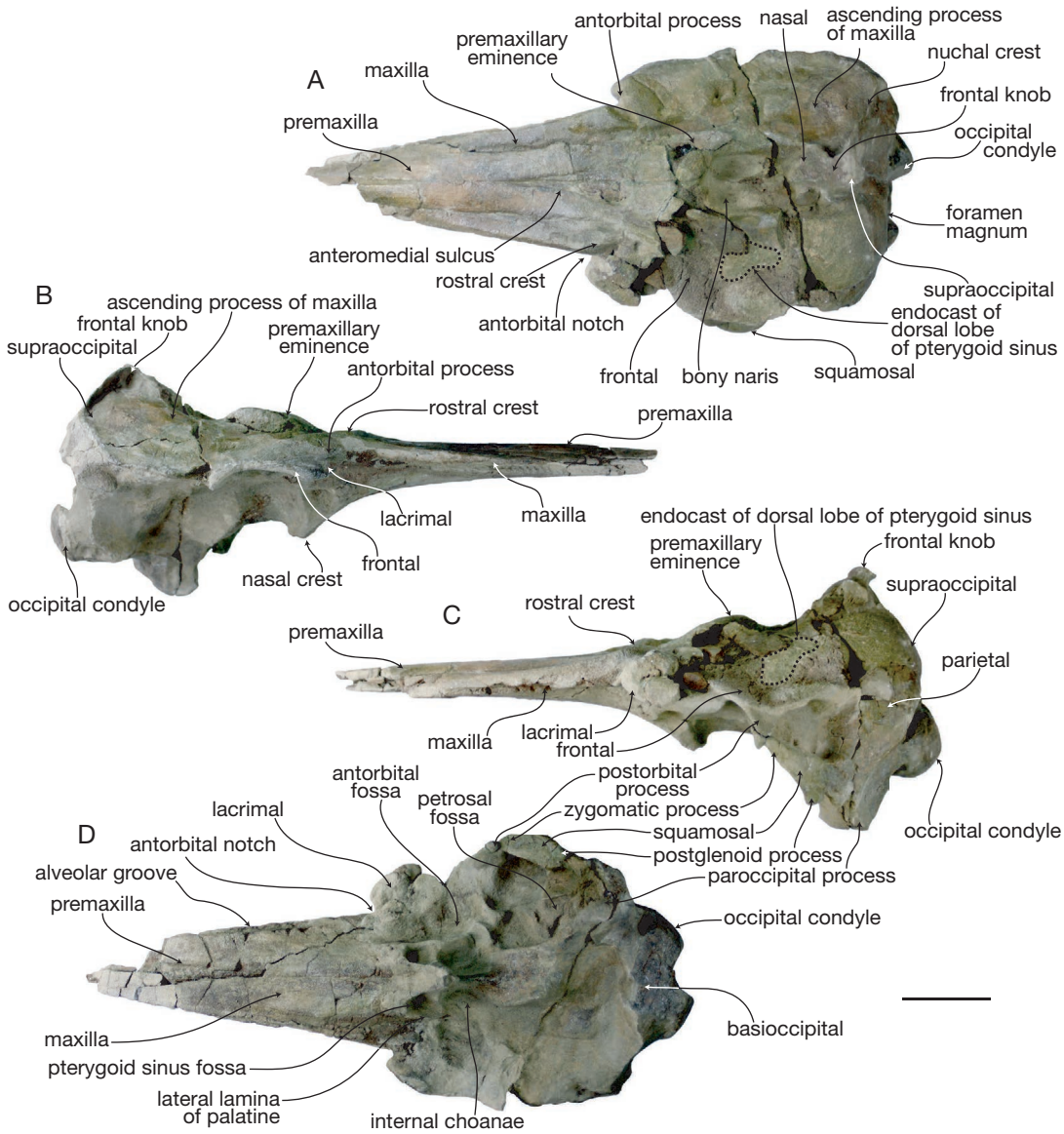

Fig. 42. — Cranium of Phocoenidae unnamed genus 2 (UCMP 219503); **A**, dorsal view; **B**, right lateral view; **C**, left lateral view; **D**, ventral view. Scale bar: 5 cm.

The zygomatic process of the squamosal is triangular in lateral view, anterodorsally directed, is dorsally flat, and bears a wide and shallow mandibular fossa ventrally; a shallow tympanosquamosal recess is present medially. The postglenoid process forms a distinct posterior margin of the fossa, and the postglenoid notch extends dorsal to the postglenoid process, distinguishing it from the rest of the squamosal. The postglenoid process is knob-like. The supramastoid crest is dorsally concave and sharp.

Part of the vomerine crest is exposed in ventral view (Fig. 42D); it merges dorsally with the trans-

TABLE 13. — Measurements (in cm) of the mandible of Phocoenidae unnamed genus 2 (UCMP 219076). Measurements given to nearest tenth of a millimeter.

Total length as preserved	37.20
Length of symphyseal portion as preserved	10.05
Transverse width at posterior end of symphysis	1.40
Dorsoventral depth at posterior end of symphysis	2.39
Transverse width at anterior end of symphysis	2.62
Dorsoventral depth at anterior end of symphysis	2.17
Transverse width of mandibular condyle	1.42
Dorsoventral depth of mandibular condyle	2.02

versely thin nasal septum; anteriorly, the nasal septum converges with the well-developed, conical, and ventrally-directed ventral tubercle. Dorsally, there is a well-developed median ridge along the mesethmoid in the region of the bony nares. Both palatines are poorly preserved, but the lateral laminae are transversely thin and nearly parallel, and delineate transversely narrow fossae for the hamular lobes of the pterygoid sinus anterior to the choanae. The maxillo-palatine suture is anterolaterally convex.

The mandibles (UCMP 219076) are fused at the symphysis (Figs 43-45; Table 13). The anterior extremity of the symphyseal portion is missing, as is the right mandibular condyle, and the dorsal margin of both coronoid crests (Fig. 43D). Anterior to the left condyle, the ventral margin is damaged. The mandibular condyle is oval-shaped and faces posteriorly. The medial surface of the condyle is hollowed out as part of the large (but incompletely preserved) mandibular foramen. The medial part of the condyle is a dorsoventrally oriented, blade-like process. The condyloid crest occurs as a slight ridge on the lateral face. On the better preserved left side, approximately 25 alveoli are preserved (Fig. 43A, D), although this is a minimum number as many interalveolar septa are missing. The toothrows are slightly laterally concave in dorsal aspect, and in lateral aspect the toothrow is slightly concave dorsally. In dorsal aspect, the toothrows are widely divergent posterior to the symphysis, but at the elongate symphysis, the toothrows are near parallel. The alveoli terminate within the alveolar groove 2 cm anterior to the posterior end of the symphyseal portion. From that level, the alveolar groove transforms into a thin, but deep sulcus; the left and right sulci are separated medially along the symphyseal portion by a high, transversely narrow median bony ridge (Fig. 43A, D). The ventral margin of the ramus is ventrally concave in lateral aspect; the horizontal ramus is dorsoventrally shallowest just posterior to the mandibular symphysis, and it deepens posteriorly and anteriorly toward the symphysis. The symphyseal portion of the mandible is elongate and transversely narrow with flat lateral surfaces. It tapers dorsoventrally toward the anterior tip in lateral view, and is slightly downturned (Figs 43B, C; 44E; 45D). Several mental foramina occur on the lateral surface of the symphyseal portion. Dorsally, a flat triangular surface is present between the alveolar grooves along the posterior portion of the symphysis; a thin median groove is visible here, and a deep, wide groove is present on the posteroventral margin of the symphysis. The rami diverge at with an angle of 24°.

REMARKS AND COMPARISONS

The skull exhibits several phocoenid synapomorphies, including the presence of a premaxillary eminence, ascending process of the premaxilla that terminates anterior to the nasal, a frontal knob, and a well-developed dorsal lobe of the pterygoid sinus fossa (Figs 42-45; Barnes 1985a; Muizon 1988a; Lambert 2008a; Murakami *et al.* 2012a, b). The skull and mandible differ from an undescribed broad-headed phocoenid from the San Diego Formation (UCMP 38340) in exhibiting a more elongate and attenuate rostrum with a distinct rostral crest medial to the antorbital notch, a much narrower antorbital notch and less prominent antorbital process, and mandibles that are fused at the symphysis and edentulous anteriorly. These two specimens from the Purisima Formation share several bizarre features with an undescribed phocoenid from the San Diego Formation preliminarily introduced by Racicot *et al.* (2007) including a fused, transversely flattened and edentulous symphyseal region of the mandible, a large, hypertrophied premaxillary eminence, and a knoblike rostral crest on the maxilla (Figs 42-45). These features distinguish the Purisima and San Diego Formation material from all other fossil and

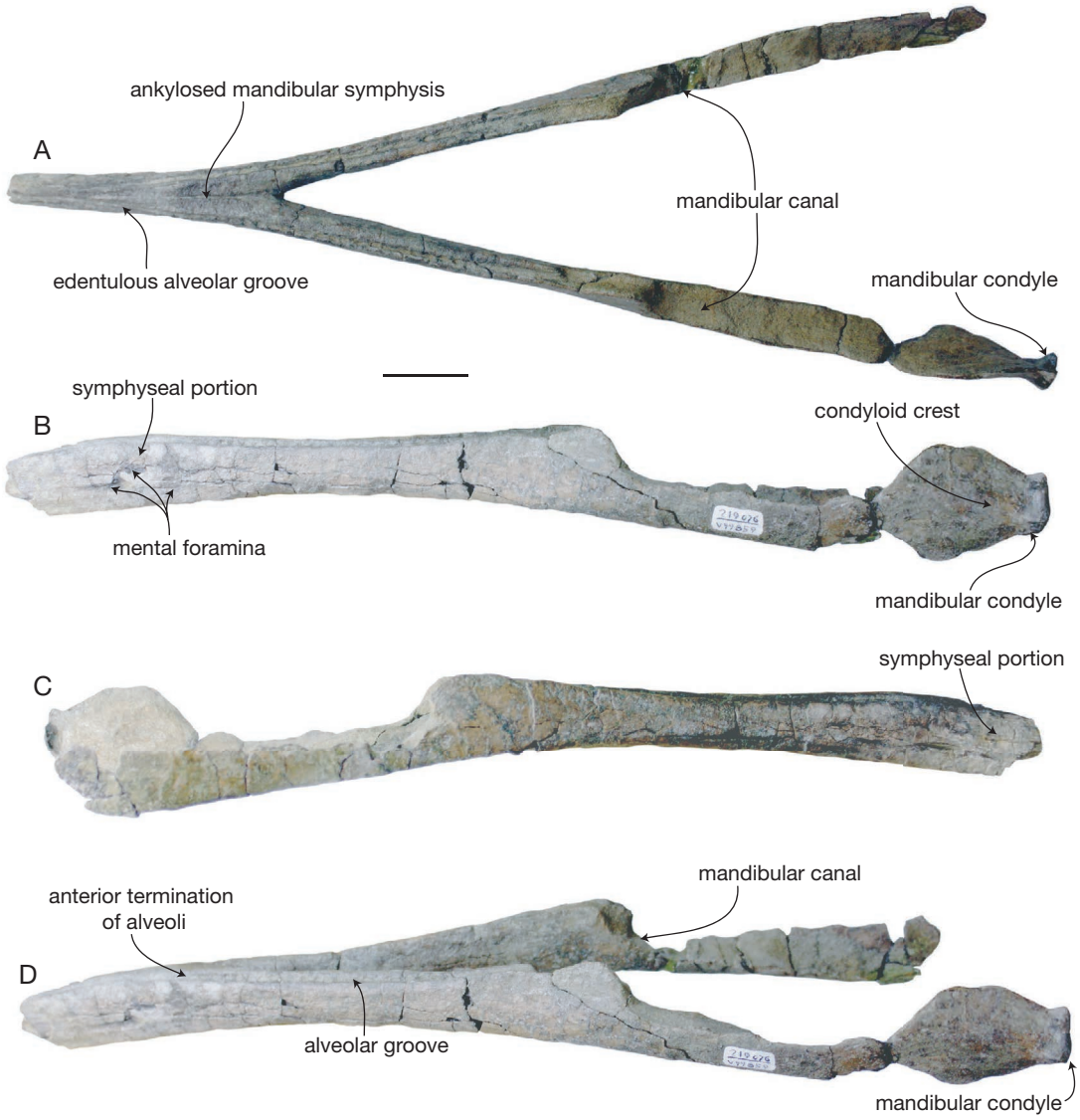

FIG. 43. — Mandibles of Phocoenidae unnamed genus 2 (UCMP 219076); **A**, dorsal view; **B**, left lateral view; **C**, right lateral view; **D**, oblique anterolateral view. Scale bar: 3 cm.

modern phocoenids. UCMP 219503 further differs from extant phocoenids in having a premaxilla wider than the maxilla at the base of the rostrum, having asymmetrical premaxillae, and a transversely convex palate. These specimens (UCMP 219503, 219076) appear to represent a taxon congeneric or conspecific with the undescribed porpoise from the San Diego Formation Racicot *et al.* (2007). More complete material of this taxon from the San Diego Formation includes a partial skeleton with skull and mandibles, partial postcranial skeleton, additional mandibles, partial crania, and petrosals (SDNHM 22452, 23194, 24710, 64742, 65276, 83724). Only a preliminary description of the Purisima

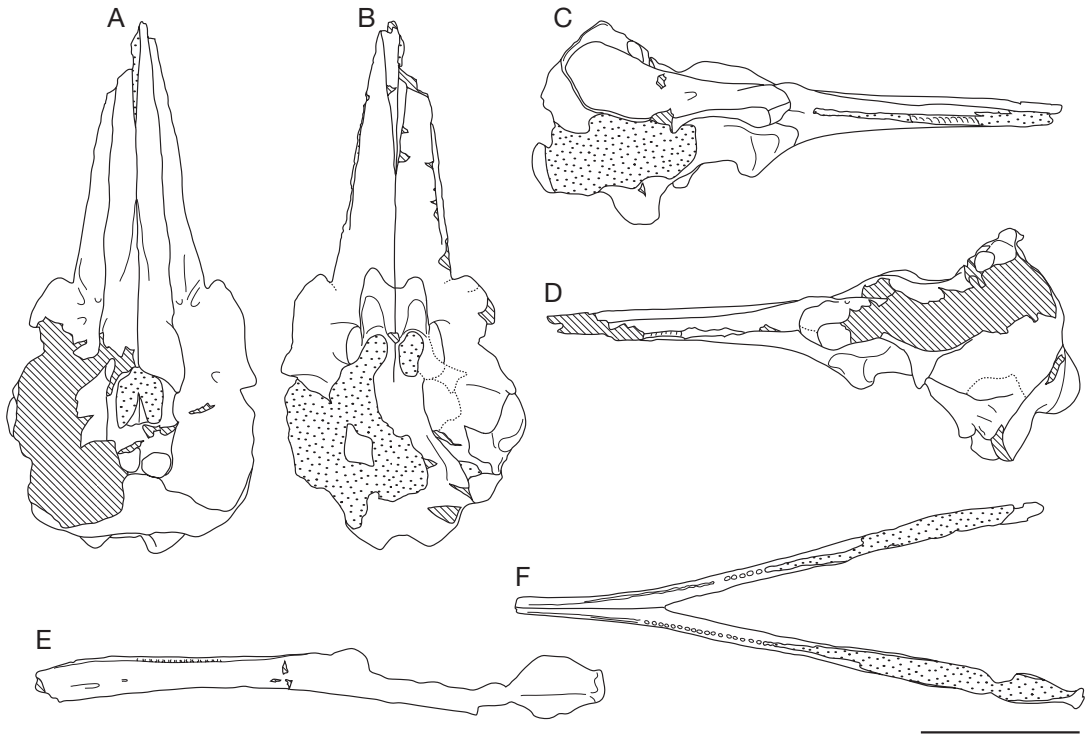

FIG. 44. — Interpretive line drawings of skull (UCMP 219503) and mandible (UCMP 219076) of Phocoenidae unnamed genus 2: **A**-**D**, skull in dorsal (**A**), ventral (**B**), right lateral (**C**) and left lateral (**D**) views; **E**, **F**, mandibles in left lateral (**E**) and dorsal (**F**) views. Scale bar: 10 cm.

Formation specimens is presented here owing to the ongoing work by Racicot and colleagues. The bizarre symphyseal portion of the mandible of this taxon is unique among phocoenids, although it is important to note that *Lomacetus ginsburgi* Muizon, 1986 exhibits a mandible with an elongate (but unfused) mandibular symphysis (Muizon 1988b; Fig. 43B, C). Furthermore, Muizon (1988a) identified strong prognathism of the mandibles as a uniting feature of *Phocoenoides dalli* True, 1885, *Phocoena dioptrica* Lahille, 1912, *Salumiphocoena stocktoni* (Wilson, 1973), and *Piscolithax* Muizon, 1983. Additional material referable to this taxon from the Santa Cruz section of the Purisima Formation includes partial rostra (UCMP 219483, 219582) and several isolated petrosals (UCMP 137472, 219484), based on comparison with the material from the San Diego Formation. Isolated petrosals of this taxon (UCMP 88582 and 88583) from the San Diego Formation were identified and figured by Barnes (1973) as Odontoceti incertae sedis.

Genus *Phocoena* Cuvier, 1816

cf. *Phocoena*

REFERRED MATERIAL. — UCMP 219123, partial skull consisting part of right maxilla and premaxilla missing the anterior portion of the rostrum, antorbital process, and most of the ascending process of the maxilla, collected by R.W. Boessenecker from UCMP locality V99833.

STRATIGRAPHIC OCCURRENCE. — Middle part of the San Gregorio section of the Purisima Formation, Early Pliocene (*c.* 5-3.35 Ma; Zanclean equivalent; Fig. 2).

DESCRIPTION

Anteriorly, the rostrum is dorsoventrally compressed with a flat dorsal surface (Fig. 46). The premaxilla

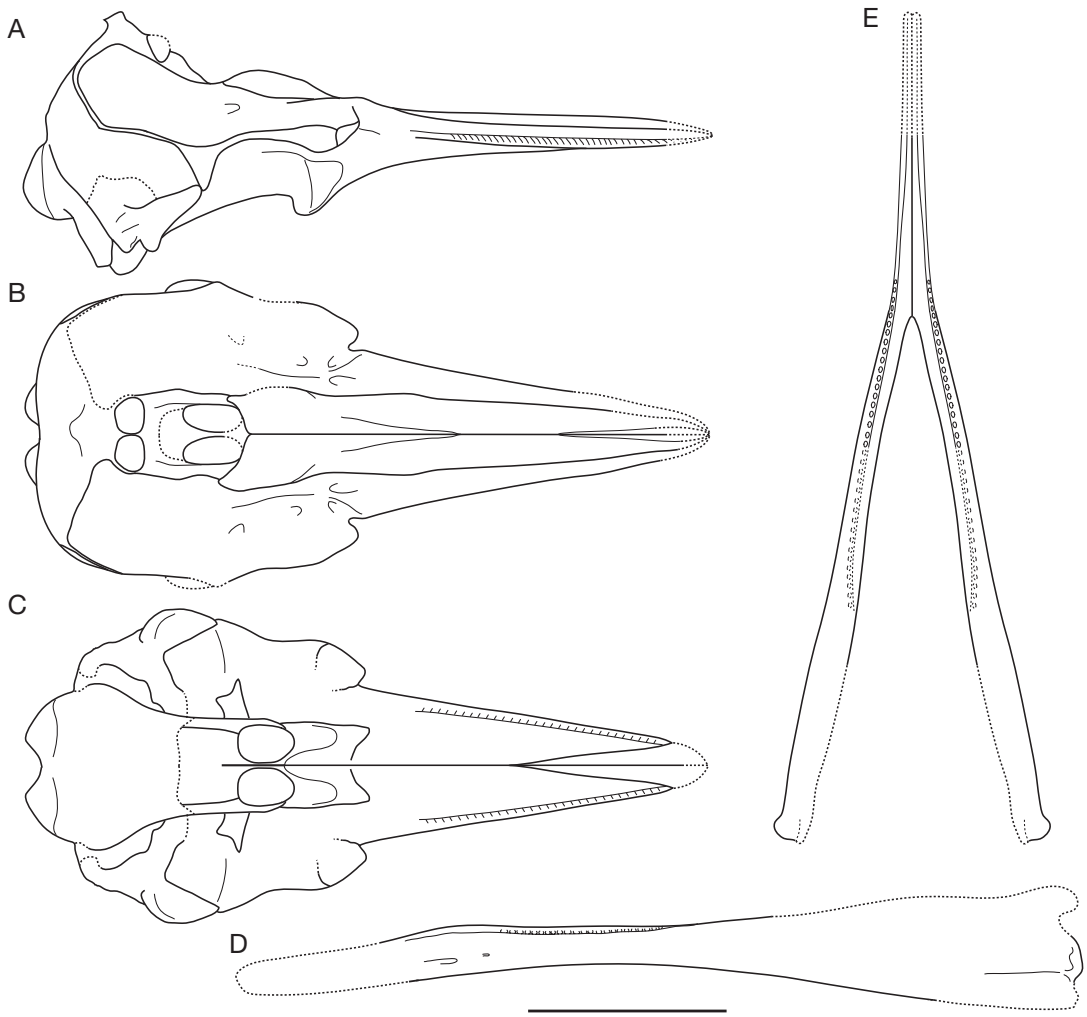

FIG. 45. — Reconstruction of skull (UCMP 219503) and mandible (UCMP 219076) of Phocoenidae unnamed genus 2: **A**-**C**, skull in lateral (**A**), dorsal (**B**) and ventral (**C**) views; **D**, **E**, mandible in lateral (**D**) and dorsal (**E**) views. Scale bar: 10 cm.

has parallel lateral and medial margins, and anteriorly, the premaxilla slopes slightly laterally. Medially, the premaxilla forms a sharp ridge along the dorsal margin of the mesorostral canal; posteriorly the medial surface is flat. The anteromedial sulcus is straight and runs posterolaterally from the margin of the mesorostral canal to the premaxillary foramen. The latter is positioned in the middle of the premaxilla anterior to the premaxillary eminence. The posteromedial sulcus is not apparent, and the posterolateral sulcus is developed lateral to the premaxillary foramen and extends posteriorly along the lateral margin of the premaxillary eminence; an additional posteromedial sulcus (*sensu* Murakami *et al.* 2012b) is not apparent. The prenarial triangle is bordered medially by the mesorostral canal and laterally by the anteromedial sulcus; it is composed of porous bone. The premaxillary eminence is elevated dorsally (Fig. 46C), dorsally convex in lateral aspect, and laterally convex in dorsal aspect (Fig. 46A). The eminence is anteroposteriorly short and laterally overhangs the maxilla; within this overhang is

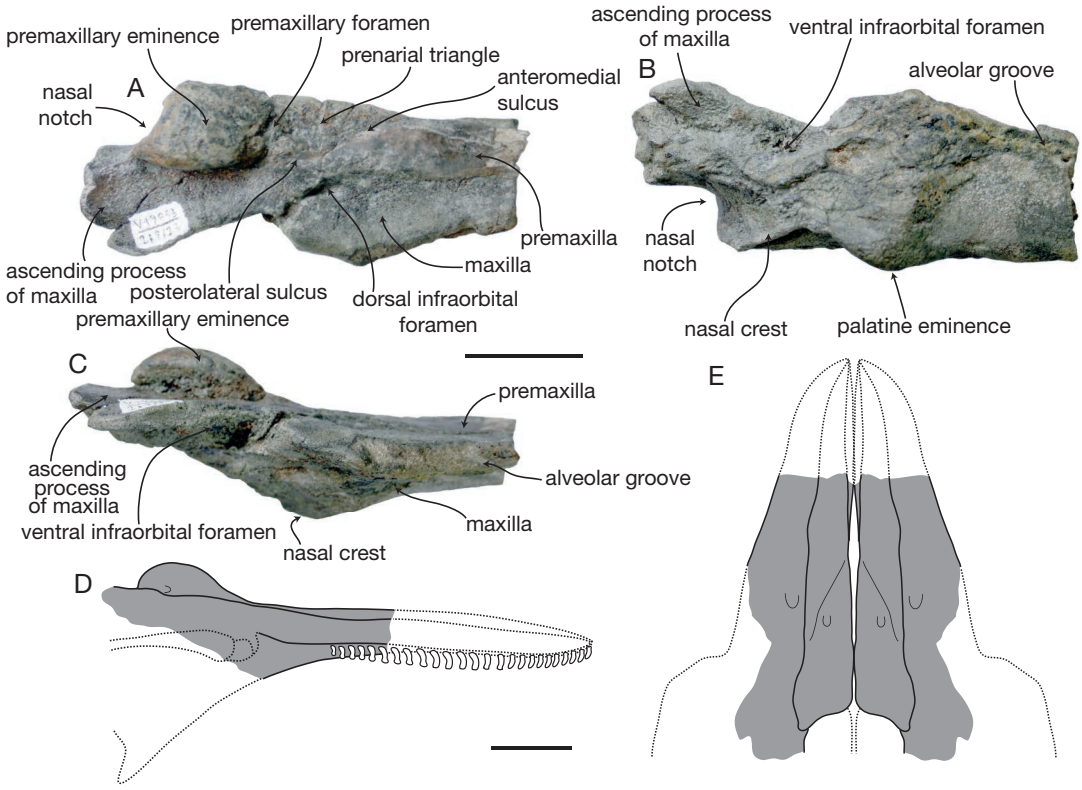

Fig. 46. — Partial skull of cf. *Phocoena* (UCMP 219123): **A**, dorsal view; **B**, ventral view; **C**, right lateral view; **D**, interpretive line drawing in right lateral view; **E**, interpretive line drawing in dorsal view, with fossil mirrored. Gray shading on line drawing represents preserved portions, and dashed line represents unknown features. Scale bars: 3 cm.

a small, laterally facing foramen in the premaxilla. There is a small indentation in the posteromedial corner of the premaxillary eminence, where the accessory exposure (= maxillary ossicle) of the maxilla was probably situated. The ascending process of the premaxilla is restricted to a small cone-shaped process extending posterolateral to the premaxillary eminence. This process dorsally overlaps the maxilla, and is short along the lateral side of the bony naris. The premaxilla/maxilla suture runs along the base of the premaxillary eminence. The dorsal surfaces of the maxilla of UCMP 219123 and ascending process of the maxilla are relatively flat (Fig. 46C). Although damaged, the rostrum clearly tapers anteriorly. The anteriormost dorsal infraorbital foramen occurs anterolateral to the premaxillary eminence and opens anteriorly. The palatal surface of the maxilla is transversely convex. A poorly preserved alveolar groove occurs adjacent to the lateral margin of the rostral portion of the maxilla.

Comparisons

This specimen exhibits many features identifying it as a phocoenid or true porpoise, including a well-developed premaxillary eminence and an ascending process of the premaxilla that does not extend posteriorly beyond the bony naris (Fig. 46A; Barnes 1985a). This specimen differs from other modern and fossil phocoenids in several ways. Although the premaxillary eminence is elevated in UCMP 219123 as in *Neophocaena phocoenoides* Cuvier, 1824, *Phocoena phocoena* Linnaeus, 1758, *Phocoena dioptrica*, *Phocoena sinus* Norris & McFarland, 1958, and *Phocoenoides dalli*, it is more elevated and more strongly dorsally convex than in

Archaeophocaena Murakami, Shimada, Hikida & Hirano, 2012, *Australithax* Muizon, 1988, *Haborophocoena*, *Lomacetus* Muizon, 1986, *Miophocaena*, *Numatophocoena* Ichishima & Kimura, 2000, *Piscolithax*, *Pterophocaena*, *Salumiphocaena* Barnes, 1985, and *Septemtriocetus* Lambert, 2008. UCMP 219123 differs from *Pterophocaena* in possessing a narrower premaxillary eminence that does not widely overhang the ascending process of the maxilla. The laterally convex margin of the premaxillary eminence in this taxon is similar with *P. phocoena*, *Phocoena spinipinnis* Burmeister, 1865, *P. dalli* and the Miocene porpoises *Archaeophocaena* and *Salumiphocoena*, while it is not as convex as in *N. phocoenoides* and *P. sinus*; all other fossil taxa exhibit a straight lateral margin (*Haborophocoena toyoshimai*, *Piscolithax*, *Septemtriocetus*) or an "angled" margin with a slight corner (*Australithax*, *Haborophocoena minutis*, *Lomacetus*, *Miophocaena*). UCMP 219123 differs from an undescribed broad-headed phocoenid from the San Diego Formation (SDNHM 38340) in its smaller size, and slightly convex palate. UCMP 219123 differs from *Archaeophocaena*, *Haborophocoena*, and *Miophocaena* in possessing a left premaxilla that terminates further anteriorly and near the anterolateral margin of the bony nares. *Phocoena dioptrica* also exhibits a relatively straight lateral margin of the premaxillary eminence. Additionally, *P. dalli* exhibits an exposure of the premaxilla lateral to the base of the eminence, as opposed to the suture running along the base as in UCMP 219123. In UCMP 219123, all extant species of *Phocoena*, and *Salumiphocaena*, the premaxillary eminence is anteroposteriorly short and dorsally highly convex; it is slightly longer in *Neophocaena* Palmer, 1899 and *Phocoenoides*, and much longer in all other fossil phocoenids. When eminence height is expressed as a percentage of anteroposterior length of the eminence, UCMP 219123 exhibits the most convex eminence at 37%, compared to 35% in *P. dioptrica*, 27% in *P. phocoena*, 25% in *P. spinipinnis* and *N. phocoenoides*, and 23% in *P. dalli*. The rostrum of *Neophocaena* is also dorsoventrally deeper than in UCMP 219123, in addition to possessing a transversely convex prenarial triangle, which is flat in UCMP 219123. Although incomplete, the morphology of the premaxilla and maxilla agree most closely with extant porpoises (*Phocoena*, *Phocoenoides*, and *Neophocaena*). In particular, the short, wide, and dorsally and laterally convex premaxillary eminence suggests that this specimen belongs to the genus *Phocoena*; no other fossil or extant phocoenids exhibit such an anteroposteriorly short and dorsally convex premaxillary eminence. However, UCMP 219123 differs from extant phocoenids and *Miophocaena* in its apparent lack of additional posterolateral sulci (*sensu* Murakami *et al.* 2012b).

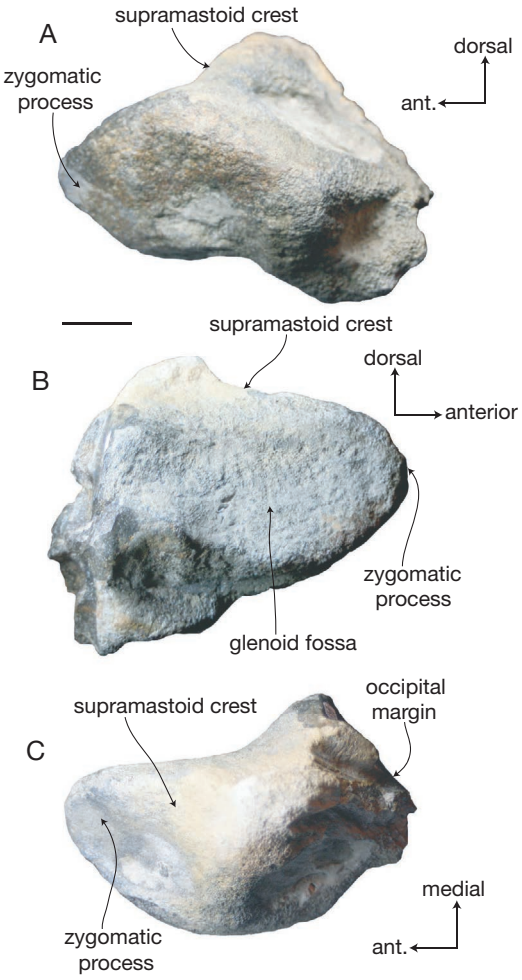

FIG. 47. — Partial left squamosal of cf. Physeteroidea gen. et sp. indet. (UCMP 219108); **A**, lateral view; **B**, medial view; **C**, dorsal view. Scale bar: 3 cm.

In UCMP 219123, as well as all other extant phocoenids and *Piscolithax*, the ascending process of the premaxilla is reduced to a small, cone shaped process that dorsally overlaps the maxilla. In *Archaeophocaena*, *H. toyoshimai*, *Miophocaena*, *Numatophocoena*, and crania of the *Haborophocoena*-like Phocoenidae unnamed genus 1 (UCMP 128285, 219504), the ascending process is formed instead as a transversely broad sheet that overlaps the maxilla (as in delphinids); in all other fossil phocoenids (*Australithax*, *H. minutis*, *Lomacetus*, *Salumiphocaena*, and Phocoenidae unnamed genus 2), the ascending process forms the anterior part of a cylindrical ridge that laterally borders the bony nares, the posterior part of which is formed by the maxilla. In this specimen, the rostral portion of the maxilla is relatively narrow, similar to *P. phocoena*, *Australithax*, *Septemtriocetus*, *H. minutis*, and *Lomacetus*. However, this differs from all other species of *Phocoena*, *Neophocaena*, *Phocoenoides*, as well as *Salumiphocaena* and *Piscolithax tedfordi* Barnes, 1984, all of which have a maxilla that is much wider than the premaxilla on the rostrum. At the other extreme, *Haborophocoena toyoshimai*, *Piscolithax boreios* Barnes, 1984, and *Piscolithax longirostris* have a rostral portion of the premaxilla that is wide and nearly wider than the maxilla on the rostrum. The small facet in the premaxillary eminence indicates that the accessory exposure of the maxilla (= maxillary ossicle) was small (although missing in UCMP 219123), like in most phocoenids (with the exception of *Lomacetus*, which had large and anteriorly extending maxillary ossicle). Lastly, unlike all extant phocoenids, UCMP 219123 exhibits a slightly convex palate, which also occurs in most fossil taxa; a convex palate appears to be plesiomorphic for phocoenids and delphinoids in general. In extant phocoenids, the palate at mid-rostrum is transversely flat or even slightly concave.

Remarks

These comparisons suggest that UCMP 219123 is most phenetically similar to the extant harbor porpoise *P. phocoena*, and is identified as cf. *Phocoena*. This is the earliest fossil record of an extant phocoenid genus, and the first fossil record of an extant phocoenid from the eastern Pacific. Previously, fossils of extant phocoenid taxa have been reported only from the Pleistocene: *N. phocaenoides* from Japan (Kimura & Hasegawa 2005) and *P. phocoena* from Champlain Sea deposits (Harington 1977). Two additional *Phocoena*-like taxa are present in Upper Pliocene strata of California: an undescribed broad-headed phocoenid with spatulate teeth from the San Diego Formation (SDNHM 38340), and a small phocoenid with a convex palate and sulci on the premaxillary eminences (USNM 23885) from the Purisima Formation near Pillar Point (San Mateo County). This proposed Pliocene record of cf. *Phocoena* has implications for the timing of divergence of crown phocoenids.

The evolutionary biogeography of phocoenids was hypothesized by Fajardo-Mellor *et al.* (2006) as follows: 1) phocoenids originated in the eastern North Pacific; 2) *Neophocaena* and the common ancestor of the *Phocoena-Phocoenoides* clade dispersed into the southern hemisphere during the Pliocene (3-2 Ma; Piacenzian-Gelasian) following cooling caused by the closure of the Panama seaway; and 3) Pleistocene cooling allowed the ancestors of *Phocoena sinus* and the common ancestor of the *P. phocoena-P. dalli* clade to each disperse northwards into the North Pacific. The presence of an Early Pliocene (4.5-3.35 Ma; Zanclean-Piacenzian equivalent) record of cf. *Phocoena* suggests that the clade may have diverged by 4 Ma. The phylogenetic relationship of the southern hemisphere *P. spinipinnis* as sister to a *Phocoenoides* + *P. phocoena* clade (Fajardo-Mellor *et al.* 2006) still supports a southern hemisphere origin for the common ancestor of these taxa, although it is possible that basal members of the entire *Phocoena-Phocoenoides* clade remained in the North Pacific during the Late Pliocene. More fossils are needed for further evaluation.

Superfamily Physeteroidea Gray, 1868

cf. Physeteroidea gen. et sp. indet.

Referred material. — UCMP 219108, an isolated and abraded squamosal collected by R.W. Boessenecker from UCMP locality V99836.

STRATIGRAPHIC OCCURRENCE. — Middle part of the San Gregorio section of the Purisima Formation, Early Pliocene (*c.* 5-3.35 Ma; Zanclean-Piacenzian equivalent; Fig. 2).

DESCRIPTION

This abraded, partial small squamosal (Fig. 47) is robust and blocky, with a blunt zygomatic process. Much of the postglenoid process is missing, although part of the external acoustic meatus is preserved at about the level of the ventral margin of the zygomatic process. An arcuate and shallow dorsomedial fossa is present on the zygomatic process. The supramastoid crest is robust and posteriorly elevated (Fig. 47A). A sharp dorsomedial ridge is present on the zygomatic process, forming the medial margin of the mandibular fossa; in dorsal aspect, it is medially convex. The mandibular fossa is broad, rectangular, and shallowly concave. A large fossa occurs on the posterolateral surface of the squamosal, and appears to have been taphonomically enlarged. A number of deep grooves on the posterior surface mark the articular surface with the exoccipital.

REMARKS AND COMPARISONS

Although clearly a cetacean squamosal, UCMP 219108 compares poorly with most groups of Neogene cetaceans; comparisons were made between this specimen and large cetaceans including mysticetes, ziphiids, physeteroids, and globicephaline delphinids. UCMP 219108 lacks features common to Neogene mysticetes including a large and paddle-shaped postglenoid process, and is transversely more robust and absolutely larger than the squamosal of extant ziphiids and globicephaline delphinids. UCMP 219108 exhibits a posterodorsally elevated supramastoid crest, which Bianucci & Landini (2006) identified as a synapomorphy of the Physeteroidea, and it is here tentatively identified to this clade. In terms of the extreme bluntness of the zygomatic, it compares relatively well with the Miocene Belgian stem physeteroid *Eudelphis mortezelensis* Du Bus, 1872; however, UCMP 219108 is significantly younger (*c.* 3.35-5 Ma, Early Pliocene; Zanclean-Piacenzian equivalent) than *Eudelphis* Du Bus, 1872 (Middle Miocene; Lambert 2008b: fig. 19). In lateral aspect, the zygomatic process exhibits a similar morphology to *Thalassocetus* Abel, 1905, *Brygmophyseter* Kimura, Hasegawa & Barnes, 2006, *Orycterocetus* Leidy, 1853, and *Aulophyseter* Kellogg, 1927 (all Early to Middle Miocene physeteroids). The zygomatic process of UCMP 219108 is shorter and more blunt than those of *Zygophyseter* Bianucci & Landini, 2006, and *Acrophyseter* Lambert, Bianucci & Muizon, 2008, and transversely thicker than all known physeteroids. Although incomplete, the squamosal of *Livyatan* Lambert, Bianucci, Post, Muizon, Salas-Gismondi, Urbina & Reumer, 2010 appears to have been more gracile and anteriorly tapering than UCMP 219108. Because *Ontocetus oxymycterus* Kellogg, 1925 lacks squamosals, it cannot be compared with UCMP 219108. This specimen is substantially larger and more robust than the squamosals of all known kogiids (e.g., *Aprixokogia* Whitmore & Kaltenbach, 2008; *Kogia* Gray, 1846; *Praekogia* Barnes, 1973; *Scaphokogia* Muizon, 1988) and can be differentiated from these taxa. Because the squamosal morphology of UCMP 219108 does not match any previously described physeteroid taxon, it cannot be confidently identified to the generic level.

DISCUSSION

The marine mammal assemblage described in this paper supplements the descriptions of fossil sharks, rays, bony fish, and birds by Boessenecker (2011a) and Boessenecker & Smith (2011) from the San Gregorio section of the Purisima Formation. Altogether, there are now 34 marine vertebrate taxa known from this locality (Fig. 48; Table 1). In comparison, there are approximately 70 marine vertebrate taxa recorded from the Santa Cruz section of the Purisima Formation, although this number is an aggregate of three stratigraphically separated assemblages (Boessenecker & Perry, unpublished data). Although various elements of the vertebrate assemblage from the well-known Santa Cruz section of the Purisima Formation have been described, including cetaceans (Barnes 1985b; Whitmore & Barnes 2008; Boessenecker *et al.* 2013) and pinnipeds (Repenning & Tedford 1977; Boessenecker & Perry 2011), the sharks, rays, bony fish, and birds have yet to be described. Additionally, there remain

many more cetacean and pinniped fossils to describe from Purisima Formation localities in the Santa Cruz and Point Reyes sections, including new taxa.

The paucity of published descriptions for the extremely rich marine vertebrate fossil record from Late Neogene strata in the eastern North Pacific (ENP) seems to be the rule rather than the exception. Despite the long history of research of Neogene marine vertebrates from this region (see reviews in Mitchell 1966a, and Barnes 2008), there are no marine vertebrate assemblages of Late Neogene age that have been described in their entirety, or where studies of most taxonomic groups have been published. For example, the marine vertebrate assemblage of the Almejas Formation in Baja California (Fig. 49) was summarized by Barnes (1992), and studies of birds (Howard 1971), pinnipeds (Repenning & Tedford 1977) and odontocetes (Barnes 1984; 1985b; 2008) have been published, but the sharks and baleen whales await study. The similarly aged Capistrano Formation assemblage of southern California (Fig. 49) includes fossil pinnipeds (Barnes & Raschke 1991; Deméré & Berta 2005), a swordfish (Fierstine 2008), and fossil birds (Smith 2011) that have been described, but virtually no other taxa from this rich assemblage have been published upon. Thus far, only birds (Howard 1982; Smith 2011, 2013) and sea cows (Domning & Deméré 1984) have been described from the uppermost Miocene to Lower Pliocene San Mateo Formation of southern California (Fig. 49), although the vertebrate assemblage was briefly summarized by Barnes *et al.* (1981), and the remainder of the assemblage is diverse and also includes sharks, odontocetes, and mysticetes (Barnes *et al.* 1981). Lastly, fossil birds (see Chandler 1990, and references therein; Smith 2011), pinnipeds (Berta & Deméré 1986; Deméré 1994b), and two cetaceans, including the lipotid dolphin *Parapontoporia sternbergi* (Gregory & Kellogg 1927; Barnes 1985b), and the poorly known mysticete *Balaenoptera davidsonii* (*sensu* Deméré 1986) have all been reported from the Pliocene San Diego Formation (Fig. 49). Even the well-documented fossil bird assemblage from the San Diego Formation requires additional study because of abundant new fossil material, in addition to the rich but virtually unstudied collection of fossil sharks and mysticetes.

In contrast, the only Neogene marine vertebrate assemblage where elements of all major vertebrate clades have been described is the Middle Miocene Sharktooth Hill Bonebed. The Sharktooth Hill local fauna has been the subject of numerous publications, and includes studies of sharks (Jordan & Hannibal 1923), sea turtles (Lynch & Parham 2003; Parham & Pyenson 2010), birds (Wetmore 1930; Miller 1961, 1962; Howard 1966, 1984; Stidham 2004), land mammals (Prothero *et al.* 2008), pinnipeds (Kellogg 1931; Mitchell 1966c; Barnes 1972, 1988; Barnes & Hirota 1995; Kohno *et al.* 1995a), odontocetes (Kellogg 1931; Barnes & Mitchell 1984; Kimura *et al.* 2006; Barnes & Reynolds 2009), mysticetes (Kellogg 1931), and taphonomy (Pyenson *et al.* 2009). However, much more material has been collected since some of these earlier studies and an enormous volume of fossil material awaits careful description and publication; abundant taxonomic problems face the fossil marine mammals in particular, and require future study and clarification.

In summary, although a wide variety of studies have focused on Neogene marine mammals and birds of the ENP, few studies have focused on marine vertebrates at the level of individual assemblages, and fewer studies have attempted to compare marine vertebrate assemblages from this region through time and space. Additionally, only a small fraction of new taxa from these assemblages have been described in the literature, and substantially more work remains to be done. With the description of this new marine mammal assemblage of Pliocene age from the San Gregorio section of the Purisima Formation, a comparison with the marine mammal assemblage of the similarly aged San Diego Formation is warranted. The aggregate marine mammal fauna of the eastern North Pacific is summarized below, and permits comparison with other Pliocene marine mammal assemblages, and a consideration of patterns and causes of marine mammal faunal provinciality and turnover during the Pliocene-Pleistocene interval. Diversity at the generic level is examined, as generic richness appears to be appropriate for discussing and analyzing Cetacean evolution (Uhen & Pyenson 2007; Marx & Uhen 2010).

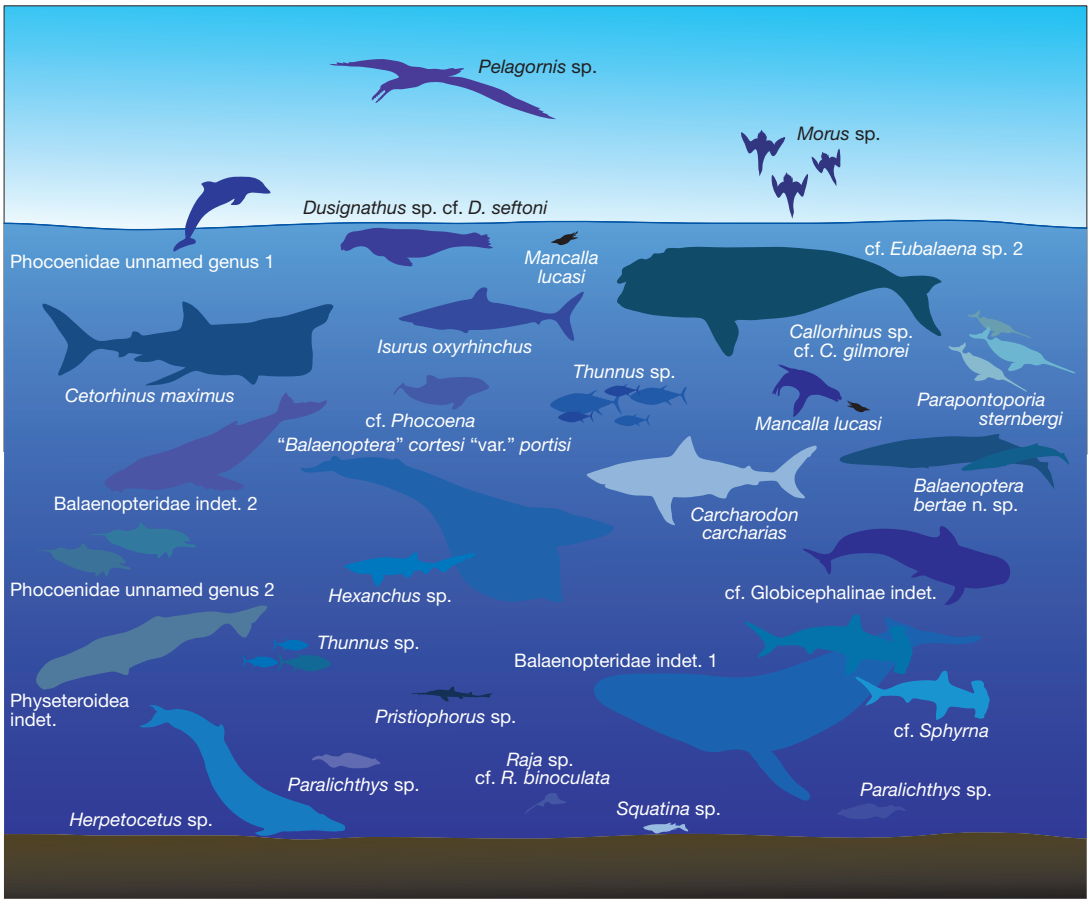

FIG. 48. — Stylized diagram of the Pliocene marine vertebrate assemblage of the San Gregorio section of the Purisima Formation, highlighting the diversity of the assemblage; as described in this study, Boessenecker (2011a), and Boessenecker & Smith (2011). Various species are shown as silhouettes, and are roughly to scale; some taxa only represented from the base of the section (latest Miocene) were omitted for space.

COMPARISON WITH THE SAN DIEGO FORMATION MARINE MAMMAL ASSEMBLAGE

Although many of the marine vertebrates from the San Diego Formation (Figs 49-51) have not yet been published, the extensive collections of marine vertebrate fossils at the San Diego Museum of Natural History and the Pliocene age of this unit (3-2 Ma, Deméré 1983; Fig. 51) make the San Diego Formation marine mammal assemblage an excellent point of comparison with the fossil mammals of the San Gregorio section of the Purisima Formation (Table 14). These two formations were deposited approximately 450 km apart, the Purisima Formation reflecting a temperate paleoclimate, and the San Diego Formation reflecting a warm temperate paleoclimate (Fig. 49; Hall 2002); such a difference in sea surface temperature may account for differences in faunal composition. Although the marine mammal assemblage of the San Diego Formation has not been described in its entirety, the pinnipeds and sirenians have been described in detail (Domning & Deméré 1984; Berta & Deméré 1986; Deméré 1994b), and parts of the cetacean assemblage have either been described or discussed in print (Barnes 1973; 1977; Deméré 1986; Deméré *et al.* 2005); additionally, a faunal list of the mam-

mal assemblage was published by Deméré (1994b: table 1). Preliminary reports of several ongoing studies of new fossil cetaceans from the San Diego Formation have been presented recently, including a new genus of eschrichtiid gray whale (Deméré & Berta 2003), a new species of *Balaenoptera* (Martin 2010), and a new genus of phocoenid (Racicot *et al.* 2007). Fossil pinnipeds from these two units are similar, and both appear to preserve the fur seal *Callorhinus gilmorei*, and the dusignathine walrus *Dusignathus seftoni*. *Callorhinus gilmorei* is now known from several geographically distant localities (Berta & Deméré 1986; Boessenecker 2011c; this study); unidentified fur seal remains from other Pliocene units (e.g., the Tirabuzón Formation, Baja California; Barnes 1998) probably represent this species as well. The third pinniped from the San Diego Formation, *Valenictus chulavistensis*, is not yet known from the San Gregorio assemblage, but well-preserved crania (e.g., UCMP 219091) and a femur (SCMNH 21366) of *Valenictus* sp. have been recovered from the Pliocene portion of the Purisima Formation near Santa Cruz. A third walrus may be represented in the San Diego Formation. A pair of short tusks with an associated incisor and several postcanine teeth (LACM 28432) exhibit globular dentine (Boessenecker pers. obs.), indicating that it represents a member of the Odobenini. Globular dentine precludes referral to the short-tusked *Dusignathus seftoni*, which along with other dusignathines lack globular dentine (Demere 1994a, b); likewise, the presence of non-canine teeth precludes referral to the "toothless" walrus *Valenictus chulavistensis* (Demere 1994a).

Curiously lacking from the San Gregorio assemblage are fossils of the gigantic sea cow *Hydrodamalis cuestae* Domning, 1978, which are abundant in the San Diego Formation (Domning & Deméré 1984); indeed, sirenian bones are completely absent from the San Gregorio assemblage. Due to the high preservation potential of sirenian bones (owing to their pachyosteosclerotic histology and large size, particularly in hydrodamalines) coupled with the large sample size of fossils from this locality, the absence of sirenian fossils from the San Gregorio assemblage appears to be genuine. Similarly, although sirenian bones are abundant within the basal bonebed of the Santa Cruz section of the Purisima Formation (referred to *Dusisiren* sp. D by Domning [1978], an informal taxon now known as *Dusisiren dewana* Takahashi, Domning & Saito, 1986), extensive field collecting (2005-2012) from higher strata of Pliocene age within the Santa Cruz section have have failed to yield any sirenian fossils (among a sample of approximately 850 vertebrate specimens). It is certainly possible that *Hydrodamalis cuestae* was restricted to warm temperate waters in southern California (Hall 2002) during the Early Pliocene (Zanclean-Piacenzian); during the Pliocene, the northernmost occurrence of hydrodamaline sirenians in the ENP is *Hydrodamalis cuestae* in the Squire Member of the Pismo Formation near San Luis Obispo, approximately 280 km to the south of the San Gregorio section of the Purisima Formation (Fig. 49).

Fossil odontocetes from both assemblages are relatively similar; both assemblages include the lipotid dolphin *Parapontoporia sternbergi* and the bizarre undescribed phocoenid (Phocoenidae unnamed genus 2) with the elongate mandibular symphysis described above and reported by Racicot *et al.* (2007). Missing from the San Diego Formation is the early globicephaline and cf. *Phocoena* (reported herein). Fossils of small-bodied delphinids and a beluga-like monodontid occur in the San Diego Formation (and the Purisima Formation at Santa Cruz), but are not yet known from the San Gregorio assemblage. Given the much smaller sample size of the latter, and the occurrence of earbones of these taxa in the Santa Cruz section of the Purisima Formation, further field investigation of the San Gregorio assemblage may well yield fossils of these taxa; indeed, isolated petrosals of small-bodied delphinids (UCMP 219485) and monodontids are known from the Pliocene section of the Purisima Formation near Santa Cruz, and more complete material is known from the uppermost Miocene portion of the Santa Cruz section of the Purisima Formation. Lastly, a *Haborophocoena*-like phocoenid (Phocoenidae unnamed genus 1) is known from the San Gregorio and Santa Cruz sections of the Purisima Formation, but has not yet been found in the San Diego Formation (or any other strata in California). An additional *Phocoena*-like diminutive porpoise

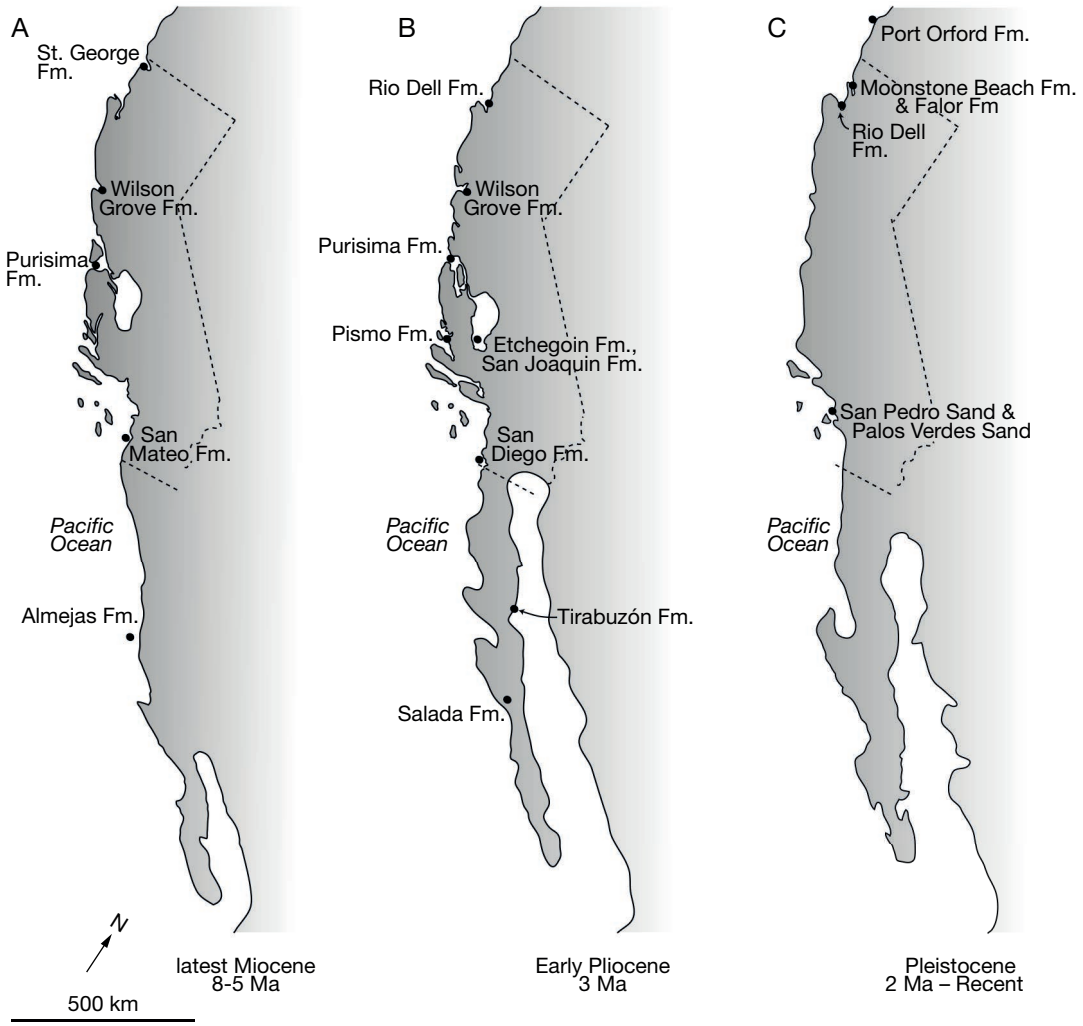

Fig. 49. — Generalized paleogeographic maps of California and Baja California. **A**, latest Miocene; **B**, Early Pliocene, **C**, Pleistocene. Maps of California redrawn from Hall (2002) and Baja California from Ledesma-Vázquez (2002), and paleogeographic maps courtesy R. Blakey. California border palinspastically corrected after Hall (2002).

(USNM 23885) is known from an Upper Pliocene locality in the Purisima Formation further north in San Mateo County; USNM 23885 is of similar size, morphology, and geologic age to cf. *Phocoena* reported herein, and may represent the same undescribed phocoenid taxon. An undescribed broad-headed phocoenid with spatulate teeth (SDNHM 38340) is present in the San Diego Formation, but is not yet known from the Purisima Formation or other strata in California (see above).

The fossil mysticetes from the San Gregorio section of the Purisima Formation and the San Diego Formation are strikingly similar. Both include the bizarre and diminutive mysticete *Herpetocetus*. Aside from the Late Miocene mandible of *Herpetocetus bramblei* from the base of the San Gregorio section, *Herpetocetus* sp. earbones and a mandible from the higher up in the section (Pliocene) share several features in common with the undescribed species of *Herpetocetus* from the San Diego Formation. The

San Gregorio specimens are probably conspecific with a new Early Pliocene species of *Herpetocetus* from the Santa Cruz section of the Purisima Formation. In contrast to the San Diego assemblage, one of the bullae reported herein belongs to the extant right whale *Eubalaena*; the extinct balaenid from the San Diego Formation represents a new fossil species of *Balaena* (Churchill *et al.* 2012). Two fossil rorquals are potentially shared by these two units: "*Balaenoptera*" *cortesi* "var." *portisi*, and *Balaenoptera* sp. The latter may represent an occurrence in the Purisima Formation of the new species of *Balaenoptera* recently reported by Martin (2010). Cranial material of this undescribed taxon from the San Diego Formation is much larger and morphologically distinct from *Balaenoptera bertae* n. sp., which is not recorded from the San Diego Formation. As discussed above, the Purisima and San Diego Formation specimens of "*B.*" *cortesi* "var." *portisi* are indistinguishable.

Although several fossil marine mammal taxa occur in the San Diego Formation but not in the San Gregorio assemblage, nearly three-quarters of fossil marine mammals from the San Gregorio assemblage occur within the San Diego Formation. The lack of certain marine mammals in the San Gregorio assemblage is probably due to the substantially smaller sample size relative to the San Diego Formation. There is a rather high degree of faunal similarity between these two rock units, and Boessenecker (2011a) utilized marine vertebrates from the San Gregorio assemblage to investigate the age of the San Gregorio section of the Purisima Formation. The occurrence of the elasmobranchs *Carcharodon carcharias* and *Raja* sp., cf. *R. binoculata*, the flightless auk *Mancalla lucasi*, and three cetaceans (including *P. sternbergi*, Phocoenidae unnamed genus 2 [=Phocoenidae new genus of Racicot *et al.* 2007], and *Herpetocetus* sp.) indicated an Early to Late Pliocene age (Piacenzian-Zanclean equivalent) for the middle and upper parts of the San Gregorio section of the Purisima Formation (Boessenecker 2011a). The occurrence of *P. sternbergi*, Phocoenidae unnamed genus 2, and *Herpetocetus* sp. led Boessenecker (2011a) to correlate this part of the Purisima Formation with the San Diego Formation, in agreement with tephrochronologic studies and recent mollusk biostratigraphy (but not earlier biostratigraphic work; see summary in Boessenecker 2011a). Additional fossil marine mammals that strengthen this correlation include the pinnipeds *Callorhinus* sp., cf. *C. gilmorei* and *Dusignathus* sp., cf. *D. seftoni*, and the early diverging balaenopterid "*B.*" *cortesi* "var." *portisi.* This high degree of similarity further supports the Early to Late Pliocene age (Piacenzian-Gelasian equivalent) determination by Boessenecker (2011a).

The Pliocene marine vertebrate assemblage of the eastern North Pacific

As discussed above, the aggregate marine vertebrate assemblage of the ENP appears to be relatively similar between localities (Table 14). Additional Pliocene odontocetes not represented in these two units include the aberrant delphinoid *Albireo savagei* Barnes, 2008 from the Upper Pliocene Pismo Formation of central California (Fig. 49; Barnes 2008), the early pilot-whale like globicephaline delphinid *Protoglobicephala mexicana* from unnamed Pliocene strata in Baja California (Aguirre-Fernández *et al.* 2009), and the bizarre kogiid sperm whale cf. *Scaphokogia* from the Pliocene Tirabuzón Formation of Baja California (Fig. 49) known previously only from the Pliocene of South America; Barnes 1998). In addition to these records, the early sea otter *Enhydritherium* has been reported from the Etchegoin, San Mateo, and San Joaquin Formations (Fig. 49; Berta & Morgan 1985).

Four pinnipeds (*Callorhinus gilmorei*, *Dusignathus seftoni*, *Valenictus chulavistensis*, *Valenictus imperialensis*, and a possible additional odobenine from the San Diego Formation) are robustly known from the aggregate Pliocene marine mammal assemblage of the eastern North Pacific. All diagnostic material thus far reported from Pliocene strata in this region have turned out to be from these taxa (Mitchell 1961; Repenning & Tedford 1977; Berta & Deméré 1986; Deméré 1994b; Barnes 1998; Boessenecker 2011c; this study). Some additional unpublished finds may slightly expand this record. Barnes (1998) further listed "aff. *Odobenus*, genus and species undetermined" from the Lower Pliocene Salada Formation (3-5 Ma) of Baja California (Fig. 49), and considered this to be a non-*Valenictus*

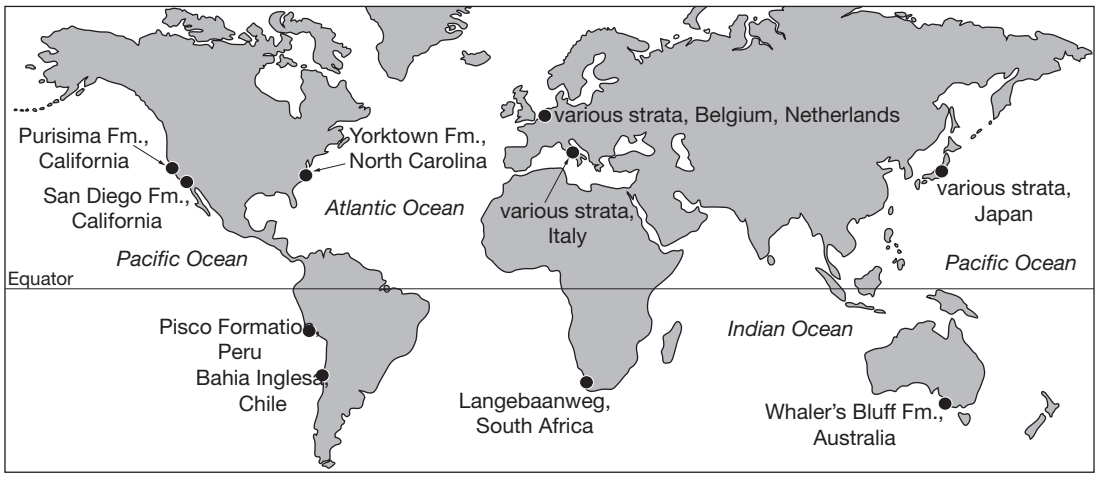

FIG. 50. — Generalized world map showing selected Pliocene marine mammal assemblages. The marine mammal assemblages from Italy and Japan are from a large number of geographically separated localities and different rock units which would be difficult to properly label at this scale.

odobenine. A set of associated postcrania including a well-preserved humerus from the Deguynos Formation (Proto-Gulf of California) apparently indicates the presence of a new dwarf species of *Valenictus* (Atterholt *et al.* 2007), attesting to Pliocene pinniped ecomorphological diversity in the region. Barnes (1998) also reported cf. *Thalassoleon* from Lower Pliocene exposures of the Almejas Formation (Fig. 49), and Deméré *et al.* (2003) listed *Thalassoleon*? sp. indet. from the Lower Pliocene Lawrence Canyon Local Fauna of the San Mateo Formation (California), suggesting that this fur seal persisted into the earliest part of the Pliocene. Only one sirenian is known, *Hydrodamalis cuestae* (Domning 1978; Domning & Deméré 1984), and all diagnostic Pliocene sirenian remains from numerous strata in the ENP (Capistrano Formation, Pismo Formation, San Diego Formation, San Mateo Formation) appear to represent this taxon (Domning 1978; Domning & Deméré 1984).

The Pliocene odontocete assemblage of the ENP is diverse, and includes a plethora of unstudied phocoenids. Five phocoenids are represented in this aggregate assemblage. Those described herein (cf. *Phocoena*, Phocoenidae unnamed genus 1, Phocoenidae unnamed genus 2) constitute the only described porpoises from the Pliocene of California. Delphinids are, in contrast, relatively rare, and include small-bodied dolphins like *Stenella* sp. and aff. *Tursiops* (Barnes 1977), as well as larger pilot whale relatives such as *Protoglobicephala* (Aguirre-Fernández *et al.* 2009) and a larger, indeterminate globicephaline (Boessenecker *et al.* 2013). Sperm whales are rare, and include some indeterminate large physeteroid bone fragments and teeth (Barnes 1977; this study), as well as smaller kogiids (cf. *Scaphokogia*; Barnes 1998). Except for some fragments from the San Diego Formation (SDNHM collections), ziphiids are nearly completely unknown from this aggregate assemblage. The lipotid dolphin *Parapontoporia* is present in most Pliocene marine strata in California and Baja California (Almejas, Capistrano, Niguel, Purisima, Salada, San Diego, San Joaquin, San Mateo, Tirabuzón, and Wilson Grove Formations; Barnes 1977, 1984, 1985b; Barnes *et al.* 1981; this study). Indeterminate monodontid fossils are known from these strata as well, and may (or may not) be congeneric with the latest Miocene *Denebola*. Altogether, there are fourteen toothed whales represented from the Pliocene of the ENP. The presence of monodontids in temperate and warm temperate waters, apparently higher richness of phocoenids, and lower richness of delphinids in the Pliocene of the ENP (in neritic environ-

ments) suggests that perhaps during this period of time, niches currently exploited by various small-bodied delphinids were exploited by phocoenids and *Albireo*, and some of the niches occupied by large globicephalines may have been occupied by *Denebola*-like monodontids and small-medium sized physeteroids ("*Scaldicetus*"-grade).

The mysticete assemblage includes the bizarre, small-bodied whale *Herpetocetus*, a number of rorquals and right whales, and a gray whale. Both genera of extant right whales (*Balaena* sp. and *Eubalaena* sp.) are present, as well as the extinct taxon *Balaenula* sp. (Barnes 1977; Churchill *et al.* 2012; this study). The balaenopterid assemblage includes several derived taxa such as *Balaenoptera bertae* n. sp. (this study), *Balaenoptera davidsonii* (Deméré 1986), and a third undescribed species of *Balaenoptera* (Martin 2010). Additional balaenopterids include an undescribed genus with *Eschrichtius*-like petrosals, the early diverging "*Balaenoptera*" *cortesi* "var." *portisi* (Deméré *et al.* 2005; this study), at least two other taxa represented by tympanic bullae (Balaenopteridae gen. et sp.indet. 1, Balaenopteridae gen. et sp. indet. 2), and "*Megaptera*" *miocaena*. In total, there are twelve mysticetes from this assemblage.

To summarize, 26 cetaceans, three pinnipeds, and a sea cow have been reported from the Pliocene of the ENP. The cetacean assemblage is roughly comparable in the number of taxa to that of the modern fauna (Leatherwood *et al.* 1988), although nearly totally distinct in its taxonomic makeup (it is worth noting that this assemblage is aggregated in time *c.* 2.5 Ma). For example, the bulk of small-bodied odontocetes are phocoenids, rather than delphinids which constitute the modern assemblage (however, at least one of these phocoenids is archaic and delphinid-like in skeletal anatomy). The modern assemblage does not include belugas (within temperate latitudes), and recent lipotids are restricted to riverine environments of eastern Asia (*Lipotes vexillifer*). While ziphiids are diverse in the ENP today, they are extremely rare in Pliocene strata of this region. Although rare in terms of the absolute number of specimens, the diversity of sperm whales (Physeteroidea) is similar to that of today (2-3 taxa). The Pliocene mysticete assemblage is more diverse (12 fossil taxa versus eight modern species), and appears to be more diverse at the generic level (nine fossil genera versus four extant genera); however debatable the utility of generic richness is, the modern mysticete fauna is dominated by closely related species of *Balaenoptera* (five out of eight modern mysticete species), which cannot be said for the Pliocene. There does appear to be greater disparity within the Pliocene mysticete assemblage, owing to the presence of *Herpetocetus*, a more diverse balaenid assemblage, and the presence of multiple early diverging balaenopterids. Most notably, nearly all Pliocene mysticetes are relatively small in comparison to their extant relatives. The modern fauna lacks sea cows and walruses, and the modern pinniped assemblage instead includes two phocids (*Phoca vitulina* Linneaus, 1758, and *Mirounga angustirostris* Gill, 1866) and four otariids (*Arctophoca townsendi* Merriam, 1897, *Callorhinus ursinus*, *Zalophus californianus* Lesson, 1828, and *Eumetopias jubatus*). Altogether, the Pliocene marine mammal fauna of the ENP appears to have been distinct from the modern fauna, and only 40% of marine mammal taxa belong to extant (or recent) genera.

Comparison with other Pliocene marine vertebrate assemblages

To address the broader context of the aggregate Pliocene marine mammal assemblage of the ENP, comparisons with coeval assemblages from other continents and ocean basins are warranted, and include the Mio-Pliocene Pisco Formation in Peru, the Lower Pliocene Yorktown Formation of the eastern United States, and the aggregate marine mammal assemblages of Pliocene age in Japan, Italy, Belgium, Australasia, and the Netherlands (Figs 50, 52; Table 15).

The marine mammal assemblage from the Lower Pliocene Sud-Sacaco and Sacaco levels of the Pisco Formation (Figs 50, 52; often abbreviated as SAS and SAO, respectively) is distinct from that of the ENP in several regards (Table 15; Muizon & DeVries 1985). It is worth noting that although formerly considered to be Early Pliocene in age, the age of the Sud-Sacaco and Sacaco levels of the Pisco Formation have recently been reassessed with new zircon U-Pb dating and strontium-ratio isotope dating

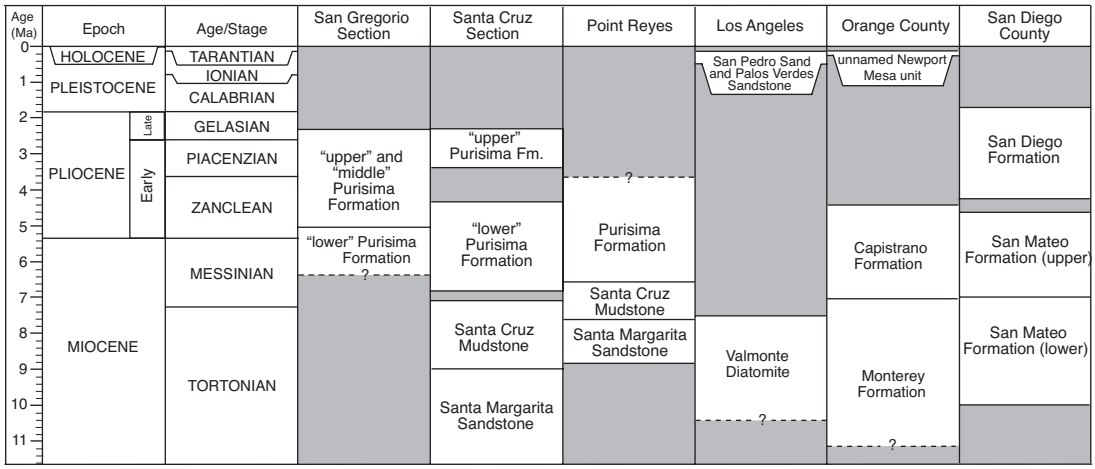

FIG. 51. — Generalized comparison of ages of marine mammal-bearing Neogene strata in California. Stratigraphic data are as follows: San Gregorio section of Purisima Formation from Boessenecker (2011a and sources therein); Purisima Formation, Santa Cruz Mudstone, and Santa Margarita Sandstone near Santa Cruz from Repenning & Tedford (1977), Clark (1981), Powell *et al.* (2007, and sources therein); Purisima Formation, Santa Cruz Mudstone, and Santa Margarita Sandstone at Point Reyes from Powell *et al*. (2007: fig. 4), Clark *et al*. (1984), and Galloway (1977); Valmonte Diatomite from Repenning and Tedford (1977); San Pedro Sand and Palos Verdes Sand from Powell & Ponti (2007); Orange County stratigraphy from Barnes (1985b), Ingle (1979), Powell *et al*. (2004b); Deméré & Berta (2005); San Diego County stratigraphy from Deméré (1983), Domning & Deméré (1984), and Vendrasco *et al.* (2012), with NALMA ages from Tedford *et al*. (2004).

by Ehret *et al.* (2012), who concluded that these two vertebrate-bearing levels of the Pisco Formation are latest Miocene in age (6-8 Ma). However, considering the typical Pliocene age which most previous researchers have considered this unit to be, comparison of the Pisco marine mammal assemblages with Pliocene marine mammal assemblages is warranted, in spite of the possibly older dates of Ehret *et al.* (2012). The combined marine mammal assemblage from these localities includes pinnipeds such as a fur seal (*Hydrarctos lomasiensis*) and several true seals (*Acrophoca* Muizon, 1981, *Hadrokirus* Ansom & Muizon, 2013, *Piscophoca* Muizon, 1981, Monachinae indet.), but no walruses (Muizon 1978; 1981; Muizon & DeVries 1985; Pilleri 1990). Walrus fossils have thus far not been found further south than about 25°N latitude, and did not invade the southern hemisphere (Deméré *et al.* 2003); curiously, the bizarre walrus-convergent odontocete *Odobenocetops* Muizon, 1993 has been found in the Pisco Formation at the Sacaco and Sud-Sacaco levels (Muizon 1993; Muizon & Domning 2002), in addition to the putatively durophagous and possibly molluskivorous phocid *Hadrokirus* (Ansom & Muizon 2013). A single physeteroid is present, *Scaphokogia* n. sp. (Lambert & Muizon 2013). Although there are only two phocoenids present at Sud-Sacaco (*Piscolithax longirostris* and an indeterminate porpoise), along with a ziphiid (*Ninoziphius platyrostris* Muizon, 1983), the rest of the cetacean assemblage is relatively similar: *Balaenoptera siberi*, *Balaenoptera* sp., and several undescribed balaenopterids are present, as well as a small cetotheriid closely related to *Herpetocetus* (*Piscobalaena nana*), a mysticete of uncertain affinities (*Piscocetus sacaco* Pilleri & Pilleri, 1989), two sperm whales (Kogiidae indet., Physeteridae indet.), the pontoporiid *Pliopontos littoralis* Muizon, 1983, two delphinine delphinids (cf. *Stenella*, cf. *Delphinus*) and two globicephaline delphinids, including *Hemisyntrachelus oligodon* (Pilleri & Pilleri 1989a, b; Pilleri & Siber 1989a-c; Muizon & DeVries 1985; Muizon 1984; Bouetel & Muizon 2006). *Hemisyntrachelus oligodon* was originally described as a species of *Tursiops*, but subsequently referred to *Hemisyntrachelus* by Post & Bosselaers (2005). An indeterminate monodontid is also present (Muizon & DeVries 1985). Additionally present

is a small dugongine sirenian similar to *Nanosiren* Domning & Aguilera, 2008 (Muizon & Domning 1985), and the bizarre aquatic sloth *Thalassocnus* Muizon & McDonald, 1995. Although there is little overall similarity at the generic level between eastern North and South Pacific marine mammal assemblages (Muizon & DeVries 1985), the eastern South Pacific also exhibits many differences with the modern fauna, such as a high number of extinct taxa (e.g., *Ninoziphius*; *Piscobalaena*; *Piscolithax*; *Piscophoca*), as well as taxa with novel adaptations (*Acrophoca*; *Odobenocetops*; *Thalassocnus*) and taxa with "extralimital" ranges with respect to their modern relatives (e.g., the pontoporiid *Pliopontos*). Of the various Pliocene assemblages discussed herein, the Pisco Formation has the lowest proportion of extant taxa (16.6%); however, this may instead simply reflect an older age of these levels of the Pisco Formation as concluded by Ehret *et al.* (2012). Regardless, differences of fossil marine mammals from the Pisco Formation and the Bahía Inglesa Formation in Chile and the modern fauna attest to widespread faunal turnover in the eastern South Pacific sometime in the Pliocene or Early Pleistocene (Walsh & Naish 2002; Valenzuela-Toro *et al.* 2013). In these regards, the Pliocene assemblages from the Pisco Formation mirror the San Gregorio and San Diego assemblages from California.

The marine mammal assemblage of the Yorktown Formation (Figs 50, 52) is vastly different from that described above for the ENP (Table 15). Like most other marine mammal fossil assemblages from the Neogene of the Atlantic, there are no otariids present, and the majority of pinnipeds are phocids. According to Koretsky & Ray (2008), there are six phocids from the aggregate Pliocene assemblage from the eastern United States. In addition, the odobenine walrus *Ontocetus emmonsi* Leidy, 1859 is ubiquitous in the Yorktown Formation and other northern Atlantic fossil localities, including the Pliocene of South Carolina, Florida, England, Belgium, the Netherlands, and Morocco (Kohno & Ray 2008). Pinniped diversity in the ENP is substantially lower than the North Atlantic. The odontocete assemblage of the Yorktown Formation is nearly modern in its composition, and is mostly composed of extant genera (Whitmore 1994; Whitmore & Kaltenbach 2008). In fact, only four of the odontocetes belong to extinct genera: the beaked whale *Ninoziphius* (however, see Lambert *et al.* 2013, who consider these fossils to represent a different extinct ziphiid), the pontoporiid *Auroracetus* Gibson & Geisler, 2009, the monodontid *Bohaskaia* Vélez-Juarbe & Pyenson, 2012 and the early diverging kogiid *Aprixokogia* (Whitmore & Kaltenbach 2008; Gibson & Geisler 2009; Vélez-Juarbe & Pyenson 2012). Extant odontocetes are nearly entirely composed of delphinids (*Delphinus* sp., *Globicephala* sp., *Lagenorhynchus harmatuki* Whitmore & Kaltenbach, 2008, *Lagenorhynchus* sp., *Pseudorca* sp., *Stenella rayi* Whitmore & Kaltenbach, 2008, *Tursiops* sp.; Whitmore & Kaltenbach 2008). In contrast to Whitmore & Kaltenbach (2008), Bianucci (2013) hypothesizes that many Pliocene delphinids identified to extant genera from numerous localities worldwide are in fact misidentified, fragmentary specimens of extinct genera. However, pending reevaluation of Yorktown Formation delphinids, this study follows the identifications of Whitmore & Kaltenbach (2008) with the potential caveat of Bianucci (2013) in mind. Two extant ziphiids are also present – *Mesoplodon longirostris* Cuvier, 1824 and *Ziphius* sp., cf. *Z. cavirostris* Cuvier, 1824 (Whitmore & Kaltenbach 2008). Notably, no phocoenids are recorded in the Yorktown Formation. The mysticete assemblage is similar in sharing the strange mysticete *Herpetocetus*, but differs in having a higher proportion of extant balaenopterids (*Balaenoptera* and *Megaptera*), and a gray whale (*Gricetoides* Whitmore & Kaltenbach, 2008). The presence of two balaenids (*Balaena* and *Balaenula*) is similar to the ENP Pliocene (Westgate & Whitmore 2002; Whitmore & Kaltenbach 2008). In particular, the diverse number of phocids and delphinids contrasts with the Pliocene of the ENP, as does the representation of extant genera; 53.1% of taxa identified to the generic level from the Yorktown Formation belong to extant genera (Table 15). Additional marine mammals not present in the Yorktown assemblage are recorded from the Pliocene of South Carolina and Florida. The aquatic mustelid *Enhydritherium terraenovae* Berta & Morgan, 1985 is present in the Early Pliocene Palmetto fauna of the Bone Valley Formation

(Morgan 1994), while the pinnipeds are identical to that of the Yorktown Formation. Mysticetes from the Palmetto fauna include *Balaenoptera floridana*, which Deméré *et al.* (2005) considered to be a junior synonym of "*Balaenoptera*" *cortesi* "var." *portisi*. Odontocetes include *Tusciziphius atlanticus* Bianucci, Miján, Lambert, Post & Mateus, 2013 from the Early Pliocene of South Carolina (Post *et al.* 2008), and the iniid *Goniodelphis hudsoni* Allen, 1941 and the sperm whales *Kogiopsis floridana* Kellogg, 1944, and *Physeterula* sp., from the Palmetto fauna (Morgan 1994). A single sirenian, *Corystosiren varguezi* Domning, 1990, is present in the Palmetto fauna (Morgan 1994). An interesting link to the ENP is the otter *Enhydritherium*, which appears to have inhabited the shoreline of Florida and southern California, including the Pliocene remnant of the inland Temblor Sea.

The extensive assemblage of Pliocene marine mammals from Japan (Fig. 50) is similar in some regards to that of the ENP. As evidenced by the list published by Oishi & Hasegawa (1995b), the majority of Pliocene cetacean fossils from Japan remains to be described. The mysticete assemblage is nearly identical to the ENP, with the exception of a Pliocene record of *Eschrichtius* sp. (Ichishima *et al.* 2006), and includes archaic taxa like *Herpetocetus*, "*Megaptera*" *miocaena*, and *Balaenula*, as well as several extant genera such as *Balaenoptera* (including "*Burtinopsis*", a junior synonym of *Balaenoptera*; Deméré 1986), *Eubalaena*, and *Balaena* (Oishi & Hasegawa 1995a, b). Delphinid odontocetes are apparently better represented and include nearly all modern genera of globicephalines endemic to the North Pacific; however, these generic identifications are based on isolated teeth and earbones, and because the majority of these specimens are undescribed, the level of precision associated with the identifications in Oishi & Hasegawa (1995b) is unclear. Archaic phocoenids include *Numatophocoena* (Ichishima & Kimura 2000), *Haborophocoena* (Ichishima & Kimura 2005; 2009), and an indeterminate narrow-snouted phocoenid (Murakami *et al.* 2013); additionally, isolated periotics of albireonid dolphins have recently been reported (Murakami & Koda 2013). The report of a *Haborophocoena*-like phocoenid herein (Phocoenidae unnamed genus 1), and the shared presence of albireonids, are notable similarities between odontocetes from the Pliocene of Japan and the ENP. Some parallels exist within the pinniped fossil record of the Pliocene of Japan and California, including the complete absence of phocids (Miyazaki *et al.* 1995). However, although *Callorhinus gilmorei* is present along both shores of the North Pacific during the Pliocene (Berta & Deméré 1986; Kohno & Yanagisawa 1997; Boessenecker 2011c) other otariids are noteworthy, including a late record of *Thalassoleon* (Kohno 1992; earliest Pliocene), and early records of the Steller's sea lion, *Eumetopias* (Miyazaki *et al.* 1995). An interesting potential link between the western and eastern North Pacific Early Pliocene pinniped assemblages is the possibility that *Thalassoleon inouei* Kohno, 1992 may be a junior synonym of *Thalassoleon macnallyae* (Deméré & Berta 2005). Dusignathine walruses are absent, but a number of odobenine walruses are present, including *Protodobenus* Horikawa, 1995, and *Ontocetus* Leidy, 1859 (Horikawa 1995; Kohno *et al.* 1998; the extant walrus, *Odobenus*, first appears in the Late Pliocene in Japan (Kohno *et al.* 1995b). Although the walrus assemblages are different in their taxonomic composition, the western North Pacific and ENP are unique in exhibiting multispecies walrus assemblages. Pliocene sirenians from Japan are identical to those of California, and also include *Hydrodamalis cuestae* and many records of *Hydrodamalis* sp. (Furusawa 1988; Domning & Furusawa 1995). The aggregate assemblage from Japan is most similar to that of the ENP.

A meager aggregate assemblage of Pliocene marine mammals has been reported from Australia and New Zealand. Pinnipeds are scarce in this region, and include fragmentary specimens of monachine phocids and indeterminate phocids from Australia (Fordyce & Flannery 1983; Fitzgerald 2004; 2005) and *Ommatophoca* sp. from New Zealand (King 1973); otariids are notably absent from the Pliocene of Australia and New Zealand, although the Pliocene marine mammal record of this region is limited (Deméré *et al.* 2003; Fitzgerald 2005). Fossil cetaceans are relatively similar to the Yorktown Formation assemblage, and appear essentially modernized in the Pliocene (Fitzgerald 2005). Pliocene mysticetes include indeterminate

balaenids and *Balaenoptera* sp. from Australia and New Zealand (Fitzgerald 2004, 2005; King *et al.* 2009), and cf. *Balaena*, cf. *Balaenoptera*, cf. *Megaptera*, *Megaptera* sp., *Megaptera* n. sp. 1, and "Cetotheriidae" indet. from Australia (Fitzgerald 2004; 2005). Pliocene odontocetes recorded both from Australia and New Zealand include Delphinidae indet., *Delphinus* sp. or *Stenella* sp., and Physeteridae indet. (Fitzgerald 2005; King *et al.* 2009). Pliocene odontocetes recorded in Australia (but not yet from New Zealand) include Kogiidae indet., cf. *Mesoplodon* sp., *M. longirostris*, cf. *Physeter* sp., *Physeter* sp., "*Scaldicetus*" sp., "*Scaldicetus*" *macgeei*, cf. *Tursiops*, and Ziphiidae indet. (Fitzgerald 2004, 2005). Several delphinids occur in the Pliocene of New Zealand but not Australia, and include *Globicephala* sp., *Orcinus*? sp., and *Pseudorca*? sp. (King *et al.* 2009). Pliocene sirenians from this region are restricted to a single record of cf. *Dugong* from Australia (Fitzgerald 2004). In summary, aside from rare cases of archaic cetaceans (e.g., "*Scaldicetus*"-grade physeteroids), the majority of the aggregate marine mammal assemblage from the Pliocene of Australia and New Zealand is composed of extant genera (Fitzgerald 2005), unlike that of the ENP.

Marine mammals from the Pliocene of Belgium and the Netherlands (Fig. 50) include several cetaceans similar to those of the Yorktown Formation assemblage. The archaic mysticete *Herpetocetus scaldiensis* is present in addition to extinct members of extant mysticete families such as the balaenids *Balaenula*, *Balaenella*, and *Eubalaena belgica* Abel, 1941, and the balaenopterid *Diunatans* (Misonne 1958; Bisconti 2005; Whitmore & Barnes 2008; Bosselaers & Post 2010). Although Whitmore & Kaltenbach (2008) noted similarities in the fossil balaenopterids between Belgium and the Yorktown Formation, all of the balaenopterid taxa described from Belgium in the late nineteenth century by P. J. Van Beneden were recently considered to be *nomina dubia* by Bosselaers & Post (2010); nevertheless, these taxa reflect the occurrence of numerous balaenopterids in the Belgian assemblage. The odontocete assemblage from the eastern North Atlantic includes an unidentified beluga-like monodontid (Lambert & Gigase 2007), the phocoenid porpoise *Septemtriocetus* (Lambert 2008a), globicephaline delphinids including *Hemisyntrachelus* (Post & Bosselaers 2005) and the pilot-whale like *Platalearostrum* Post & Kompanje, 2010 (Plio-Pleistocene in age; Post & Bosselaers 2005). Furthermore, Lambert (2005) reported that some ziphiids of uncertain stratigraphic origin published during the 19th century may be Early Pliocene in age (or alternatively Late Miocene), including *Aporotus dicyrtus* du Bus, 1868, *Ziphirostrum recurvus* (du Bus, 1868), and *Ziphirostrum turniense* du Bus, 1868. Numerous undescribed cetaceans are known from Pliocene to Pleistocene deposits on the North Sea Floor off the coast of the Netherlands, including "*Balaenoptera*-, *Delphinapterus*-, *Eubalaena*-, *Globicephala*-, *Hemisyntrachelus*-, *Mesoplodon*-, *Orcinus*-, *Physeter*-, *Stenella*/*Delphinus*- and *Tursiops*-like genera" (Post & Kompanje 2010); however, this material awaits description, and the stratigraphic control of these specimens is uncertain. The pinniped assemblage from the Pliocene of the eastern North Atlantic includes only one odobenid, the odobenine walrus *Ontocetus emmonsi* (Kohno & Ray 2008), and possibly up to seven extinct phocids (Van Beneden 1876; Misonne 1958; Ray 1977; Koretsky & Ray 2008). However, these fragmentary phocid fossils require extensive revision and redescription. The Pliocene marine mammal assemblage from the eastern North Atlantic mirrors that of the western North Atlantic, both in sharing similar extinct taxa (*Herpetocetus*, *Ontocetus*), having a high number of extant genera (*Mesoplodon* Gervais, 1850, *Eubalaena*), and comparatively few extinct genera (*Septemtriocetus*, *Platalearostrum*), and shares a large number of taxa with the Yorktown Formation assemblage. Although a single phocoenid is present, there instead appear to be a wide variety of small-bodied delphinids (reported as Plio-Pleistocene by Post & Kompanje 2010), and this assemblage lacks the phocoenid diversity of the ENP during the Pliocene. There is little overlap with the pinniped assemblage, as there are several phocids (absent in the North Pacific Pliocene) and there are no otariids (present in the North Pacific); however, the walrus *Ontocetus* is present in the Pliocene of Japan, Europe, the eastern United States, and Morocco (Kohno & Ray 2008). Sirenians are also absent from the Belgian Pliocene (Misonne 1958). There is little similarity in general with Pliocene marine mammal assemblages from the Pacific Ocean.

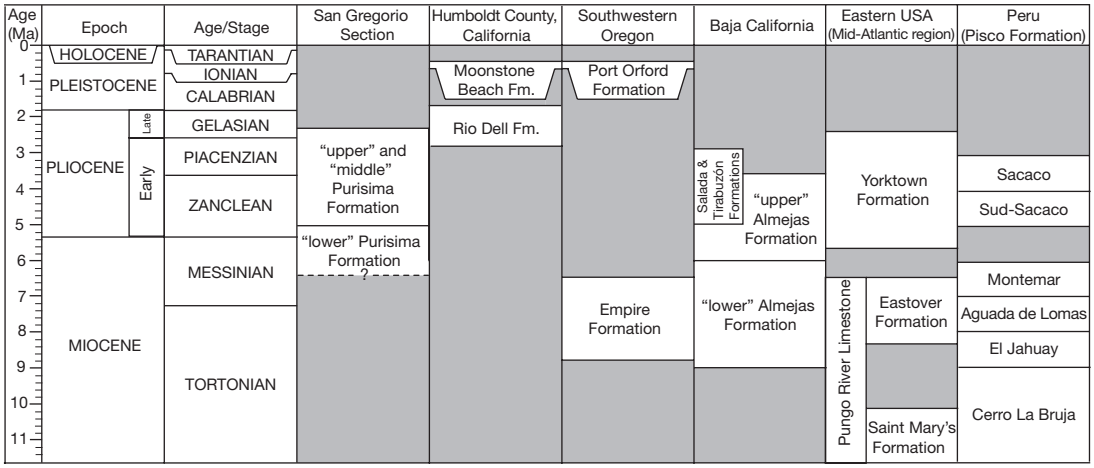

Fig. 52. — Generalized comparison of geochronologic ages of marine mammal-bearing Neogene strata in the eastern North Pacific outside California, the Mid-Atlantic region of the eastern United States, and the Pisco Basin of Peru; San Gregorio section of Purisima Formation from Boessenecker (2011a and sources therein); Humboldt County stratigraphy from Haller (1980) and Roth (1979); southwestern Oregon stratigraphy after Roth (1979) and Prothero *et al*. (2001); stratigraphy of Baja California from Barnes (1998) and Barnes (2008); strata of the mid-Atlantic region of the Eastern United States after Gottfried *et al*. (1994); Pisco Formation stratigraphy after Muizon & DeVries (1985) and Muizon & Bellon (1986). Note that Ehret *et al*. (2012) recently published new radiometric and strontium isotope dates from the Pisco Formation resulting in somewhat older ages for the Sacaco, Sud-Sacaco, Montemar, and Aguado de Lomas levels.

The marine mammal assemblage from the Italian Pliocene (Fig. 50) is diverse with respect to cetaceans, and depauperate with respect to pinnipeds. Only one pinniped is known from the Pliocene of Italy (Tavani 1941), the phocid *Pliophoca etrusca* Tavani, 1941. Several balaenopterids are reported, including "*Balaenoptera*" *cortesii*, "*B.*" *cortesi* "var." *portisi*, *Cetotheriophanes capellinii*, *Protororqualus cuvieri*, and several other taxa needing revision (Deméré *et al.* 2005; Bisconti 2009). Several balaenids are present, including *Balaena montalionis* Capellini, 1904, *Balaenula astensis*, and *Eubalaena* (Trevisan 1942; Bisconti 2000, 2002, 2003); additionally, the early gray whale *Eschrichtioides* Bisconti, 2008 is known from the Pliocene of Italy (Bisconti 2008). The odontocete assemblage is dominated by delphinids, and includes a number of small-bodied delphinids (*Astadelphis*, *Etruridelphis*, *Stenella*, *Tursiops*) as well as several globicephaline delphinids (*Arimidelphis* Bianucci, 2005, *Globicephala*, "*Grampus*-group", *Hemisyntrachelus*, *Orcinus*; Bianucci 1996, 2005; Bianucci *et al.* 2009). Other odontocetes include unidentified physeteroids and the pygmy sperm whale *Kogia pusilla* Pilleri, 1987, and several beaked whales including *Mesoplodon* and *Tusciziphius crispus* Bianucci, 1997 (Bianucci 1997). Also present are late surviving records of the dugongid sirenian *Metaxytherium* de Christol, 1840 (Sorbi & Vaiani 2007; Sorbi *et al.* 2012). Certain aspects of the Pliocene Mediterranean marine mammal assemblage appear to be endemic (i.e. many of the unique delphinid taxa, the early gray whale *Eschrichtioides*, and a late surviving *Metaxytherium*), while certain other taxa appear to have been widespread, such as "*B.*" *cortesi* "var." *portisi*, *Tusciziphius*, *Hemisyntrachelus*, *Globicephala*, and the balaenids). The assemblage from the Italian Pliocene is most similar to that of the western and eastern North Atlantic, and unlike the Northern Pacific assemblages, exhibits many delphinids, lacks *Herpetocetus* (and apparently is the only major Northern Hemisphere marine mammal assemblage that lacks *Herpetocetus* thus far), and lacks a large number of phocoenids. The presence of the same three genera of balaenids (*Balaena*, *Balaenula*, and *Eubalaena*) mirrors the North Pacific, as does the occurrence of "*Balaenoptera*" *cortesi* "var." *portisi*; however, these balaenid genera appear to be present in most of the other assemblages as well and there is overall little similarity with the Pacific Pliocene assemblages.

Aberrant marine mammals in Pliocene assemblages

Several authors (Whitmore 1994; Oishi & Hasegawa 1995b; Fordyce *et al.* 2002; Fitzgerald 2005) have previously noted that Pliocene marine mammal assemblages are often characterized by a mix of later diverging fossil taxa closely related to modern species (e.g., *Callorhinus gilmorei* Berta & Deméré, 1986; Boessenecker 2011c), taxa with novel or seemingly bizarre adaptations (e.g., *Australodelphis* Fordyce, Quilty & Daniels, 2002; *Odobenocetops* Muizon, 1993), archaic taxa with smaller body sizes (Bisconti 2003; Bisconti 2009), and other taxa with aberrant geographic ranges relative to modern relatives (e.g., the subtropical walrus *Valenictus* [Deméré 1994b]; temperate-warm temperate water beluga relatives *Denebola* and *Bohaskaia*; Barnes 1984; Vélez-Juarbe & Pyenson 2012). Additionally, aspects of these assemblages appear more diverse than their counterparts of modern faunas (e.g., mysticetes, Oishi & Hasegawa 1995b, Bisconti 2009; pinnipeds, Koretsky & Ray 2008). An additionally noted aspect is the apparently higher provinciality of marine mammal assemblages during the Pliocene (see The emergence of the modern marine mammal fauna).

The marine mammal assemblages of the ENP are no exception, and are excellent examples of the strange composition of Pliocene marine mammal faunas. The California Pliocene includes extinct species within extant genera that appear seemingly modern (e.g., *Balaenoptera bertae* n. sp., *Balaenoptera davidsonii*, cf. *Balaenoptera*, *Balaena* n. sp., *Callorhinus gilmorei*, cf. *Phocoena*; Berta & Deméré 1986; Deméré 1986; Churchill *et al.* 2012; this study), taxa with bizarre or novel adaptations (e.g., Phocoenidae unnamed genus 2, *Valenictus chulavistensis*, *Dusignathus seftoni*, *Herpetocetus*; see Deméré 1994b; Racicot *et al.* 2007; this study), dwarf or archaic taxa (*Albireo*, "*Balaenoptera*" *cortesi* "var." *portisi*, *Balaenula*, and taxa both archaic and small such as *Herpetocetus*; Barnes 1977, 2008; Deméré *et al.* 2005; Boessenecker 2013a; this study), and many taxa which have distributions that are geographically or latitudinally disparate from modern relatives (e.g., *Parapontoporia*, on the other side of the Pacific from its sister taxon *Lipotes*, and temperate to subtropical monodontids and walruses; Barnes 1985; Deméré 1994b).

The peculiarities of the Pliocene balaenid assemblages from the Mediterranean and Japan have been the subject of recent discourse by Bisconti (2003; 2009) and Kimura (2009), and are a microcosm of the greater marine mammal assemblage. Pliocene balaenid assemblages are characterized by extant genera (*Eubalaena* and *Balaena*) approaching the gigantic size of modern species (Bisconti 2003) and co-occur with relict taxa that are both archaic and small-bodied; these assemblages all occur within temperate settings. In contrast, modern balaenids are not sympatric, are restricted to polar and subpolar settings, and are all gigantic. Bisconti (2003) hypothesized that the more diverse Pliocene balaenid assemblage could have been fostered by: 1) higher primary productivity which removed competitive pressures between balaenid species; 2) lower competitive pressures permitting the persistence of relict small-bodied whales like *Balaenella* and *Balaenula*; and 3) predatory pressures by the large shark *Carcharocles megalodon* which kept "dominant" advanced balaenids from competitively excluding the relict taxa. Similarly, Kimura (2009) reported that higher diversity of balaenids in Japan corresponded to periods of higher diatom productivity, a relationship that is corroborated by the finding that cetacean diversity through time is correlated with and tracks diatom diversity (Marx & Uhen 2010).

It is certainly possible that the strange composition of Pliocene marine mammal assemblages is due to relaxed competition during a period of higher primary productivity, as bottom-up controls on cetacean evolution have been previously identified (Marx & Uhen 2010); it is further possible that more niches were available during the Pliocene. The hypothesis presented by Bisconti (2003) may be applied to other Pliocene marine mammal clades, as most of these (pinnipeds, sirenians, odontocetes, and other mysticetes) exhibit similar patterns (e.g., relict and bizarre taxa), but it is beyond the scope of this study to investigate causes for this strange faunal composition. It is, however, worth noting that these strange marine mammal assemblages appear to have been more ecologically diverse than the modern fauna and included many taxa inhabiting niches that have since been vacated, as well as exhibiting much higher disparity. Future research

should be directed at changes in marine vertebrate food webs during the Pliocene and Pleistocene, as this avenue of study may yield enlightening insights into modern marine mammal ecology.

Pleistocene marine mammals of the eastern north Pacific

A discussion of Pleistocene marine mammal assemblages from the ENP is warranted for comparison with Pliocene marine mammal-bearing localities, such as the San Gregorio assemblage reported herein. In contrast to the abundance of Miocene and Pliocene marine mammal localities along the Pacific coast of North America, there are comparatively few Pleistocene marine mammal-bearing rock units in this region. Only localities with at least small assemblages (more than one taxon) are discussed, as Upper Pleistocene localities that have produced isolated specimens are numerous and scattered. A summary of all relevant Late Miocene, Pliocene, and Pleistocene marine mammal taxa previously reported from the temperate ENP (Baja California to British Columbia) appears in Appendix.

The Port Orford Formation of southwestern Oregon (Figs 49, 52) is Middle Pleistocene in age, dated to 700-500 Ka (Ionian equivalent) by amino acid racemization and mollusk biostratigraphy (Wehmiller *et al.* 1978; Roth 1979), although it was erroneously referred to as Upper Pliocene by Barnes *et al.* (2006). A meager marine mammal assemblage has been reported from this locality, including a sea otter (*Enhydra* sp.), a possible fur seal (?*Callorhinus* sp.), a possible California sea lion (?*Zalophus* sp.), a *Eumetopias*-like sea lion (*Proterozetes ulysses* Barnes *et al.* 2006), a harbor seal (*Phoca* sp., cf. *P. vitulina*), a right whale (*Balaena* sp.), and a rorqual, *Balaenoptera* sp. (Packard 1947; Leffler 1964; Barnes & Mitchell 1975; Barnes *et al.* 2006; Boessenecker 2013b).

A number of Pleistocene marine mammals have been reported from a few localities in Humboldt County, California (Fig. 49). The *c.* 700-470 Ka (Wehmiller *et al.* 1978; Roth 1979) Moonstone Beach Formation (including the Crannel Junction deposit) has yielded a meager assemblage, including an extinct sea otter (*Enhydra macrodonta* Kilmer, 1972), a harbor seal (*Phoca* sp.), and a sea lion, *Eu-*

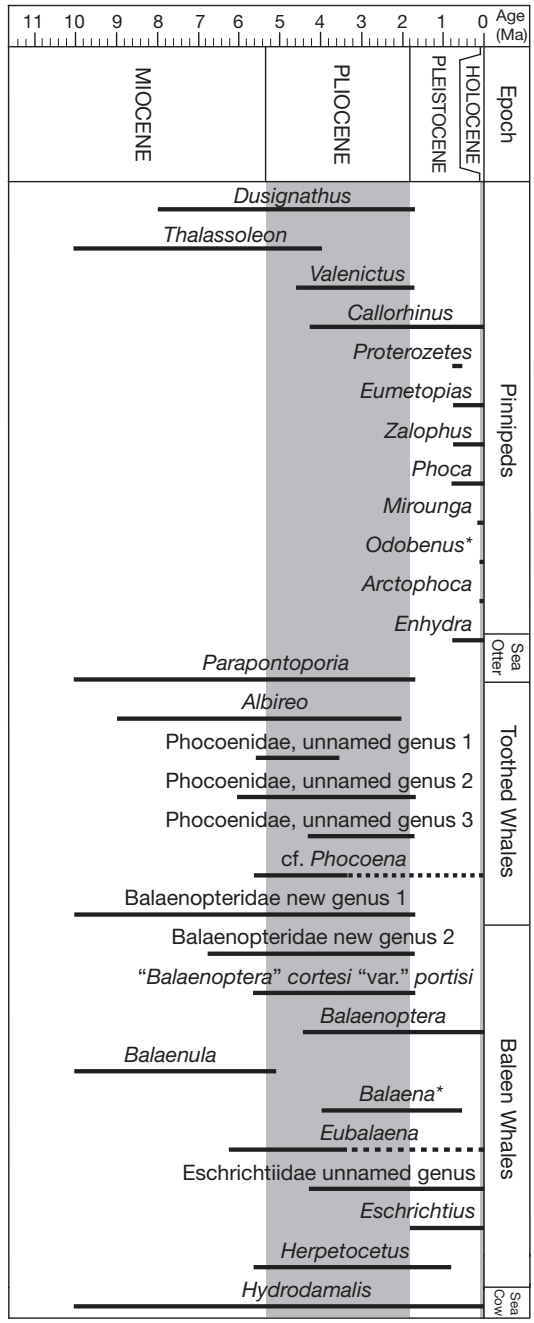

Fig. 53. — Geochronologic ranges of selected Pliocene and Pleistocene marine mammals; see Appendix for ages of various taxa. *, denotes extant marine mammals that do not currently inhabit the eastern North Pacific. Dashed lines indicate extant marine mammals represented by Pliocene (but not Pleistocene) fossil records.

metopias jubatus (Kilmer 1972; Kohl 1974; Barnes & Mitchell 1975). Boessenecker (2011c) reported the fur seal *Callorhinus* sp. from the Lower Pleistocene portion of the Rio Dell Formation at Scotia Bluffs; additional specimens at Sierra College include a possible gray whale tympanic bulla (cf. *Eschrichtius*; VMW 27) and an indeterminate delphinoid atlas (VMW 14), and a partial tusk and calcaneum of an indeterminate odobenid reside in a private collection. Recently, an unusually late occurring record of *Herpetocetus* was reported from the Lower-Middle Pleistocene Falor Formation (Boessenecker 2013a); unpublished fossils from this same locality include a large vertebra identifiable as *Hydrodamalis* sp., and an unprepared balaenopterid cranium (R.W. Boessenecker, personal observation).

Stratigraphic units in southern California have produced more diverse marine mammal assemblages than those from further north. These include the San Pedro Sand and Palos Verdes Sand (Fig. 49), both of Late Pleistocene age and exposed on the Palos Verdes Peninsula (Woodring *et al.* 1946; Powell & Ponti 2007), and unnamed fossiliferous strata at the Newport Mesa near Newport Beach, California, also of Late Pleistocene age (Powell *et al.* 2004b). The combined assemblage from the San Pedro Sand and Palos Verdes Sand includes sea otters (*Enhydra* sp., cf. *E. lutris*), harbor and elephant seals (*Phoca* sp., cf. *P. vitulina*, *Mirounga* sp., cf. *M. angustirostris*), California sea lions (*Zalophus californicus*), an arctocephaline fur seal, delphinid odontocetes, a gray whale (*Eschrichtius* sp., cf. *E. robustus*), and indeterminate mysticetes (Mitchell 1966b; Miller 1971; Barnes & Mitchell 1975; Langenwalter 1975; Barnes & McLeod 1984; Jefferson 1991). The Newport Mesa locality has yielded a sea otter (*Enhydra lutris* Linneaus, 1758), an indeterminate otariid, an elephant seal (*Mirounga* sp., cf. *M. angustirostris*), and a delphinid dolphin, *Lagenorhynchus* sp. Gray, 1846 (Miller 1971; Jefferson 1991).

Some isolated Pleistocene marine mammal occurrences are also worth noting. Sporadic Late Pleistocene examples of the modern walrus (*Odobenus rosmarus*) are known from temperate and cold temperate latitudes of the ENP, much further to the south of their current range of the Pacific walrus in the Bering Sea. These records include a partial skeleton of *O. rosmarus* from British Columbia, dated at >40 Ka and considered latest Pleistocene in age (Harington & Beard 1992), and a partial skull of *O. rosmarus* dredged from the San Francisco Bay, dated at 27 Ka (latest Pleistocene; Harington 1984). Additional evidence for walruses at temperate latitudes in the ENP includes trace evidence of *O. rosmarus* feeding in Middle Pleistocene sediments in southwestern Washington, USA (Gingras *et al.* 2007). These southern records reflect southward migration of walruses during glacial maxima (Harington 2008). Jones (1967) reported an isolated braincase of *Hydrodamalis gigas* dredged from the floor of Monterey Bay, which was C-14 dated to 18.94±1.1 Ka (latest Pleistocene), and another dredged Late Pleistocene *Hydrodamalis* specimen was reported by Jefferson (1991) from the mouth of San Francisco Bay.

With the exception of the Rio Dell Formation, all of these localities are Middle to Upper Pleistocene (Ionian-Tarantian equivalent). However, despite the relatively meager nature of these assemblages, several features distinguish them from Pliocene marine mammal assemblages. Firstly, true sea otters (*Enhydra* Fleming, 1822), harbor seals (*Phoca* Linneaus, 1858), and elephant seals (*Mirounga* Gray, 1827) are present, which are entirely absent from Pliocene (and older) deposits in this region (Fig. 53; Mitchell 1966b; Barnes & Mitchell 1975; Boessenecker 2011c; *contra* Harnik *et al.* 2012: figure II, who erroneously show a *c.* 3 Ma long fossil record of *Enhydra* in the ENP). Extinct walrus genera are absent, and non-*Callorhinus* otariids are present (formerly absent during the Pliocene in the ENP; Deméré *et al.* 2003; Boessenecker 2011c). Delphinids and the extant gray whale *Eschrichtius* are also present, which are rare and absent (respectively) during the Pliocene (Fig. 53).

The emergence of the modern marine mammal fauna

Although modernization of the Atlantic and western South Pacific marine mammal fauna appears to have occurred within the Pliocene (Whitmore 1994; Fordyce *et al.* 2002; Fitzgerald 2005), the apparent discord between the Pliocene marine mammal assemblage and modern fauna of the

ENP suggests a much different situation than what Whitmore (1994) described for that of the North Atlantic. The relatively modern aspect of the cetacean assemblage from the Yorktown Formation of the eastern United States led Whitmore (1994) to suggest that altered circulation patterns, cooling, and steepened temperature gradients led to the appearance of the modern marine mammal fauna during the latest Miocene and earliest Pliocene (i.e. physical events occurring prior to deposition of the Yorktown Formation).

In contrast, Pliocene marine mammal assemblages from California and Baja California share little in common with the modern fauna. The Pliocene marine mammal record includes many taxa which are now extinct in the ENP, and several of these extinct taxa also exhibit strange adaptations. Other fossil marine mammals are in vastly different environments or otherwise geographically far removed from their modern relatives. A few taxa are genuine occurrences of extant genera, but unlike the western North Atlantic assemblage, the proportion of extant taxa is relatively low. Approximately 35.3% of genera (or taxa identified to a more inclusive clade and clearly distinct from extant taxa, e.g., cf. Physeteroidea, Balaenopteridae indet. morphotypes 1 and 2) from the San Gregorio assemblage are extant, versus 53% for the Yorktown Formation (Table 15).

While the modern marine mammal fauna was already present in much of its modern taxonomic composition by the Early Pliocene in the western North Atlantic (Whitmore 1994), review of the ENP assemblage indicates that only a few modern taxa appeared prior to the Pleistocene. Considering the bulk Pliocene marine mammal assemblage from the ENP (Table 14), there are a total of 35 taxa diagnostic at the genus level (e.g., named and unnamed genera in addition to those in Table 14, including *Albireo savagei*, aff. *Denebola*, *Enhydritherium terraenovae*, aff. *Globicephala*, aff. *Kogia* sp., aff. *Lagenorhynchus* sp., *Parabalaenoptera* sp., *Pliopedia pacifica*, cf. *Pontoporia* sp., *Protoglobicephala mexicana*, cf. *Scaphokogia* sp., *Thalassoleon*, and aff. *Tursiops*; see also Appendix; Kellogg 1921; Berta & Morgan 1986; Barnes 1998, 2008; Aguirre-Fernández *et al.* 2009). Fourteen of these taxa are extant (or "recent"; e.g., *Hydrodamalis*), and 40% of the assemblage represents recent or extant taxa.

It appears that the emergence of the modern marine mammal fauna in the ENP was delayed relative to that of the North Atlantic as reflected by the Yorktown Formation, previously outlined by Whitmore (1994). Furthermore, it is worth noting that the Pisco Formation assemblage appears to show a similar phenomenon, and a later timing of faunal "modernization". In fact, only 16.6% of the taxa from the Pliocene assemblages from the Sacaco and Sud-Sacaco levels of the Pisco Formation are extant (Table 15; however, as noted above, this may be due to a possible older age of these levels of the Pisco Formation; Ehret *et al.* 2012). In contrast to both the North Atlantic and eastern North and eastern South Pacific, the modern pinniped assemblage appeared in the western North Pacific during the Early Pliocene, as reflected by pinniped assemblages from Japan (Miyazaki *et al.* 1995). The different timing of modernization of marine mammal assemblages during the Pliocene in different regions of ocean basins points towards some degree of faunal provinciality during the Pliocene. The pinniped assemblages of the eastern and western North Pacific, for example, have little taxonomic overlap (sharing one fur seal, *Callorhinus gilmorei*, but having different suites of odobenids and other otariids), although Pliocene cetaceans from the ENP and western North Pacific share more taxa in common (Oishi & Hasegawa 1995a, b). Similarly, many of the bizarre and distinctive marine mammals from the southern hemisphere in general (e.g., *Australodelphis*, *Acrophoca*, *Odobenocetops*, *Thalassocnus*) have yet to be discovered in geographically distant locations and appear to not have been cosmopolitan, although cetaceans belonging to modern genera appear to have established cosmopolitan distributions in the southern ocean during the Pliocene (Fitzgerald 2005), further suggesting that the North Pacific and eastern South Pacific regions exhibited provincial faunas lacking many marine mammal genera which currently reside there.

Faunal provinciality during the Pliocene was likely fostered by the presence of several physical and temperature-related barriers absent in the Pacific realm earlier in the Miocene and later in the Pleis-

tocene and Holocene. Although the Bering Strait appears to have opened as early as *c.* 5 Ma, it did not act as a pathway for the dispersal of mollusks, pinnipeds, and cetaceans until the "Middle" Pliocene (*c.* 3.5 Ma; Kohno *et al.* 1995b; Marincovich 2000; Lambert 2008a), indicating the persistence of a northern barrier until near the end of the Pliocene. Similarly, although the Panama seaway did not completely close until the Late Pliocene (Coates & Obando 1996), uplift of this landmass began to affect inter-ocean currents and restrict dispersal of invertebrates as early as the Late Miocene (8-6 Ma; Collins *et al.* 1996) with increased current inhibition and salinity contrasts forming during the Early Pliocene (4.2 Ma; Haug *et al.* 2001). A few shared marine mammals between the Pisco and Yorktown formations suggest at least limited faunal interchange between the eastern South Pacific and western North Atlantic (Muizon & DeVries 1985; Lambert & Gigase 2007), although some Yorktown fossils no longer appear to be congeneric with those from the Pisco (e.g., *Ninoziphius*; Lambert *et al.* 2013). In addition to physical barriers restricting or preventing dispersal to or from the north (Arctic) and east (North Atlantic), there appears to have been a "thermal barrier" in equatorial waters. The Early Pliocene was a brief period of warming climate, with permanent El Nino conditions in the equatorial Pacific (Wara *et al.* 2005; Fedorov *et al.* 2013) and sea surface temperatures *c.* 3°C higher than today (Filippelli & Flores 2009). Many extant marine mammals exhibit antitropical distributions in the Pacific and Atlantic (e.g., *Arctocephalus*, *Balaenoptera*, *Eubalaena*, *Globicephala*, *Phocoena*) and molecular divergence dating in concert with biogeographic data indicate that phocoenids dispersed from north to south (or vice versa) during "window" periods of equatorial cooling (Fajardo-Mellor *et al.* 2006), and it is possible that Early Pliocene warming maintained a warm equatorial belt (Wara *et al.* 2005) which acted as a "sieve" or partial barrier to marine mammal dispersal during this time period. Physical barriers to the north (until 3.5 Ma), east (beginning 8-6 Ma, totally closed by 2.5 Ma), and a partial thermal barrier to the south (until *c.* 2.5 Ma) appear to have fostered provinciality of marine mammal faunas by restricting dispersal to and from the North Pacific, as well as the eastern South Pacific, thereby explaining patterns of Pliocene marine mammal diversity across the globe.

It is evident that a high degree of faunal overturn took place after deposition of the Purisima and San Diego Formations, and the Pleistocene marine mammal record (outlined above) can be used to constrain the timing of this event (or events). Middle and Late Pleistocene marine mammal assemblages (e.g., Port Orford Formation, Moonstone Beach Formation, Palos Verdes Sand, San Pedro Sand) are nearly completely composed of extant marine mammal taxa (Table 15; Fig. 53; Boessenecker 2011c, 2013a). Although meager and scattered, these Pleistocene assemblages are crucial in constraining the timing of faunal overturn to a period of time before the Middle Pleistocene (Ionian, > 700 Ka). The San Diego Formation, estimated to be 2 Ma at its youngest, also constrains the earliest timing for faunal overturn. In summary, the modern marine mammal fauna appears to have appeared between 2 Ma and 700 Ka in the ENP (Boessenecker 2013a). The Early Pleistocene, then, will unfortunately serve as a "black box" until additional fossils and localities are discovered; the fossil record from this period of time is currently restricted to a single locality in the ENP (Rio Dell Formation; Boessenecker 2011c). During this period of time, a number of faunal changes are inferred based on contrasting Pliocene and Pleistocene marine mammal assemblages, including: 1) extinction of the walruses *Dusignathus* and *Valenictus*; 2) extinction of archaic balaenopterids and balaenids; 3) extinction of *Parapontoporia*; 4) extirpation (or extinction) of temperate Pacific monodontids; 5) extinction of archaic and bizarre phocoenids; 6) invasion of the region by *Enhydra*, *Eumetopias*, *Phoca*, *Mirounga*, *Zalophus*, *Odobenus*, and *Eschrichtius* (all of which, except for *Mirounga*, are known from the Late Pliocene of the western North Pacific or Arctic Ocean; Repenning & Tedford 1977; Repenning 1983; Miyazaki *et al.* 1995; Deméré *et al.* 2003; Ichishima *et al.* 2006); 7) invasion of the region by additional delphinid and ziphiid taxa; and 8) restriction of monodontids, odobenids, balaenids, and certain phocids to polar regions. Among the marine mammals, there are only four lineages

TABLE 14. — Faunal comparison checklist of Pliocene marine mammal assemblages in California, compiled from Kellogg (1927); Gregory & Kellogg (1927); Barnes (1973, 1977, 1985b, 2008); Repenning & Tedford (1977); Domning (1978); Barnes *et al.* (1981); Domning & Deméré (1984); Berta & Morgan (1985); Berta & Deméré (1986); Deméré (1986, 1994a); Deméré & Berta (2003, 2005); Deméré *et al.* (2003); Boessenecker (2011a); Boessenecker & Smith (2011); Churchill *et al.* (2012); Boessenecker (pers. obs., Purisima Formation at Point Reyes and Santa Cruz); Deméré (pers. comm. 2011); and this study. Bold denotes extant genera. Abbreviations: **SCS**, Santa Cruz section; **SGS**, San Gregorio section; **PRS**, Point Reyes section.

	Purisima Formation (SGS)	Purisima Formation (SCS)	Purisima Formation (PRS)	San Diego Formation	San Mateo Formation	Pismo Formation
Mustelidae						
Enhydritherium					×	
Pinnipedia						
Callorhinus	×	×		×		
Thalassoleon			×		×	
Otariidae indet.						×
Dusignathus	×			×		
Valenictus		×		×		
Odobenidae indet.		×	×	×	×	
Mysticeti						
Balaenula					×	
Balaena				×		
Eubalaena	×	×				
Balaenidae indet.		×	×	×	×	
"*Megaptera*" *miocaena*			×	×	×	×
Balaenoptera *davidsonii*				×		
Balaenoptera *bertae* n. sp.	×	×				
Balaenoptera spp.	×	×		×		
Balaenopteridae unnamed genus				×	×	
Herpetocetus	×	×	×	×	×	
Odontoceti						
Albireo			×			×
Delphinus or ***Stenella***		×		×	×	
Globicephalinae indet.	×	×		×		
Delphinapterinae indet.		×	×	×	×	
Parapontoporia	×	×		×	×	
Phocoenidae unnamed genus 1	×	×				
Phocoenidae unnamed genus 2	×	×		×		
Phocoenidae unnamed genus 3				×		
?Phocoenidae unnamed genus 4			×		×	
Piscolithax		×			×	
Phocoena	×					
Physeteroidea indet.	×			×	×	
Sirenia						
Hydrodamalis			×	×	×	×

which have been identified as remaining endemic to the region since the Pliocene (Fig. 53): the fur seal *Callorhinus* (Boessenecker 2011c), the sea cow *Hydrodamalis* (Domning 1978), the mysticete *Balaenoptera* (Deméré 1986; this study), and the porpoise *Phocoena* (this study); further study of the balaenids is warranted, as *Eubalaena* may be a fifth taxon to have remained endemic (although it is not yet recorded from the Pleistocene of the ENP). Similar to these taxa, *Herpetocetus* survived extinctions that affected many other marine mammals at the close of the Pliocene, only becoming extinct during the Middle Pleistocene (Boessenecker 2013a). Given that the common ancestor of *Phocoena phocoena* and *Phocoenoides dalli* probably lived in the southern hemisphere (Fajardo-Mellor *et al.* 2006), perhaps

only *Callorhinus*, *Balaenoptera*, and *Hydrodamalis* have remained in the region, with *Phocoena phocoena* and *Phocoenoides* dispersing into the north Pacific late in the Pleistocene (Fajardo-Mellor *et al.* 2006). As outlined above, provincial marine mammal faunas of the Pliocene were apparently succeeded by a more cosmopolitan modern fauna, and faunal turnover was characterized by many dispersal and "invasion" events within a short period of time coinciding with extinctions of multiple taxa. This suggests a period of intense faunal restructuring, constraining the events outlined above to a period between 2 Ma and 700 Ka. Interestingly, megafaunal extinctions in the ENP appear to have predated the Late Pleistocene megafaunal extinctions at 45-9 Ka (Barnosky *et al.* 2004) by approximately 1-2 Ma, suggesting that the causes of Plio-Pleistocene extinctions among marine and terrestrial mammals are discordant. Furthermore, many marine organisms appear to have fared well during the Late Pleistocene in spite of rapidly fluctuating climate and sea level (Valentine & Jablonski 1991; Pyenson & Lindberg 2011; Harnik *et al.* 2012), and marine mammals appear to have emerged unscathed given the near identical nature of Middle and Late Pleistocene marine mammal assemblages (with the exception of *Herpetocetus*; Boessenecker 2013a). The occurrence of marine mammals characteristic of Pliocene assemblages such as *Herpetocetus* in the Early-Middle Pleistocene – a period of time when the modern pinniped assemblage was present in the ENP – indicates that the modern marine mammal fauna may have arisen in a piecemeal or stepwise fashion (Boessenecker 2013a).

The situation regarding Pliocene marine mammals outlined above contrasts starkly with genetic divergence of Late Neogene kelp, invertebrates, fish, and marine birds from the ENP (Jacobs *et al.* 2004); many extant genera and families of kelp, sand dollars, abalones, surfpeches, rockfishes, salmonids, and auks (Alcidae) all underwent radiations during the latest Miocene (Jacobs *et al.* 2004). Although some groups of marine birds underwent dispersals and succumbed to extinctions and extirpations in the ENP during the Plio-Pleistocene interval, sea bird turnover appears to have been different to marine mammal turnover during this period, both in terms of severity and timing. Warheit (1992) noted two primary differences between the Late Pliocene seabird assemblage (Fauna IV of Warheit 1992) and the modern fauna: the presence of abundant flightless alcids (*Mancalla* spp.) and an abnormally diverse record of sulids, namely gannets (*Morus* spp.) and boobies (*Sula* spp.), which no longer inhabit the ENP. *Mancalla* and the Mancallinae are now wholly extinct, and gannets are not present in the modern bird fauna of the ENP; however, these groups are present in Middle Pleistocene strata of the Moonstone Beach Formation, Humboldt County, and the Late Pleistocene Newport Mesa in Orange County, California, respectively (Miller 1971; Kohl 1974). Harnik *et al.* (2012: figure II) erroneously show the *Mancalla* lineage persisting up to the Pleistocene-Holocene boundary; however, the youngest confirmed record of *Mancalla* in the ENP is from the Middle Pleistocene (700-500 Ka; Roth 1979) Moonstone Beach Formation (Kohl 1974; Smith 2011), with a possible record in an unnamed Late Pleistocene unit at Newport Mesa (Miller 1971). In addition to these taxa, the recent discovery of Pliocene (Piacenzian-Gelasian equivalent) pelagornithids in the San Gregorio section of the Purisima Formation (Boessenecker & Smith 2011) adds another distinctive bird group to succumb to extinction after the Pliocene. Seabird assemblages from the ENP appear to have been slightly more diverse during the Pliocene than the Late Miocene, and differed principally in the diversification and appearance of larids (gulls) and phalacrocoracids (cormorants and shags); otherwise, the Pliocene seabird assemblage was characteristically modern (Warheit 1992). The timing of the marine bird extinctions in this region appear to have been later, during the Late Pleistocene (although it may have been earlier for pelagornithids; Boessenecker & Smith 2011) and not in concert with marine mammal turnover, which appears to have occurred during the Early Pleistocene (Boessenecker 2011c; 2013a).

Delayed faunal turnover in the ENP appears to be linked with several large scale physical changes in the Pacific realm during the Pliocene. These include initial closure (8-6 Ma) and final closure (3-2.5 Ma) of the Panama Seaway from (Coates & Obando 1996), opening of the Bering strait and the arctic

TABLE 15. — Faunal comparison of marine mammal assemblages from the Pliocene part of the San Gregorio section of the Purisima Formation (compiled from Boessenecker 2011a; Boessenecker & Smith 2011; this study), San Diego Formation (compiled from Barnes 1973, 1977; Berta & Deméré 1986; Deméré 1994a: table 1; Deméré & Berta 2003; Racicot *et al.* 2007; Martin 2010; Churchill *et al.* 2012; and Deméré pers. comm. 2012), Sacaco and Sud-Sacaco horizons of the Pisco Formation (compiled from Muizon 1978, 1981, 1984, 1993; Muizon & Domning 2002; Ansom & Muizon 2013; Lambert *et al.* 2013), and Yorktown Formations (compiled from Whitmore 1994; Westgate & Whitmore 2002; Kohno & Ray 2008; Koretsky & Ray 2008; Whitmore & Kaltenbach 2008; Gibson & Geisler 2009; Vélez-Juarbe & Pyenson 2012). Extant vs extinct taxon counts for the Purisima Formation include Balaenopteridae gen. et sp. indet. morphotypes 1 and 2, as both of these are demonstrably not from extant *Balaenoptera* or *Megaptera*. Abbreviation: **SGS**, San Gregorio section.

	Purisima Fm. (SGS)	**San Diego Fm.**	**Pisco Fm.**	**Yorktown Fm.**
Pinnipedia	***Callorhinus*** sp., cf. *C. gilmorei* *Dusignathus* sp., cf. *D. seftoni* Otariidae indet.	***Callorhinus*** *gilmorei* *Dusignathus seftoni* *Valenictus chulavistensis*	*Hydrarctos lomasiensis* *Acrophoca longirostris* *Hadrokirus martini* *Piscophoca pacifica* Monachinae indet.	*Callophoca obscura* *Pliophoca etrusca* *Homiphoca capensis* *Phocanella pumila* *Platyphoca vulgaris* *Gryphoca similis* *Ontocetus emmonsi*
Mysticeti	cf. ***Eubalaena* sp. 1** cf. ***Eubalaena* sp. 2** ***Balaenoptera*** *bertae* n. sp. "*Balaenoptera*" *cortesi* "var." *portisi* cf. ***Balaenoptera*** Balaenopteridae indet. 1 Balaenopteridae indet. 2 *Herpetocetus bramblei* *Herpetocetus* sp.	***Balaena*** n. sp. Balaenidae indet. "*Megaptera*" *miocaena* ***Balaenoptera*** *davidsonii* ***Balaenoptera*** sp. "*Balaenoptera*" *cortesi* "var." *portisi* cf. *Parabalaenoptera* Balaenopteridae new genus *Herpetocetus* n. sp.	Balaenopteridae indet. ***Balaenoptera*** *siberi* *Piscocetus sacaco* *Piscobalaena nana*	*Balaenula* sp. ***Balaena*** *ricei* ***Balaenoptera*** sp. ***Balaenoptera acutorostrata*** ***Megaptera*** sp. cf. "*Plesiocetus*" *Gricetoides aurorae* *Herpetocetus transatlanticus* Cetotheriidae indet.
Odontoceti	Odontoceti indet. Delphinidae indet. cf. Globicephalinae indet. *Parapontoporia sternbergi* Phocoenidae indet. Phocoenidae unnamed genus 1 Phocoenidae unnamed genus 2 **cf. *Phocoena*** Physeteroidea indet.	***Delphinus*** or ***Stenella*** Globicephalinae indet. Delphinapterinae indet. *Parapontoporia sternbergi* Phocoenidae unnamed genus 2 Phocoenidae unnamed genus 3 Physeteroidea indet.	cf. ***Delphinus*** cf. ***Stenella*** *Hemisyntrachelus oligodon* Globicephalinae indet. *Piscorhynchus aenigmaticus* *Piscolithax longirostris* Phocoenidae indet. Monodontidae indet. Delphinoidea indet. *Pliopontos littoralis* *Odobenocetops leptodon* *Odobenocetops peruvianus* Physeteridae indet. *Scaphokogia* n. sp. Kogiidae indet. *Ninoziphius platyrostris*	***Delphinus*** sp. ***Lagenorhynchus*** *harmatuki* ***Lagenorhynchus*** sp. ***Stenella*** *rayi* cf. ***Stenella*** sp. ***Tursiops*** sp. ***Globicephala*** sp. ***Pseudorca*** sp. cf. ***Pontoporia*** *Bohaskaia monodontoides* cf. ***Monodon*** *Auroracetus bakerae* *Aprixokogia kelloggi* Kogiidae indet. Physeteroidea indet. Physeteridae indet. *Ninoziphius* sp., cf. *N. platyrostris* ***Mesoplodon longirostris*** ***Ziphius*** sp., cf. ***Z. cavirostris***
Sirenia	–	***Hydrodamalis*** *cuestae*	cf. *Nanosiren*	–
% Recent Genera	35.3% (N=6)	37.5% (N=6)	16.6% (N=3)	53.1% (N=17)
# Taxa	21	21	25	35
# Taxa identified to generic level	17	16	18	32

portal from *c.* 3.5 Ma (Marincovich 2000), further cooling related to northern hemisphere glaciation at about 3 Ma (Zachos *et al.* 2001), decrease in marine upwelling during the Early Pliocene (3.6-2.588 Ma; Piacenzian equivalent; Barron 1998), and an upwelling-driven spike in primary productivity, Pacific *Chaetoceros* Explosion Event-2 (Suto *et al.* 2012). The final closure of the Panama Seaway is the implicated cause of increased upwelling and major changes in current patterns in the Pacific, including reversal of flow through the Bering Strait (Marincovich 2000). Changes in marine climate, the availability of food, currents, availability of haul out areas, and paleogeographic barriers (whether physical or temperature related) are all possible influences on these faunal perturbations (Fordyce *et al.* 2002; Walsh & Naish 2002; Fitzgerald 2005; Boessenecker 2013a; Valenzuela-Toro *et al.* 2013), and it is clear that many large scale physical processes could have driven marine vertebrate extinctions during the Pleistocene, in addition to ecological shifts (e.g., Harington 2008; Pyenson & Lindberg 2011; Foote *et al.* 2013). Apparently higher faunal provinciality during the Pliocene appears to have been fostered by restriction of dispersal routes to the Arctic, North Atlantic, and South Pacific, and provinciality may certainly have contributed to greater vulnerability of these faunas at their demise. Perhaps rapidly cooling climates driven by northern hemisphere glaciation (Zachos *et al.* 2001) drove the extinction of elements of these faunas towards the end of the Pliocene, and fostered dispersal of cosmopolitan marine mammals adapted to cooler waters into the North Pacific through the newly opened Arctic portal (Marincovich 2000), and across substantially cooled equatorial waters in the Pleistocene (Fajardo-Mellor *et al.* 2006). Indeed, many extant marine mammals are known or hypothesized to have survived drastic changes in marine climate and sea level during the Late Pleistocene by retaining flexible feeding ecology (Pyenson & Lindberg 2011) and tracking optimal climatic conditions north and south during interglacial and glacial periods (Harington 2008; Foote *et al.* 2013). Plio-Pleistocene changes in coastal geography may have affected a subset of the ENP marine mammal fauna. Large, shallow embayments were abundant during the Miocene and Pliocene along the California coastline (Hall 2002), which were subsequently eliminated owing to uplift of the coast ranges and infilling from increasing sedimentation related to Sierra Nevada uplift (Hall 2002), resulting in a change from a Pliocene coastline with numerous protected embayments to a Pleistocene-Holocene coastline with abundant rocky shore habitats (Jacobs *et al.* 2004). The loss of these embayments likely reduced the range of various marine mammals, ultimately leading to the extinction of *Parapontoporia* (Pyenson 2009). Development of the modern rocky shore likely fostered the dispersal of sea lions (rocky shore breeders) in addition to kelp forest foragers such as sea otters into the ENP during the Pleistocene. Future research should be directed at describing additional Pliocene marine mammals from California and Mexico, refining the geochronologic range of Plio-Pleistocene marine mammals, discovering new Pleistocene marine mammal-bearing localities, integrating paleobiogeographic and molecular phylogenetic data, and identifying possible causes for end-Pliocene marine mammal turnover.

CONCLUSIONS

The uppermost Miocene and Pliocene Purisima Formation has historically yielded a number of stratigraphically separated marine vertebrate assemblages. Recent field research in the San Gregorio section of Purisima Formation of uppermost Miocene and Pliocene age has yielded a diverse assemblage of 34 marine vertebrates. Of these, 21 marine mammals are here described, while the sharks, bony fish, and birds have been previously published. The marine mammal assemblage from the San Gregorio section of the Purisima Formation includes a fur seal (*Callorhinus* sp., cf. *C. gilmorei*), a walrus (*Dusignathus* sp., cf. *D. seftoni*) and an indeterminate otariid (Otariidae gen. et sp. indet.), two right whales (cf. *Eubalaena* sp. 1, cf. *Eubalaena* sp. 2) several balaenopterid mysticetes (*Balaenoptera* sp., "*Balaenoptera*" *cortesi* "var." *portisi*, Balaenopteridae gen. et sp. indet. morphotype 1, Balaenopteridae gen. et sp. indet. morphotype 2), a new species of balaenopterid (*Balaenoptera bertae* n. sp.), two

stratigraphically separated herpetocetine whales (*Herpetocetus bramblei*, *Herpetocetus* sp.), an indeterminate odontocete, an indeterminate delphinid, a pilot whale-like delphinid (cf. Globicephalinae gen. et sp. indet.), a long-beaked lipotid dolphin (*Parapontoporia sternbergi*), four true porpoises (cf. *Phocoena*, Phocoenidae unnamed genus 1, Phocoenidae unnamed genus 2, Phocoenidae indet.), and an unidentified sperm whale (cf. Physeteroidea gen. et sp. indet.). The new species of *Balaenoptera* exhibits many features in common with extant *Balaenoptera* spp., including a squamosal crease (but differs in retaining a narrow vertex and subvertical medial portion of frontal) and represents one of the few well documented fossil species of *Balaenoptera*. A new skull of *Parapontoporia sternbergi* is noteworthy as it preserves the first known earbones for this genus, confirming the earbone referrals of previous authors.

The San Gregorio assemblage is similar to the marine mammal assemblage from the Upper Pliocene San Diego Formation, and these two assemblages share several pinniped, mysticete, and odontocete taxa. The aggregate Late Pliocene assemblage from the ENP appears to exhibit a much higher number of extinct taxa at the generic level than other well known Pliocene assemblages from the North Atlantic, such as the Yorktown Formation. This suggests that the ENP harbored a more archaic marine mammal fauna for longer into the Pliocene than the North Atlantic realm, and that faunal turnover was temporally diachronous between the two oceanic basins. Furthermore, the ENP fauna either was affected by large-scale drivers geochronologically later, or was more resistant to such drivers. Meager Middle and Late Pleistocene marine mammal assemblages from the ENP are virtually completely constituted by extant genera, which indicate that the modern fauna appeared in this region between 2 Ma and 700 Ka. This appears to coincide with the 3.5-2 Ma closure of the Panama Seaway, a period of time which witnessed increasingly colder sea surface temperature, a shutdown of upwelling, and the initiation of continental glaciation in North America. Modern marine mammal species are now at risk due to changes in sea surface temperature, haul-out geography, pack ice, prey availability, and even prey-switching. Future research into Plio-Pleistocene faunal turnover may provide an additional "deep time" background for the conservation of marine mammals.

Acknowledgements
First and foremost, I would like to thank my undergraduate advisor, D. Varricchio, who encouraged me in 2003 to start fieldwork for this project, which began in 2005 and resulted in two other publications. Thanks go to the local surfer who directed me to "cool bones", resulting in the discovery of the San Gregorio fossil locality. Many other students and colleagues have provided assistance with fieldwork at these localities, including C. Argento, S. Boessenecker, M. Berrini, L. Ferrer, D. Fowler, E. Freedman, V. Jacklich, E. Johnson, D. Maxwell, T. Palladino, A. Poust, C. Powell, and especially C. Pirrone. Thanks to J. Horner, R. Harmon, and C. Ancell for use of the Museum of the Rockies preparation laboratory, and to C. Ancell, B. Baziak, S. Boessenecker, E. Freedman, R. Harmon, R. Hua, J. Jette, E. Morschauser, D. Varricchio, and C. Woodruff, who provided additional laboratory assistance. Thanks to S. Boessenecker for assistance with figure construction. This study benefited from numerous discussions on various aspects of marine mammal paleontology, and I am grateful for discussions with the following: G. Aguirre-Fernández, L. G. Barnes, A. Berta, G. Bianucci, M. Churchill, T. A. Deméré, J. Duran, J. El Adli, R. E. Fordyce, D. Fowler, E. Freedman-Fowler, J. H. Geisler, L. Hall, M. Knell, O. Lambert, C. Loch-Silva, F. G. Marx, F. A. Perry, A. Poust, C. L. Powell, II, R. Racicot, J. Scannella, N. A. Smith, Y. Tanaka and C. H. Tsai. Comments from R. E. Fordyce and F. G. Marx greatly improved an earlier version of this study, and their assistance is appreciated. Constructive reviews from G. Bianucci and O. Lambert vastly improved the quality of this study. French abstract was translated by Didier Merle and Sevket Sen (MNHN). I would also like to thank those who facilitated many museum and collections visits, including L. G. Barnes and S. McLeod (LACM), J. Demouthe and M. Flannery (CAS), R. Hilton and G. Bromm (Sierra College), P. Holroyd and M. Goodwin (UCMP), K. Randall, T. A.

Deméré, and J. El Adli (SDNHM), and F. A. Perry (SCMNH). I would like to thank T. A. Deméré, J. El Adli, O. Lambert, F. G. Marx, M. Murakami, R. Racicot, and J. Vélez-Juarbe for providing comparative photos of various fossil and modern cetaceans. Thanks to M. Colbert (UT Austin) for taking CT scans and constructing 3D models, and thanks to J. H. Geisler (NYCOM) for providing funding for CT scanning. I am particularly indebted to P. Holroyd, whose assistance was invaluable in curation and cataloging of this fossil collection, and in tolerating so many visits to UCMP. Lastly, special thanks go to employees of California State Parks, including S. Brown for facilitating and granting the collections permits for this study, J. Kerbavez for reviewing excavation sites in the field, and the Halfmoon Bay Ranger Lifeguards, whose coordination ensured my safety in the field, occasional heavy lifting, and the safe removal of the *Balaenoptera bertae* n. sp. holotype from the beach.

REFERENCES

AGUIRRE-FERNÁNDEZ G., BARNES L. G., ARANDA-MANTECA F. J. & FERNÁNDEZ-RIVERA J. R. 2009. — *Protoglobicephala mexicana*, a new genus and species of Pliocene fossil dolphin (Cetacea; Odontoceti; Delphinidae) from the Gulf of California, Mexico. *Boletín de la Sociedad Geológica Mexicana* 61 (2): 245-265.

ANSOM E. & MUIZON C. DE. (2013). — A new durophagous phocid (Mammalia: Carnivora) from the Late Neogene of Peru and considerations on monachine seals phylogeny. *Journal of Systematic Palaeontology*. http://dx.doi.org/10.1080/14772019.2013.799610

ATTERHOLT J., JEFFERSON G. & SCHACHNER E. 2007. — New marine vertebrates from the Yuha Member of the Deguynos Formation of Anza-Borrego Desert State Park. *Journal of Vertebrate Paleontology* 27 (3, supplement): 42A.

AUBRY M. P., BERGGREN W. A., VAN COUVERING J., MCGOWAN B., HILGEN F., STEININGER F. & LOURENS L. 2009. — The Neogene Quaternary: chronostratigraphic compromise or nonoverlapping magisteria? *Stratigraphy* 6: 1-16.

BARNES L. G. 1972. — Miocene Desmatophocinae (Mammalia: Carnivora) from California. *University of California Publications in Geological Sciences* 89: 1-76.

BARNES L. G. 1973. — Pliocene cetaceans of the San Diego Formation, San Diego, California, *in* ROSS A. & DOWLEN R. J. (eds), *Studies on the Geology and Geologic Hazards of the Greater San Diego Area, California*. San Diego Association of Geologists, San Diego, California: 37-42.

BARNES L. G. 1977. — Outline of eastern North Pacific fossil cetacean assemblages. *Systematic Zoology* 25: 321-343.

BARNES L. G. 1979. — Fossil enaliarctine pinnipeds (Mammalia: Otariidae) from Pyramid Hill, Kern County, California). *Contributions in Science, Natural History Museum of Los Angeles County* 318: 1-41.

BARNES L. G. 1984. — Fossil odontocetes (Mammalia: Cetacea) from the Almejas Formation, Isla Cedros, Mexico. *PaleoBios* 42: 1-46.

BARNES L. G. 1985a. — Evolution, taxonomy and antitropical distributions of the porpoises (Phocoenidae, Mammalia). *Marine Mammal Science* 1: 149-165.

BARNES L. G. 1985b. — Fossil pontoporiid dolphins (Mammalia: Cetacea) from the Pacific coast of North America. *Contributions in Science, Natural History Museum of Los Angeles County* 363: 1-34.

BARNES L. G. 1988. — A new fossil pinniped (Mammalia: Otariidae) from the Middle Miocene Sharktooth Hill Bonebed, California. *Contributions in Science, Natural History Museum of Los Angeles County* 396: 1-11.

BARNES L. G. 1992. — The fossil marine vertebrate fauna of the latest Miocene Almejas Formation, Isla Cedros, Baja California, Mexico, *in* CARRILLO-CHÁVEZ A. & ALVAREZ-ARELLANO A. (eds), *Primera Reunión Internacional sobre Geología de la Península de Baja California, Memorias*. Universidad Autónoma de Baja California Sur La Paz, Baja California Sur, Mexico: 147-166.

BARNES L. G. 1998. — The sequence of fossil marine mammal assemblages in Mexico, *in* CARRANZA-CASTAÑEDA O. & CÓRDOBA-MÉNDEZ D. A. (eds), *Avances en Investigación. Paleontología de Vertebrados. Publicación Especial 1*. Instituto de Investigaciones en Ciencias de la Tierra, Universidad Autónoma del Estado de Hidalgo, Pachucha, Hidalgo, Mexico: 26-79.

BARNES L. G. 2008. — Miocene and Pliocene Albireonidae (Cetacea, Odontoceti), rare and unusual fossil dolphins from the eastern North Pacific Ocean. *Natural History Museum of Los Angeles County Science Series* 41: 99-152.

BARNES L. G. & MITCHELL E. D. 1975. — Late Cenozoic northeast Pacific Phocidae. *Conseil International pour l'Exploration de la Mer, Rapports et Procès verbaux des Réunions* 169: 34-62.

BARNES L. G. & MCLEOD S. A. 1984. — The fossil record and phyletic relationships of gray whales, *in* JONES M. L., SWARTZ S. L. & LEATHERWOOD S. (eds) *The Gray Whale: Eschrichtius robustus*. Academic Press, Orlando, Florida: 3-32.

BARNES L. G. & MITCHELL E. D. 1984. — *Kentriodon obscurus* (Kellogg, 1931), a fossil dolphin (Mammalia: Kentriodontidae) from the Miocene Sharktooth Hill Bonebed in California. *Contributions in Science, Natural History Museum of Los Angeles County* 353: 1-23.

BARNES L. G. & PERRY F. A. 1989. — A toothless walrus from the Purisima Formation in California, U.S.A. *Abstracts, Eighth Biennial Conference on the Biology of Marine Mammals. Pacific Grove, California, December 1989*, 8: 5.

BARNES L. G. & RASCHKE R. E. 1991. — *Gomphotaria pugnax*, a new genus and species of Late Miocene dusignathine otariid pinniped (Mammalia: Carnivora) from California. *Contributions in Science, Natural History Museum of Los Angeles County* 426: 1-16.

BARNES L. G. & HIROTA K. — 1995. Miocene pinnipeds of the otariid subfamily Allodesminae in the North Pacific Ocean: Systematics and relationships. *The Island Arc* 3: 329-360.

BARNES L. G. & REYNOLDS R. E. 2009. — A new species of Early Miocene allodelphinid dolphin (Cetacea, Odontoceti, Platanistoidea) from Cajon Pass, Southern California, U.S.A. *Museum of Northern Arizona Bulletin* 65: 483-507.

BARNES L. G., HOWARD H., HUTCHISON J. H. & WELTON B. J. 1981. — The vertebrate fossils of the marine Cenozoic San Mateo Formation at Oceanside, California, *in* ABBOTT P. L. & O'DUNN S. (eds), *Geologic Investigations of the coastal plain, San Diego County, California*. San Diego Association of Geologists, San Diego, California: 53-70.

BARNES L. G., KIMURA M., FURUSAWA H. & SAWAMURA H. 1995. — Classification and distribution of Oligocene Aetiocetidae (Mammalia; Cetacea; Mysticeti) from western North America and Japan. *The Island Arc* 3: 392-431.

BARNES L. G., RAY C. E. & KORETSKY I. A. 2006. — A new Pliocene sea lion, *Proterozetes ulysses* (Mammalia: Otariidae) from Oregon, U.S.A., *in* CSIKI Z. (ed), *Mesozoic and Cenozoic Vertebrates and Paleoenvironments: Tributes to the Career of Prof. Dan Grigorescu*. Bucharest, Romania: 57-77.

BARNES L. G., KIMURA T. & GODFREY S. J. 2010. — The evolutionary history and phylogenetic relationships of the Superfamily Platanistoidea, *in* RUIZ-GARCIA M. & SHOSTELL J. (eds), *Biology, Evolution, and Conservation of River Dolphins Within South America and Asia*. Nova Science Publishers, New York: 445-488.

BARNOSKY A. D., KOCH P. L., FERANEC R. S., WING S. L. & SHABEL A. B. 2004. — Assessing the causes of Late Pleistocene extinctions on the continents. *Science* 306: 70-75.

BARRON J. A. 1998. — Late Neogene changes in diatom sedimentation in the North Pacific. *Journal of Asian Earth Science* 16: 85-95.

BARRON J. A. & ISAACS C. M. 2001. — Updated chronostratigraphic framework for the California Miocene, *in* Isaacs C. M. & Rullkotter J. (eds), *The Monterey Formation – From Rocks to Molecules*. Columbia University Press, New York: 393-395.

BEATTY B. L. 2009. — New material of *Cornwallius sookensis* (Mammalia: Desmostylia) from the Yaquina Formation of Oregon. *Journal of Vertebrate Paleontology* 29 (3): 894-909.

BERTA A. & MORGAN G. S. 1985. — A new sea otter (Carnivora: Mustelidae) from the Late Miocene and Early Pliocene (Hemphillian) of North America. *Journal of Paleontology* 59: 809-819.

BERTA A. & DEMÉRÉ T. A. 1986. — *Callorhinus gilmorei* n. sp., (Carnivora: Otariidae) from the San Diego Formation (Blancan) and its implications for otariid phylogeny. *Transactions of the San Diego Society of Natural History* 21 (7): 111-126.

BERTA A. & WYSS A. R. 1994. — Pinniped phylogeny. *Proceedings of the San Diego Society of Natural History* 29: 33-56.

BERTA A., RAY C. E. & WYSS A. R. 1989. — Skeleton of the oldest known pinniped, *Enaliarctos mealsi*. *Science* 244: 60-62.

BIANUCCI G. 1996. — The Odontoceti (Mammalia, Cetacea) from Italian Pliocene. Systematics and phylogenesis of Delphinidae. *Palaeontolographica Italica* 83: 73-167.

BIANUCCI G. 1997. — The Odontoceti (Mammalia, Cetacea) from Italian Pliocene. The Ziphiidae. *Palaeontographia Italica* 84: 163-192.

BIANUCCI G. 2005. — *Arimidelphis sorbinii* a new small killer whale-like dolphin from the Pliocene of Marecchia River (Central eastern Italy) and a phylogenetic analysis of the Orcininae (Cetacea: Odontoceti). *Rivista Italiana di Paleontologia e Stratigrafia* 111: 329-344.

BIANUCCI G. 2013. — *Septidelphis morii*, n. gen. et sp., from the Pliocene of Italy: new evidence of the explosive radiation of true dolphins (Odontoceti, Delphinidae). *Journal of Vertebrate Paleontology* 33: 722-740.

BIANUCCI G. & LANDINI W. 2006. — Killer sperm whale: a new basal physeteroid (Mammalia, Cetacea) from the Late Miocene of Italy. *Zoological Journal of the Linnaean Society* 148: 103-131.

BIANUCCI G., VAIANI S. C. & CASATI S. 2009. — A new delphinid record (Odontoceti, Cetacea) from the Early Pliocene of Tuscany (Central Italy): systematics and biostratigraphic considerations. *Neus Jahrbuch fur Geologie und Paläontologie Abhandlungen* 254: 275-292.

BIANUCCI G., LAMBERT O. & POST K. 2010. — High concentration of long-snouted beaked whales (genus *Messapicetus*) from the Miocene of Peru. *Palaeontology* 53: 1077-1098.

BISCONTI M. 2000. — New description, character analysis and preliminary phyletic assessment of two Balaenidae skulls from the Italian Pliocene. *Paleontographica Italica* 87: 37-66.

BISCONTI M. 2001. — Morphology and postnatal growth trajectory of rorqual petrosal. *Italian Journal of Zoology* 68: 87-93.

BISCONTI M. 2002. — An Early Late Pliocene right whale (Genus *Eubalaena*) from Tuscany (Central Italy). *Bollettino della Societa Paleontologica Italiana* 41: 83-91.
BISCONTI M. 2003. — Evolutionary history of Balaenidae. *Cranium* 20: 9-50.
BISCONTI M. 2005. — Skull morphology and phylogenetic relationships of a new diminutive balaenid from the lower Pliocene of Belgium. *Palaeontology* 48: 793-816.
BISCONTI M. 2007a. — A new basal balaenopterid whale from the Pliocene of northern Italy. *Palaeontology* 50: 1103-1122.
BISCONTI M. 2007b. — Taxonomic revision and phylogenetic relationships of the rorqual-like mysticete from the Pliocene of Mount Pulgnasco, northern Italy (Mammalia, Cetacea, Mysticeti). *Palaeontographica Italica* 91: 85-108.
BISCONTI M. 2008. — Morphology and phylogenetic relationships of a new eschrichtiid genus (Cetacea: Mysticeti) from the Early Pliocene of northern Italy. *Zoological Journal of the Linnean Society* 153: 161-186.
BISCONTI M. 2009. — Taxonomy and evolution of the Italian Pliocene Mysticeti (Mammalia, Cetacea); a state of the art. *Bollettino della Società Paleontologica Italiana* 48: 147-156.
BISCONTI M. 2010a. — A new balaenopterid whale from the Late Miocene of the Stirone River, Northern Italy (Mammalia, Cetacea, Mysticeti). *Journal of Vertebrate Paleontology* 30: 943-958.
BISCONTI M. 2010b. — New description of "*Megaptera*" *hubachi* Dathe, 1983 based on the holotype skeleton held in the Museum fur Naturkunde, Berlin. *Quaderni del Museuo di Storia Naturale di Livorno* 23: 37-58.
BOESSENECKER R. W. 2006. — A new marine vertebrate assemblage from the Late Neogene Purisima Formation at Pomponio State Beach, California. *Journal of Vertebrate Paleontology* 26 (3, supplement): 43A.
BOESSENECKER R. W. 2007. — New records of fur seals and walruses (Carnivora: Pinnipedia) from the Late Neogene of Northern California. *Journal of Vertebrate Paleontology* 27 (3, supplement): 50A.
BOESSENECKER R. W. 2011a. — A new marine vertebrate assemblage from the Late Neogene Purisima Formation in central California, Part I: Fossil sharks, bony fish, birds, and implications for the age of the Purisima Formation west of the San Gregorio Fault. *PalArch's Journal of Vertebrate Paleontology* 8(4): 1-30.
BOESSENECKER R. W. 2011b. — Herpetocetine (Cetacea: Mysticeti) dentaries from the Upper Miocene Santa Margarita Sandstone of Central California. *PaleoBios* 30(1): 1-12.
BOESSENECKER R. W. 2011c. — New records of the fur seal *Callorhinus* (Carnivora: Otariidae) from the Plio-Pleistocene Rio Dell Formation of Northern California and comments on otariid dental evolution. *Journal of Vertebrate Paleontology* 31: 454-467.
BOESSENECKER R. W. 2013a. — Pleistocene survival of an archaic dwarf baleen whale (Mysticeti: Cetotheriidae). *Naturwissenschaften* 100: 365-371.
BOESSENECKER R. W. 2013b. — Taphonomic implications of barnacle encrusted sea lion bones from the Middle Pleistocene Port Orford Formation, coastal Oregon. *Journal of Paleontology* 87: 657-663.
BOESSENECKER R. W. & GEISLER J. H. 2008. — New material of the bizarre whale *Herpetocetus bramblei* from the latest Miocene Purisima Formation of Central California. *Journal of Vertebrate Paleontology* 28 (3, supplement): 54A.
BOESSENECKER R. W. & PERRY F. A. 2011. — Mammalian bite marks on juvenile fur seal bones from the Late Neogene Purisima Formation of Central California. *Palaios* 26: 115-120.
BOESSENECKER R. W. & SMITH N. A. 2011. — Latest Pacific basin record of a bony-toothed bird (Aves, Pelagornithidae) from the Pliocene Purisima Formation of California, U.S.A. *Journal of Vertebrate Paleontology* 31: 652-657.
BOESSENECKER R. W., PERRY F. A. & GEISLER J. H. 2013. — Globicephaline whales from the Mio-Pliocene Purisima Formation of central California, USA. *Acta Palaeontologica Polonica*. http://dx.doi.org/10.4202/app.2013.0019
BOSSELAERS M. & POST K. 2010. — A new fossil rorqual (Mammalia, Cetacea, Balaenopteridae) from the Early Pliocene of the North Sea, with a review of the rorqual species described by Owen and Van Beneden. *Geodiversitas* 32: 331-363. http://dx.doi.org/10.5252/g2010n2a6
BOUETEL V. & MUIZON C. DE. 2006. — The anatomy and relationships of *Piscobalaena nana* (Cetacea, Mysticeti), a Cetotheriidae s.s. from the Early Pliocene of Peru. *Geodiversitas* 28: 319-395.
CHANDLER R. M. 1990. — Fossil birds of the San Diego Formation, Late Pliocene, Blancan, California. *Ornithological Monographs* 44: 77-161.
CHURCHILL M., BERTA A. & DEMÉRÉ T. A. 2012. — The systematics of right whales (Mysticeti: Balaenidae). *Marine Mammal Science* 28: 497-521.
CLARK J. C. 1981. — Stratigraphy, paleontology, and geology of the central Santa Cruz Mountains, California Coast Ranges. *United States Geological Survey Professional Paper* 1168: 1-51.
CLARK J. C. 1997. — *Neotectonics of the San Gregorio Fault Zone-age dating controls on offset history and slip rate*. National Earthquake Hazards Reduction Program, Menlo Park, California: 30p.
CLARK J. C., BRABB E. E., GREENE H. G. & ROSS D. C. 1984. — Geology of Point Reyes Peninsula and implications for San Gregorio Fault history, *in* Crouch J. K. & Bachman S. B. (eds), *Tectonics and sedimentation along the California margin*. Pacific Section SEPM, Los Angeles, California: 67-86.

CLARK J. M. 1991. — A new Early Miocene species of *Paleoparadoxia* (Mammalia: Desmostylia) from California. *Journal of Vertebrate Paleontology* 11: 490-508.

COATES A. G. & OBANDO J. A. 1996. — Geological evolution of the Central American Isthmus *in* JACKSON J. B. C., BUDD A. F. & COATES A. G. (eds), *Evolution and Environment in Tropical America*. University of Chicago Press, Chicago: 21-56.

COLLINS L. S., COATES A. G., BERGGREN W. A., AUBRY M. P. & ZHANG J. 1996. — The Late Miocene Panama isthmian strait. *Geology* 24: 687-690.

CUMMINGS J. C., TOURING R. M. & BRABB E. E. 1962. — Geology of the northern Santa Cruz Mountains, California. *California Division of Mines and Geology Bulletin* 181: 179-220.

DEMÉRÉ T. A. 1983. — The Neogene San Diego Basin: a review of the marine Pliocene San Diego Formation of southern California, *in* LARUE D. K. & STEEL R. J. (eds), *Cenozoic Marine Sedimentation, Pacific Margin, U.S.A.* Society of Economic Paleontologists and Mineralogists, Los Angeles, California: 187-195.

DEMÉRÉ T. A. 1986. — The fossil whale, Balaenoptera davidsonii (Cope 1872), with a review of other Neogene species of *Balaenoptera* (Cetacea: Mysticeti). Marine Mammal Science 2: 277-298.

DEMÉRÉ T. A. 1993. — Fossil mammals from the Imperial Formation (Upper Miocene-lower Pliocene), Coyote Mountains, Imperial County, California. *San Bernardino County Museum Association Special Publication* 93-1: 82-85.

DEMÉRÉ T. A. 1994a. — The family Odobenidae: a phylogenetic analysis of fossil and living taxa. *Proceedings of the San Diego Society of Natural History* 29: 99-123.

DEMÉRÉ T. A. 1994b. — Two new species of fossil walruses (Pinnipedia: Odobenidae) from the Upper Pliocene San Diego Formation, California. *Proceedings of the San Diego Society of Natural History* 29: 77-98.

DEMÉRÉ T. A. & BERTA A. 2002. — The Miocene pinniped *Desmatophoca oregonensis* Condon, 1906 (Mammalia: Carnivora) from the Astoria Formation, Oregon. *Smithsonian Contributions to Paleobiology* 93: 113-147.

DEMÉRÉ T. A. & BERTA A. 2003. — A new species of baleen whale (Cetacea, Mysticeti) from the Pliocene of California and its implications for higher mysticete phylogenetic relationships. *Journal of Vertebrate Paleontology* 23 (3, supplement): 45A.

DEMÉRÉ T. A. & BERTA A. 2005. — New skeletal material of *Thalassoleon* (Otariidae: Pinnipedia) from the Late Miocene–Early Pliocene (Hemphillian) of California. *Bulletin of the Florida Museum of Natural History* 45: 379-411.

DEMÉRÉ T. A., BERTA A. & ADAM P. J. 2003. — Pinnipedimorph evolutionary biogeography. *Bulletin of the American Museum of Natural History* 13: 32-76.

DEMÉRÉ T. A., BERTA A. & MCGOWEN M. R. 2005. — The taxonomic and evolutionary history of modern balaenopteroid mysticetes. *Journal of Mammalian Evolution* 12: 99-143.

DOMNING D. P. 1978. — Sirenian evolution in the North Pacific Ocean. *University of California Publications in Geological Sciences* 18: 1-176.

DOMNING D. P. & DEMÉRÉ T. A. 1984. — New material of *Hydrodamalis cuestae* (Mammalia; Dugongidae) from the Miocene and Pliocene of San Diego County, California. *Transactions of the San Diego Society of Natural History* 20: 169-188.

DOMNING D. P. & BARNES L.G. 2007. — A new name for the "Stanford Skeleton" of *Paleoparadoxia* (Mammalia, Desmostylia). *Journal of Vertebrate Paleontology* 27: 748-751.

DOMNING D. P. & FURUSAWA H. 1995. — Summary of taxa and distribution of Sirenia in the North Pacific Ocean. *The Island Arc* 3: 506-512.

DOMNING D. P., RAY C. E. & MCKENNA M. C. 1986. — Two new Oligocene desmostylians and a discussion of Tethytherian systematics. *Smithsonian Contributions to Paleobiology* 59: 1-56.

DORNBURG A., BRANDLEY M. C., MCGOWEN M. R. & NEAR T. J. 2012. — Relaxed clocks and inferences of heterogeneous patterns of nucleotide substitution and divergence time estimates across whales and dolphins (Mammalia: Cetacea). *Molecular Biology and Evolution* 29: 721-736.

DURHAM J. W. & MORGAN S. R. 1978. — New sand dollars (Echinoidea) of the genera *Merriamaster* and *Dendraster* from Purisima Formation, California. *Proceedings of the California Academy of Sciences* 41: 297-305.

DUKE W. L., ARNOTT R. W. C. & CHEEL R. J. 1991. — Shelf sandstones and hummocky cross-stratification: new insights on a stormy debate. *Geology* 19: 625-628.

EHRET D. J., MACFADDEN B. J., JONES D. S., DEVRIES T. J., FOSTER D. A. & SALAS-GISMONDI R. 2012. — Origin of the white shark *Carcharodon* (Lamniformes: Lamnidae) based on recalibration of the Upper Neogene Pisco Formation of Peru. *Palaeontology* 55: 1139-1153.

EKDALE E. G., BERTA A. & DEMÉRÉ T. A. 2011. — The comparative osteology of the petrotympanic complex (ear region) of extant baleen whales (Cetacea: Mysticeti). *Plos One* 6 (6): 1-42.

EMLONG D. 1966. — A new archaic cetacean from the Oligocene of Northwest Oregon. *Bulletin of the Museum of Natural History, University of Oregon* 3: 1-51.

FAJARDO-MELLOR L., BERTA A., BROWNELL R. L., BOY C. C. & GOODALL R. N. 2006. — The phylogenetic relationships and biogeography of true porpoises (Mammalia: Phocoenidae) based on morphological data. *Marine Mammal Science* 22: 910-932.

FEDOROV A. V., BRIERLY C. M., LAWRENCE K. T., LIU Z., DEKENS P. S. & RAVELO A. C. 2013. — Patterns and mechanisms of Early Pliocene warmth. *Nature* 496: 43-49.

FIERSTINE H. L. 2008. — A fossil skull of the extant blue marlin (*Makaira nigricans* Lacépède, 1802) from the Late Miocene of Orange County, California. *Bulletin of the Southern California Academy of Science* 107: 45-56.

FILIPPELLI G. M. & FLORES. J. A. 2009. — From the warm Pliocene to the cold Pleistocene: a tale of two oceans. *Geology* 37: 959-960.

FITZGERALD E. M. G. 2004. — A review of the Tertiary fossil Cetacea (Mammalia) localities in Australia. *Memoirs of the Museum of Victoria* 61 (2): 183-208.

FITZGERALD E. M. G. 2005. — Pliocene marine mammals from the Whalers Bluff Formation of Portland, Victoria, Australia. Memoirs of Museum Victoria 62 (1): 67-89.

FOOTE A. D., KASCHNER K., SCHULTZE S. E. GARILAO C., HO S. Y. W., POST K., HIGHAM T. F. G., STOKOWSKA C., ES H. VAN DER, EMBLING C. B., GREGERSEN K., JOHANSSON F., WILLERSLEV E. & GILBERT M. T. P. 2013. — Ancient DNA reveals that bowhead whale lineages survived Late Pleistocene climate change and habitat shifts. *Nature Communications* 4: 1677.

FORDYCE R. E. 1994. — *Waipatia maerewhenua*, new genus and new species, Waipatiidae, new family, an archaic Late Oligocene dolphin (Cetacea: Odontoceti: Platanistoidea) from New Zealand. *Proceedings of the San Diego Society of Natural History* 29: 147-176.

FORDYCE R. E. & FLANNERY T. F. 1983. — Fossil phocid seals from the Late Tertiary of Victoria. *Proceedings of the Royal Society of Victoria* 95: 99-100.

FORDYCE R. E., QUILTY P. G. & DANIELS J. 2002. — *Australodelphis mirus*, a bizarre new toothless ziphiid-like fossil dolphin (Cetacea: Delphinidae) from the Pliocene of Vestfold Hills, East Antarctica. *Antarctic Science* 14: 37-54.

FURUSAWA H. 1988. — *A new species of hydrodamaline Sirenia from Hokkaido, Japan*. Takikawa Museum of Art and Natural History, Takikawa, 73 p.

GALLOWAY A. J. 1977. — Geology of the Point Reyes Peninsula, Marin County, California. *California Division of Mines and Geology Bulletin* 202: 1-72.

GAVIGAN C. L. 1984. — *Composition and Stratigraphy of the Purisima Formation in the Central California Coast Ranges*. Unpublished M. S. thesis, Stanford University, Stanford, California, 111 p.

GEISLER J. H. & LUO Z. 1996. — The petrosal and inner ear of *Herpetocetus* sp. (Mammalia: Cetacea) and their implications for the phylogeny and hearing of archaic mysticetes. *Journal of Paleontology* 70 (6): 1045-1066.

GEISLER J. H. & SANDERS A. E. 2003. — Morphological Evidence for the Phylogeny of Cetacea. *Journal of Mammalian Evolution* 10 (1/2): 23-129.

GEISLER J. H., MCGOWEN M. R., YANG G. & GATESY J. 2011. — A supermatrix analysis of genomic, morphological, and paleontological data from crown Cetacea. *BMC Evolutionary Biology* 11 (112): 1-33.

GEISLER J. H., GODFREY S. J. & LAMBERT O. 2012. — A new genus and species of Late Miocene inioid (Cetacea, Odontoceti) from the Meherrin River, North Carolina, U.S.A. *Journal of Vertebrate Paleontology* 32: 198-211.

GIBBARD P. L., HEAD M. J., WALKER M. J. & Subcommittee on Quaternary Stratigraphy 2009. — Formal ratification of the Quaternary System/Period and the Pleistocene Series/Epoch with a base at 2.58 Ma. *Journal of Quaternary Science* 25: 96-102.

GIBSON M. L. & GEISLER J. H. 2009. — A new Pliocene dolphin (Cetacea: Pontoporiidae) from the Lee Creek Mine, North Carolina. *Journal of Vertebrate Paleontology* 29:966-971.

GINGRAS M. K., ARMITAGE I. A., PEMBERTON G. & CLIFTON H. E. 2007. — Pleistocene walrus herds in the Olympic Peninsula area: trace-fossil evidence of predation by hydraulic jetting. *Palaios* 22: 539-545.

GLEN W. 1959. — Pliocene and lower Pleistocene of the western part of the San Francisco peninsula. *University of California Publications in Geological Sciences* 36: 147-198.

GOLOBOFF P., FARRIS J. & NIXON K. 2008. — TNT, a free program for phylogenetic analysis. *Cladistics* 24: 774-786.

GOTTFRIED M. D., BOHASKA D. J. & WHITMORE F. C. 1994. — Miocene cetaceans of the Chesapeake Group. *Proceedings of the San Diego Society of Natural History* 29: 229-238.

GRADSTEIN F. M., OGG J. G. & SMITH A. G. 2004. — *A Geologic Timescale 2004*. Cambridge University Press, Cambridge, 589 p.

GREGORY W. K. & KELLOGG R. 1927. — A fossil porpoise from California. *American Museum Novitates* 269: 1-7.

HALL C. A. JR. 2002. — Nearshore marine paleoclimatic regions, increasing zoogeographic provinciality, molluscan extinctions, and paleoshorelines, California: Late Oligocene (27 Ma) to Late Pliocene (2.5 Ma). *Geological Society of America Special Papers 2002* 357: 1-489.

HALLER C. R. 1980. — Pliocene biostratigraphy of California. *American Association of Petroleum Geologists Studies in Geology* 11: 183-341.

HARINGTON C. R. 1977. — Marine mammals in the Champlain Sea and the Great Lakes. *Annals of the New York Academy of Sciences* 288: 508-537.

HARINGTON C. R. 1984. — Quaternary marine and land mammals and their paleoenvironmental implications – some examples from northern North America. *Carnegie Museum of Natural History, Special Publication* 8: 511-525.

HARINGTON C. R. 2008. — The evolution of Arctic marine mammals. *Ecological Applications* 18: S23-S40.
HARINGTON C. R. & BEARD G. 1992. — The Qualicum walrus: a Late Pleistocene walrus (*Odobenus rosmarus*) skeleton from Vancouver Island, British Columbia, Canada. *Annales Zoologici Fennici* 28: 311-319.
HARNIK P. G., LOTZE H. K., ANDERSON S. C., FINKEL Z. V., FINNEGAN S., LINDBERG D. R., LIOW L. H., LOCKWOOD R., MCCLAIN C. R., MCGUIRE J. L., O'DEA A., PANDOLFI J. M., SIMPSON C. & TITTENSOR D. P. 2012. — Extinctions in ancient and modern seas. *Trends in Ecology & Evolution* 27: 608-617.
HAUG G. H., TIEDEMANN R., ZAHN R. & RAVELO A. C. 2001. — Role of Panama uplift on oceanic freshwater balance. *Geology* 29: 207-210.
HILGEN F. J., LOURENS L. J. & VAN DAM J. A. 2012. — The Neogene period, *in* GRADSTEIN F. M., OGG J. G., SCHMITZ M. & OGG G. (eds), *The Geologic Time Scale 2012*. Elsevier, Amsterdam: 923-978.
HORIKAWA H. 1995. — A primitive odobenine walrus of Early Pliocene age from Japan. *The Island Arc* 3: 309-328.
HOWARD H. 1966. — Additional avian records from the Miocene of Sharktooth Hill, California. *Contributions in Science, Natural History Museum of Los Angeles County* 114: 1-11.
HOWARD H. 1971. — Pliocene avian remains from Baja California. *Contributions in Science, Natural History Museum of Los Angeles County* 217: 1-17.
HOWARD H. 1982. — Fossil birds from Tertiary marine beds at Oceanside, San Diego County, California, with descriptions of two species of the genera *Uria* and *Cepphus* (Aves: Alcidae). *Contributions in Science, Natural History Museum of Los Angeles County* 341: 1-15.
HOWARD H. 1984. — Additional avian records from the Miocene of Kern County, California, USA with the description of a new species of fulmar (Aves: Procellariidae). *Bulletin of the Southern California Academy of Sciences* 83:84-89.
ICHISHIMA H. & KIMURA M. 2000. — A new fossil porpoise (Cetacea; Delphinoidea; Phocoenidae) from the Early Pliocene Horokaoshirarika Formation, Hokkaido, Japan. *Journal of Vertebrate Paleontology* 20: 561-576.
ICHISHIMA H. & KIMURA M. 2005. — *Haborophocoena toyoshimai*, a new Early Pliocene porpoise (Cetacea, Phocoenidae) from Hokkaido, Japan. *Journal of Vertebrate Paleontology* 25: 655-664.
ICHISHIMA H. & KIMURA M. 2009. — A new species of *Haborophocoena*, an Early Pliocene phocoenid cetacean from Hokkaido, Japan. *Marine Mammal Science* 25: 855-874.
ICHISHIMA H., SATO E., SAGAYAMA T. & KIMURA M. 2006. — The oldest record of Eschrichtiidae (Cetacea: Mysticeti) from the Late Pliocene, Hokkaido, Japan. *Journal of Paleontology* 80: 367-379.
INGLE J. C. 1979. — Biostratigraphy and paleoecology of Early Miocene through Early Pleistocene benthonic and planktonic foraminifera, San Joaquin Hills-Newport Bay-Dana Point area, Orange County, California, *in* STUART C. J. (ed), *Miocene Lithofacies and Depositional Environments, Coastal Southern California and Northwestern Baja California*. Society of Economic Paleontologists and Mineralogists, Pacific Section, Los Angeles: 53-77.
JACOBS D. K., HANEY T. A. & LOUIE K. D. 2004. — Genes, diversity, and geologic process on the Pacific coast. *Annual Review of Earth and Planetary Sciences* 32: 601-652.
JEFFERSON G. T. 1991. — A catalogue of Late Quaternary vertebrates from California: part two, mammals. *Natural History Museum of Los Angeles County Technical Report* 7: 1-129.
JONES R. E. 1967. — A *Hydrodamalis* skull fragment from Monterey Bay, California. *Journal of Mammalogy* 48: 143-144.
JORDAN D. S. & HANNIBAL H. 1923. — Fossil sharks and rays of the Pacific Slope of North America. *Bulletin of the Southern California Academy of Science* 22: 27-63.
KAZÁR E. & BOHASKA D. J. 2008. — Toothed whale (Mammalia: Cetacea: Odontoceti) limb bones of the Lee Creek Mine, North Carolina. *Virginia Museum of Natural History Special Publication* 14: 271-324.
KELLOGG R. 1921. — A new pinniped from the Upper Pliocene of California. *Journal of Mammalogy* 2: 212-226.
KELLOGG R. 1922. — Description of the skull of *Megaptera miocaena*, a fossil humpback whale from the Miocene diatomaceous earth of Lompoc, California. *Proceedings of the United States National Museum* 61: 1-18.
KELLOGG R. 1927. — Fossil Pinnipeds from California. *Contributions to Palaeontology from the Carnegie Institution of Washington* 348: 27-37.
KELLOGG R. 1931. — Pelagic mammals from the Temblor Formation of the Kern River region, California. *Proceedings of the California Academy of Sciences* 19: 217-397.
KELLOGG R. 1944. — Fossil Cetaceans from the Florida Tertiary. *Bulletin of the Museum of Comparative Zoology at Harvard College* 44: 433-471.
KILMER F. H. 1972. — A new species of sea otter from the Late Pleistocene of northwestern California. *Bulletin of the Southern California Academy of Sciences* 71: 150-157.
KIMURA T. 2009. — Review of the fossil balaenids from Japan with a re-description of *Eubalaena shinshuensis* (Mammalia, Cetacea, Mysticeti). *Quaderni del Museo di Storia Naturale di Livorno* 22: 3-21.
KIMURA T. & HASEGAWA Y. 2005. — Fossil finless porpoise, *Neophocaena phocaenoides*, from the Seto Island Sea, Japan. *Bulletin of the Gunma Museum of Natural History* 9: 65-72.

KIMURA T., HASEGAWA Y. & BARNES L. G. 2006. — Fossil sperm whales (Cetacea, Physeteridae) from Gunma and Ibaraki prefectures, Japan; with observations on the Miocene fossil sperm whale *Scaldicetus shigensis* Hirota and Barnes, 1995. *Bulletin of the Gunma Museum of Natural History* 10: 1-23.

KING J. E. 1973. — Pleistocene Ross seal (*Ommatophoca rossi*) from New Zealand. *New Zealand Journal of Marine and Freshwater Research* 7: 391-397.

KING C. M., ROBERTS C. D., BELL B. D., FORDYCE R. E., NICOLL R. S., WORTHY T. H., PAULIN C. D., HITCHMOUGH R. A., KEYES I. W., BAKER A. N., STEWART A. L., HILLER N., MCDOWALL R. M., HOLDAWAY R. N., MCPHEE R. P., SCHWARZHANS W. W., TENNYSON A. J. D., RUST S. & MACADIE I. 2009. — Phylum Chordata. Lancelets, fish, amphibians, reptiles, birds, and mammals, *in* GORDON D. P. (ed.), *The New Zealand Inventory of Biodiversity: A Species 2000 Symposium Review*. University of Canterbury Press, Christchurch: 433-553.

KOHL R. F. 1974. — A new Late Pleistocene fauna from Humboldt County, California. *The Veliger* 17: 211-219.

KOHNO N. 1992. — A new Pliocene fur seal (Carnivora: Otariidae) from the Senhata Formation on the Boso Peninsula, Japan. *Natural History Research* 2: 15-28.

KOHNO N. 2006. — A new Miocene odobenid (Mammalia: Carnivora) from Hokkaido, Japan, and its implications for odobenid phylogeny. *Journal of Vertebrate Paleontology* 26: 411-421.

KOHNO N. & YANAGISAWA Y. 1997. — The first record of the Pliocene Gilmore fur seal in the Western North Pacific Ocean. *Bulletin of the National Science Museum, Tokyo* 23: 119-130.

KOHNO N. & RAY C. E. 2008. — Pliocene walruses from the Yorktown Formation of Virginia and North Carolina, and a systematic revision of the North Atlantic Pliocene walruses. *Virginia Museum of Natural History Special Publication* 14: 39-80.

KOHNO N., BARNES L. G. & HIROTA K. 1995a. — Miocene fossil pinnipeds of the genera *Prototaria* and *Neotherium* (Carnivora; Otariidae; Imagotariinae) in the North Pacific Ocean: Evolution, relationships and distribution. *The Island Arc* 3: 285-308.

KOHNO N., TOMIDA Y., HASEGAWA Y. & FURUSAWA H. 1995b. — Pliocene tusked odobenids (Mammalia: Carnivora) in the Western North Pacific, and their paleobiogeography. *Bulletin of the National Science Museum, Tokyo Series C (Geology & Paleontology)* 21: 111-131.

KOHNO N., NARITA K. & KOIKE H. 1998. — An Early Pliocene odobenid (Mammalia: Carnivora) from the Joshita Formation, Nagano Prefecture, central Japan. *Research Reports of the Shinshushinmachi Fossil Museum* 1: 1-7.

KORETSKY I. A. & RAY C. E. 2008. — Phocidae of the Pliocene of eastern USA. *Virginia Museum of Natural History Special Publication* 14: 81-140.

LAMBERT O. 2005. — Systematics and phylogeny of the fossil beaked whales *Ziphirostrum* du Bus, 1868 and *Choneziphius* Duvernoy, 1851 (Mammalia, Cetacea, Odontoceti), from the Neogene of Antwerp (north of Belgium). *Geodiversitas* 27: 443-497.

LAMBERT O. 2008a. — A new porpoise (Cetacea, Odontoceti, Phocoenidae) from the Pliocene of the North Sea. *Journal of Vertebrate Paleontology* 28: 863-872.

LAMBERT O. 2008b. — Sperm whales from the Miocene of the North Sea: a re-appraisal. *Bulletin del'Institut Royal des Sciences Naturelles de Belgique, Sciences de la Terre* 78: 277-316.

LAMBERT O. & GIGASE P. 2007. — A monodontid cetacean from the Early Pliocene of the North Sea. *Bulletin de l'Institut Royal des Sciences Naturelles de Belgique Sciences de la Terre* 77: 197-210.

LAMBERT O. & MUIZON C. DE. 2013. — A new long-snouted species of the Miocene pontoporiid dolphin Brachydelphis and a review of the Mio-Pliocene marine mammal levels in the Sacaco Basin, Peru. *Journal of Vertebrate Paleontology* 33: 709-721.

LAMBERT O., MUIZON C. DE & BIANUCCI G. 2013. — The most basal beaked whale *Ninoziphius platyrostris* Muizon, 1983: clues on the evolutionary history of the family Ziphiidae (Cetacea: Odontoceti). *Zoological Journal of the Linnean Society* 167: 569-598.

LANGENWALTER P. E. 1975. — Chordates: The fossil vertebrates of the Los Angeles-Long Beach harbors region. *Marine studies of San Pedro Bay, California* 9: 36-54.

LEATHERWOOD S., HOBBS L. J. & DAVIS F. A. 1988. — *Whales, dolphins, and porpoises of the eastern North Pacific and adjacent Arctic waters.* Dover Publications, New York. 256p.

LEDESMA-VÁZQUEZ J. 2002. — A gap in the Pliocene invasion of seawater to the gulf of California. *Revista Mexicana de Ciencias Geológicas* 19: 145-151.

LEFFLER S. R. 1964. — Fossil mammals from the Elk River Formation, Cape Blanco, Oregon. *Journal of Mammalogy* 45: 53-61.

LOOMIS K. B. 1992. — New K-Ar ages from the tuffs in the Etchegoin Formation, San Joaquin basin, California. *Isochron/West* 58: 3-7.

LYNCH S. C. & PARHAM J. F. 2003. — The first report of hard-shelled sea turtles (Cheloniidae sensu lato) from the Miocene of California, including a new species (*Euclastes hutchisoni*) with unusually plesiomorphic characters. *PaleoBios* 23: 21-35.

MADRID V. M., STUART R. M. & VEROSUB K. L. 1986. — Magnetostratigraphy of the Late Neogene Purisima Formation, Santa Cruz County, California. *Earth and Planetary Science Letters* 79: 431-440.

MARINCOVICH L. 2000. — Central American paleogeography controlled Pliocene Arctic Ocean molluscan migrations. *Geology* 28: 551-554.

MARTIN J. 2010. — A new fossil balaenopterid (Cetacea, Mysticeti) from the Late Pliocene San Diego Formation, California. *Journal of Vertebrate Paleontology* 30 (3, Supplement): 130A.

MARX F. G. 2011. — The more the merrier? A large cladistic analysis of mysticetes, and comments on the transition from teeth to baleen. *Journal of Mammalian Evolution* 18 (2): 77-100.

MARX F. G. & UHEN M. D. 2010. — Climate, critters, and cetaceans: Cenozoic drivers of the evolution of modern whales. *Science* 327: 993-996.

MCGOWEN M. R., SPAULDING M. & GATESY J. 2009. — Divergence date estimation and a comprehensive molecular tree of extant cetaceans. *Molecular Phylogenetics and Evolution* 53: 891-906.

MEAD J. G. & FORDYCE R. E. 2009. — The therian skull: a lexicon with emphasis on the odontocetes. *Smithsonian Contributions to Zoology* 627: 1-248.

MILLER L. 1961. — Birds from the Miocene of Sharktooth Hill, California. *The Condor* 63: 399-402.

MILLER L. 1962. — A new albatross from the Miocene of California. *The Condor* 64: 471-472.

MILLER W. E. 1971. — Pleistocene vertebrates of the Los Angeles Basin and vicinity (exclusive of Rancho La Brea). *Bulletin of the Los Angeles County Museum of Natural History, Science* 10: 1-124.

MISONNE X. 1958. — Faune du Tertiaire et du Pléistocène inférieur de Belgique (oiseaux et mammifères). *Bulletin de l'Institut Royal des Sciences Naturelles de Belgique* 34: 1-36.

MITCHELL E. D. 1961. — A new walrus from the imperial Pliocene of Southern California: with notes on odobenid and otariid humeri. *Contributions in Science, Natural History Museum of Los Angeles County* 44: 1-28.

MITCHELL E. D. 1962. — A walrus and a sea lion from the Pliocene Purisima Formation at Santa Cruz, California; with remarks on the type locality and geologic age of the sea lion *Dusignathus santacruzensis* Kellogg. *Contributions in Science, Natural History Museum of Los Angeles County* 44: 1-24.

MITCHELL E. D. 1966a. — *History of research at Sharktooth Hill, Kern County, California*. Kern County Historical Society, Bakersfield, California, 45 p.

MITCHELL E. D. 1966b. — Northeastern Pacific Pleistocene sea otters. *Journal of the Fisheries Research Board of Canada* 23: 1897-1911.

MITCHELL E. D. 1966c. — The Miocene pinniped *Allodesmus*. *University of California Publications in Geological Sciences* 61: 1-105.

MITCHELL E. D. & TEDFORD R. H. 1973. — The Enaliarctinae: A new group of extinct aquatic Carnivora and a consideration of the origin of the Otariidae. *Bulletin of the American Museum of Natural History* 151: 203-284.

MIYAZAKI S., HORIKAWA H., KOHNO N., HIROTA K., KIMURA M., HASEGAWA Y., TOMIDA Y., BARNES L. G. & RAY C. E. 1995. — Summary of the fossil record of pinnipeds of Japan, and comparisons with that from the eastern North Pacific. *The Island Arc* 3: 361-372.

MORGAN G. S. 1994. — Miocene and Pliocene marine mammal faunas from the Bone Valley Formation of central Florida. *Proceedings of the San Diego Society of Natural History* 29: 239-268.

MUIZON C. DE 1978. — *Arctocephalus* (*Hydrarctos*) *lomasiensis*, subgen. nov. et nov sp., un nouvel Otariidae du Mio-Pliocene de Sacaco. *Bulletin de l'Institute Francais d'Etudes Andines* 7: 169-189.

MUIZON C. DE 1981. — Les vertébrés fossiles de la Formation Pisco (Pérou). Première parti : deux nouveaux Monachinae (Phocidae, Mammalia) du Pliocène de Sud-Sacaco. *Recherche sur les grandes Civilisations Mémoire* 1981: 1-150.

MUIZON C. DE 1984. — Les vertébrés fossiles de la Formation Pisco (Pérou), Deuxieme partie: Les odontocètes (Cetacea, Mammalia) du Pliocène inférieur de Sud-Sacaco. *Travaux de l'Institut français d'Études Andines* 50: 1-188.

MUIZON C. DE 1988a. — Les relations phylogenetiques des Delphinida (Cetacea, Mammalia). *Annales de Paleontologie* 74: 159-227.

MUIZON C. DE 1988b. — Les vertébrés fossiles de la Formation Pisco (Perou). Troisième partie : les odontocètes (Cetacea, Mammalia) du Miocène. *Éditions Recherche sur les Civilisations* 78: 1-244.

MUIZON C. DE 1993. — Walrus-like feeding adaptation in a new cetacean from the Pliocene of Peru. *Nature* 365: 745-748.

MUIZON C. DE & BELLON H. 1986. — Nouvelles données sur l'âge de la Formation Pisco (Pérou). *Comptes-Rendus de l'Académie des Sciences Paris. Série II. Mécanique-Physique-Chimie, Sciences de l'Univers, Sciences de la Terre* 303: 1401-1404.

MUIZON C. DE & DEVRIES T. J. 1985. — Geology and paleontology of Late Cenozoic marine deposits in the Sacaco area (Peru). *Geologische Rundschau* 74: 547-563.

MUIZON C. DE & DOMNING D. P. 1985. — The first records of fossil sirenians in the southeastern Pacific Ocean. *Bulletin du Muséum National de'Histoire Naturelle* 3: 189-213.

MUIZON C. DE & DOMNING D. P. 2002. — The anatomy of *Odobenocetops* (Delphinoidea, Mammalia), the walrus-like dolphin from the Pliocene of Peru and its palaeobiological implications. *Zoological Journal of the Linnean Society* 134: 423-452.

MURAKAMI M., SHIMADA C., HIKIDA Y. & HIRANO H. 2012a. — A new basal porpoise, *Pterophocaena nishinoi* (Cetacea, Odontoceti, Delphinoidea), from the Upper Miocene of Japan and its phylogenetic relationships. *Journal of Vertebrate Paleontology* 32: 1157-1171.

MURAKAMI M., SHIMADA C., HIKIDA Y. & HIRANO, H. 2012b. — Two new extinct basal phocoenids (Cetacea, Odontoceti, Delphinoidea) from the Upper Miocene

Koetoi Formation of Japan and their phylogenetic significance. *Journal of Vertebrate Paleontology* 32: 1172-1185.

MURAKAMI M. & KODA Y. 2013. — The first Pliocene albireonid (Cetacea, Delphinoidea) periotic from the western North Pacific and paleobiogeographic significance of fossil delphinoid ear bones of Na-arai Formation of Choshi, Chiba, central Japan. *Japan Cetology* 23: 13-20.

MURAKAMI M., SHIMADA C., HIKIDA Y. & HIRANO H. (in press). — New fossil remains from the Pliocene Koetoi Formation of Northern Japan provide insights into growth rates and the vertebral evolution of porpoises. *Acta Palaeontologica Polonica*. http://dx.doi.org/10.4202/app.2012.0127

NIKAIDO M., HAMILTON H., MAKINO H., SASAKI T., TAKAHASHI K., GOTO M., KANDA N., PASTENE L. A. & OKADA N. 2006. — Baleen whale phylogeny and a past extensive radiation event revealed by SINE insertion analysis. *Molecular Biology and Evolution* 23: 866-873.

NILSEN T. H. & CLARK S. H. 1989. — Late Cenozoic basins of Northern California. *Tectonics* 8: 1137-1158.

NORRIS R. D. 1986. — Taphonomic gradients in shelf fossil assemblages: Pliocene Purisima Formation, California. *Palaios* 1: 256-270.

OISHI M. & HASEGAWA Y. 1995a. — A list of fossil cetaceans in Japan. *The Island Arc* 3: 493-505.

OISHI M. & HASEGAWA Y. 1995b. — Diversity of Pliocene mysticetes from eastern Japan. *The Island Arc* 3: 346-452.

ORR P. C. 1960. — Radiocarbon dates from Santa Rosa Island. *Bulletin of the Geological Society of America* 71: 1113-1120.

PACKARD E. L. 1947. — A fossil sea lion from Cape Blanco, Oregon. *Oregon State Monographs, Studies in Geology* 6: 13-21.

PARHAM J. F. & PYENSON N. D. 2010. — New sea turtle from the Miocene of Peru and iterative evolution of feeding ecomorphologies since the Cretaceous. *Journal of Paleontology* 84: 231-247.

PECK J. 1960. — Paleontology and correlation of the Ohlson Ranch Formation. *University of California Publications in Geological Sciences* 36: 233-241.

PERRY F. A. 1977. — *Fossils of Santa Cruz County*. Santa Cruz Museum Association, Santa Cruz, 32 p.

PILLERI G. 1990. — Zweiter fund von *Arctocephalus lomasiensis* und *Acrophoca longirostris* (Pinnipedia, Otariidae) in der Pisco Formation Perus, *in* PILLERI G. (ed.), *Beiträge zur Paläontologie der Cetacean und Pinnipedier der Pisco Formation Perus II*. Hirnanatomisches Institut der Universitat Bern, Ostermundigen: 237-240.

PILLERI G. & PILLERI O. 1989a. — *Balaenoptera siberi*, ein neuer balaenopterid (Cetacea) aus der Pisco-Formation Perus I, *in* PILLERI G. (ed.), *Beiträge zur Paläontologie der Cetacean Perus*. Hirnanatomisches Institut der Universitat Bern, Ostermundigen: 63-106.

PILLERI G. & PILLERI O. 1989b. — Bartenwale aus der Pisco-Formation Perus, *in* PILLERI G. (ed.), *Beiträge zur Paläontologie der Cetacean Perus*. Hirnanatomisches Institut der Universitat Bern, Ostermundigen: 11-38.

PILLERI G. & SIBER H. J. 1989a. — Neuer delphinid (Cetacea, Odontoceti) aus der Pisco-Formation Perus, *in* PILLERI G. (ed.), *Beiträge zur Paläontologie der Cetacean Perus*. Hirnanatomisches Institut der Universitat Bern, Ostermundigen, Switzerland: 167-175.

PILLERI G. & SIBER H. J. 1989b. — Neuer spättertiärer cetotherid (Cetacea, Mysticeti) aus der Pisco-Formation Perus, *in* PILLERI G. (ed), *Beiträge zur Paläontologie der Cetacean Perus*. Hirnanatomisches Institut der Universitat Bern, Ostermundigen: 108-115

PILLERI G. & SIBER H. J. 1989c. — *Piscorhynchus aenigmaticus*, ein neuer Miozaner Zahnwal aus der Pisco-Formation Perus, *in* PILLERI G. (ed.), *Beiträge zur Paläontologie der Cetacean Perus*. Hirnanatomisches Institut der Universitat Bern, Ostermundigen: 195-203.

PORTIS A. 1885. — Catalogo descrittivo dei Talassoterii rinvenuti nei terreni terziarii del Piemonte e della Liguria. *Memoire della R. Accademia delle scienze di Torino, Turin* 37: 247-365.

POST K. & BOSSELAERS M. 2005. — Late Pliocene occurrence of *Hemisyntrachelus* (Odontoceti, Delphinidae) in the southern North Sea. *Deinsea* 11: 29-45.

POST K. & KOMPANJE E. J. O. 2010. — A new dolphin (Cetacea, Delphinidae) from the Plio-Pleistocene of the North Sea. *Deinsea* 14: 1-12.

POST K., LAMBERT O. & BIANUCCI G. 2008. — First record of *Tusciziphius crispus* (Cetacea, Ziphiidae) from the Neogene of the US east coast. *Deinsea* 12: 1-10.

POWELL C. L. II. 1998. — The Purisima Formation and related rocks (Upper Miocene-Pliocene), greater San Francisco Bay area, central California – Review of literature and USGS collections (now housed at the Museum of Paleontology, University of California, Berkeley). *United States Geological Survey Open-File Report* 98-594: 1-101.

POWELL C. L. II & PONTI D. J. 2007. — Paleontologic and stratigraphic reevaluation of Deadman Island, formerly in San Pedro Bay, *in* BROWN A. R., SHLEMON R. J. & COOPER J. D. (eds), *Geology and Paleontology of Palos Verdes Hills, California: A 60th Anniversary Revisit to Commemorate the 1946 Publication of U.S. Geological Survey Professional Paper 207*. Society of Economic Mineralogists and Paleontologists, Pacific Section, Los Angeles: 101-120.

POWELL C. L. II, ALLEN J. R. & HOLLAND P. J. 2004a. — Invertebrate paleontology of the Wilson Grove Formation (Late Miocene to Late Pliocene), Sonoma and Marin Counties, California, with some observations on its stratigraphy, thickness, and structure. *U.S. Geological Survey Open File Report* 2004-1017: 1-106.

POWELL C. L. II, GRANT L. B. & CONKLING S. W. 2004b. — Paleoecologic analysis and age of a Late Pleistocene fossil assemblage at a locality in Newport Beach, upper Newport Bay, Orange County, California. *The Veliger* 47: 171-180.

POWELL C. L. II, BARRON J. A., SARNA-WOJCICKI A. M., CLARK J. C., PERRY F. A., BRABB E. E. & FLECK R. J. 2007. — Age, stratigraphy, and correlation of the Late Neogene Purisima Formation, central California coast ranges. *US Geological Survey Professional Paper* 1740: 1-32.

POWELL C. L. II, FISK L. H., MALONEY D. F. & HAASL D. M. 2010. — Biostratigraphy of the San Joaquin Formation in borrow-source area B-17, Kettleman Hills Landfill, North Dome, Kettleman Hills, Kings County, California. *US Geological Society Open File Report* 2010-1140: 1-29.

PROTHERO D. R., LAU J. N. & ARMENTROUT J. M. 2001. — Magnetic stratigraphy of the Upper Miocene (Wishkahan) Empire Formation, Coos County, Oregon, *in* PROTHERO D. R. (ed), *Magnetic stratigraphy of the Pacific Coast Cenozoic*. Society of Economic Paleontologists and Mineralogists, Pacific Section, Los Angeles: 284-292.

PROTHERO D. R., LITER M. R., BARNES L. G., WANG X., MITCHELL E. D., MCLEOD S. A., WHISTLER D. P., TEDFORD R. H. & RAY C. E. 2008. — Land mammals from the Middle Miocene Sharktooth Hill bonebed, Kern County, California. *Bulletin of the New Mexico Museum of Natural History and Science* 44: 299-314.

PYENSON N. D. 2009.— Requiem for *Lipotes*. *Marine Mammal Science* 25: 714-724.

PYENSON N. D. & LINDBERG D. R. 2011. — What happened to Gray Whales during the Pleistocene? The ecological impact of sea-level change on feeding areas in the North Pacific Ocean. *Plos One* 6: e21295.

PYENSON N. D., IRMIS J. H., LIPPS J. H., BARNES L. G., MITCHELL E. D. & MCLEOD S. A. 2009. — The origin of a widespread marine bonebed deposited during the Middle Miocene Climatic Optimum. *Geology* 37: 519-522.

RACICOT R., DEMÉRÉ T. A. & ROWE T. 2007. — Morphology of a bizarre new fossil porpoise (Cetacea: Phocoenidae) from the Pliocene San Diego Formation of southern California. *Journal of Vertebrate Paleontology* 27 (3, supplement): 132A.

RAY C. E. 1977. — Geography of phocid evolution. *Systematic Zoology* 25: 391-406.

REPENNING C. A. 1983. — New evidence for the age of the Gubik Formation, Alaskan North Slope. *Quaternary Research* 19: 356-372.

REPENNING C. A. & TEDFORD R. H. 1977. — Otarioid seals of the Neogene. *US Geological Survey Professional Paper* 992: 1-87.

REPENNING C. A., PETERSON R. S. & HUBBS C. L. 1971. — Contributions to the systematics of the southern fur seals, with particular reference to the Juan Hernandez and Guadalupe species. *Antarctic Research Series* 18: 1-34.

RICK R. C., DELONG R. L., ERLANDSON J. M., BRAJE T. J., JONES T. L., KENNETT D. J., WAKE T. A. & WALKER P. L. 2009. — A trans-Holocene archaeological record of Guadalupe fur seals (*Arctocephalus townsendi*) on the California coast. *Marine Mammal Science* 25: 487-502.

ROBINETTE H. R. & STAINS H. J. 1970. — Comparative study of the calcanea of the Pinnipedia. *Journal of Mammalogy* 51 (3): 527-541.

ROBINSON D. T., AALTO K. R., BARRON J. A., ERWIN D. M. & JAYKO A. S. 2001. — Marine inundation of a Late Miocene forest: stratigraphy and tectonic evolution of the Saint George Formation, Crescent City, California. *California Geology* 6: 10-22.

ROTH B. 1979. — *Late Cenozoic Marine Invertebrates from Northwest California and Southwest Oregon.* Unpublished Ph.D. dissertation. University of California, Berkeley, California, 803 p.

RYCHEL A. L., REEDER T. W. & BERTA A. 2004.— Phylogeny of mysticete whales based on mitochondrial and nuclear data. *Molecular Phylogenetics and Evolution* 32: 892-901.

SACCO F. 1880. — Sopra una mandibola di *Balaenoptera* dell' Astigiana. *Atti della R. Accademia delle scienze di Torino, Turin* 25: 3-8.

SARNA-WOJCICKI A. M., LAJOIE K. R., MEYER C. E., ADAM D. P. & RIECK H. J. 1991. — Tephrochronologic correlation of Upper Neogene sediments along the Pacific margin, conterminous United States, *in* MORRISON R. B. (ed.), *Quaternary Nonglacial Geology: Conterminous U.S.* Geological Society of America, Boulder, Colorado: 117-140.

SCHÄFER W. 1972. — *Ecology and Paleoecology of Marine Environments*. University of Chicago press, Chicago, Illinois, 568 p.

SMITH N. A. 2011. — Taxonomic revision and phylogenetic analysis of the flightless Mancallinae (Aves, Pan-Alcidae). *Zookeys* 91: 1-116.

SMITH N. A. 2013. — The fossil record and phylogeny of the auklets (Pan-Alcidae, Aethiini). *Journal of Systematic Palaeontology*. http://dx.doi.org/10.1080/14772019.2012.742147

SORBI S. & VAIANI S. C. 2007. — New sirenian record form lower Pliocene sediments of Tuscany (Italy). *Rivista Italiana di Paleontologia e Stratigrafia* 113: 299-304.

SORBI S., DOMNING D. P., VAIANI S. C. & BIANUCCI G. 2012. — *Metaxytherium subappeninum* (Bruno, 1839) (Mammalia, Dugongidae), the latest surviving sirenian of the Mediterranean Basin. *Journal of Vertebrate Paleontology* 32: 686-707.

STANTON R. J. & DODD J. R. 1984. — *Teichichnus pescaderoensis* – new ichnospecies in the Neogene shelf and slope sediments, California. *Facies* 11: 219-228.

STEEMAN M. E. 2007. — Cladistic analysis and a revised classification of fossil and recent mysticetes. *Zoological Journal of the Linnean Society* 150: 875-894.

STEEMAN M. E., HEBSGAARD M. B., FORDYCE R. E., HO S. Y. W., RABOSKY D. L., NIELSEN R., RAHBEK C., GLENNER H., SORENSON M. V. & WILLERSLEV E. 2009. — Radiation of extant cetaceans driven by restructuring of oceans. *Systematic Biology* 58: 573-585.

STEWART J. D. & PERRY F. A. 2002. — First paleomagnetic framework for *Isurus-Carcharodon* transition in the Pacific basin: the Purisima Formation, Central California. *Journal of Vertebrate Paleontology* (3, supplement): 111A.

STIDHAM T. A. 2004. — New skull material of *Osteodontornis orri* (Aves: Pelagornithidae) from the Miocene of California. *PaleoBios* 24: 7-12.

SUTO I., KAWAMURA K., HAGIMOTO S., TERAISHI A. & TANAKA Y. 2012. — Changes in upwelling mechanisms drove the evolution of marine organisms. *Palaeogeography, Palaeoclimatology, Palaeoecology* 339-341: 39-51.

TAVANI G. 1941. — Revisione dei resti del pinnipede conservato nel museo di geologia di Pisa. *Palaeontographia Italica* 40: 97-112.

TEDFORD R. H., ALBRIGHT B. III, BARNOSKY A. D., FERRUSQUIA-VILLAFRANCA I., HUNT R. M. JR., STORER J. E., SWISHER C. C. III, VOORHIES M. R., WEBB S. D. & WHISTLER D. P. 2004. — Mammalian biochronology of the Arikareean through Hemphillian interval (late Oligocene through early Pliocene epochs), *in* WOODBURNE M. O. (ed.), *Late Cretaceous and Cenozoic Mammals of North America: Biostratigraphy and Geochronology.* Columbia University Press, New York: 169-231.

TREVISAN L. 1942. — Una nuova specie de *Balaenula* Pliocenica. *Palaeontographia Italica* 40: 1-13.

UHEN M. D. & PYENSON N. D. 2007. — Diversity estimates, biases, and historiographic effects: resolving cetacean diversity in the Tertiary. *Palaeontologia Electonica* 10: 11A: 1-22.

VALENTINE J. W. & JABLONSKI D. 1991. — Biotic effects of sea level change: the Pleistocene test. *Journal of Geophysical Research* 96: 6873-6878.

VALENZUELA-TORO A., GUTSTEIN C. S., VARAS-MALCA R. M., SUAREZ M. E. & PYENSON, N. D. 2013. — Pinniped turnover in the South Pacific Ocean: new evidence from the Plio-Pleistocene of the Atacama Desert, Chile. *Journal of Vertebrate Paleontology* 33: 216-223.

VAN BENEDEN P. J. 1876. — Les phoques fossiles du bassin d'Anvers. *Bulletins de l'Academie royale des Sciences, des Lettres et des Beaux-Arts de Belgique* 41: 783-803.

VEDDER J. G. 1972. — Review of stratigraphic names and megafaunal correlation of Pliocene rocks along the southeast margin of the Los Angeles basin, California, *in* STINEMEYER E. H. (ed), *Proceedings of the Pacific Coast Miocene Biostratigraphic Symposium*. Society of Economic Paleontologists and Mineralogists, Pacific Section, Los Angeles: 158-172.

VÉLEZ-JUARBE J. & PYENSON N. D. 2012. — *Bohaskaia monodontoides*, a new monodontid (Cetacea, Odontoceti, Delphinoidea) from the Pliocene of the western North Atlantic Ocean. *Journal of Vertebrate Paleontology* 32: 476-484.

VENDRASCO M. J., EERNISSE D. J., POWELL C. L. II & FERNANDEZ C. Z. 2012. — Polyplacophora (Mollusca) from the San Diego Formation: a remarkable assemblage of fossil chitons from the Pliocene of Southern California. *Contributions in Science, Natural History Museum of Los Angeles County* 520: 15-72.

WALSH S. & NAISH D. 2002. — Fossils seals from Late Neogene deposits in South America: a new pinniped (Carnivora, Mammalia) assemblage from Chile. *Palaeontology* 45: 821-842.

WARA M. W., RAVELO A. C. & DELANEY M. L. 2005.— Permanent El-Nino-like conditions during the Pliocene warm period. *Science* 309: 758-761.

WARHEIT K. I. 1992. — A review of the fossil seabirds from the Tertiary of the north Pacific: plate tectonics, paleoceanography, and faunal change. *Paleobiology* 18: 401-424.

WEHMILLER J. F., LAJOIE K. R., SARNA-WOJCICKI A. M., YERKES R. F., KENNEDY G. L., STEPHENS T. L. & KOHL R. F.1978. — Amino acid racemization dating of Quaternary mollusks, Pacific Coast, United States. *U.S. Geological Survey Open-file Report* 78-701: 1-4.

WESTGATE J. W. & WHITMORE F. C. 2002. — *Balaena ricei*, a new species of bowhead whale from the Yorktown Formation (Pliocene) of Hampton, Virginia. *Smithsonian Contributions to Paleobiology* 93: 295-312.

WETMORE A. 1930. — Fossil bird remains from the Temblor Formation near Bakersfield, California. *Proceedings of the California Academy of Sciences.* 19: 85-93.

WHITMORE F. C. 1994. — Neogene climatic change and the emergence of the modern whale fauna of the North Atlantic Ocean. *Proceedings of the San Diego Society of Natural History* 29: 223-227.

WHITMORE F. C. & BARNES L. G. 2008. — The Herpetocetinae, a new subfamily of extinct baleen whales (Mammalia, Cetacea, Cetotheriidae). *Virginia Museum of Natural History Special Publication* 14: 141-180.

WHITMORE F. C. & KALTENBACH J. A. 2008. — Neogene Cetacea of the Lee Creek Phosphate Mine, North Carolina. *Virginia Museum of Natural History Special Publication* 14: 181-269.

WOLFF R. G. 1973. — Hydrodynamic sorting and ecology of a Pleistocene mammalian assemblage from California (U.S.A.). *Palaeogeography, Palaeoclimatology, Palaeoecology* 13:91-101.

WOODRING W. P., BRAMLETTE M. N. & KEW W. S. W. 1946. — Geology and paleontology of Palos Verdes Hills, California. *US Geological Survey Professional Paper* 207: 1-145.

ZACHOS J., PAGANI M., SLOAN L., THOMAS E. & BILLUPS K. 2001. — Trends, rhythms, and aberrations in global climate 65 Ma to present. *Science* 292: 686-693.

ZEIGLER C. V., CHAN G. L. & BARNES L. G. 1997. — A new Late Miocene balaenopterid whale (Cetacea: Mysticeti), *Parabalaenoptera baulinensis*, (new genus and species) from the Santa Cruz Mudstone, Point Reyes Peninsula, California. *Proceedings of the California Academy of Sciences* 50 (4): 115-138.

Submitted on 25 September 2012;
accepted on 15 May 2013;
published on 27 December 2013.

APPENDIX

Stratigraphic occurrence data of latest Messinian-recent marine mammals recorded from the eastern North Pacific (excluding records not identified to at least the genus level, and marine mammals from the San Gregorio section of the Purisima Formation described herein). *, denotes NALMA ages from Tedford *et al.* (2004). †, denotes diatom zone ages from Barron & Isaacs (2001).

Taxon	Stratigraphic occurrence	Reference	Age of Occurrence	Reference
Callorhinus gilmorei	San Diego Fm.	Berta & Deméré (1986)	4.2-1.8 Ma	Deméré (1983)
Callorhinus gilmorei and *Callorhinus* sp.	Rio Dell Fm.	Boessenecker (2011c)	3-1.2 Ma	Boessenecker (2011c)
cf. *Callorhinus*	Etchegoin Fm.	Repenning & Tedford (1977)	>5 Ma	Loomis (1992)
Thalassoleon mexicanus	Almejas Fm.	Repenning & Tedford (1977)	8-6 Ma	Barnes (2008)
Thalassoleon mexicanus	Capistrano Fm.	Deméré & Berta (2005)	6.42-4.89 Ma	Deméré & Berta (2005)
Thalassoleon sp.	San Mateo Fm.	Deméré *et al.* (2003)	10-4.6 Ma*	Domning & Deméré (1984)
Thalassoleon macnallyae	Purisima Fm., Pt. Reyes	Repenning & Tedford (1977)	<6.4-5.6 Ma	Clark *et al.* (1984)
Thalassoleon macnallyae	Purisima Fm., Santa Cruz	Repenning & Tedford (1977)	6.9-5.33 Ma	Powell *et al.* (2007)
Thalassoleon n. sp.	Almejas Fm.	Barnes (1998)	8-6 Ma	Barnes (2008)
cf. *Thalassoleon*	Almejas Fm.	Barnes (1998)	latest Miocene-Early Pliocene	Barnes (1998)
Aivukus cedrosensis	Almejas Fm.	Repenning & Tedford (1977)	8-6 Ma	Barnes (2008)
Valenictus chulavistensis	San Diego Fm.	Deméré (1994a)	4.2-1.8 Ma	Vendrasco *et al.* (2012)
Valenictus chulavistensis	San Joaquin Fm.	Repenning & Tedford (1977)	4.5-2.5 Ma	Powell *et al.* (2010)
Valenictus imperialensis	Deguynos Fm.	Mitchell (1961)	4-2 Ma	Deméré (1993)
Valenictus sp.	Purisima Fm., Santa Cruz	Boessenecker (pers. obs.)	5.6-4.5 Ma	Powell *et al.* (2007)
Valenictus n. sp.	Deguynos Fm.	Atterholt *et al.* (2007)	4.4-4.1 Ma	Atterholt *et al.* (2007)
cf. *Valenictus imperialensis*	Salada Fm.	Barnes (1998)	5-3 Ma	Barnes (1998)
aff. *Valenictus*	Salada Fm.	Barnes (1998)	5-3 Ma	Barnes (1998)
Pliopedia pacifica	Paso Robles Fm.	Kellogg (1921)	6-5 Ma	Deméré (1994b)
Pliopedia pacifica	Etchegoin Fm.	Repenning & Tedford (1977)	>5 Ma	Loomis (1992)
Odobenus rosmarus	submerged deposit	Jefferson (1991)	Late Pleistocene	Jefferson (1991)
Odobenus rosmarus	Dashwood Drift	Harington & Beard (1992)	>40 Ka	Harington & Beard (1990)
Odobeninae indet.	San Diego Fm.	Boessenecker (pers. obs.)	4.2-1.8 Ma	Vendrasco *et al*. (2012)
Dusignathus santacruzensis	Purisima Fm., Santa Cruz	Kellogg (1927)	6.9-5.33 Ma	Powell *et al.* (2007)
Dusignathus sp.	St. George Fm., Crescent City	Boessenecker (2007)	6.4-6 Ma	Robinson *et al.* (2001)
Dusignathus santacruzensis	Wilson Grove Fm.	Boessenecker (pers. obs.)	7.8-6 Ma	Powell *et al.* (2004a)
Dusignathus santacruzensis	Almejas Fm.	Repenning & Tedford (1977)	8-6 Ma	Barnes (2008)
Dusignathus seftoni	San Diego Fm.	Deméré (1994a)	4.2-1.8 Ma	Vendrasco *et al.* (2012)
Dusignathus sp.	San Mateo Fm.	Deméré *et al.* (2003)	10-7 Ma*	Domning & Deméré (1984)

APPENDIX. — Continuation.

cf. *Imagotaria*	Purisima Fm., Santa Cruz	Boessenecker (pers. obs.)	6.9-5.6 Ma	Powell *et al.* (2007)
Proterozetes ulysses	Port Orford Fm.	Barnes *et al.* (2006)	700-500 Ka	Roth (1979)
Eumetopias sp.	Palos Verdes Sand	Miller (1971)	130-85 Ka	Powell & Ponti (2007)
Eumetopias sp.	Moonstone Beach Fm.	Kilmer (1972)	700 Ka	Roth (1979)
Zalophus sp.	San Pedro Sand	Langenwalter (1975)	500-200 Ka	Powell & Ponti (2007)
Zalophus sp.	Palos Verdes Sand	Jefferson (1991)	130-85 Ka	Powell & Ponti (2007)
Phoca sp.	Moonstone Beach Fm.	Barnes & Mitchell (1975)	700 Ka	Roth (1979)
Phoca sp., cf. *P. vitulina*	Palos Verdes Sand	Barnes & Mitchell (1975)	130-85 Ka	Powell & Ponti (2007)
Phoca sp., cf. *P. vitulina*	Port Orford Fm.	Barnes & Mitchell (1975)	700-500 Ka	Roth (1979)
Mirounga sp., cf. *M. angustirostris*	Palos Verdes Sand	Miller (1971)	130-85 Ka	Powell & Ponti (2007)
Arctophoca townsendi	Archaeological sites	Rick *et al.* (2009)	9-1 Ka	Rick *et al.* (2009)
Enhydra macrodonta	Moonstone Beach Fm.	Kilmer (1972)	700 Ka	Roth (1979)
Enhydra sp., cf. *E. lutris*	Port Orford Fm.	Leffler (1964)	700-500 Ka	Roth (1979)
Enhydra sp., cf. *E. lutris*	San Pedro Sand	Mitchell (1966b)	500-200 Ka	Powell & Ponti (2007)
Enhydra sp., cf. *E. lutris*	Palos Verdes Sand	Jefferson (1991)	130-85 Ka	Powell & Ponti (2007)
Enhydra sp., cf. *E. lutris*	Timms Point Silt	Mitchell (1966b)	500-300 Ka	Powell & Ponti (2007)
Enhydra sp., cf. *E. lutris*	Newport Bay Mesa	Miller (1971)	105-85 Ka	Powell *et al.* (2004b)
Enhydra lutris	Santa Rosa Island Fm.	Mitchell (1966b)	>33-12 Ka	Orr (1960)
Enhydra lutris	Montezuma Fm.	Jefferson (1991)	Late Pleistocene	Wolff (1973)
Enhydra lutris	San Miguel Island deposits	Jefferson (1991)	143-12 Ka	Jefferson (1991)
Enhydritherium terraenovae	San Mateo Fm.	Berta & Morgan (1985)	7-4.6 Ma*	Domning & Deméré (1984)
Enhydritherium sp.	San Joaquin Fm.	Berta & Morgan (1985)	4.5-2.5 Ma	Powell *et al.* (2010)
Enhydritherium terraenovae	Etchegoin Fm.	Berta & Morgan (1985)	>5 Ma	Loomis (1992)
aff. *Lagenorhynchus* sp.	Almejas Fm.	Barnes (1998)	latest Miocene-early Pliocene	Barnes (1998)
aff. *Lagenorhynchus* sp.	Salada Fm.	Barnes (1998)	5-3 Ma	Barnes (1998)
aff. *Lagenorhynchus* sp.	Tirabuzón Fm.	Barnes (1998)	4-3 Ma	Barnes (1998)
Delphinus sp. or *Stenella* sp.	Almejas Fm.	Barnes (1998)	latest Miocene-early Pliocene	Barnes (1998)
Delphinus sp. or *Stenella* sp.	Salada Fm.	Barnes (1998)	5-3 Ma	Barnes (1998)
Delphinus sp. or *Stenella* sp.	Capistrano Fm.	Barnes (1977)	Pliocene	Barnes (1977)
Delphinus sp. or *Stenella* sp.	Niguel Fm.	Barnes (1977)	Pliocene	Barnes (1977)
Delphinus sp. or *Stenella* sp.	San Diego Fm.	Barnes (1977)	3-2 Ma	Deméré (1983)
Delphinus sp. or *Stenella* sp.	Tirabuzón Fm.	Barnes (1998)	4-3 Ma	Barnes (1998)
Delphinus sp. or *Stenella* sp.	Purisima Fm., Santa Cruz	Barnes (1977)	6.9-4.5 Ma	Powell *et al.* (2007)
Delphinus sp. or *Stenella* sp.	San Mateo Fm.	Barnes (1977)	10-4.6 Ma*	Domning & Deméré (1984)

Appendix. — Continuation.

aff. *Globicephala*	Capistrano Fm.	Barnes (1977)	Pliocene	Barnes (1977)
aff. *Tursiops*	Capistrano Fm.	Barnes (1977)	Pliocene	Barnes (1977)
Parapontoporia pacifica	Almejas Fm.	Barnes (1984)	8-6 Ma	Barnes (2008)
Parapontoporia sternbergi	San Diego Fm.	Barnes (1985b)	4.2-1.8 Ma	Vendrasco *et al.* (2012)
Parapontoporia sternbergi	San Joaquin Fm.	Barnes (1973)	4.5-2.5	Powell *et al.* (2010)
Parapontoporia wilsoni	Purisima Fm., Santa Cruz	Barnes (1985b)	6.9-4.5 Ma	Powell *et al.* (2007)
Parapontoporia sp.	Capistrano Fm.	Boessenecker (pers. obs.)	6.42-4.89 Ma	Deméré & Berta (2005)
Parapontoporia sp.	Capistrano Fm.	Barnes (1977)	Pliocene	Barnes (1977)
Parapontoporia sp.	San Mateo Fm.	Barnes *et al.* (1981)	10-4.6 Ma*	Domning & Deméré 1984)
Parapontoporia sp.	Almejas Fm.	Barnes (1998)	Latest Miocene-earliest Pliocene	Barnes (1998)
Parapontoporia sp.	Wilson Grove Fm.	Barnes (1977)	Late Pliocene	Powell *et al.* (2004a)
Parapontoporia sp.	Niguel Fm.	Barnes (1977)	Pliocene	Barnes (1977)
Parapontoporia sp.	San Joaquin Fm.	Barnes (1973)	4.5-2.5 Ma	Powell *et al.* (2010)
cf. *Parapontoporia* sp.	Salada Fm.	Barnes (1998)	5-3 Ma	Barnes (1998)
aff. *Pontoporia* sp.	Tirabuzón Fm.	Barnes (1998)	4-3 Ma	Barnes (1998)
Phocoenidae unnamed genus 1	Purisima Fm., Santa Cruz	Boessenecker (pers. obs.)	5.6-3.5 Ma	Powell *et al.* (2007)
Denebola brachycephala	Almejas Fm.	Barnes (1984)	8-6 Ma	Barnes (2008)
Denebola sp.	Almejas Fm.	Barnes (1984)	8-6 Ma	Barnes (2008)
Denebola sp.	Purisima Fm., Point Reyes	Barnes (1977)	Latest Miocene-Early Pliocene	Clark *et al.* (1984)
aff. *Denebola* sp.	Salada Fm.	Barnes (1998)	5-3 Ma	Barnes (1998)
Phocoenidae unnamed genus 2	San Diego Fm.	Racicot *et al.* (2007)	4.2-1.8 Ma	Vendrasco *et al.* (2012)
Phocoenidae unnamed genus 2	Niguel Fm.	Barnes (1977)	6-4 Ma	Vedder (1972)
Phocoenidae unnamed genus 2	"Upper" Capistrano Fm.	Barnes (1977)	<5 Ma	Deméré & Berta (2005)
Phocoenidae unnamed genus 2	Purisima Fm., Santa Cruz	Boessenecker (pers. obs.)	5.6-3.5 Ma	Powell *et al.* (2007)
Phocoenidae unnamed genus 3	San Diego Fm.	T.A. Deméré (pers. comm.)	4.2-1.8 Ma	Vendrasco *et al.* (2012)
Piscolithax boreios and *Piscolithax tedfordi*	Almejas Fm.	Barnes (1984)	8-6 Ma	Barnes (2008)
Piscolithax sp.	Capistrano Fm.	Barnes (1977)	6.4-5.6 Ma	Deméré & Berta (2005)
Piscolithax sp.	Santa Cruz Mudstone	Boessenecker (pers. obs.)	7.5-6.5†	Zeigler *et al.* (1997)
cf. *Piscolithax*	Purisima Fm., Santa Cruz	Boessenecker (pers. obs.)	6.9-5.6 Ma	Powell *et al.* (2007)
aff. *Kogia* sp.	Salada Fm.	Barnes (1998)	5-3 Ma	Barnes (1998)
aff. *Kogia* sp.	Tirabuzón Fm.	Barnes (1998)	4-3 Ma	Barnes (1998)
Praekogia cedrosensis	Almejas Fm.	Barnes (1984)	8-6 Ma	Barnes (2008)
cf. *Scaphokogia* sp.	Tirabuzón Fm.	Barnes (1998)	4-3 Ma	Barnes (1998)
Albireo whistleri	Almejas Fm.	Barnes (1984)	8-6 Ma	Barnes (2008)
aff. *Albireo whistleri*	Almejas Fm.	Barnes (2008)	Latest Miocene-Early Pliocene	Barnes (2008)
Albireo savagei	Pismo Fm.	Barnes (2008)	3-2 Ma	Barnes (2008)
cf. *Albireo*	Santa Cruz Mudstone	Boessenecker (pers. obs.)	7.5-6.5†	Zeigler *et al.* (1997)
cf. *Albireo*	Purisima Fm., Santa Cruz	Boessenecker (pers. obs.)	6.9-5.6 Ma	Powell *et al.* (2007)

APPENDIX. — Continuation.

cf. Albireo	Purisima Fm., Point Reyes	Boessenecker (pers. obs.)	Latest Miocene-early Pliocene	Clark *et al.* (1984)
Balaenula sp.	San Mateo Fm.	Barnes (1977)	7-4.6 Ma*	Domning & Deméré (1984)
Balaenula sp.	Wilson Grove Fm.	Barnes (1977)	Late Pliocene	Powell *et al.* (2004a)
Balaena sp.	Port Orford Fm.	Barnes *et al.* (2006)	700-500 Ka	Roth (1979)
"*Balaenoptera*" *cortesi* "var." *portisi*	San Diego Fm.	Deméré *et al.* (2005)	4.2-1.8 Ma	Vendrasco *et al.* (2012)
"*Balaenoptera*" *cortesi* "var." *portisi*	Purisima Fm., Santa Cruz	Boessenecker (pers. obs.)	5.6-4.5 Ma	Powell *et al.* (2007)
Balaenoptera sp.	Almejas Fm.	Barnes (1992)	8-6 Ma	Barnes (2008)
Balaenoptera sp., cf. *B. acutorostrata*	Port Orford Fm.	Barnes *et al.* (2006)	700-500 Ka	Roth (1979)
Balaenoptera davidsonii	San Diego Fm.	Deméré (1986)	4.2-1.8 Ma	Vendrasco *et al.* (2012)
Balaenoptera n. sp.	San Diego Fm.	Martin (2010)	4.2-1.8 Ma	Vendrasco *et al.* (2012)
"*Megaptera*" *miocaena* (Balaenopteridae unnamed genus 1)	Purisima Fm., Santa Cruz	Boessenecker (pers. obs.)	6.9-5.6 Ma	Powell *et al.* (2007)
"*Megaptera*" *miocaena* (Balaenopteridae unnamed genus 1)	Purisima Fm., Point Reyes	Boessenecker (pers. obs.)	Latest Miocene-Early Pliocene	Clark *et al*. (1984)
"*Megaptera*" *miocaena* (Balaenopteridae unnamed genus 1)	San Mateo Fm.	T. A. Deméré (pers. comm.)	Latest Miocene	Domning & Deméré (1984)
"*Megaptera*" *miocaena* (Balaenopteridae unnamed genus 1)	San Diego Fm.	T. A. Deméré (pers. comm.)	4.2-1.8 Ma	Vendrasco *et al.* (2012)
Parabalaenoptera baulinensis	Santa Cruz Mudstone	Zeigler *et al.* (1997)	7.5-6.5†	Zeigler *et al.* (1997)
Parabalaenoptera sp.	Purisima Fm., Santa Cruz	Boessenecker (pers. obs.)	5.6-4.5 Ma	Powell *et al.* (2007)
aff. "*Plesiocetus*"	Almejas Fm.	Barnes (1992)	8-6 Ma	Barnes (2008)
Balaenopteridae unnamed genus 2	San Mateo Fm.	T. A. Deméré (pers. comm.)	latest Miocene	Domning & Deméré (1984)
Balaenopteridae unnamed genus 2	San Diego Fm.	T. A. Deméré (pers. comm.)	4.2-1.8 Ma	Vendrasco *et al.* (2012)
Balaenopteridae unnamed genus 2	Purisima Fm., Santa Cruz	Boessenecker (pers. obs.)	5.6-3.5 Ma	Powell *et al.* (2007)
Eschrichtiidae new genus	San Diego Fm.	Deméré & Berta (2003)	4.2-1.8 Ma	Vendrasco *et al.* (2012)
cf. *Eschrichtius*	Rio Dell Fm.	Boessenecker (pers. obs.)	2.1-1.2 Ma	Boessenecker (2011c)
Eschrichtius sp., cf. *E. robustus*	Palos Verdes Sand	Barnes & McLeod (1984)	130-85 Ka	Powell & Ponti (2007)
Herpetocetus bramblei	Purisima Fm., Santa Cruz	Whitmore & Barnes (2008)	5.6-4.5 Ma	Powell *et al.* (2007)
Herpetocetus sp.	Purisima Fm., Point Reyes	Boessenecker (pers. obs.)	<6.4-5.6 Ma	Clark *et al.* (1984)
Herpetocetus sp.	Wilson Grove Fm.	Boessenecker (pers. obs.)	Late Pliocene	Powell *et al.* (2004a)
Herpetocetus sp.	Etchegoin Fm.	Boessenecker (pers. obs.)	>5 Ma	Loomis (1992)
Herpetocetus sp.	Falor Fm.	Boessenecker (2013b)	2.1-0.7 Ma	Boessenecker (2013b)

Appendix. — Continuation.

Herpetocetus n. sp.	San Diego Fm.	Barnes (1977)	4.2-1.8 Ma	Vendrasco *et al.* (2012)
Herpetocetus n. sp.	Purisima Fm., Santa Cruz	Boessenecker (pers. obs.)	5.4-4.5 Ma	Powell *et al.* (2007)
aff. *Herpetocetus*	Capistrano Fm.	Barnes (1977)	Late Miocene	Barnes (1977)
cf. *Herpetocetus*	Almejas Fm.	Barnes (1984)	8-6 Ma	Barnes (2008)
Nannocetus sp.	San Mateo Fm.	Barnes *et al.* (1981)	10-4.6 Ma	Domning & Deméré 1984)
Nannocetus sp.	Purisima Fm., Santa Cruz	Boessenecker (pers. obs.)	6.9-5.6 Ma	Powell *et al.* (2007)
aff. *Nannocetus*	Almejas Fm.	Barnes (1984)	8-6 Ma	Barnes (2008)
Dusisiren dewana	Santa Cruz Mudstone	Domning (1978)	7.5-6.5†	Zeigler *et al.* (1997)
Dusisiren dewana	Purisima Fm., Santa Cruz	Domning (1978)	6.9-5.6 Ma	Powell *et al.* (2007)
Hydrodamalis cuestae	Pismo Fm.	Domning (1978)	3-2 Ma	Barnes (2008)
Hydrodamalis cuestae	San Diego Fm.	Domning & Deméré (1984)	4.2-1.8 Ma	Vendrasco *et al.* (2012)
Hydrodamalis cuestae	San Mateo Fm.	Domning & Deméré (1984)	10-4.6 Ma	Domning & Deméré (1984)
Hydrodamalis cuestae	Capistrano Fm.	Domning (1978)	Pliocene	Domning (1978)
Hydrodamalis cuestae	unnamed unit	Domning (1978)	Pliocene	Domning (1978)
Hydrodamalis sp.	Falor Fm.	Boessenecker (pers. obs.)	2.1-0.7 Ma	Boessenecker (2013b)
Hydrodamalis sp.	submerged deposit	Jefferson (1991)	Late Pleistocene	Jefferson (1991)
Hydrodamalis gigas	submerged deposit	Jefferson (1991)	Late Pleistocene	Jefferson (1991)
Hydrodamalis gigas	submerged deposit	Jones (1967)	18.94 Ka	Jones (1967)
aff. *Hydrodamalis* sp.	Almejas Fm.	Barnes (1998)	8-6 Ma	Barnes (2008)
aff. *Hydrodamalis* sp.	Purisima Fm., Point Reyes	Boessenecker (pers. obs.)	latest Miocene-early Pliocene	Clark *et al*. (1984)